NATIONAL ENERGY TECHNOLOGY LABORATORY

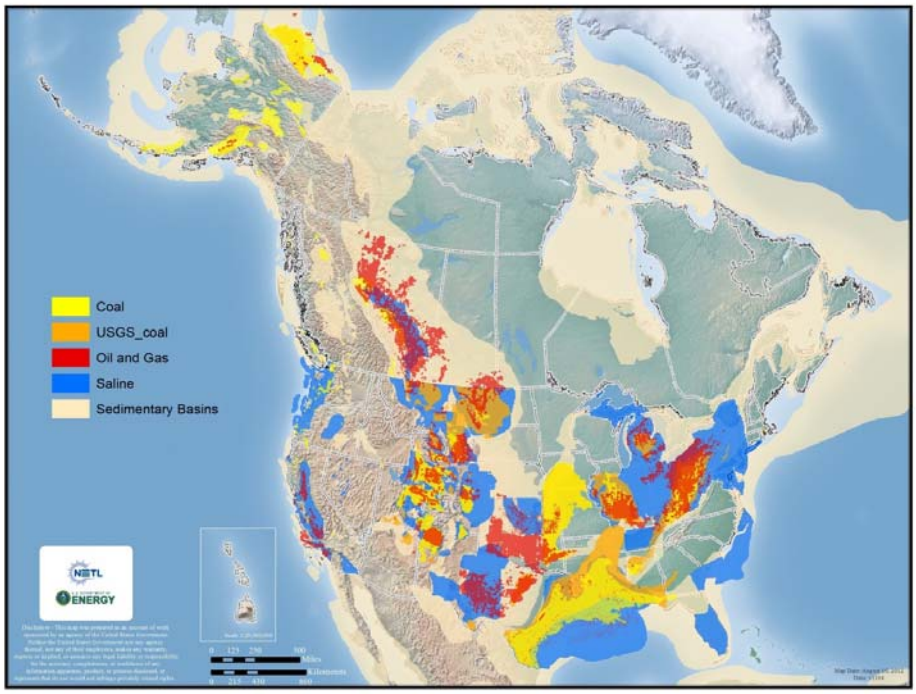

Comparison of Publicly Available Methods for Development of Geologic Storage Estimates for Carbon Dioxide in Saline Formations

12 March 2013

U.S. DEPARTMENT OF ENERGY

Office of Fossil Energy

NETL-TRS-1-2013

Disclaimer

This report was prepared as an account of work sponsored by an agency of the United States Government. Neither the United States Government nor any agency thereof, nor any of their employees, makes any warranty, express or implied, or assumes any legal liability or responsibility for the accuracy, completeness, or usefulness of any information, apparatus, product, or process disclosed, or represents that its use would not infringe privately owned rights. Reference therein to any specific commercial product, process, or service by trade name, trademark, manufacturer, or otherwise does not necessarily constitute or imply its endorsement, recommendation, or favoring by the United States Government or any agency thereof. The views and opinions of authors expressed therein do not necessarily state or reflect those of the United States Government or any agency thereof.

Cover Illustration: This map highlights potential regions of carbon dioxide storage for oil and gas reservoirs, saline formations, and coal beds that were assessed by the Regional Carbon Sequestration Partnerships and other sources and compiled by NATCARB.

Suggested Citation: Goodman, A.; Bromhal, G.; Strazisar, B.; Rodosta, T.; Guthrie, G. *Comparison of Publicly Available Methods for Development of Geologic Storage Estimates for Carbon Dioxide in Saline Formations*; NETL-TRS-1-2013; NETL Technical Report Series; U.S. Department of Energy, National Energy Technology Laboratory: Morgantown, WV, 2013; p 182.

An electronic version of this report can be found at: http://netl.doe.gov/onsite_research

Comparison of Publicly Available Methods for Development of Geologic Storage Estimates for Carbon Dioxide in Saline Formations

Angela Goodman[1], Grant Bromhal[2], Brian Strazisar[1], Traci Rodosta[2], George Guthrie[1], and William F. Guthrie[3]

[1]U.S. Department of Energy, National Energy Technology Laboratory, 626 Cochrans Mill Road, Pittsburgh, PA 15236

[2]U.S. Department of Energy, National Energy Technology Laboratory, 3610 Collins Ferry Road, Morgantown, WV 26507

[3]National Institute of Standards and Technology, 100 Bureau Drive, Stop 8980, Gaithersburg, MD 20899

NETL-TRS-1-2013

12 March 2013

NETL Contacts:

Angela Goodman, Principal Investigator

Brian Strazisar, Technical Coordinator

George Guthrie, Focus Area Lead

This page intentionally left blank.

Table of Contents

EXECUTIVE SUMMARY **1**

1. IMPORTANCE OF PROSPECTIVE CO_2 STORAGE METHODOLOGIES FOR SALINE FORMATIONS **3**

2. OVERVIEW OF SELECT PROSPECTIVE CO_2 STORAGE METHODS FOR SALINE FORMATIONS **5**

2.1 CO_2 STORAGE CAPACITY ESTIMATION: METHOD AND GAPS 6

2.2 U.S. DOE METHOD FOR THE DEVELOPMENT OF GEOLOGIC STORAGE RESOURCE FOR CARBON DIOXIDE AT THE NATIONAL AND REGIONAL SCALE 6

2.3 A PROBABILISTIC ASSESSMENT METHODOLOGY FOR THE EVALUATION OF GEOLOGIC CARBON DIOXIDE STORAGE 8

2.4 LIFETIME OF CARBON CAPTURE AND STORAGE AS A CLIMATE-CHANGE MITIGATION TECHNOLOGY 9

2.5 A METHOD FOR QUICK ASSESSMENT OF CO_2 STORAGE CAPACITY IN CLOSED AND SEMI-CLOSED SALINE FORMATIONS 10

3. DESCRIPTION OF SALINE FORMATION DATA SET **12**

4. RESULTS - COMPARISON OF SIX PUBLICLY-AVAILABLE CO_2 STORAGE METHODS TO 13 SALINE FORMATION DATA SETS **15**

4.1 COMPARISON OF ALL METHODS 15

4.2 COMPARISON OF DOE-NETL ATLAS III, IV METHOD WITH THE OTHER METHODS 23

4.3 COMPARISON OF THE CO_2 STORAGE EFFICIENCY FOR ALL METHODS 31

5. CONCLUSION **35**

6. REFERENCES **37**

APPENDIX A: A-1

APPENDIX B: B-1

APPENDIX C: C-1

APPENDIX D: D-1

APPENDIX E: E-1

APPENDIX F: F-1

APPENDIX G: G-1

This page intentionally left blank.

List of Figures

Figure 1. Saline formation net and gross thickness. 13
Figure 2. Multi-colored bars represent estimates of CO_2 storage resource in gigatonnes (GT) at the 50th percentile for Formations A through F for the following methods: CSLF: Bachu et al. (2007), DOE-NETL Atlas I, II (2007, 2008), DOE-NETL Atlas III, IV (2010, 2012), USGS: Brennan et al. (2010), Szulczewski et al. (2012), and Zhou et al. (2008). 16
Figure 3. Multi-colored bars represent estimates of CO_2 storage resource in gigatonnes (GT) at the 50th percentile for Formations G through M for the following methods: CSLF: Bachu et al. (2007), DOE-NETL Atlas I, II (2007, 2008), DOE-NETL Atlas III, IV (2010, 2012), USGS: Brennan et al. (2010), Szulczewski et al. (2012), and Zhou et al. (2008). 17
Figure 4. Simultaneous 95% uncertainty interval for all pair-wise differences between all methods for Formations A-H. 20
Figure 5. Simultaneous 95% uncertainty interval for all pair-wise differences between all methods for Formations I-M. 21
Figure 6. Summary graphs for Formations A and B, comparing the predicted distributions of the pair-wise differences between the method used in the DOE/NETL Atlas III, IV with (a) CSLF, (b) Atlas I, II, (c) USGS, (d) Szulczewski et al., and (e) Zhou et al. 24
Figure 7. Summary graphs for Formations C and D, comparing the predicted distributions of the pair-wise differences between the method used in the DOE/NETL Atlas III, IV with (a) CSLF, (b) Atlas I, II, (c) USGS, (d) Szulczewski et al., and (e) Zhou et al. 25
Figure 8. Summary graphs for Formations E and F, comparing the predicted distributions of the pair-wise differences between the method used in the DOE/NETL Atlas III, IV with (a) CSLF, (b) Atlas I, II, (c) USGS, (d) Szulczewski et al., and (e) Zhou et al. 26
Figure 9. Summary graphs for Formations G and H, comparing the predicted distributions of the pair-wise differences between the method used in the DOE/NETL Atlas III, IV with (a) CSLF, (b) Atlas I, II, (c) USGS, (d) Szulczewski et al., and (e) Zhou et al. 27
Figure 10. Summary graphs for Formations I and J, comparing the predicted distributions of the pair-wise differences between the method used in the DOE/NETL Atlas III, IV with (a) CSLF, (b) Atlas I, II, (c) USGS, (d) Szulczewski et al., and (e) Zhou et al. 28
Figure 11. Summary graph for Formations K and L, comparing the predicted distributions of the pair-wise differences between the method used in the DOE/NETL Atlas III, IV with (a) CSLF, (b) Atlas I, II, (c) USGS, (d) Szulczewski et al., and (e) Zhou et al. 29
Figure 12. Summary graph for Formations M, comparing the predicted distributions of the pair-wise differences between the method used in the DOE/NETL Atlas III, IV with (a) CSLF, (b) Atlas I, II, (c) USGS, (d) Szulczewski et al., and (e) Zhou et al. 30
Figure 13. Multi-colored bars represent overall efficiency for CO_2 storage estimates at the 50th percentile for formations A through F for the following methods: CSLF: Bachu et al. (2007), DOE-NETL Atlas I, II (2007, 2008), DOE-NETL Atlas III, IV (2010, 2012), USGS: Brennan et al. (2010), Szulczewski et al. (2012), and Zhou et al. (2008)..... 33
Figure 14. Multi-colored bars represent overall efficiency for CO_2 storage estimates at the 50th percentile for formations G through M for the following methods: CSLF: Bachu et al. (2007), DOE-NETL Atlas I, II (2007, 2008), DOE-NETL Atlas III, IV (2010, 2012), USGS: Brennan et al. (2010), Szulczewski et al. (2012), and Zhou et al. (2008)..... 34

List of Tables

Table 1. Summary of all pair-wise differences between methods at the 95% uncertainty interval for Formations A-M. 22

Acronyms, Abbreviations, and Symbols

Term	Description
CCUS	Carbon capture, utilization, and storage
CSLF	Carbon Sequestration Leadership Forum
DOE	Department of Energy
EERC	Energy & Environmental Research Center
EPA	U.S. Environmental Protection Agency
GT	Gigatonnes
IEAGHG	International Energy Agency Greenhouse Gas
LBNL	Lawrence Berkeley National Laboratory
NATCARB	National Carbon Sequestration Database and Geographic Information System
NETL	National Energy Technology Laboratory
RCSP	Regional Carbon Sequestration Partnerships
USGS	United States Geological Survey

This page intentionally left blank.

Acknowledgments

This work was conducted as part of the intramural research activities at the National Energy Technology Laboratory (NETL) in support of the Department of Energy's (DOE) Office of Fossil Energy's CO_2 Storage Program, as managed by NETL's Strategic Center for Coal.

The authors would also like to thank: John Litynski, Energy Efficiency & Renewable Energy Program Operations, U.S. DOE – Advanced Manufacturing Office , Washington, DC; Stefan Bachu, CO_2 Storage Alberta Innovates – Technology Futures, Edmonton, AB, Canada; Sean Brennan, U.S. Geological Survey, Reston, Virginia; Ruben Juanes, Civil and Environmental Engineering and Center for Computational Engineering, Massachusetts Institute of Technology, Cambridge, MA; Michael L. Szulczewski, Civil and Environmental Engineering, Massachusetts Institute of Technology, Cambridge, MA; Quanlin Zhou, Lawrence Berkeley National Laboratory (LBNL), Earth Sciences Division, Berkeley, CA; Scott Frailey, Illinois State Geologic Survey, Midwest Geological Sequestration Consortium, Champaign, IL; Charlie Gorecki, Energy & Environmental Research Center (EERC), University of North Dakota, Grand Forks, ND; Kelly Rose, U.S. DOE NETL, Albany, Oregon; Bob Dilmore, U.S. DOE NETL, Pittsburgh, PA; and Doug Allen, Salem State University, Salem, MA for reviewing calculations and helpful discussions.

This page intentionally left blank.

EXECUTIVE SUMMARY

Prospective CO_2 storage resource estimates for application to saline formations at the national, regional, and basin scale are required to assess the potential for carbon capture, utilization, and storage (CCUS) technologies to reduce CO_2 emissions. Both private and public entities worldwide rely on CO_2 storage resource estimates for broad energy-related government policy and business decisions. As prospective estimates, they embody inherent uncertainties arising from simplifying assumptions and data limitations pertaining to subsurface geology. CO_2 storage-resource estimates provide important bounds for energy planning at the national and regional levels. Several methods have been developed to provide storage-resource estimates, originating with efforts as early as 1993. This study compares estimates that several commonly used methods produce when applied to common data sets to assess the impact that the choice of method has on the results.

The methods assessed in this study include the following:

- **CSLF: Bachu (2007)**: This method was developed for the Carbon Sequestration Leadership Forum (CSLF) and assumes open-boundary conditions; it is detailed in Bachu et al. (2007)
- **DOE-NETL Atlas I, II (2007, 2008):** This method was developed for the first and second editions of the United States Department of Energy-National Energy Technology Laboratory (DOE-NETL) Carbon Sequestration Atlas of the United States and Canada; it assumes open-boundary conditions and is detailed in DOE-NETL (2007, 2008)
- **DOE-NETL Atlas III, IV (2010, 2012)**: This method was developed for the third and fourth editions of the DOE-NETL Carbon Sequestration Atlas of the United States and Canada; it assumes open-boundary conditions and is detailed in DOE-NETL (2010a, 2012) and Goodman et al. (2011)
- **USGS: Brennan et al. (2010)**: This probabilistic method was developed by the United States Geological Survey; it assumes open-boundary conditions and is detailed in Brennan et al. (2010). An updated USGS method is currently in press (Blondes et al., 2013)
- **Szulczewski et al. (2012)**: This migration- and pressure-limited method can be applied to both open-boundary and closed-boundary conditions and is detailed in Szulczewski et al. (2012)
- **Zhou et al. (2008)**: This method can be applied to both closed-boundary and semi-closed-boundary conditions and is detailed in Zhou et al. (2008)

The following general trends were determined for the methods for the median CO_2 storage resource estimates (i.e. the 50th percentile):

1) The closed-boundary method by Zhou et al. (2008), typically, reports the lowest CO_2 storage resource
2) The open-boundary method by USGS: Brennan et al. (2010), typically, reports the highest CO_2 storage resource

3) In most cases, the migration limited estimates by Szulczewski et al. (2012) are similar to the closed-boundary estimates provided by Zhou et al. (2008) for CO_2 storage resource
4) The open-boundary estimates by CSLF: Bachu et al. (2007), DOE-NETL Atlas I, II (2007, 2008), and DOE-NETL Atlas III, IV (2010, 2012) typically fall between the open-boundary estimates by USGS: Brennan et al. (2010) and closed-boundary estimates by Zhou et al. (2008) for CO_2 storage resource

Statistical conclusions stemming from a pair-wise comparison of stochastic inputs using the Šidák inequality to control for false positives arising from multiple comparisons are as follows:

1) In almost all open-boundary method cases the methods do not differ in a statistically significant way in each of the saline formation cases that were studied
2) Although there are definite differences in the underlying assumptions for open- and closed-boundary methods, for most of the saline formation cases that were studied the variability in underlying parameters was still so great that the estimates of CO_2 storage resource from the closed-boundary method could not be statistically distinguished from those generated by the open-boundary methods. In some cases, however, the open-boundary methods do give statistically significant different results when compared to the closed-boundary method.
3) In general, the uncertainty in the underlying parameters has a much greater impact on overall estimates of CO_2 storage resource than the choice of method does, especially within subsets of methods defined by their boundary assumptions

1. IMPORTANCE OF PROSPECTIVE CO_2 STORAGE METHODOLOGIES FOR SALINE FORMATIONS

Prospective CO_2 storage resource estimates for application to saline formations at the national, regional, and basin scale are required to assess the potential for carbon capture, utilization, and storage (CCUS) technologies to reduce CO_2 emissions. Both private and public entities worldwide rely on CO_2 storage resource estimates for broad energy-related government policy and business decisions. Prospective estimates of CO_2 geologic storage resource are subject to relatively large uncertainties, however, because the assessments rely on simplifying assumptions due to the deficiency or absence of data from the subsurface associated with areas of potential storage in saline formations and the natural heterogeneity of geologic formations in general, resulting in undefined rock properties. As site characterization progresses to individual CO_2 storage sites, additional site-specific data will likely be collected and analyzed that will allow for the refinement of prospective CO_2 storage resource estimates and development of CO_2 storage capacities. Until such detailed characterization can be documented, dependable prospective CO_2 storage estimates are essential to ensure successful widespread deployment of CCUS technologies (Bachu et al., 2007; Bradshaw et al., 2007; Goodman et al., 2011).

Initiatives for assessing CO_2 geologic storage potential have been conducted since 1993. These initiatives vary from an overview description of assessment tools to a detailed, comprehensive method (Bachu et al., 2007; Bradshaw et al., 2007; DOE NETL, 2007, 2008, 2010a; Economides and Ehlig-Economides, 2009; Gorecki et al., 2009; Koide et al., 1992; Szulczewski and Juanes, 2009; Szulczewski et al., 2012; van de Meer, 1993; van de Meer and Egberts, 2008a; van de Meer and Egberts, 2008b; van de Meer and Yavuz, 2009; Zhou et al., 2008). Prospective CO_2 storage estimates have been published for regions in the United States (DOE NETL, 2010a), Canada (NACSA, 2012), Mexico (NACSA, 2012), Japan (Takahashi et al., 2009), Ireland (Lewis et al., 2009), India (Garg and Shukla, 2009), Greece (Koukouzas et al., 2009), China (Dahowski et al., 2009), Poland (Radoslaw et al., 2009), and South Africa (Surridge and Cloete, 2009) using various methods that require deterministic or probabilistic input parameters. Although dependable prospective CO_2 storage estimates are essential to ensure successful deployment of CCUS technologies, it is difficult to completely assess the uncertainty of these estimates without knowing how the current methods targeted at prospective CO_2 storage resource estimates for saline formations compare to one another.

In this study, we compare prospective CO_2 methods for development of geologic storage estimates for CO_2 in saline formations to determine if the method used for estimation of storage resource significantly impacts the results. The purpose of this study is not to validate data sets, endorse methods, or release CO_2 estimates for specific formations. This study compares methods using the same input data to assess significant differences between the various methods. Specifically, six publicly-available, transparent methods were applied to 13 saline formation data sets.

The methods applied are listed as follows:

- **CSLF: Bachu (2007)**: This method was developed for the Carbon Sequestration Leadership Forum (CSLF) and assumes open-boundary conditions; it is detailed in Bachu et al. (2007)

- **DOE-NETL Atlas I, II (2007, 2008):** This method was developed for the first and second editions of the United States Department of Energy-National Energy Technology Laboratory (DOE-NETL) Carbon Sequestration Atlas of the United States and Canada; it assumes open-boundary conditions and is detailed in DOE-NETL (2007, 2008)
- **DOE-NETL Atlas III, IV (2010, 2012)**: This method was developed for the third and fourth editions of the DOE-NETL Carbon Sequestration Atlas of the United States and Canada; it assumes open-boundary conditions and is detailed in DOE-NETL (2010a, 2012) and Goodman et al. (2011)
- **USGS: Brennan et al. (2010)**: This probabilistic method was developed by the United States Geological Survey; it assumes open-boundary conditions and is detailed in Brennan et al. (2010). An updated USGS method is currently in press (Blondes et al., 2013)
- **Szulczewski et al. (2012)**: This migration- and pressure-limited method can be applied to both open-boundary and closed-boundary conditions and is detailed in Szulczewski et al. (2012)
- **Zhou et al. (2008)**: This method can be applied to both closed-boundary and semi-closed-boundary conditions and is detailed in Zhou et al. (2008)

The authors worked accordingly with the corresponding authors of the methods applied in this study to ensure that each method was applied to the general saline formation data sets correctly.

The saline formations targeted were characterized by Szulczewski et al. (2012). While detailed information regarding the formations is available (Szulczewski et al., 2012), location names were not used in order to focus the study on comparing methods and to avoid implying any specific endorsement of this data set.

2. OVERVIEW OF SELECT PROSPECTIVE CO_2 STORAGE METHODS FOR SALINE FORMATIONS

Methods for CO_2 storage in saline formations selected for this comparison study were publicly-available, referenced in the literature, and transparent in that all input parameters were defined and could be readily applied to an existing data set. These methods target CO_2 storage resource estimates which represent the fraction of pore volume in a formation of interest that will be occupied by CO_2 injected through drilled and completed wellbores. CO_2 storage resource estimates consider only physical trapping of CO_2 (Bachu et al., 2007; Kopp et al., 2009; Xie and Economides, 2009). Economic, legal, and regulatory considerations are not included in these methods. Injectivity issues are considered by one method (Szulczewski et al., 2012). All methods assumed these basic criteria: (1) pressure and temperature conditions in the saline formation are adequate to keep the CO_2 liquid or supercritical; (2) a suitable seal system, such as a caprock, is present to limit vertical flow of the CO_2 to the surface; and (3) a combination of hydrogeologic conditions isolates the CO_2 within the saline formation. The methods target CO_2 storage resource estimates at a high-level such as the national, regional, basin or formation scale. At present, a universal standard CO_2 storage classification structure is not generally accepted although several CO_2 storage classifications systems have been proposed (Bachu et al., 2007; Burruss et al., 2009; DOE-NETL, 2010c; Gorecki et al., 2009; IEAGHG, 2009). Site-specific CO_2 storage estimates are not considered in these methods.

The boundary conditions for the saline formation subsurface comparison were considered to be open or closed, depending on the method. Open systems are permeable fluid-filled reservoirs where in-situ fluids will either be displaced away from the injection location into other parts of the formation and/or into neighboring formations or managed by means of fluid production, treatment, and disposal in accordance with current technical, regulatory, and economic guidelines (Birkholzer and Zhou, 2009; Gorecki et al., 2009; IEAGHG, 2009; Nicot, 2008; Zhou et al., 2008). Subsequently, the primary constraints on the percentage of pore space that can be filled with CO_2 in open systems are due to displacement efficiencies, rather than pressure increases, although there will often be a need to define a maximum bottom-hole injection pressure to reduce risks associated with injection (Gorecki et al., 2009; IEAGHG, 2009; Zhou et al., 2008). Closed systems are fluid-filled reservoirs where in-situ fluid movement is restricted within the formation by means of impermeable barriers (Birkholzer and Zhou, 2009; Gorecki et al., 2009; IEAGHG, 2009; Nicot, 2008; Zhou et al., 2008). Storage volume in closed systems is then constrained by the compressibility of the formation's native fluid and rock matrix (van de Meer, 1992, 1993, 1995; van de Meer and Egberts, 2008a; van de Meer and Yavuz, 2009). In addition, the CO_2 injection pressure cannot exceed the maximum allowable pressure of the formation, and no mechanism for pressure relief (such as brine production) is considered (Burruss et al., 2009; Gorecki et al., 2009; Zhou et al., 2008). The very low compressibility of formation fluids and rocks limit the capacity of closed systems to a very small percentage of total pore volume (Gorecki et al., 2009; Xie and Economides, 2009; Zhou et al., 2008).

A brief description of the select CO_2 storage methods and how we applied the methods to the saline formations in this study is in the following sections.

2.1 CO_2 STORAGE CAPACITY ESTIMATION: METHOD AND GAPS (CSLF: BACHU ET AL., 2007)

This method stems from the Technical Group Taskforce on CO_2 storage estimates led by the Carbon Sequestration Leadership Forum (CSLF) (Bachu et al., 2007). In this effort, multi-faceted aspects of CO_2 storage capacity estimation were examined including types of geological media, operating time frames, resource-reserve pyramid classification, and assessment of scale and resolution.

For saline aquifers, the boundary conditions are considered to be open. The general equation used for storing CO_2 in structural and stratigraphic traps as static trapping is:

$$M_{CO_2e} = V_{trap}\phi(1 - S_{wirr})\rho CO_2 C_c = Ah\phi(1 - S_{wirr})\rho CO_2 C_c \quad (1)$$

where M_{CO2e} is the effective storage capacity as designated in the resource-reserve classification pyramid by CO_2 mass representing a subset of the theoretical capacity (Bachu et al., 2007). This estimate usually changes with the acquisition of new data and or knowledge. V_{trap} is the geometric volume of the structural or stratigraphic trap down to the spill point, ϕ is the porosity, S_{wirr} is the irreducible water saturation, ρCO_2 is the CO_2 density at the temperature and pressure of the aquifer, C_c is a capacity coefficient that incorporates the cumulative effects of trap heterogeneity, CO_2 buoyancy and sweep efficiency, and A and h are the trap area and average gross thickness, respectively. At the time of publication of Bachu et al. (2007), no values in the literature were available for this capacity coefficient, which is site-specific and must be determined through numerical simulations and/or field work. Recent work by the International Energy Agency Greenhouse Gas (IEAGHG) R&D Programme (IEAGHG, 2009) cites C_c at the formation and site-specific scale specific to this method. Formation (C_c) values range between 2.4% and 10% based on their 10th to 90th percentiles. The IEAGHG (2009) also determined that the CSLF method is equivalent to the DOE method as long as the same parameters are applied to each method. Worldwide CO_2 storage estimates are primarily based on either CSLF or DOE methods.

In this comparison effort, baseline values for parameters A, h, ϕ, ($1-S_{wirr}$) and ρCO_2 shown in Equation 1 were applied to the CSLF: Bachu et al. (2007) method for each saline formation (see **Appendix A** for baseline values for saline formations A through M). For the capacity coefficient, we applied the following formation $C_c*(1-S_{wirr})$ values cited by the IEAGHG (2009) as a function of lithology based on their 10th, 50th, and 90th percentiles: Clastics (1.86, 2.70, and 6.00)%; Dolomite (2.58, 3.26, and 5.54)%; and Limestone (1.41, 2.04, and 3.27)%.

2.2 U.S. DOE METHOD FOR THE DEVELOPMENT OF GEOLOGIC STORAGE RESOURCE FOR CARBON DIOXIDE AT THE NATIONAL AND REGIONAL SCALE [DOE-NETL ATLAS I, II (2007, 2008) AND DOE-NETL ATLAS III, IV (2010, 2012)]

The U.S. Department of Energy (DOE) method is intended for external users such as the Regional Carbon Sequestration Partnerships (RCSP), future project developers, and governmental entities to produce prospective CO_2 resource assessments of potential CO_2 storage reservoirs in the United States and Canada at the regional and national scale (DOE NETL, 2007, 2008, 2010a; Goodman et al., 2011). The method, however, is general enough to be applied globally. The CO_2 storage estimates are considered to be prospective storage resources according

to the DOE storage classification structure (DOE-NETL, 2010c). The CO_2 storage resource reported in DOE's assessment is intended to be distributed online by a geographic information system in the National Carbon Sequestration Database and Geographic Information System (NATCARB) (DOE NETL, 2010b) and made available in hard copy in the Carbon Sequestration Atlas of the United States and Canada (DOE-NETL, 2007, 2008, 2010a, 2012). The DOE-NETL Atlas I, II (2007, 2008) method was developed for the first and second editions of the Carbon Sequestration Atlas of the United States and Canada; it assumes open-boundary conditions and is detailed in DOE-NETL (2007, 2008). The DOE-NETL Atlas III, IV (2010, 2012) method was developed for the third edition of the Carbon Sequestration Atlas of the United States and Canada; it assumes open-boundary conditions and is detailed in DOE-NETL (2010a) and Goodman et al. (2011). DOE's method will be regularly refined, incorporating results of the Development Phase projects conducted by the RCSPs from 2008 through 2018. Estimates will be formally updated every two years in subsequent versions of the Carbon Sequestration Atlas of the United States and Canada.

Structural and hydrodynamic trapping are initially the dominant trapping mechanisms and are the focus of the DOE method. The boundary conditions are considered to be open. The volumetric equation to calculate the CO_2 storage resource mass estimate (G_{CO2}) for geologic storage in saline formations for DOE-NETL Atlas I, II (2007, 2008) and DOE-NETL Atlas III, IV (2010, 2012) is:

$$G_{CO_2} = A_t h_g \phi_{tot} \rho E_{saline} \tag{2}$$

Where A_t is the total geographical area that defines the basin or region being assessed for CO_2 storage, h_g is the gross thickness of the saline formation for which CO_2 storage is assessed within the basin or region defined by A_t, ϕ_{tot} is the total porosity in volume defined by the net thickness, ρ is the density of CO_2 evaluated at the pressure and temperature that represents storage conditions anticipated for a specific geologic unit averaged over h_g and A_t.

E_{saline} is the CO_2 storage efficiency factor that reflects a fraction of the total pore volume that is filled by CO_2. In DOE-NETL Atlas I, II (2007, 2008), efficiency is averaged over four stochastic simulation cases that are based on 1) normal distributions with one standard deviation, 2) normal distributions with one half standard deviation, 3) uniform distributions, and 4) a mixture of distributions such as normal, lognormal, and uniform. For DOE-NETL Atlas I, II (2007, 2008), efficiency ranged between 0.7% and 4.7% based on their 15th to 85th percentiles (DOE-NETL, 2007, 2008). In DOE-NETL Atlas III, IV (2010, 2012), E_{saline} for saline formations as estimated by Monte Carlo sampling is based directly on the range of their 10th and 90th percentiles for net-to-gross thickness, effective-to-total porosity, volumetric displacement, and microscopic displacement as reported by IEAGHG (2009) (Goodman et al., 2011). Because no documented data for the net-to-total area term are available, it was assumed that CO_2 will occupy between 20% and 80% of the formation for the purposes of Monte Carlo sampling simulations. For DOE-NETL Atlas III, IV (2010, 2012), E_{saline} factors range between 0.40% and 5.5% based on their 10th to 90th percentiles (DOE-NETL, 2010a).

CO_2 storage resource estimates for DOE-NETL Atlas I, II, III, and IV were calculated by Monte Carlo simulation using the program GoldSim (see **Appendix B** for the GoldSim Model description for DOE-NETL Atlas I, II and III). Baseline values for parameters A_t, h_g, ϕ_{tot}, and ρ shown in Equation 2 were applied to the DOE-NETL Atlas I, II (2007, 2008) and DOE-NETL Atlas III, IV (2010, 2012) methods for each saline formation (see **Appendix A** for baseline

values for saline formations A through M). For DOE-NETL Atlas I, II (2007, 2008), E_{saline} values applied were 0.7, 2.1, and 4.7% based on their 15th, 50th, and 85th percentiles. For DOE-NETL Atlas III, IV (2010, 2012), E_{saline} values applied were based on lithology at their 10th, 50th, and 90th percentiles and are as follows: Clastics (0.5, 2.0 and 5.4) %; Dolomite (0.64, 2.2, and 5.5) %; and Limestone (0.40, 1.5, and 4.1) %.

2.3 A PROBABILISTIC ASSESSMENT METHODOLOGY FOR THE EVALUATION OF GEOLOGIC CARBON DIOXIDE STORAGE (USGS: BRENNAN ET AL., 2010)

In 2007, the Energy Independence and Security Act (Public Law 110-140) authorized the United States Geological Survey (USGS) to conduct a national assessment of potential geologic storage resources for CO_2 in cooperation with the U.S. Environmental Protection Agency (EPA) and the DOE. As a result of this legislation, USGS developed a method that is intended to be used by the USGS's geologists for assessments of CO_2 storage resource in the United States at scales ranging from regional to sub-basinal in which storage assessment units are defined on the basis of common geologic and hydrologic characteristics (Brennan et al., 2010). The USGS plans to report CO_2 storage assessments stemming from this Act in 2013. An updated USGS method is currently in press (Blondes et al., 2013). As described by Brennan et al. (2010), this method estimates the technically accessible storage resource by probabilistic assessment, which is the mass of CO_2 that can be stored in the pore volume of the saline storage formation. The boundary conditions are considered to be open. This resource is the product of CO_2 density and storage volume, which is the fraction of the pore volume that will retain injected CO_2. The storage formation pore volume ($_{S}F_{PV}$) is calculated and then allocated between the pore volume available for buoyantly trapped CO_2 and residually trapped CO_2:

$$SF_{PV} = A_{SF} T_{PI} \phi_{PI} \tag{3}$$

where A_{SF} is the area of storage assessment unit, T_{PI} is the mean thickness of the net porous interval, and ϕ_{PI} is the mean porosity. The buoyant trapping and residual trapping are calculated separately because they are modified by different geologic uncertainties and storage efficiencies. Storage efficiency is the value that represents the fraction of the total available pore space that will retain free-phase CO_2. The technically accessible storage volume (TA_{SV}) for the storage formation as a whole is the summation of the buoyantly and residually trapped CO_2:

$$TA_{SV} = R1_{SV} + R2_{SV} + R3_{SV} + B_{SV} \tag{4}$$

where $R1_{SV}$, $R2_{SV}$, $R3_{SV}$ are the residually trapped CO_2 storage volume for rock class 1, where permeability is greater than 1 darcy (d), class 2, where permeability ranges between 1 millidarcy and 1 darcy, and class 3, where permeability is less than 1 millidarcy. B_{SV} is the buoyantly trapped CO_2 storage volume. Buoyant trapping efficiencies range between 10% and 60% and residual trapping efficiencies range between 1% and 15% by rock class based on their 5th and 95th percentiles. The technically accessible storage resource by CO_2 mass is determined by multiplying the TA_{SV} by the density of CO_2 by using a probabilistic distribution of the density of CO_2 calculated by the assessment team based on the upper and lower depth boundaries of the storage formation, temperature and pressure gradients appropriate for the area, and an equation of state for CO_2.

In this comparison effort, all parameters were treated stochastically in the Monte Carlo simulation program GoldSim for the USGS: Brennan et al. (2010) method (See **Appendix C** for

GoldSim Model description). Minimum, baseline, and maximum values in a triangular distribution were applied to A_{SF}, T_{PI}, ϕ_{PI}, CO_2 density, and residual trapping efficiency (see **Appendix A** for baseline values for saline formations A through M). Buoyant trapping was set to 0% because the caprock for the saline formation data sets was assumed to be roughly linear ensuring that structural trapping would not occur at the top of an anticline or in a tilted fault block (Szulczewski et al., 2012). Minimum, baseline, and maximum values for residual trapping efficiency as a function of permeability are as follows: Class 1 with permeability greater than 0.9869233 µm² (1 d): (1, 5, and 7) % efficiency, Class 2 with permeability between 0.9869233×10^{-3} µm² and 0.9869233 µm² (1 md and 1000 md): (1, 7, and 15) % efficiency, and Class 3 with permeability less than 0.9869233×10^{-3} µm² (1 md): (0, 0, and 7) % efficiency. Eleven saline data formation sets were found to have Class 2 permeability. Two formations were found to have Class 1 and 2 permeability ranges where it was assumed that Class 1 accounted for 5% and Class 2 accounted for 95% of permeability range. Technically accessible CO_2 storage estimates are reported at their 5th, 50th, and 95th percentiles.

2.4 LIFETIME OF CARBON CAPTURE AND STORAGE AS A CLIMATE-CHANGE MITIGATION TECHNOLOGY (SZULCZEWSKI ET AL., 2012)

According to Szulczewski et al. (2012), the storage capacity of a saline aquifer is the maximum amount of CO_2 that could be injected and securely stored under geologic constraints, such as the aquifer's size and the integrity of its caprock. Both residual trapping, in which zones of CO_2 become immobilized by capillary forces, and solubility trapping, in which CO_2 dissolves into the groundwater are considered. This method is applicable to both open and closed systems depending upon the geology of the formation of interest. How much CO_2 can be trapped in the pore space of the formation is partitioned by CO_2 trapping and migration-limited capacity, a time independent component, and CO_2 capacity due to limitations on the injection rate through pressure dissipation and pressure-limited capacity, a time dependent component. Accordingly, CO_2 storage supply is constrained by CO_2 dissipation and pressure-limited capacity for short injection times and CO_2 trapping and migration-limited capacity for longer injection times. Thus, the total CO_2 storage supply estimate is determined by the more conservative capacity curve: the dissipation and pressure-limited curve or the CO_2 trapping and migration-limited curve. This method reports CO_2 storage capacities at several injection times between 25 years and 600 years.

The mass of CO_2 (C_t) stored for the CO_2 trapping and migration-limited method at the basin scale, is calculated by:

$$C_t = \rho_g L_t W H \phi (1 - S_{wc}) \frac{2}{\varepsilon_T} \tag{5}$$

where ρ_g is the CO_2 density, L_t is the length of domain for migration model, W is the width of the well array, H is the net aquifer thickness, ϕ is the porosity, S_{wc} is the connate water saturation, and $2/\varepsilon_T$ is the efficiency factor. The efficiency factor is calculated using a reservoir model to simulate CO_2 migration through an aquifer as well as solubility and capillary trapping.

The mass of CO_2 (C_p) stored for the CO_2 dissipation and pressure-limited method at the basin scale, is calculated by:

$$C_p = \rho_g HW\sqrt{\frac{k_{aq}cT}{\mu_w}}\ \frac{P_{fraq} - (\rho_o + \overline{\rho_w} gD)}{4\tilde{p}_{max}} \tag{6}$$

where ρ_g is the CO_2 density, H is the net aquifer thickness, W is the width of the well array, k_{aq} is the aquifer permeability, c is the compressibility, T is the temperature, μ_w is the brine viscosity, P_{fraq} is the fracture pressure, ρ_o is the density, ρ_w is the brine density, g is the gravitational acceleration, D is the depth to the top of aquifer, and p_{max} is maximum dimensionless pressure.

This comparison effort is focused on time-independent storage resource in the absence of injectivity limitations. Therefore, only the CO_2 trapping and migration-limited capacity was considered. This is equivalent to the reported capacities by Szulczewski et al. (2012) in the limit of long injection times. The storage volumes reported by Szulczewski et al. (2012) had reached the volumetric limit by 300 years for 12 of the 13 formations used in this comparison. For the 13th, the time-independent resource was communicated to us directly by the authors. In this comparison effort, the CO_2 trapping and migration-limited CO_2 storage resource estimates were used directly from Szulczewski et al. (2012) for each saline formation considered. Szulczewski et al. (2012) reported baseline storage capacities based on a normal distribution where one standard deviation is used as an appropriate measure of uncertainty from the probability density function. Because of the assumed normality of the distribution, one standard deviation was taken to be the half-range of the 16th and 84th percentiles of baseline storage capacity.

2.5 A METHOD FOR QUICK ASSESSMENT OF CO_2 STORAGE CAPACITY IN CLOSED AND SEMI-CLOSED SALINE FORMATIONS (ZHOU ET AL., 2008)

As described in detail by Zhou et al. (2008), this is a simple method for assessing the storage capacity of closed and semi-closed storage formations. In this comparison study, only closed systems were considered. The basic principle is that CO_2 injection into these systems will lead pressure build-up, because an additional volume of fluid needs to be stored. The injected CO_2 displaces an equivalent volume of native brine, which may either be stored in the expanded pore space due to compression of the rock, or be stored in the expanded pore space in the seals. The method is designed to provide capacity estimates at early stages of site selection and characterization, when quick assessments of multiple sites may be needed and site characterization data is sparse. More specifically, the estimated pressure increase caused by injection and storage of a specified volume of CO_2 can be compared to a sustainable pressure threshold, which is the maximum pressure that the formation can sustain without geomechanical damage. Alternatively, one may determine the maximum CO_2 volume that can be injected without jeopardizing the geomechanical structure of the formation seal system.

In a closed system for saline formations, the available volume for storage of CO_2 is provided only by the expansion of the pore volume in the formation and seals and the increased brine density in response to pressure buildup in the storage formation. It is implied that in-situ mobile fluids will neither be displaced by the injected CO_2 into distant parts of the same formation or neighboring formations, nor be managed by means of fluid production, treatment, and disposal in accordance with current technical, regulatory, and economic guidelines.

The storage capacity by CO_2 mass for the closed systems ($M_{CO2}(t_I)$) is:

$$M_{CO_2}(t_I) = (\beta_p + \beta_w)\Delta P(t_I)\rho V_f = (\beta_p + \beta_w)\Delta P(t_I)\rho\phi_f AB_f \tag{7}$$

where β_p and β_w are the pore compressibility and native brine compressibility, respectively, ΔP is the sustainable pressure build-up at time t_I, and ρ is the CO_2 density at temperature and pressure of the formation. V_f is the volume of the formation and is equal to the initial porosity (ϕ_f), horizontal area (A), and gross thickness (B_f) of the formation. The storage efficiency (E) in a closed system is derived by simplifying Equation 7.

$$E = (\beta_p + \beta_w)\Delta P(t_I) \tag{8}$$

Reported efficiency factors for saline formations with closed boundaries range between 0.35% and 1% near the CO_2 injection well (Economides and Ehlig-Economides, 2009; Gorecki et al., 2009; Okwen et al., 2010; van de Meer, 1992, 1993, 1995; van de Meer and Egberts, 2008a; van de Meer and Yavuz, 2009; Xie and Economides, 2009; Zhou et al., 2008).

In this comparison effort, the storage resource was calculated stochastically by the Monte Carlo simulation program GoldSim for the method by Zhou et al. (2008) (see **Appendix C** for GoldSim Model description). The parameters, β_p, β_w, ρ ϕ_f, A, and B_f, were treated stochastically assuming the values for each quantity follow a triangular distribution and ΔP was treated deterministically (see **Appendix A** for baseline values for saline formations A through M). CO_2 storage estimates are reported at their 10th, 50th, and 90th percentiles.

3. DESCRIPTION OF SALINE FORMATION DATA SET

A recent publication authored by Szulczewski et al. (2012) provides detailed input parameters regarding saline formations throughout the United States. This data set has been peer-reviewed and is readily available to the public (Szulczewski et al., 2012). Szulczewski et al. (2012) selected rectangular volumes representative of various formations found in the United States that met the following criteria: 1) the depth must exceed 800 m so that CO_2 is stored efficiently as a high-density, supercritical fluid; 2) the aquifer and caprock must be laterally continuous over long distances; and 3) there must be very few faults that could serve as leakage pathways. In the selected rectangular volumes, it was assumed that the caprock is roughly linear ensuring that the CO_2 could be trapped by hydrodynamic, residual, and solubility trapping. Structural trapping, where the CO_2 is trapped at the top of an anticline or in a tilted fault block, and mineral trapping, where dissolved CO_2 reacts with the reservoir rock to form carbonate minerals, were not considered. Select data and formations from Szulczewski et al. (2012) were applied as input parameters for the six methods discussed above. Parameters selected directly from Szulczewski et al. (2012) for comparison of methods for saline formations A through M include the following and are listed in Appendix A: net aquifer thickness (H), length of trapping-model domain (L_T), width of well array (W), porosity (ϕ), CO_2 density (ρ_g), connate water saturation (S_{wc}), aquifer permeability (k_{aq}), surface temperature (T_s), temperature gradient (G_T), depth to the top of the aquifer (D), brine density (ρ_w,), and salinity (s). Formations with salinity less than 1% were omitted in order to concur with drinking water regulations stated by the EPA (EPA, 2010).

The methods by CSLF: Bachu et al. (2007), DOE-NETL Atlas I, II (2007, 2008), DOE-NETL Atlas III, IV (2010, 2012), and Zhou et al. (2008) require gross thickness, while the methods by USGS: Brennan et al. (2010) and Szulczewski et al. (2012) require net thickness. Gross thickness is the mean thickness of the saline formation for which CO_2 storage is assessed within the basin or region defined by the area. Net thickness considers a percentage of the gross thickness that meets a set of minimum standards based on porosity and permeability within the basin or region defined by the area. For methods that use gross thickness, the net thickness percentage is incorporated into the efficiency factor. As described in the U.S. DOE method, net-to-gross thickness efficiency was estimated by Monte Carlo sampling for saline formations based directly on the 10th and 90th percentiles of net-to-gross thickness as reported by IEAGHG (Goodman et al., 2011). Mean net-to-gross thickness efficiency as a function of lithology was calculated to be 0.48 for clastics, 0.41 for dolomite, and 0.35 for limestone formations. Gross thickness (H_g) was estimated by dividing the net thickness for individual saline formations provided in the article by Szulczewski et al. (2012) by net-to gross thickness efficiency (see **Figure 1** and **Appendix A** for information regarding saline formations A through M). Black solid error bar lines represent the minimum and maximum thickness as calculated by the uncertainty analysis provided in the article by Szulczewski et al. (2012).

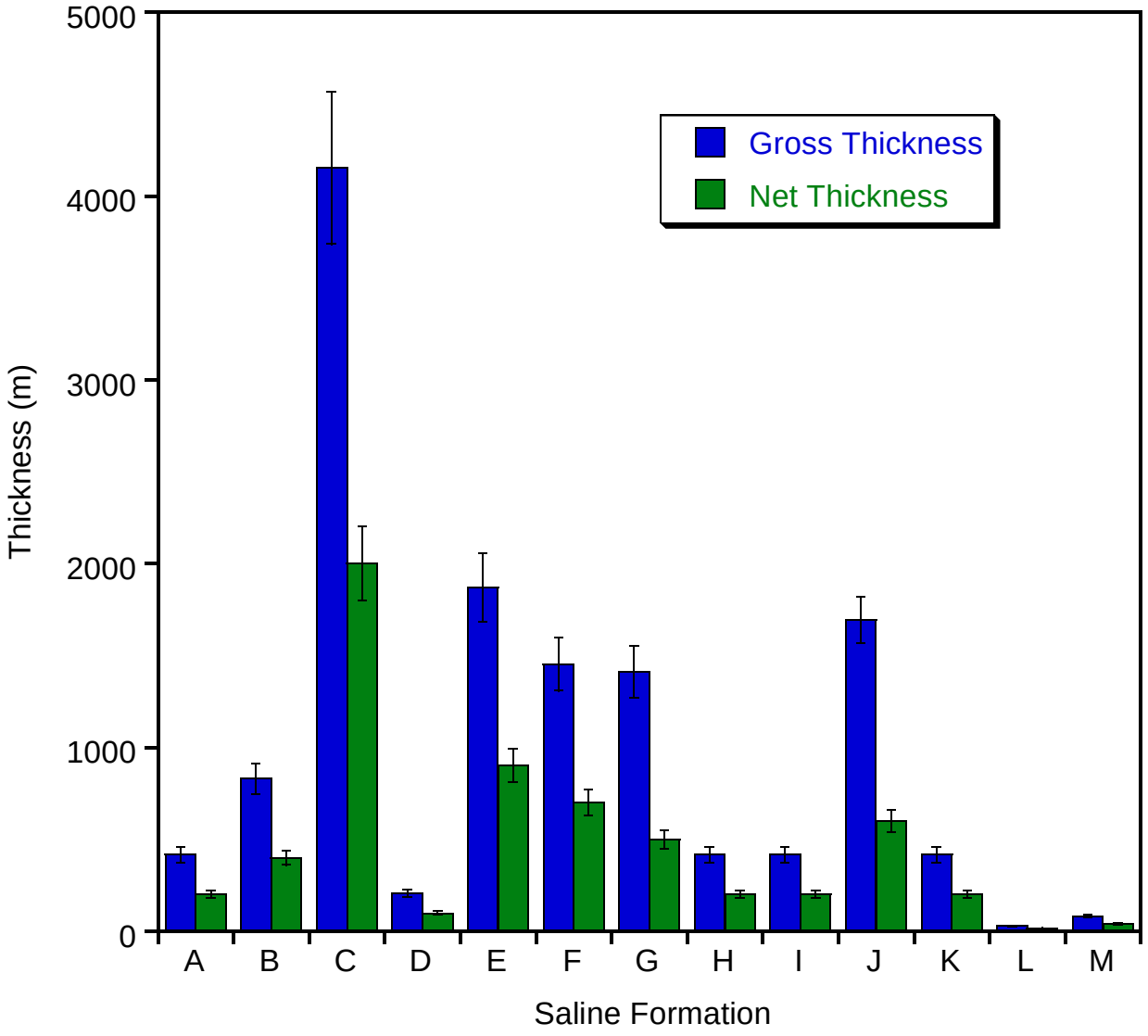

Figure 1. Saline formation net and gross thickness. Green bars: baseline net thickness in meters (m) for individual saline formations directly provided in the article by Szulczewski et al. (2012). Blue bars: baseline gross thickness in meters (m) estimated by dividing the baseline net thickness by a net-to-gross thickness efficiency term. The mean net-to-gross thickness efficiency term as a function of lithology was calculated to be 0.48 for clastics, 0.41 for dolomite, and 0.35 for limestone formations. Black solid error bar lines represent the minimum and maximum thickness as calculated by the uncertainty analysis provided by Szulczewski et al. (2012). See Appendix A for tabulated values for formations A through M.

Pore compressibility, brine compressibility, and sustainable pressure build-up are required by the closed system method authored by Zhou et al. (2008). Pore compressibility (B_p) varies widely depending upon subsurface material. Szulczewski et al. (2012) set an average compressibility for each formation to $1x10^{-10}$ Pa^{-1} because little or no data was available for compressibility of the aquifers and caprocks chosen in their work. The IEAGHG (2009) reported pore compressibility between $2.8x10^{-10}$ Pa^{-1} and $6.9x10^{-10}$ Pa^{-1} as a function of lithology and depositional environment based on numerical simulation and data from the average global database of hydrocarbon reservoir properties. Zhou et al. (2008) reported pore compressibility for deep formations ranging from ($4.5x10^{-11}$ to $4.5x10^{-9}$) Pa^{-1}. Others reported compressibility for sandstones and limestones between ($1x10^{-11}$ and $1x10^{-10}$) Pa^{-1} (Domenico and Schwartz, 1998; Fjar et al., 1991). In this study, pore compressibility (B_p) is set to range between $1x10^{-10}$ Pa^{-1} and $5x10^{-10}$ Pa^{-1}. Brine compressibility (B_w) for each formation was directly calculated as described by Battistelli et al. (1997) while assuming the brine could be represented by a sodium chloride solution. Sustainable pressure build-up refers to a pressure that the storage formation can accommodate without undergoing geo-mechanical damage such as microfracturing and fault reactivation of the sealing structures (Neuzil, 2003). In this study, sustainable pressure build-up (ΔP) was calculated by taking 50% of the initial hydrostatic pressure at the top of the storage formation of interest (see **Appendix A**). The initial hydrostatic pressure was calculated by multiplying the depth at the top of the formation (D) by the hydrostatic pressure gradient for fresh water (0.009792 MPa/m) (Schlumberger, 2012).

4. RESULTS - COMPARISON OF SIX PUBLICLY-AVAILABLE CO_2 STORAGE METHODS TO 13 SALINE FORMATION DATA SETS

4.1 COMPARISON OF ALL METHODS [CSLF: BACHU ET AL. (2007), DOE-NETL ATLAS I, II (2007, 2008), DOE-NETL ATLAS III, IV (2010, 2012), USGS: BRENNAN ET AL. (2010), SZULCZEWSKI ET AL. (2012), AND ZHOU ET AL. (2008)]

The methods by CSLF: Bachu et al. (2007), DOE-NETL Atlas I, II (2007, 2008), DOE-NETL Atlas III, IV (2010, 2012), USGS: Brennan et al. (2010), Szulczewski et al. (2012), and Zhou et al. (2008), were applied to 13 saline formation data sets labeled A-M. Low, middle, and high estimates of CO_2 storage resource for the methods are represented in **Figure 2** for formations A through F and **Figure 3** for formations G through M. Note the change in scale on the y-axis in **Figures 2** and **3**. The specific input parameters for formations A through M are tabulated in **Appendix A**. Location names were not used in order to focus the study on comparing methods and to avoid implying any specific endorsement of this data set. **Figures 2** and **3** allow for direct comparison of estimates of CO_2 storage resource among the methods. The solid multi-color bars represent the middle CO_2 storage resource estimates, which are based on their 50th percentile. The black solid error bars represent low and high estimates of CO_2 storage resource at the 10th and 90th percentiles, respectively.

Low, middle, and high CO_2 storage estimates derived from each method are compiled in **Appendix D**. The methods by CSLF: Bachu et al. (2007), DOE-NETL Atlas III, IV (2010, 2012), and Zhou et al. (2008) produce CO_2 storage resource at the 10th, 50th, and 90th percentiles. The method by DOE-NETL Atlas I, II (2007, 2008) produces CO_2 storage resource values at the 15th, 50th, and 85th percentiles. The method by USGS: Brennan et al. (2010) produces CO_2 storage resource values at the 5th, 50th, and 95th percentiles. The method by Szulczewski et al. (2012) produces a low, baseline, and high storage estimate where one standard deviation is used as an appropriate measure of uncertainty from the probability density function. Because of the assumed normality of the distribution, one standard deviation was taken to be the half-range of the 16th and 84th percentiles of the storage values.

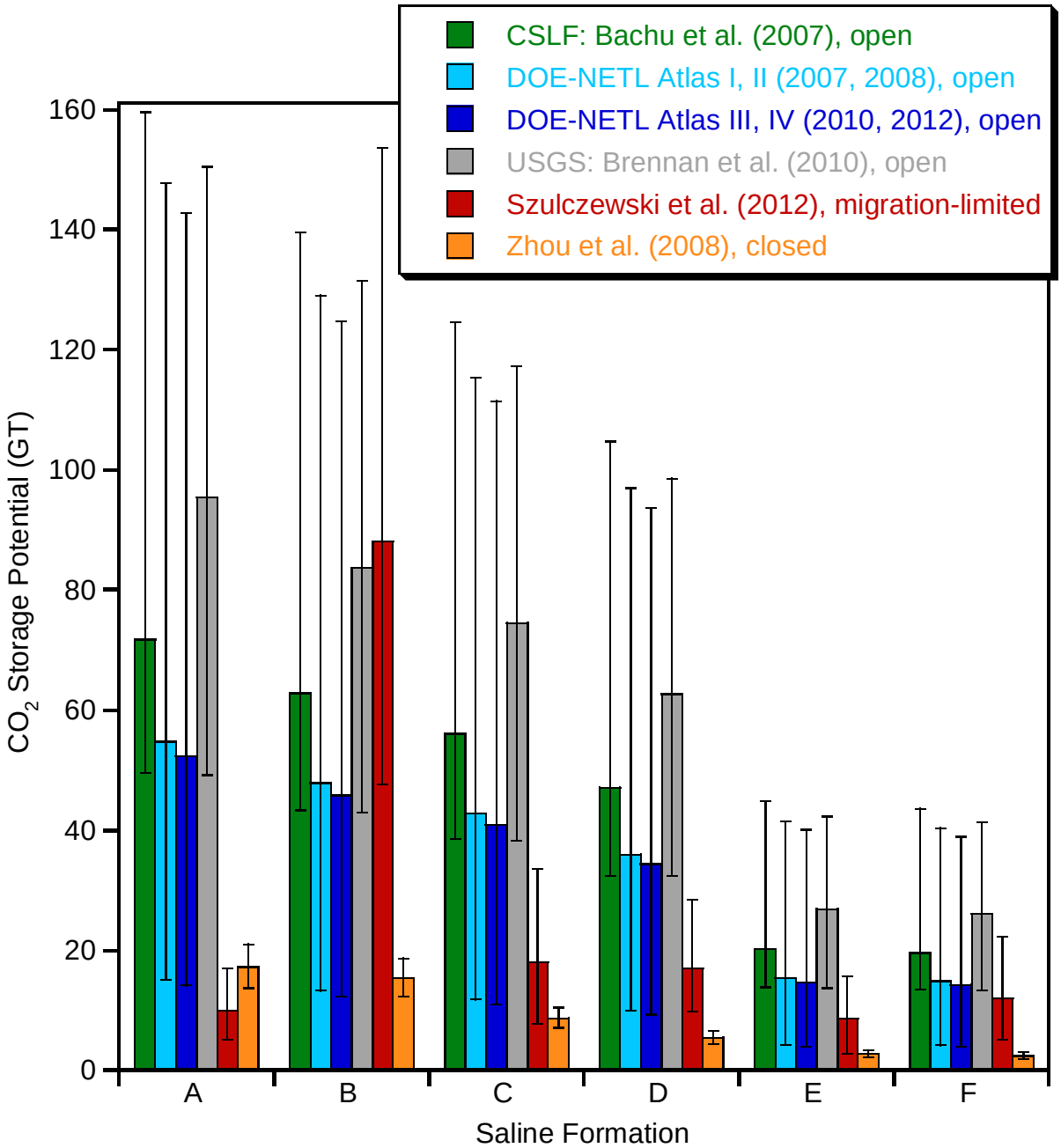

Figure 2. Multi-colored bars represent estimates of CO_2 storage resource in gigatonnes (GT) at the 50th percentile for Formations A through F for the following methods: CSLF: Bachu et al. (2007), DOE-NETL Atlas I, II (2007, 2008), DOE-NETL Atlas III, IV (2010, 2012), USGS: Brennan et al. (2010), Szulczewski et al. (2012), and Zhou et al. (2008). Black solid error bars represent low and high estimates of CO_2 storage resource based on their 10th and 90th percentiles, respectively. See Appendix D for tabulated values for percent probability ranges specifically prescribed by each method.

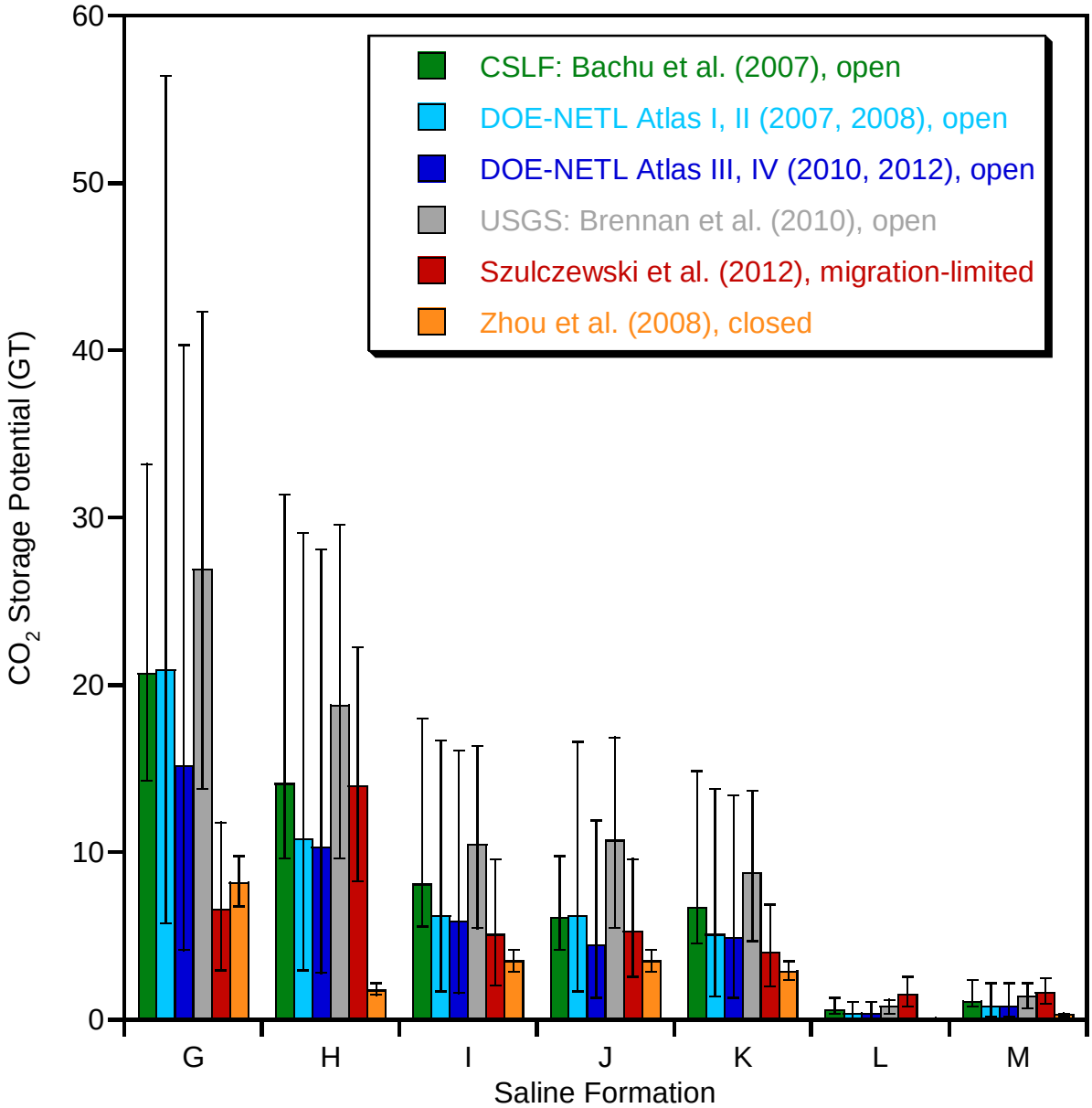

Figure 3. Multi-colored bars represent estimates of CO_2 storage resource in gigatonnes (GT) at the 50th percentile for Formations G through M for the following methods: CSLF: Bachu et al. (2007), DOE-NETL Atlas I, II (2007, 2008), DOE-NETL Atlas III, IV (2010, 2012), USGS: Brennan et al. (2010), Szulczewski et al. (2012), and Zhou et al. (2008). Black solid error bars represent low and high estimates of CO_2 storage resource as represented by their 10th and 90th percentiles, respectively. See Appendix D for tabulated values for percent probability ranges specifically prescribed by each method.

This study attempted to apply uniform input parameters for each method; however, certain methods required some input parameters to be different. Inputs for length, width, porosity, and CO_2 density, for example, were consistently applied for each method. Gross or net thickness was applied as prescribed by the method. In the cases where gross thickness was used, the efficiency factor accounted for the net-to-gross thickness where the fraction of total geologic unit meets the minimum porosity and permeability requirements for injection. In the cases where net thickness was used, the efficiency factor did not account for net-to-gross thickness. As discussed in more detail below, the efficiency term itself was unique to each method.

Aside from these differences, the following general trends were determined for all of the methods [CSLF: Bachu et al. (2007), DOE-NETL Atlas I, II (2007, 2008) and DOE-NETL Atlas III, IV (2010, 2012), USGS: Brennan et al. (2010), Szulczewski et al. (2012), and Zhou et al. (2008)] for the median CO_2 storage resource estimates (i.e. the 50th percentile):

1) The closed-boundary method by Zhou et al. (2008), typically, reports the lowest CO_2 storage resource
2) The open-boundary method by USGS: Brennan et al. (2010), typically, reports the highest CO_2 storage resource
3) In most cases, the migration limited estimates by Szulczewski et al. (2012) are similar to the closed-boundary estimates provided by Zhou et al. (2008) for CO_2 storage resource
4) The open-boundary estimates by CSLF: Bachu et al. (2007), DOE-NETL Atlas I, II (2007, 2008), and DOE-NETL Atlas III, IV (2010, 2012) fall between the open-boundary estimates by USGS: Brennan et al. (2010) and closed-boundary estimates by Zhou et al. (2008) for CO_2 storage resource

In order to compare the methods with more rigor and determine if any of these methods produce statistically significant differences in CO_2 storage resource, a pair-wise comparison of the results obtained from each method was carried out, using the Šidák inequality to control for false positives arising from multiple comparisons (Abdi, 2007). The family-wise confidence level for each set of comparisons for a particular formation was set at the 95% confidence level.

Although more powerful multiple comparison methods, such as control of the false discovery rate (Benjamini and Hochberg, 1995), have been developed recently, the decision to use the Šidák inequality in this report was made because of its ability to be used to compute uncertainty intervals as well as for hypothesis testing and its general applicability for any type of dependence among the parameters studied. The procedure of Benjamini and Hochberg (1995) requires a set of p-values as inputs and therefore is most naturally suited for hypothesis testing. Benjamini and Yekutieli (2005) published a generally-applicable method for controlling the false coverage rate of multiple confidence intervals for selected parameters, but it was not used here since uncertainty intervals for all pair-wise differences of the parameters are reported and no parameter selection has been carried out.

The following methods were compared in pairs: CSLF: Bachu et al. (2007), DOE-NETL Atlas I, II (2007, 2008), DOE-NETL Atlas III, IV (2010, 2012), USGS: Brennan et al. (2010), Szulczewski et al. (2012), and Zhou et al. (2008). This allowed for fifteen different comparison scenarios, or all possible pairs of six methods.

Because the results for each method were computed using stochastic input values generated by the GoldSim Monte Carlo simulation software[1], it seemed natural to compare the results from each method using Monte Carlo simulation as well. The probability distribution for each pair-wise difference between methods was simulated by reading the GoldSim simulation output for each method into the open-source statistical software R (R Development Core Team, 2008) and then computing pair-wise differences. Since the GoldSim output for each method is a vector of 50 000 individual simulated values, the result for each pairwise difference is a vector of 50 000 differences. Quantiles from the distribution of these values were then used to determine an uncertainty interval for each comparison using the Šidák inequality to set the confidence level for each individual interval to achieve the desired family-wise confidence level for all comparisons within each formation.

After obtaining an approximation to the probability distribution for each difference, the values were smoothed using a kernel density estimation procedure with the R function density and plotted, as shown in Appendix F for formations A through M.

This type of uncertainty analysis, based on the propagation of probability distributions, is a standard approach to uncertainty analysis in the measurement science community. The rationale and techniques for this method are laid out in the *Supplement 1 to the Guide to the Expression of Uncertainty in Measurement* written by the Joint Committee on Guides in Metrology (JCGM, 2008).

The R code used to carry out the pair-wise comparison is given in **Appendix E**.

Using this approach, the open-boundary methods in general gave estimates that do not statistically differ from one another at the 95% confidence level. **Figures 4** and **5** and **Table 1** show a combined summary of the pair-wise statistical analysis for formations A through M); the individual pair-wise analyses of formations A through M is compiled in **Appendix F**. In these analyses, a statistically significant result is evident when the difference in the estimated CO_2 storage resource does not contain zero. Statistically different method pairs are highlighted in yellow. In the case for Formation H, for example, the method pairs USGS: Brennan et al. (2010) and Zhou et al. (2008); CSLF: Bachu et al. (2007) and Zhou et al. (2008); and Szulczewski et al. (2012), and Zhou et al. (2008) were found to be statistically different. In the case for Formation G and J, no methods were found to be statistically different. Importantly, the estimates for the open-boundary methods were not found to differ statistically, as mentioned in general above.

[1]The models used to describe the uncertainty in the input values for each method are described in Appendix C.

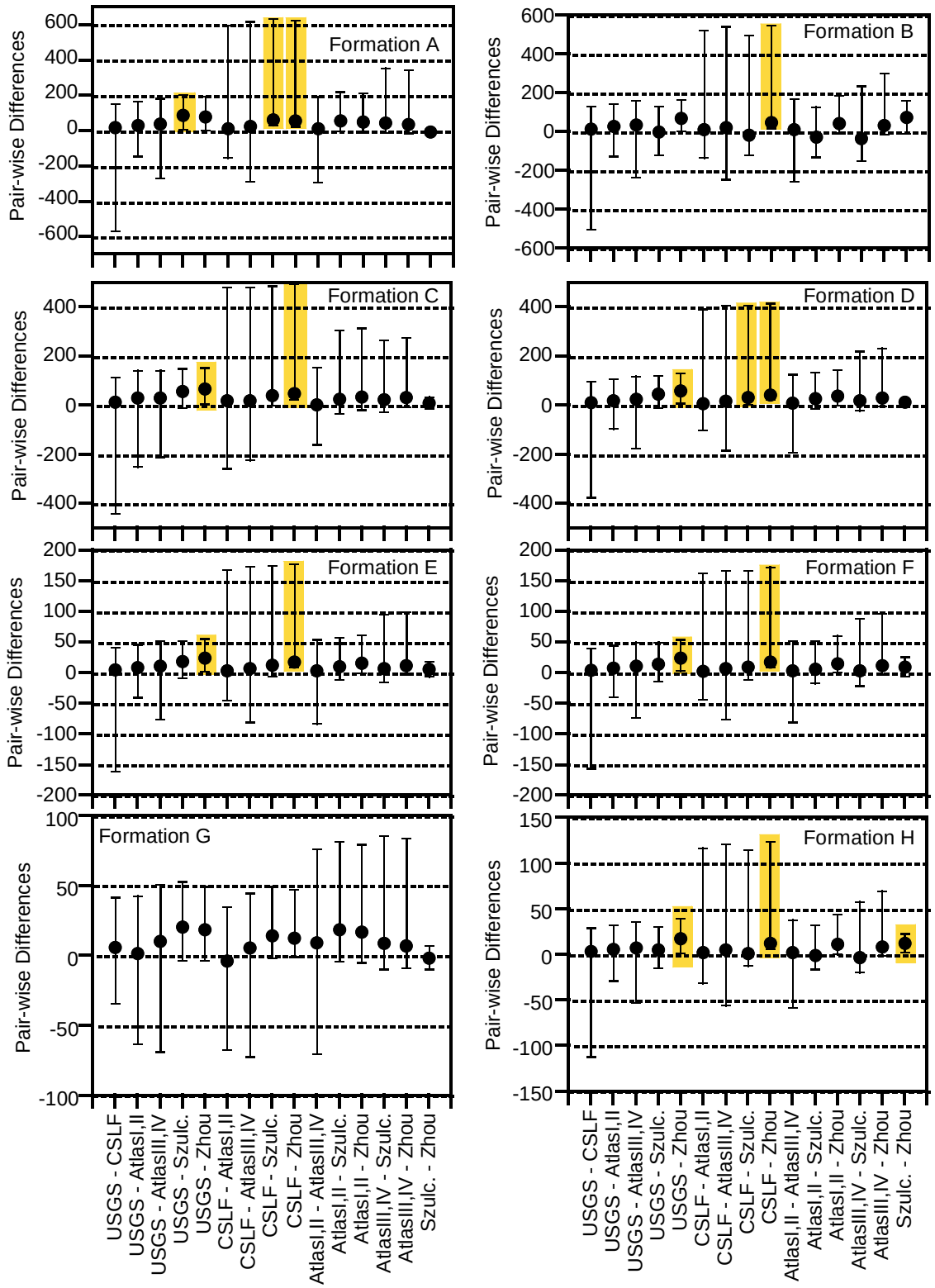

Figure 4. Simultaneous 95% uncertainty interval for all pair-wise differences between all methods for Formations A-H. Statistically different method pairs are highlighted in yellow.

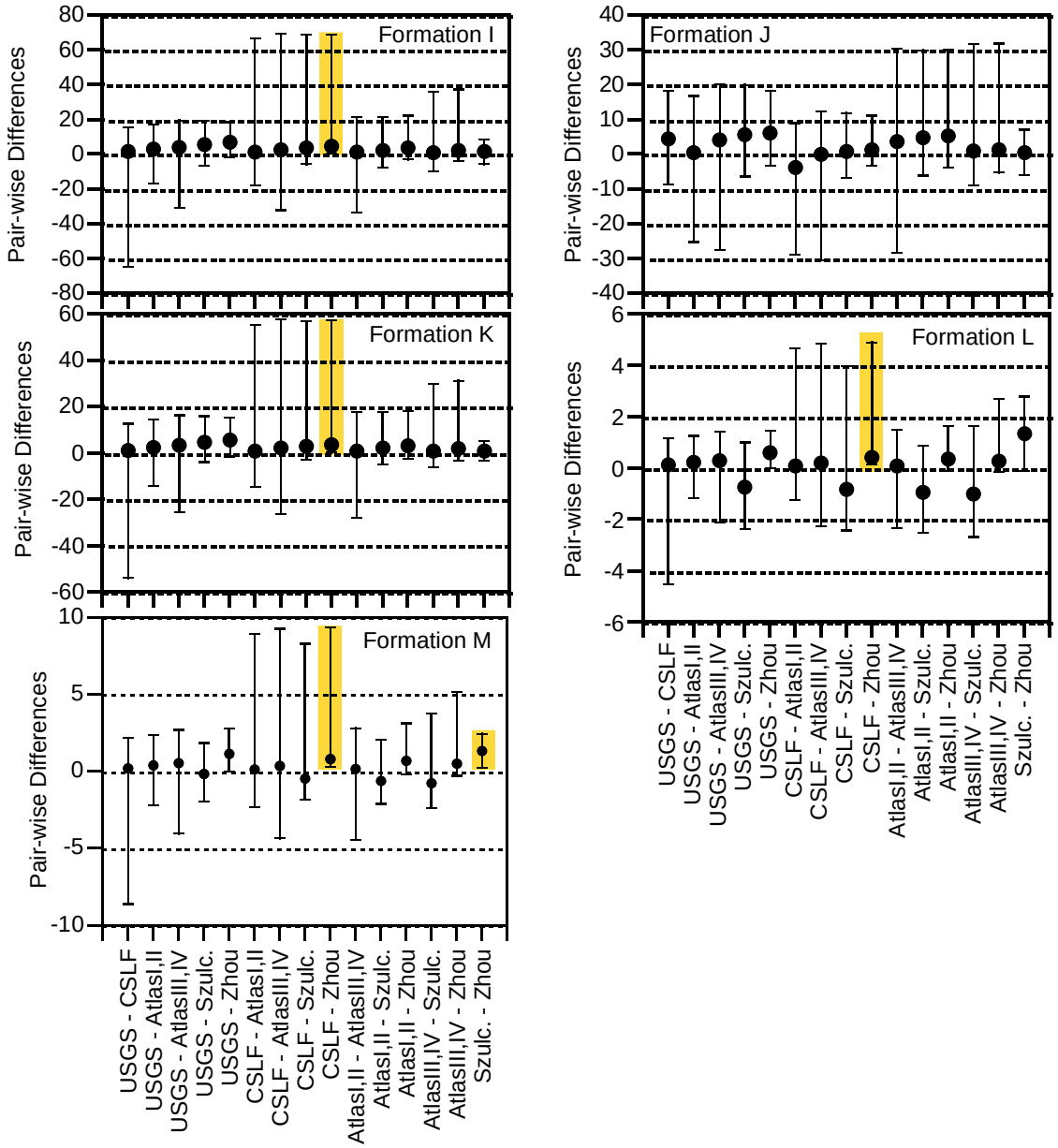

Figure 5. Simultaneous 95% uncertainty interval for all pair-wise differences between all methods for Formations I-M. Statistically different method pairs are highlighted in yellow.

Table 1. Summary of all pair-wise differences between methods at the 95% uncertainty interval for Formations A-M. The crossed boxes (X) represent statistically different method pairs.

	Formation												
Pair-wise Differences	A	B	C	D	E	F	G	H	I	J	K	L	M
USGS - CSLF													
USGS – Atlas I, II													
USGS – Atlas III, IV													
USGS - Szulc.	X												
USGS - Zhou			X	X	X	X		X					
CSLF – Atlas I, II													
CSLF – Atlas III, IV													
CSLF - Szulc.	X	X		X									
CSLF - Zhou	X		X	X	X	X		X	X		X	X	X
Atlas I, II – Atlas III, IV													
Atlas I, II - Szulc.													
Atlas I, II - Zhou													
Atlas III, IV - Szulc.													
Atlas III, IV - Zhou													
Szulc. - Zhou								X					X

Statistical conclusions stemming from a pair-wise comparison of differences in the CO_2 storage resource between different methods at each of the 13 sites, using the Šidák inequality to control for false positives potentially arising from the multiple comparisons within each site, are as follows:

1) For the open-boundary methods, in almost all cases the methods do not differ in a statistically significant way in each of the saline formation cases that were studied
2) Although there are definite differences in the underlying assumptions for open- and closed-boundary methods, for most of the saline formation cases that were studied the variability in underlying parameters was still so great that the estimates of CO_2 storage resource from the closed-boundary method could not be statistically distinguished from

those generated by the open-boundary methods. In some cases, however, the open-boundary methods do give statistically significantly different results when compared to the closed-boundary method.

3) In general, the uncertainty in the underlying parameters has a much greater impact on overall estimates of CO_2 storage resource than the choice of method does, especially within subsets of methods defined by their boundary assumptions.

4.2 COMPARISON OF DOE-NETL ATLAS III, IV (2010, 2012) METHOD WITH THE OTHER METHODS [CSLF: BACHU ET AL. (2007), DOE-NETL ATLAS I, II (2007, 2008), USGS: BRENNAN ET AL. (2010), SZULCZEWSKI ET AL. (2012), AND ZHOU ET AL. (2008)]

A specific analysis of the comparison of the DOE-NETL Atlas III, IV (2010, 2012) method to the other methods is shown in **Figures 6** through **12** for formations A through M. These figures show distributions of the differences in the storage resource estimated by the Atlas III, IV method and each of the other five methods, (a) CSLF, (b) Atlas I, II, (c) USGS, (d) Szulczewski et al., and (e) Zhou et al. In all cases, the uncertainty bounds based on these distributions contain zero at the 95% confidence level, demonstrating that the results from the Atlas III, IV method do not differ statistically from the results from the other methods for this data set. The middle red lines, which indicate the median value for each distribution, provide a measure of how well the methods compare; as can be seen, methods (a) CSLF, (b) Atlas I, II, (c) USGS, and (d) Szulczewski et al., compare very well. A complete set of analyses for the Atlas III, IV method are provided in **Appendix F**.

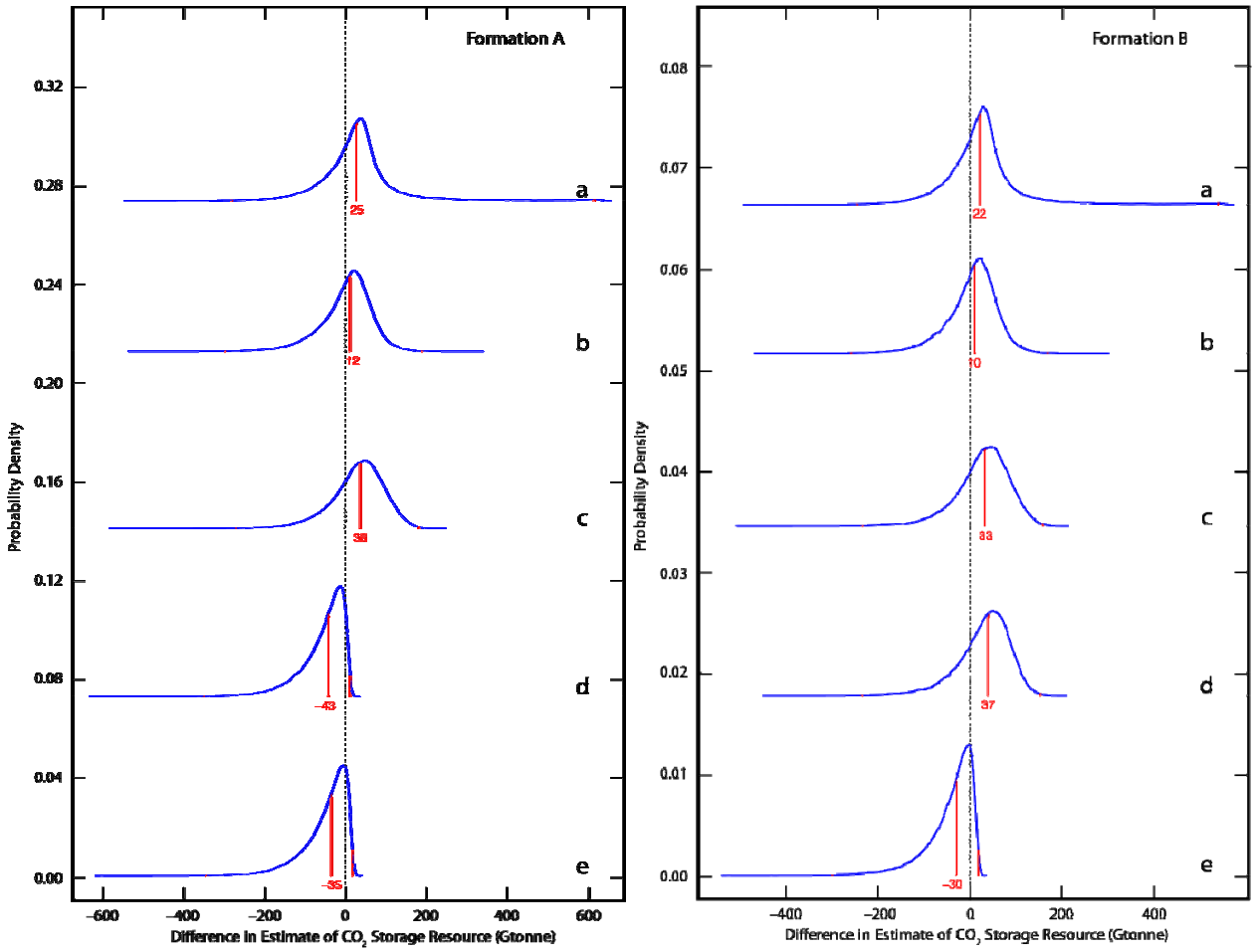

Figure 6. Summary graphs for Formations A and B, comparing the predicted distributions of the pair-wise differences between the method used in the DOE/NETL Atlas III, IV with (a) CSLF, (b) Atlas I, II, (c) USGS, (d) Szulczewski et al., and (e) Zhou et al.

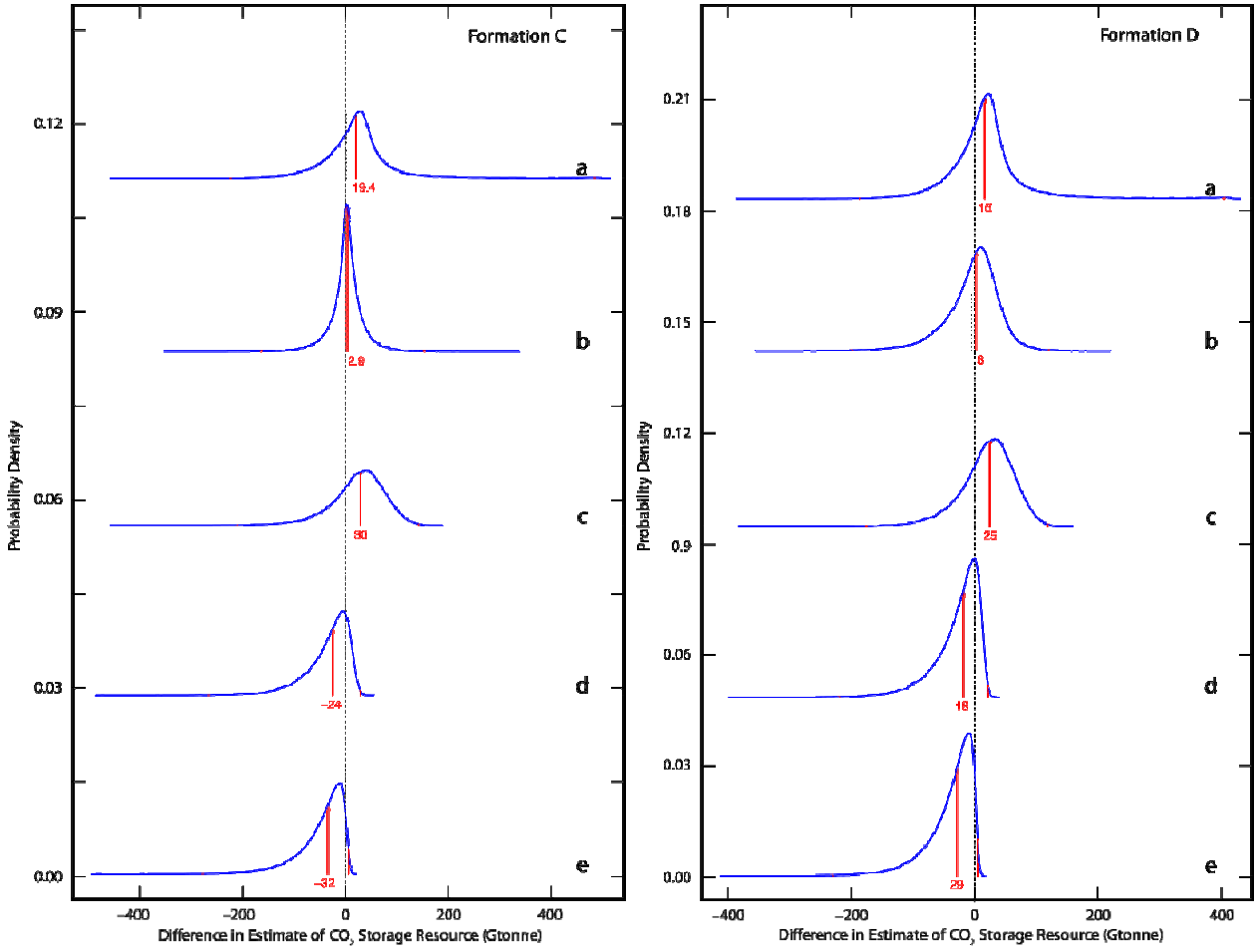

Figure 7. Summary graphs for Formations C and D, comparing the predicted distributions of the pair-wise differences between the method used in the DOE/NETL Atlas III, IV with (a) CSLF, (b) Atlas I, II, (c) USGS, (d) Szulczewski et al., and (e) Zhou et al.

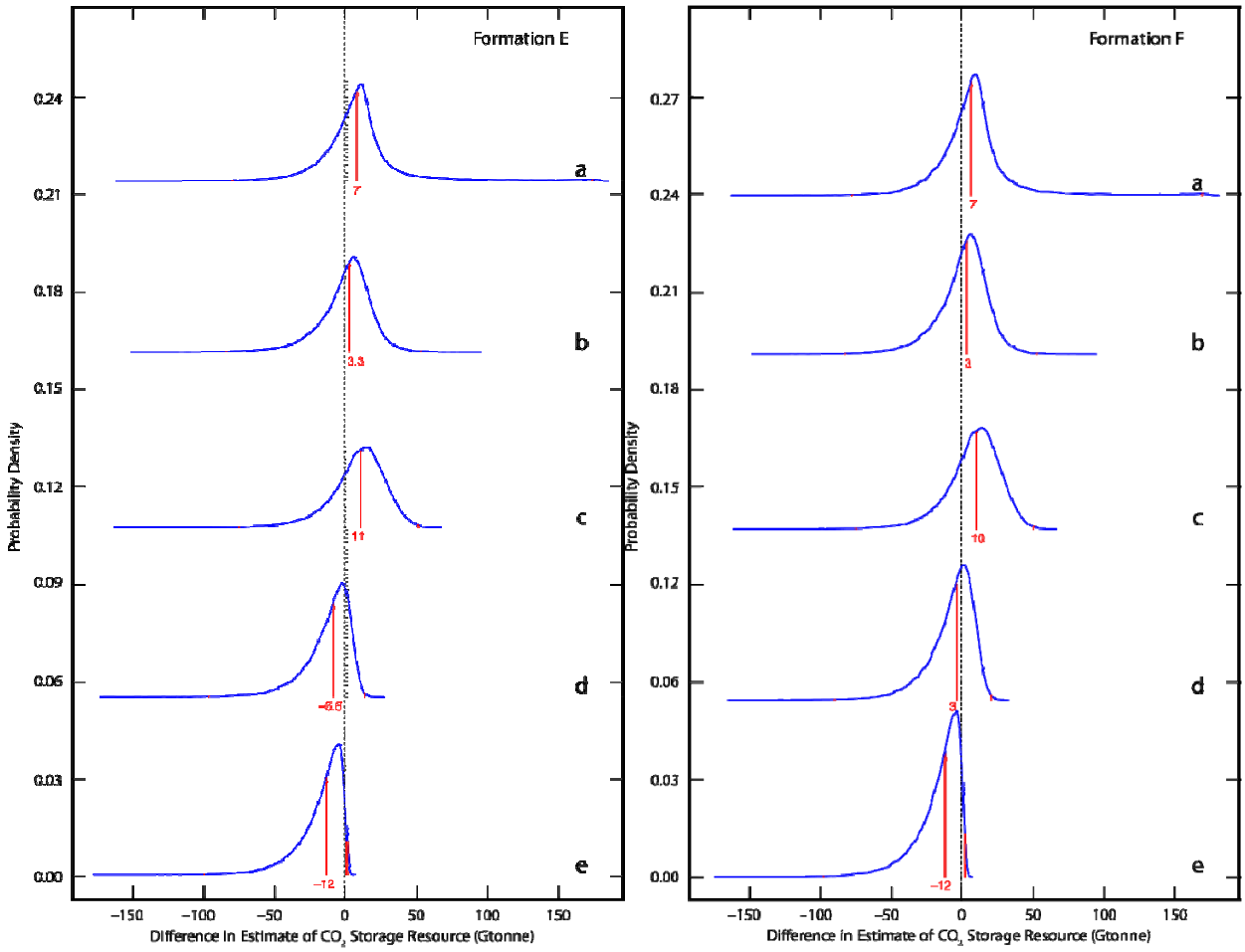

Figure 8. Summary graphs for Formations E and F, comparing the predicted distributions of the pair-wise differences between the method used in the DOE/NETL Atlas III, IV with (a) CSLF, (b) Atlas I, II, (c) USGS, (d) Szulczewski et al., and (e) Zhou et al.

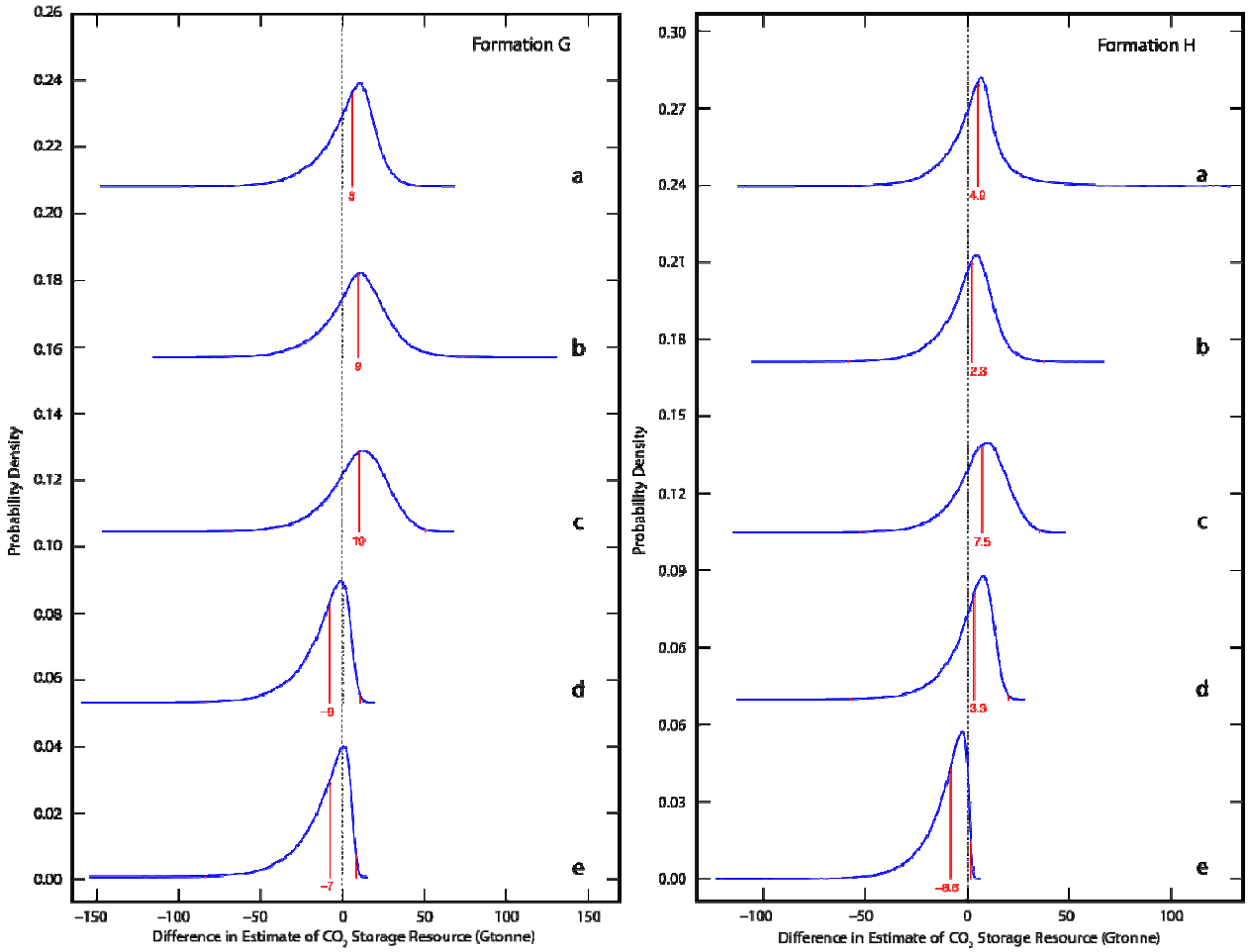

Figure 9. Summary graphs for Formations G and H, comparing the predicted distributions of the pair-wise differences between the method used in the DOE/NETL Atlas III, IV with (a) CSLF, (b) Atlas I, II, (c) USGS, (d) Szulczewski et al., and (e) Zhou et al.

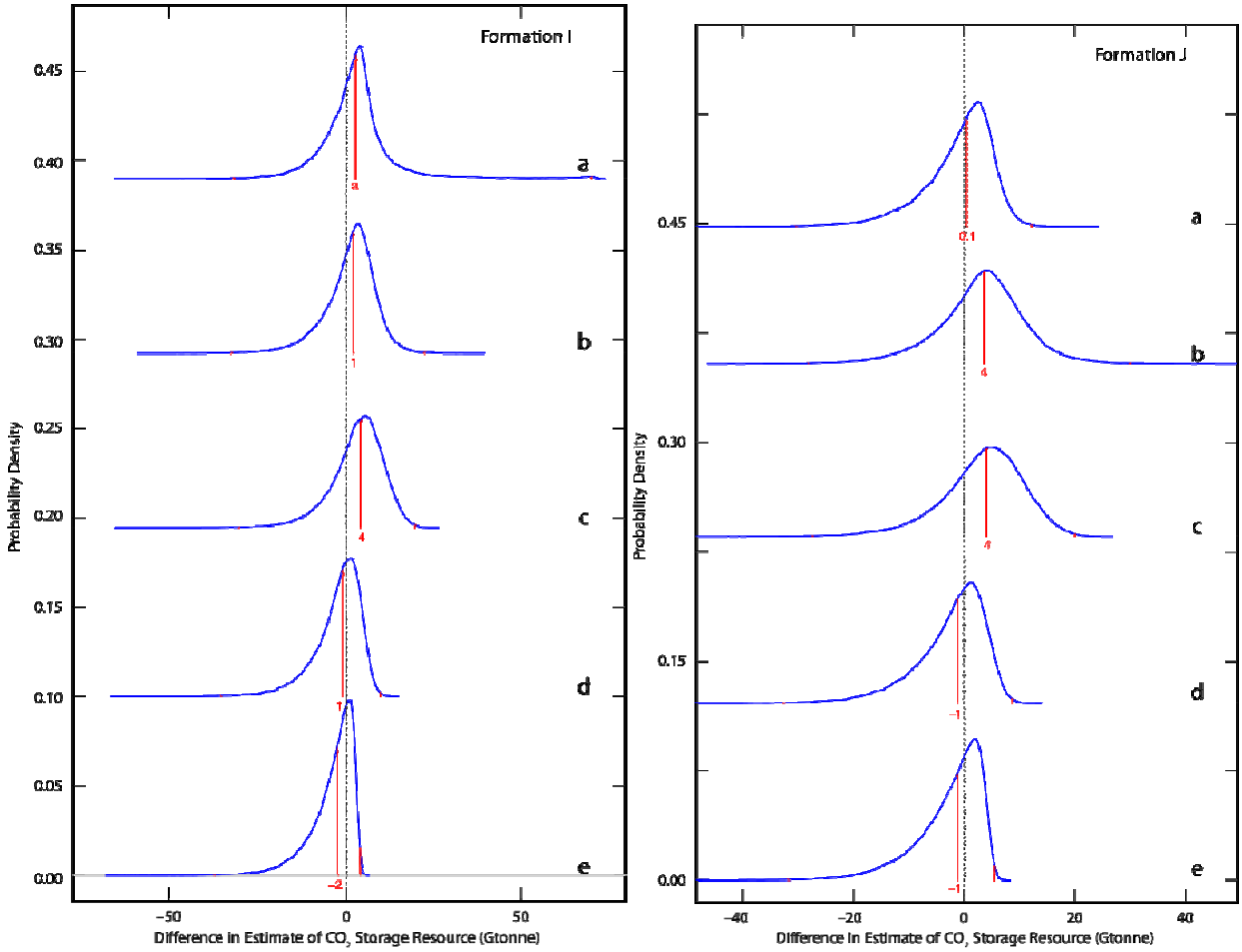

Figure 10. Summary graphs for Formations I and J, comparing the predicted distributions of the pair-wise differences between the method used in the DOE/NETL Atlas III, IV with (a) CSLF, (b) Atlas I, II, (c) USGS, (d) Szulczewski et al., and (e) Zhou et al.

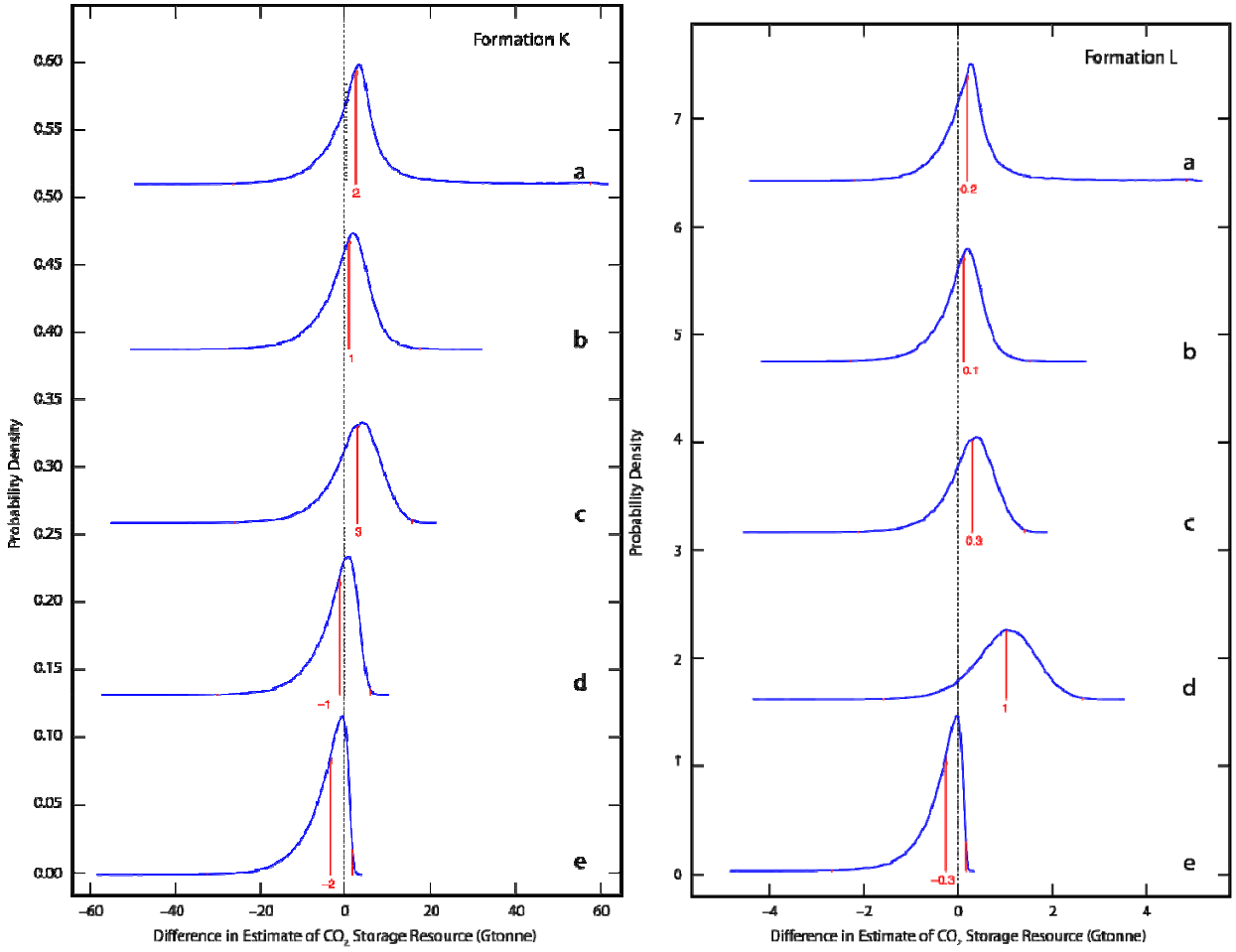

Figure 11. Summary graph for Formations K and L, comparing the predicted distributions of the pair-wise differences between the method used in the DOE/NETL Atlas III, IV with (a) CSLF, (b) Atlas I, II, (c) USGS, (d) Szulczewski et al., and (e) Zhou et al.

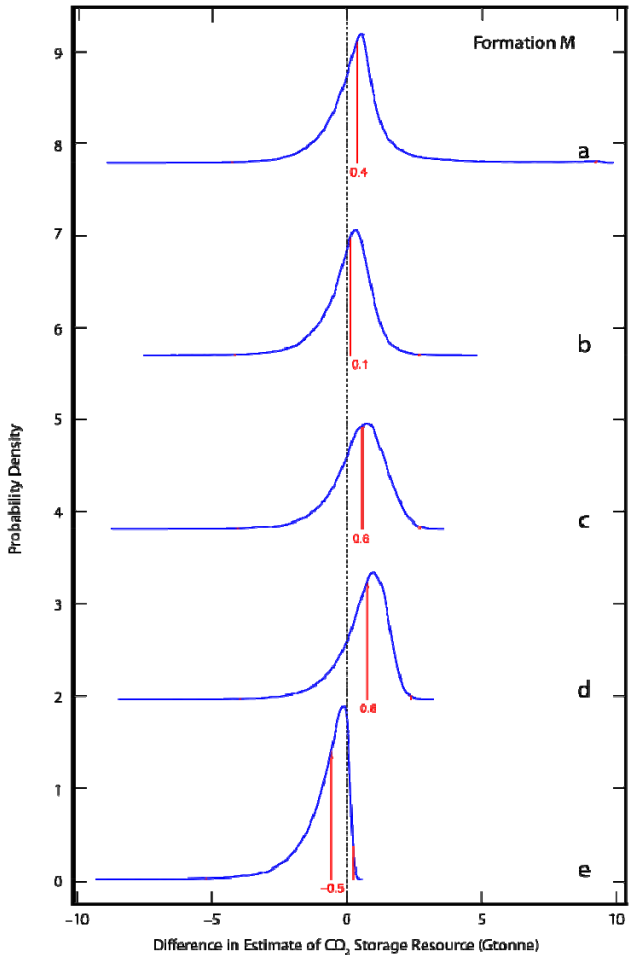

Figure 12. Summary graph for Formations M, comparing the predicted distributions of the pair-wise differences between the method used in the DOE/NETL Atlas III, IV with (a) CSLF, (b) Atlas I, II, (c) USGS, (d) Szulczewski et al., and (e) Zhou et al.

4.3 COMPARISON OF THE CO_2 STORAGE EFFICIENCY FOR ALL METHODS: CSLF: BACHU ET AL. (2007), DOE-NETL ATLAS I, II (2007, 2008), DOE-NETL ATLAS III, IV (2010, 2012), USGS: BRENNAN ET AL. (2010), SZULCZEWSKI ET AL. (2012), AND ZHOU ET AL. (2008)

As discussed previously, efficiency was a uniquely applied by each method. Carbon dioxide storage efficiency gauges the fraction of the accessible pore volume that will be occupied by the injected CO_2. In general, a generic efficiency can be broadly applied to formations of interest or a unique efficiency can be calculated for individual formations. Each method in this comparison effort defines and describes the application of storage efficiency in different ways. In most open boundary methods, the fraction of accessible pore volume is typically estimated by the use of geologic terms: area, thickness, and porosity; and displacement terms: areal, vertical, gravity, and microscopic displacement (Lake, 1989). In closed systems, the fraction of accessible pore volume is estimated by compressibility of the formation, compressibility of the in-situ fluid, and the maximum allowable pressure. Other open and closed boundary methods approximate efficiency with capillary trapping numbers and mobility factors (Szulczewski and Juanes, 2009).

In addition to accessing the fraction of accessible pore volume, the efficiency term also accommodates CO_2 trapping mechanisms, lithology properties, and rock permeability class. For example, structural trapping, while not considered in the data input model by Szulczewski et al. (2009), is incorporated in the efficiency term prescribed by the CSLF: Bachu et al. (2007), DOE-NETL Atlas I, II (2007, 2008), DOE-NETL Atlas III, IV (2010, 2012), USGS: Brennan et al. (2010), and Zhou et al. (2008) methods. While the USGS: Brennan et al. (2010) method offers the flexibility to adjust the percentage of CO_2 structural trapping, the other three methods do not. Hydrodynamic and residual trapping were considered for all methods except by Szulczewski et al. (2012), where only residual and solubility trapping were considered.

Comparison of the CO_2 storage efficiency uniquely applied by each method is not useful because of the wide variety of definitions and rules prescribed by the individual methods for applying efficiency. Thus, we developed the concept of a general efficiency that would allow comparison among all the methods by defining an *overall efficiency* that is equal to the total estimate of CO_2 storage resource predicted by each method divided by the total reservoir pore space available for CO_2 storage specific to each formation.

$$\text{Overall Efficiency} = \frac{\text{Total } CO_2 \text{ Storage Estimate unique to each method (GT)}}{\text{Total Reservoir Pore Space specific to each formation (GT)}} \tag{9}$$

Under this definition, the overall efficiency is normalized and CO_2 storage efficiency can be directly compared amongst the six methods. This then allows us to attribute the differences in estimates of CO_2 storage resource predicted by each method to differences in the efficiency value.

Direct comparisons of low, middle, and high estimates of CO_2 storage efficiency for the methods are represented in **Figures 13** and **14**. The solid multi-color bars represent the median CO_2 storage efficiency values (the 50th percentile). The black solid error bars represent low and high estimates of CO_2 storage efficiency values at the 10th and 90th percentiles, respectively. Low, middle, and high CO_2 storage efficiency prescribed by each method are compiled in **Appendix G**. The methods by CSLF: Bachu et al. (2007), DOE-NETL Atlas III, IV (2010, 2012), and Zhou et al. (2008) produce CO_2 storage efficiency at the 10th, 50th, and 90th percentiles. The method by DOE-NETL Atlas I, II (2007, 2008) produces CO_2 storage efficiency at the 15th, 50th, and 85th

percentiles. The method by USGS: Brennan et al. (2010) produces CO_2 storage efficiency at the 5th, 50th, and 95th percentiles. The method by Szulczewski et al. (2012) produces a low, baseline, and high storage efficiency where one standard deviation is used as an appropriate measure of uncertainty from the probability density function. Because of the assumed normality of the distribution, one standard deviation was taken to be the half-range of the 16th and 84th percentiles of the storage efficiency.

The overall efficiencies for the open system methods CSLF: Bachu et al. (2007), DOE-NETL Atlas I, II (2007, 2008), DOE-NETL Atlas III, IV (2010, 2012), and USGS: Brennan et al. (2010) range between 1.5% and 3.6% at the 50th percentile. The efficiency for the closed system method by Zhou et al. (2008) ranges between 0.3% and 1.2% at the 50th percentile. The efficiency for the method by Szulczewski et al. (2012), which considers migration-limited storage based on the geology of the formation, ranges between 0.4% and 7.2% at the 50th percentile. All values are compiled in **Appendix G**.

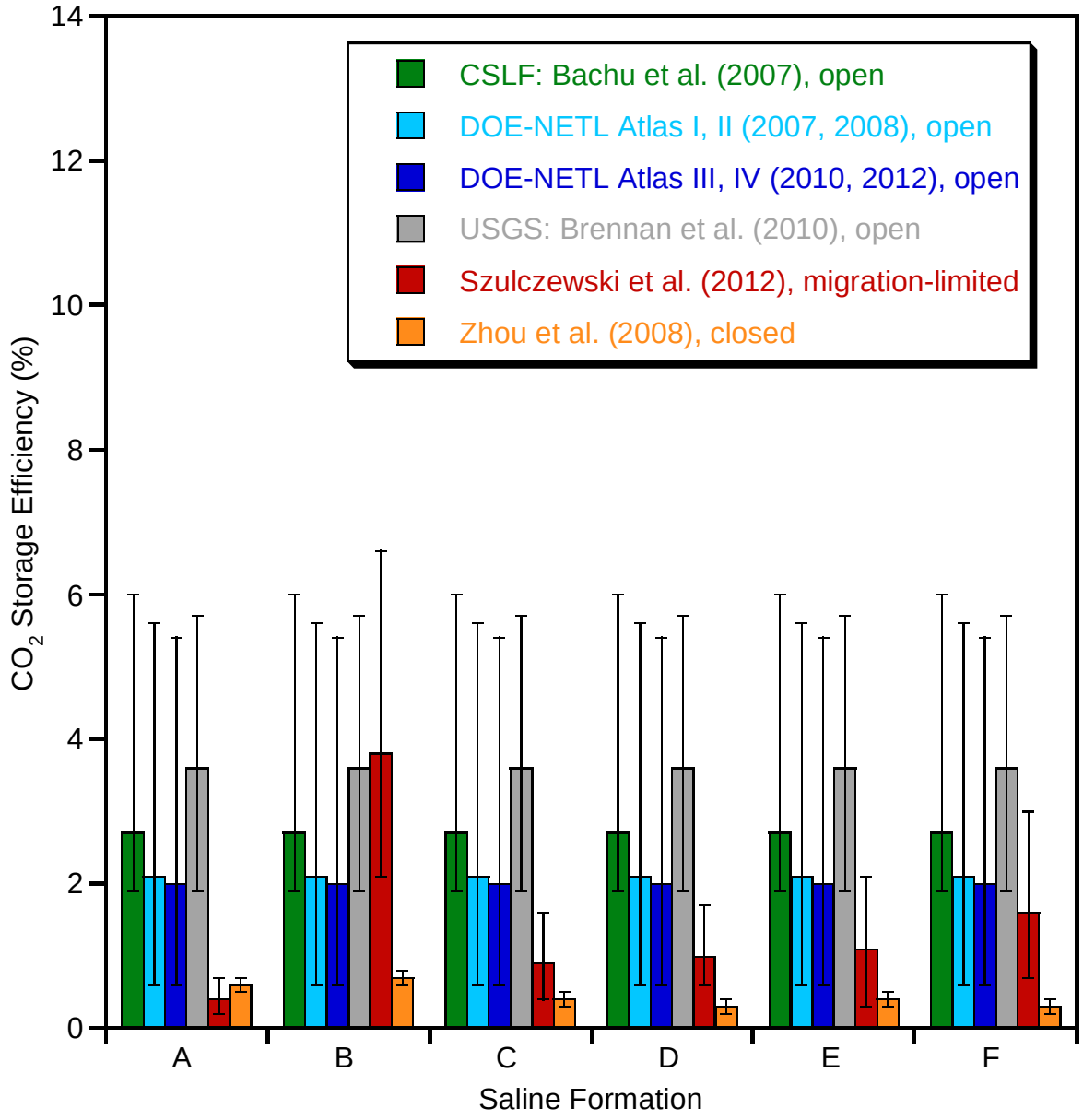

Figure 13. Multi-colored bars represent overall efficiency for CO_2 storage estimates at the 50th percentile for formations A through F for the following methods: CSLF: Bachu et al. (2007), DOE-NETL Atlas I, II (2007, 2008), DOE-NETL Atlas III, IV (2010, 2012), USGS: Brennan et al. (2010), Szulczewski et al. (2012), and Zhou et al. (2008). Black solid error bars represent low and high estimates of overall CO_2 storage efficiency as represented by the 10th and 90th percentiles of overall efficiency, respectively. See Appendix G for tabulated values for percentiles specifically prescribed by each method.

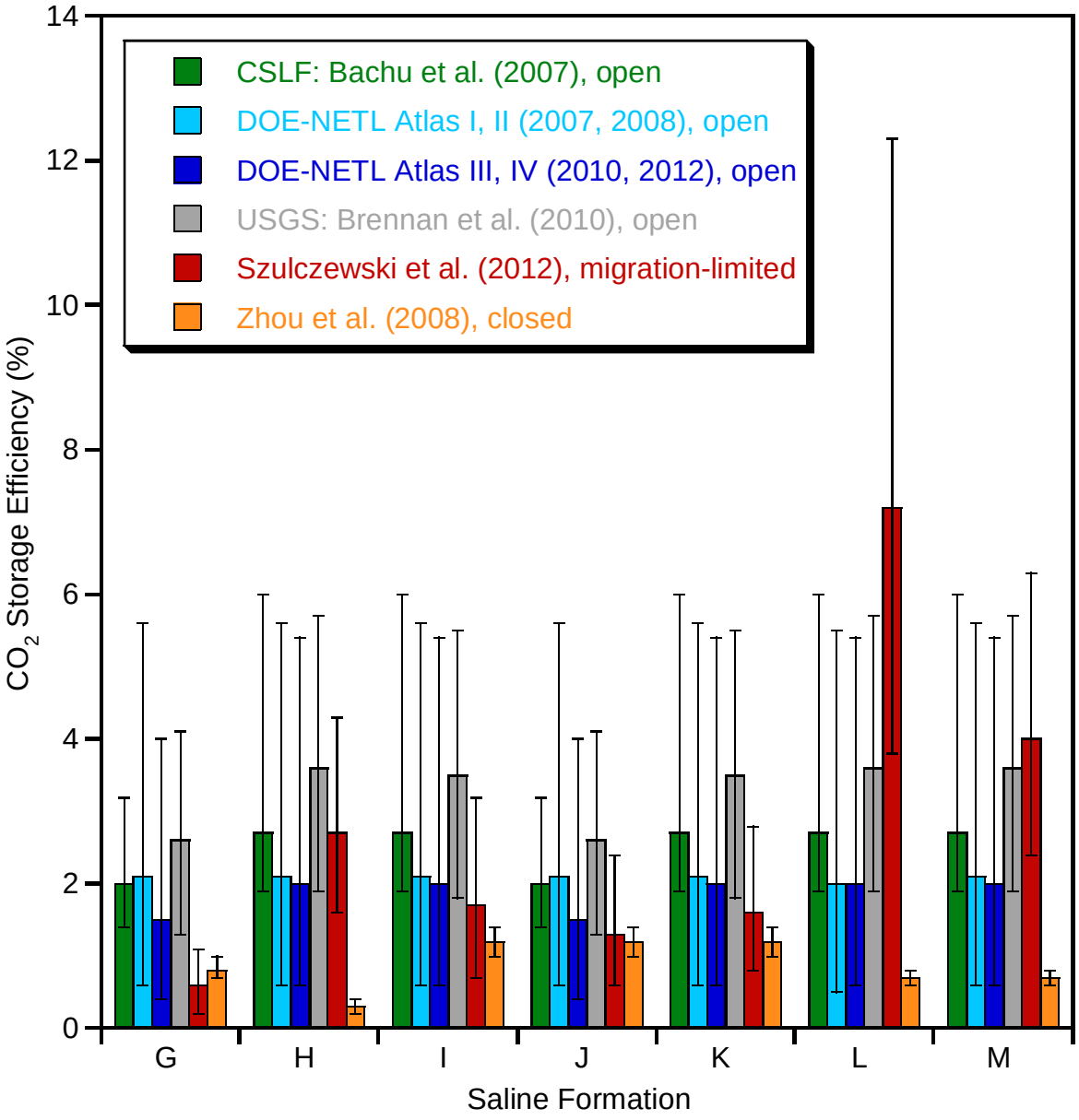

Figure 14. Multi-colored bars represent overall efficiency for CO_2 storage estimates at the 50th percentile for formations G through M for the following methods: CSLF: Bachu et al. (2007), DOE-NETL Atlas I, II (2007, 2008), DOE-NETL Atlas III, IV (2010, 2012), USGS: Brennan et al. (2010), Szulczewski et al. (2012), and Zhou et al. (2008). Black solid error bars represent low and high estimates of overall CO_2 storage efficiency as represented by the 10th and 90th percentiles, respectively. See Appendix G for tabulated values for percentiles specifically prescribed by each method.

5. CONCLUSION

Several different resource estimation methods [CSLF: Bachu et al. (2007); DOE-NETL Atlas I, II (2007, 2008); DOE-NETL Atlas III, IV (2010, 2012); USGS: Brennan et al. (2010); Szulczewski et al. (2012); and Zhou et al. (2008)] were applied to a wide range of different sites. As is typical for these types of estimates for carbon storage in saline fields, the data sets were very sparse. This study attempted to apply uniform input parameters for each method; however, certain methods required some input parameters to be different. Inputs for length, width, porosity, and CO_2 density, for example, were consistently applied for each method. Gross or net thickness was applied as prescribed by the method. The efficiency term was unique to each method.

The following general trends were determined for the methods for the middle CO_2 storage resource estimates, which are based on the 50th percentile:

1) The closed-boundary method by Zhou et al. (2008), typically, reports the lowest CO_2 storage resource
2) The open-boundary method by USGS: Brennan et al. (2010), typically, reports the highest CO_2 storage resource
3) In most cases, the migration limited estimates by Szulczewski et al. (2012) are similar to the closed-boundary estimates provided by Zhou et al. (2008) for CO_2 storage resource
4) The open-boundary estimates by CSLF: Bachu et al. (2007), DOE-NETL Atlas I, II (2007, 2008), and DOE-NETL Atlas III, IV (2010, 2012) typically fall between the open-boundary estimates by USGS: Brennan et al. (2010) and closed-boundary estimates by Zhou et al. (2008) for CO_2 storage resource.

Statistical conclusions stemming from a pair-wise comparison of stochastic inputs using the Šidák inequality to control for false positives arising from this multiple comparison effort are as follows:

1) For the open-boundary methods, in almost all cases the methods do not differ in a statistically significant way in each of the saline formation cases that were studied
2) Although there are definite differences in the underlying assumptions for open- and closed-boundary methods, for most of the saline formation cases that were studied the variability in underlying parameters was still so great that the estimates of CO_2 storage resource from the closed-boundary method could not be statistically distinguished from those generated by the open-boundary methods. In some cases, however, the open-boundary methods do give statistically significantly different results when compared to the closed-boundary method.
3) In general, the uncertainty in the underlying parameters has a much greater impact on overall estimates of CO_2 storage resource than the choice of method does, especially within subsets of methods defined by their boundary assumptions

In a specific analysis of the comparison of the Atlas III, IV method to the other methods:

1) In all cases, the uncertainty bounds based on these distributions contain zero at the 95% confidence level, demonstrating that the results from the Atlas III, IV method do not differ statistically from the results from the other methods for this data set

A direct comparison of the overall efficiency amongst the six methods produced the following storage efficiency ranges:

2) The overall efficiencies for the open system methods [CSLF: Bachu et al. (2007); DOE-NETL Atlas I, II (2007, 2008); DOE-NETL Atlas III, IV (2010, 2012); and USGS: Brennan et al. (2010)] range between 1.5% and 3.6% at the 50th percentile. The efficiency for the closed system method by Zhou et al. (2008) ranges between 0.3% and 1.2% percent at the 50th percentile. The efficiency for the method by Szulczewski et al. (2012), which considers migration-limited storage based on the geology of the formation, ranges between 0.4% and 7.2% at the 50th percentile.

Most of the open system methods gave median results that were well within the uncertainty bounds of the others, suggesting that the uncertainty accounted for within each method is higher than the variability between the methods. Thus, the uncertainty in the underlying parameters has a much greater impact on overall estimates of CO_2 storage resource than uncertainty in the choice of method. Assessments of CO_2 storage potential made with different methods currently can be treated as giving comparable results relative to our typical knowledge of the relevant input values when assessing CO_2 storage potential at a high level.

The closed system estimates were consistently lower than those of the open system methods, but the estimated values from the closed system were also mostly well within the uncertainty bounds of the open system estimates. The fact that the closed methods often give lower results than the open methods suggests that statistically significant differences will ultimately be found in many cases, but maybe not in all cases, as uncertainty in the underlying parameters decreases.

6. REFERENCES

Abdi, H. *The Bonferonni and Šidák Corrections for Multiple Comparisons*; Thousand Oaks, CA, 2007.

Bachu, S.; Bonijoly, D.; Bradshaw, J.; Burruss, R.; Holloway, S.; Christensen, N. P.; Mathiassen, O.M. CO2 storage capacity estimation: methodology and gaps. *International Journal of Greenhouse Gas Control* **2007,** *1*, 430–443.

Battistelli, A.; Calore, C.; Pruess, K. The simulator Tough2/EWASG for Modeling Geothermal Reservoirs with Brines and Non-condensible Gas. *Geothermics* **1997,** *26*, 437–464.

Benjamini, Y.; Hochberg, Y, Controlling the False Discovery Rate: A Practical and Powerful Approach to Multiple Testing. *Journal of the Royal Statistical Society, Series B* **1995,** *57*, 289–300.

Benjamini, Y.; Yekutieli, D. False Discovery Rate-Adjusted Multiple Confidence Intervals for Selected Parameters. *Journal of the American Statistical Association* **2005,** *100*, 71–81.

Birkholzer, J. T.; Zhou, Q. Basin-scale hydrogeologic impacts of CO2 storage: capacity and regulatory implications. *International Journal of Greenhouse Gas Control* **2009,** *3*, 745–756.

Blondes, M. S.; Brennan, S. T.; Merrill, M. D.; Buursink, M. L.; Warwick, P. D.; Cahan, S. M.; Cook, T. A.; Corum, M. D.; Craddock, W. H.; DeVera, C. A.; Drake, R. M.; Drew, L. J.; Freeman, P. A.; Lohr, C. D.; Olea, R. A.; Roberts-Ashby, T. L.; Slucher, E. R.; Varela, B. A. *National assessment of geologic carbon dioxide storage resources–methodology implementation*; U.S. Geological Survey Open-File Report 2013-1055; in press.

Bradshaw, J.; Bachu, S.; Bonijoy, D.; Burruss, R.; Holloway, S.; Christensen, N. P.; Mathiassen, O. M. CO2 storage capacity estimation: issues and development of standards. *International Journal of Greenhouse Gas Control* **2007,** *1*, 62–68.

Brennan, S. T.; Burruss, R. C.; Merrill, M. D.; Freeman, P. A.; Ruppert, L. F. *A Probabilistic Assessment Methodology for the Evaluation of Geologic Carbon Dioxide Storage*; Open-File Report 2010–1127; U.S. Geological Survey, 2010; pp 1–31.

Burruss, R. C.; Brennan, S. T.; Freeman, P. A.; Merrill, M. D.; Ruppert, L. F.; Becker, M. F.; Herkelrath, W. N.; Kharaka, Y. K.; Neuzil, C. E.; Swanson, S. M.; Cook, T. A.; Klett, T. R.; Nelson, P. H.; Schenk, C. J. *Development of a probabilistic assessment methodology for evaluation of carbon dioxide storage*; Open-File Report 2009–1035; U.S. Geological Survey, 2009; pp 1–81.

Dahowski, R.; Li, X.; Davidson, C.; Wei, N.; Dooley, J.; Gentile, R. A Preliminary Cost Curve Assessment of Carbon Dioxide Capture and Storage Potential in China. *Energy Procedia* **2009,** *1*, 2849–2856.

DOE-NETL. *Carbon Sequestration Atlas of the United States and Canada.* U.S. Department of Energy, National Energy Technology Laboratory, Office of Fossil Energy, 2007.

DOE-NETL. *Carbon Sequestration Atlas of the United State and Canada, second edition*. U.S. Department of Energy, National Energy Technology Laboratory, Office of Fossil Energy, 2008.

DOE-NETL. *Carbon Sequestration Atlas of the United State and Canada, third edition.* U.S. Department of Energy, National Energy Technology Laboratory, Office of Fossil Energy, 2010a.

DOE-NETL. *NATCARB.* U.S. Department of Energy, National Energy Technology Laboratory, 2010b. http://www.netl.doe.gov/technologies/carbon_seq/natcarb/

DOE-NETL. *Site Screening, Selection and Characterization for Storage of CO2 in Deep Geologic Formations*. United State Department of Energy: National Energy Technology Laboratory, 2010c. http://www.netl.doe.gov/technologies/carbon_seq/refshelf/BPM-SiteScreening.pdf

DOE-NETL.*The United States 2012 Carbon Utilization and Storage Atlas, fourth edition.* U.S. Deparment of Energy, National Energy Technology Laboratory, Office of Fossil Energy, 2012.

Domenico, P. A.; Schwartz, F. W. *Physical and Chemical Hydrogeology, 2nd edition.* John Wiley & Sons: New York, 1998.

Economides, M. J.; Ehlig-Economides, C. A. *Sequestering carbon dioxide in a closed underground volume*; SPE 124430; 2009; pp 1–9.

EPA. *Safe Drinking Water Act, Office of Ground Water & Drinking Water.* U.S. Environmental Protection Agency, 2010. http://www.epa.gov/safewater/sdwa

Fjar, E.; Holt, R. M.; Horsrud, P.; Raaen, A. M. *Petroleum Related Rock Mechanics*. Elsevier: Amsterdam, 1991.

Garg, A.; Shukla, P. Coal and Energy Security for India: Role of Carbon Dioxide Capture and Storage. *Energy* **2009,** *34*, 1032–1041.

Goodman, A.; Hakala, A.; Bromhal, G.; Deel, D.; Rodosta, T.; Frailey, S.; Small, M.; Allen, D.; Romanov, V.; Fazio, J.; Huerta, N.; McIntyre, D.; Kutchko, B.; Guthrie, G. U.S. DOE methodology for the development of geologic storage potential for carbon dioxide at the national and regional scale. *International Journal of Greenhouse Gas Control* **2011,** *5*, 952–965.

Gorecki, C. D.; Sorensen, J. A.; Bremer, J. M.; Knudsen, D. J.; Smith, S. A.; Steadman, E. N.; Harju, J.A. Development of storage coefficients for determining the effective CO2 storage resource in deep saline formations. Society of Petroleum Engineers International Conference on CO2 Capture, Storage, and Utilization, San Diego, California, 2009; PE 126444-MS-P.

IEAGHG. *Development of Storage Coefficients for CO2 Storage in Deep Saline Formations*; International Energy Agency Greenhouse Gas R&D Programme, 2009.

JCGM. *Evaluation of Measurement Data -Supplement 1 to the "Guide to the Expression of Uncertainty in Measurement" - Propagation of Distributions Using a Monte Carlo Method*; Joint Committee for Guides in Metrology, 2008. http://www.bipm.org/utils/common/documents/jcgm/JCGM_101_2008_E.pdf.

Koide, H.; Tazaki, Y.; Noguchi, Y.; Nakayama, S.; Iijima, M.; Ito, K.; Shindo, Y. Subterranean Containment and Long-term Storage of Carbon Dioxide in Unused Aquifers and in

Depleted Natural Gas Reservoirs. *Energy Conversion and Management* **1992,** *33*, 619–626.

Kopp, A.; Class, H.; Helmig, R. Investigations on CO2 storage capacity in saline aquifers Part 2. Estimation of storage capacity coefficients. *International Journal of Greenhouse Gas Control* **2009,** *3*, 277–287.

Koukouzas, N.; Zigou, F.; Gemeni, V., Preliminary Assessment of CO2 geological Storage Opportunities in Greece. *International Journal of Greenhouse Gas Control* **2009,** *3*, 502–513.

Lake, L.W. *Enhanced Oil Recovery.* Prentice Hall: Englewood Cliffs, NJ, 1989.

Lewis, D.; Bentham, M.; Cleary, T.; Vernon, R.; O'neill, N.; Kirk, K.; Chadwick, A.; Hilditch, D.; Michael, K.; Allinson, G.; Neal, P.; Ho, M. Assessment of the potential for geological storage of carbon dioxide in Ireland and Northern Ireland. *Energy Procedia* **2009,** *1*, 2655–2662.

NACSA. *The North American Carbon Storage Atlas.* This document was prepared as an account of work jointly undertaken by the governments of Canada, Mexico, and the United States, 2012.

Neuzil, C.E. Hydromechanical coupling in geologic processes. *Hydrogeology Journal* **2003,** *11*, 41–83.

Nicot, J.-P. Evaluation of large-scale CO2 storage on fresh-water sections of aquifers: an example from the Texas Gulf Coast Basin. *International Journal of Greenhouse Gas Control* **2008,** *2*, 582–593.

Okwen, R.T.; Stewart, M., T.; Cunningham, J.A. Analytical solution for estimating storage efficiency of geologic sequestration of CO2. *International Journal of Greenhouse Gas Control* **2010,** *4*, 102–107.

R Development Core Team. *R: A Language and Environment for Statistical Computing.* R Foundation for Statistical Computing, Vienna, Austria, 2008. http://www.R-project.org

Radoslaw, T.; Barbara, U.-M.; Adam, W. CO2 Storage Capacity of Deep Aquifers and Hydrocarbon Fields in Poland-EU GeoCapacity Project Results. *Energy Procedia* **2009,** *1*, 2671–2677.

Schlumberger. *Oilfield Glossary*, 2012. http://www.glossary.oilfield.slb.com/

Surridge, A. D.; Cloete, M. Carbon Capture and Storage in South Africa. *Energy Procedia* **2009,** *1*, 2741–2744.

Szulczewski, M.; Juanes, R. A simple but rigorous model for calculating CO2 storage capacity in deep saline aquifers at the basin scale. *Energy Procedia* **2009,** *1*, 3307–3314.

Szulczewski, M.; MacMinn, C. W.; Herzog, H. J.; Juanes, R. Lifetime of carbon capture and storage as a climate-change mitigation technology. Proc. Natl. Acad. Sci. **2012,** *109*, 5185–5189.

Takahashi, T.; Ohsumi, T.; Nakayama, K.; Koide, K.; Miida, H. Estimation of CO2 Aquifer Storage Potential in Japan. *Energy Procedia* **2009,** *1*, 2361–2638.

van de Meer, L. G. H. Investigations Regarding the Storage of Carbon Dioxide in Aquifers in the Netherlands. *Energy Conversion and Management* **1992,** *33*, 611–618.

van de Meer, L. G. H. The conditions limiting CO2 storage in aquifers. *Energy Conversion and Management* **1993,** *34*, 959–966.

van de Meer, L. G. H. The CO2 storage efficiency of aquifers. *Energy Conversion and Management* **1995,** *36*, 513–518.

van de Meer, L. G. H.; Egberts, P. J. P. Calculating subsurface CO2 storage capacities. *The Leading Edge* **2008a,** *27*, 502–505.

van de Meer, L. G. H.; Egberts, P. J. P. A general method for calculating subsurface CO2 storage capacity. Offshore Technology Conference, May 5-8, 2008, Houston, TX, 2008b; OTC 19309, 887–895.

van de Meer, L. G. H.; Yavuz, F. CO2 storage capacity calculations for the Dutch subsurface. *Energy Procedia* **2009,** *1*, 2615–2622.

Xie, X.; Economides, M. J. The impact of carbon geological sequestration. *Journal of Natural Gas Science and Engineering* **2009,** *1*, 103–111.

Zhou, Q.; Birkholzer, J. T.; Tsang, C.-F.; Rutqvist, J. A method for quick assessment of CO2 storage capacity in closed and semi-closed saline formation. *International Journal of Greenhouse Gas Control* **2008,** *2*, 626–639.

APPENDIX A:

Appendix A contains tables with detailed information for Formations A through M (see below).

Baseline values were used directly from Szulczewski et al. (2012). Minimum and maximum values were calculated by the uncertainty analysis provided by Szulczewski et al. (2012).

Gross thickness (H_g) was estimated by dividing the net thickness for individual saline formations provided in the article by Szulczewski et al. (2012) by net-to gross thickness efficiency. As described in the DOE-NETL method, net-to-gross thickness efficiency was estimated by Monte Carlo sampling for saline formations based directly on the P_{10} and P_{90} ranges for net-to-gross thickness as reported by IEAGHG (Goodman et al., 2011). Mean net-to-gross thickness efficiency as a function of lithology was calculated to be 0.48 for clastics, 0.41 for dolomite, and 0.35 for limestone formations.

The irreducible water saturation (S_{wirr}) corresponds to the lowest water saturation that can be achieved in a core plug by displacing the water by oil or gas. The state is usually achieved by flowing oil or gas through a water-saturated sample, or spinning it in a centrifuge to displace the water with oil or gas. The term is somewhat imprecise because the irreducible water saturation is dependent on the final drive pressure when flowing oil or gas or the maximum speed of rotation in a centrifuge. The related term, connate water saturation, is the lowest water saturation found in situ (Schlumberger, 2012). In this study, the value of connate water saturation is used to represent irreducible water saturation.

Sustainable pressure build-up refers to a pressure that the storage formation can accommodate without undergoing geo-mechanical damage such as microfracturing and fault reactivation of the sealing structures (Neuzil, 2003). As discussed by Zhou et al. (2008) , sustainable pressure build-up (ΔP) was calculated by taking 50 % of the initial hydrostatic pressure at the top of the storage formation of interest. The initial hydrostatic pressure was calculated by multiplying the depth at the top of the formation (D) by the hydrostatic pressure gradient for fresh water (0.009792 MPa/m) (Schlumberger, 2012).

Area (A) was calculated by multiplying length of the trapping-model domain (L_T) by net aquifer thickness (H) or gross aquifer thickness (H_{gross}) depending upon what is prescribed by the method.

Table A.1. Formation A

Symbol	Parameters	Units	Formula for Uncertainty	Uncertainty	Minimum	Baseline	Maximum	Source
H	Net aquifer thickness	m	$\psi=\Delta P/P$	0.2	180	200	220	Szulczewski et al. (2012)
L_T	Length of trapping-model domain	m	$\psi=\Delta P/P$	0.1	190000	200000	210000	Szulczewski et al. (2012)
W	Width of well array	m	$\psi=\Delta P/P$	0.2	180000	200000	220000	Szulczewski et al. (2012)
ϕ	Porosity		$\psi=\Delta P/P$	0.1	0.16	0.2	0.24	Szulczewski et al. (2012)
ρ_g	CO_2 density	kg/m^3	ΔP	20	790	800	810	Szulczewski et al. (2012)
S_{wc}	Connate water saturation		ΔP	0.2	0.3	0.4	0.5	Szulczewski et al. (2012)
k_{aq}	Aquifer permeability	mD	Ψ	0.03	93	100	107	Szulczewski et al. (2012)
T_s	Surface temperature	^oC				9		Szulczewski et al. (2012)
G_T	Geothermal gradient	$^oC/km$				20		Szulczewski et al. (2012)
D	depth to top of aquifer	m				2000		Szulczewski et al. (2012)
ρ_w	Brine density	kg/m^3				1000		Szulczewski et al. (2012)
s	Salinity	g/L				200		Szulczewski et al. (2012)
H_{gross}	Gross aquifer thickness	m	$\psi=\Delta P/P$	0.2	374	416	457	calculated in this study
B_p	Pore compressibility	Pa^{-1}			1E-10	3E-10	5E-10	calculated in this study
B_w	Brine compressibility	Pa^{-1}			3.5E-10	3.5E-10	3.6E-10	Battistelli et al. (1997)
G_P	Pressure gradient for fresh water	MPa/m				0.009792		Schlumberger Oilfield Glossary
P	Hydrostatic pressure	MPa				20		calculated in this study
ΔP	Sustainable pressure buildup	Mpa				10		calculated in this study

Table A.2. Formation B

Symbol	Parameters	Units	Formula for Uncertainty	Uncertainty	Minimum	Baseline	Maximum	Source
H	Net aquifer thickness	m	$\psi=\Delta P/P$	0.2	360	400	440	Szulczewski et al. (2012)
L_T	Length of trapping-model domain	m	$\psi=\Delta P/P$	0.1	95000	100000	105000	Szulczewski et al. (2012)
W	Width of well array	m	$\psi=\Delta P/P$	0.1	190000	200000	210000	Szulczewski et al. (2012)
ϕ	Porosity		$\psi=\Delta P/P$	0.4	0.16	0.2	0.24	Szulczewski et al. (2012)
ρ_g	CO_2 density	kg/m^3	ΔP	20	690	700	710	Szulczewski et al. (2012)
S_{wc}	Connate water saturation		ΔP	0.2	0.3	0.4	0.5	Szulczewski et al. (2012)
k_{aq}	Aquifer permeability	mD	Ψ	0.03	93	100	107	Szulczewski et al. (2012)
T_s	Surface temperature	^oC				10		Szulczewski et al. (2012)
G_T	Geothermal gradient	$^oC/km$				20		Szulczewski et al. (2012)
D	depth to top of aquifer	m				2000		Szulczewski et al. (2012)
ρ_w	Brine density	kg/m^3				1000		Szulczewski et al. (2012)
s	Salinity	g/L				100		Szulczewski et al. (2012)
H_{gross}	Gross aquifer thickness	m	$\psi=\Delta P/P$	0.2	748	831	914	calculated in this study
B_p	Pore compressibility	Pa^{-1}			1E-10	3E-10	5E-10	calculated in this study
B_w	Brine compressibility	Pa^{-1}			3.6E-10	3.7E-10	3.8E-10	Battistelli et al. (1997)
G_P	Pressure gradient for fresh water	MPa/m				0.009792		Schlumberger Oilfield Glossary
P	Hydrostatic pressure	MPa				20		calculated in this study
ΔP	Sustainable pressure buildup	Mpa				10		calculated in this study

Table A.3. Formation C

Symbol	Parameters	Units	Formula for Uncertainty	Uncertainty	Minimum	Baseline	Maximum	Source
H	Net aquifer thickness	m	$\psi=\Delta P/P$	0.2	1800	2000	2200	Szulczewski et al. (2012)
L_T	Length of trapping-model domain	m	$\psi=\Delta P/P$	0.1	47500	50000	52500	Szulczewski et al. (2012)
W	Width of well array	m	$\psi=\Delta P/P$	0.1	95000	100000	105000	Szulczewski et al. (2012)
ϕ	Porosity		$\psi=\Delta P/P$	0.4	0.16	0.2	0.24	Szulczewski et al. (2012)
ρ_g	CO_2 density	kg/m^3	ΔP	20	490	500	510	Szulczewski et al. (2012)
S_{wc}	Connate water saturation		ΔP	0.2	0.3	0.4	0.5	Szulczewski et al. (2012)
k_{aq}	Aquifer permeability	mD	Ψ	0.03	366	400	438	Szulczewski et al. (2012)
T_s	Surface temperature	^oC				20		Szulczewski et al. (2012)
G_T	Geothermal gradient	$^oC/km$				30		Szulczewski et al. (2012)
D	depth to top of aquifer	m				1000		Szulczewski et al. (2012)
ρ_w	Brine density	kg/m^3				1000		Szulczewski et al. (2012)
s	Salinity	g/L				50		Szulczewski et al. (2012)
H_{gross}	Gross aquifer thickness	m	$\psi=\Delta P/P$	0.2	3740	4156	4572	calculated in this study
B_p	Pore compressibility	Pa^{-1}			1E-10	3E-10	5E-10	calculated in this study
B_w	Brine compressibility	Pa^{-1}			3.9E-10	5.1E-10	7.2E-10	Battistelli et al. (1997)
G_P	Pressure gradient for fresh water	MPa/m				0.009792		Schlumberger Oilfield Glossary
P	Hydrostatic pressure	MPa				10		calculated in this study
ΔP	Sustainable pressure buildup	Mpa				5		calculated in this study

Table A.4. Formation D

Symbol	Parameters	Units	Formula for Uncertainty	Uncertainty	Minimum	Baseline	Maximum	Source
H	Net aquifer thickness	m	$\psi=\Delta P/P$	0.2	90	100	110	Szulczewski et al. (2012)
L_T	Length of trapping-model domain	m	$\psi=\Delta P/P$	0.1	285000	300000	315000	Szulczewski et al. (2012)
W	Width of well array	m	$\psi=\Delta P/P$	0.1	190000	200000	210000	Szulczewski et al. (2012)
ϕ	Porosity		$\psi=\Delta P/P$	0.4	0.16	0.2	0.24	Szulczewski et al. (2012)
ρ_g	CO_2 density	kg/m^3	ΔP	20	690	700	710	Szulczewski et al. (2012)
S_{wc}	Connate water saturation		ΔP	0.2	0.3	0.4	0.5	Szulczewski et al. (2012)
k_{aq}	Aquifer permeability	mD	Ψ	0.03	93	100	107	Szulczewski et al. (2012)
T_s	Surface temperature	^oC				10		Szulczewski et al. (2012)
G_T	Geothermal gradient	$^oC/km$				20		Szulczewski et al. (2012)
D	depth to top of aquifer	m				1000		Szulczewski et al. (2012)
ρ_w	Brine density	kg/m^3				1000		Szulczewski et al. (2012)
s	Salinity	g/L				200		Szulczewski et al. (2012)
H_{gross}	Gross aquifer thickness	m	$\psi=\Delta P/P$	0.2	187	208	229	calculated in this study
B_p	Pore compressibility	Pa^{-1}			1E-10	3E-10	5E-10	calculated in this study
B_w	Brine compressibility	Pa^{-1}			3.3E-10	3.3E-10	3.4E-10	Battistelli et al. (1997)
G_P	Pressure gradient for fresh water	MPa/m				0.009792		Schlumberger Oilfield Glossary
P	Hydrostatic pressure	MPa				10		calculated in this study
ΔP	Sustainable pressure buildup	Mpa				5		calculated in this study

Table A.5. Formation E

Symbol	Parameters	Units	Formula for Uncertainty	Uncertainty	Minimum	Baseline	Maximum	Source
H	Net aquifer thickness	m	$\psi=\Delta P/P$	0.2	810	900	990	Szulczewski et al. (2012)
L_T	Length of trapping-model domain	m	$\psi=\Delta P/P$	0.1	38000	40000	42000	Szulczewski et al. (2012)
W	Width of well array	m	$\psi=\Delta P/P$	0.1	95000	100000	105000	Szulczewski et al. (2012)
ϕ	Porosity		$\psi=\Delta P/P$	0.4	0.16	0.2	0.24	Szulczewski et al. (2012)
ρ_g	CO_2 density	kg/m^3	ΔP	20	490	500	510	Szulczewski et al. (2012)
S_{wc}	Connate water saturation		ΔP	0.2	0.3	0.4	0.5	Szulczewski et al. (2012)
k_{aq}	Aquifer permeability	mD	Ψ	0.03	366	400	438	Szulczewski et al. (2012)
T_s	Surface temperature	^oC				20		Szulczewski et al. (2012)
G_T	Geothermal gradient	$^oC/km$				30		Szulczewski et al. (2012)
D	depth to top of aquifer	m				1000		Szulczewski et al. (2012)
ρ_w	Brine density	kg/m^3				1000		Szulczewski et al. (2012)
s	Salinity	g/L				50		Szulczewski et al. (2012)
H_{gross}	Gross aquifer thickness	m	$\psi=\Delta P/P$	0.2	1683	1870	2057	calculated in this study
B_p	Pore compressibility	Pa^{-1}			1E-10	3E-10	5E-10	calculated in this study
B_w	Brine compressibility	Pa^{-1}			3.9E-10	4.4E-10	5.0E-10	Battistelli et al. (1997)
G_P	Pressure gradient for fresh water	MPa/m				0.009792		Schlumberger Oilfield Glossary
P	Hydrostatic pressure	MPa				10		calculated in this study
ΔP	Sustainable pressure buildup	Mpa				5		calculated in this study

Table A.6. Formation F

Symbol	Parameters	Units	Formula for Uncertainty	Uncertainty	Minimum	Baseline	Maximum	Source
H	Net aquifer thickness	m	$\psi=\Delta P/P$	0.2	630	700	770	Szulczewski et al. (2012)
L_T	Length of trapping-model domain	m	$\psi=\Delta P/P$	0.1	47500	50000	52500	Szulczewski et al. (2012)
W	Width of well array	m	$\psi=\Delta P/P$	0.1	95000	100000	105000	Szulczewski et al. (2012)
ϕ	Porosity		$\psi=\Delta P/P$	0.4	0.16	0.2	0.24	Szulczewski et al. (2012)
ρ_g	CO_2 density	kg/m^3	ΔP	20	490	500	510	Szulczewski et al. (2012)
S_{wc}	Connate water saturation		ΔP	0.2	0.3	0.4	0.5	Szulczewski et al. (2012)
k_{aq}	Aquifer permeability	mD	Ψ	0.03	366	400	438	Szulczewski et al. (2012)
T_s	Surface temperature	^oC				20		Szulczewski et al. (2012)
G_T	Geothermal gradient	$^oC/km$				30		Szulczewski et al. (2012)
D	depth to top of aquifer	m				1000		Szulczewski et al. (2012)
ρ_w	Brine density	kg/m^3				1000		Szulczewski et al. (2012)
s	Salinity	g/L				100		Szulczewski et al. (2012)
H_{gross}	Gross aquifer thickness	m	$\psi=\Delta P/P$	0.2	1309	1455	1600	calculated in this study
B_p	Pore compressibility	Pa^{-1}			1E-10	3E-10	5E-10	calculated in this study
B_w	Brine compressibility	Pa^{-1}			3.6E-10	3.8E-10	4.1E-10	Battistelli et al. (1997)
G_P	Pressure gradient for fresh water	MPa/m				0.009792		Schlumberger Oilfield Glossary
P	Hydrostatic pressure	MPa				10		calculated in this study
ΔP	Sustainable pressure buildup	Mpa				5		calculated in this study

Table A.7. Formation G

Symbol	Parameters	Units	Formula for Uncertainty	Uncertainty	Minimum	Baseline	Maximum	Source
H	Net aquifer thickness	m	$\psi=\Delta P/P$	0.2	450	500	550	Szulczewski et al. (2012)
L_T	Length of trapping-model domain	m	$\psi=\Delta P/P$	0.1	85500	90000	94500	Szulczewski et al. (2012)
W	Width of well array	m	$\psi=\Delta P/P$	0.1	190000	200000	210000	Szulczewski et al. (2012)
ϕ	Porosity		$\psi=\Delta P/P$	0.4	0.064	0.08	0.096	Szulczewski et al. (2012)
ρ_g	CO_2 density	kg/m^3	ΔP	20	490	500	510	Szulczewski et al. (2012)
S_{wc}	Connate water saturation		ΔP	0.2	0.3	0.4	0.5	Szulczewski et al. (2012)
k_{aq}	Aquifer permeability	mD	Ψ	0.03	56	60	64	Szulczewski et al. (2012)
T_s	Surface temperature	^oC				6		Szulczewski et al. (2012)
G_T	Geothermal gradient	$^oC/km$				40		Szulczewski et al. (2012)
D	depth to top of aquifer	m				3000		Szulczewski et al. (2012)
ρ_w	Brine density	kg/m^3				1000		Szulczewski et al. (2012)
s	Salinity	g/L				200		Szulczewski et al. (2012)
H_{gross}	Gross aquifer thickness	m	$\psi=\Delta P/P$	0.2	1271	1412	1553	calculated in this study
B_p	Pore compressibility	Pa^{-1}			1E-10	3E-10	5E-10	calculated in this study
B_w	Brine compressibility	Pa^{-1}			4.7E-10	5.1E-10	5.7E-10	Battistelli et al. (1997)
G_P	Pressure gradient for fresh water	MPa/m				0.009792		Schlumberger Oilfield Glossary
P	Hydrostatic pressure	MPa				20		calculated in this study
ΔP	Sustainable pressure buildup	Mpa				10		calculated in this study

Table A.8. Formation H

Symbol	Parameters	Units	Formula for Uncertainty	Uncertainty	Minimum	Baseline	Maximum	Source
H	Net aquifer thickness	m	$\psi=\Delta P/P$	0.2	180	200	220	Szulczewski et al. (2012)
L_T	Length of trapping-model domain	m	$\psi=\Delta P/P$	0.1	85500	90000	94500	Szulczewski et al. (2012)
W	Width of well array	m	$\psi=\Delta P/P$	0.1	95000	100000	105000	Szulczewski et al. (2012)
ϕ	Porosity		$\psi=\Delta P/P$	0.4	0.16	0.2	0.24	Szulczewski et al. (2012)
ρ_g	CO_2 density	kg/m^3	ΔP	20	690	700	710	Szulczewski et al. (2012)
S_{wc}	Connate water saturation		ΔP	0.2	0.3	0.4	0.5	Szulczewski et al. (2012)
k_{aq}	Aquifer permeability	mD	Ψ	0.03	813	900	997	Szulczewski et al. (2012)
T_s	Surface temperature	^oC				20		Szulczewski et al. (2012)
G_T	Geothermal gradient	$^oC/km$				20		Szulczewski et al. (2012)
D	depth to top of aquifer	m				1000		Szulczewski et al. (2012)
ρ_w	Brine density	kg/m^3				1000		Szulczewski et al. (2012)
s	Salinity	g/L				10		Szulczewski et al. (2012)
H_{gross}	Gross aquifer thickness	m	$\psi=\Delta P/P$	0.2	374	416	457	calculated in this study
B_p	Pore compressibility	Pa^{-1}			1E-10	3E-10	5E-10	calculated in this study
B_w	Brine compressibility	Pa^{-1}			3.7E-10	3.8E-10	3.8E-10	Battistelli et al. (1997)
G_P	Pressure gradient for fresh water	MPa/m				0.009792		Schlumberger Oilfield Glossary
P	Hydrostatic pressure	MPa				10		calculated in this study
ΔP	Sustainable pressure buildup	Mpa				5		calculated in this study

Table A.9. Formation I

Symbol	Parameters	Units	Formula for Uncertainty	Uncertainty	Minimum	Baseline	Maximum	Source
H	Net aquifer thickness	m	$\psi=\Delta P/P$	0.2	180	200	220	Szulczewski et al. (2012)
L_T	Length of trapping-model domain	m	$\psi=\Delta P/P$	0.1	28500	30000	31500	Szulczewski et al. (2012)
W	Width of well array	m	$\psi=\Delta P/P$	0.1	190000	200000	210000	Szulczewski et al. (2012)
ϕ	Porosity		$\psi=\Delta P/P$	0.4	0.16	0.2	0.24	Szulczewski et al. (2012)
ρ_g	CO_2 density	kg/m^3	ΔP	20	590	600	610	Szulczewski et al. (2012)
S_{wc}	Connate water saturation		ΔP	0.2	0.3	0.4	0.5	Szulczewski et al. (2012)
k_{aq}	Aquifer permeability	mD			40	100	4000	Szulczewski et al. (2012)
T_s	Surface temperature	^oC				6		Szulczewski et al. (2012)
G_T	Geothermal gradient	$^oC/km$				30		Szulczewski et al. (2012)
D	depth to top of aquifer	m				3000		Szulczewski et al. (2012)
ρ_w	Brine density	kg/m^3				1000		Szulczewski et al. (2012)
s	Salinity	g/L				35		Szulczewski et al. (2012)
H_{gross}	Gross aquifer thickness	m	$\psi=\Delta P/P$	0.2	374	416	457	calculated in this study
B_p	Pore compressibility	Pa^{-1}			1E-10	3E-10	5E-10	calculated in this study
B_w	Brine compressibility	Pa^{-1}			4.7E-10	4.8E-10	5.0E-10	Battistelli et al. (1997)
G_P	Pressure gradient for fresh water	MPa/m				0.009792		Schlumberger Oilfield Glossary
P	Hydrostatic pressure	MPa				29		calculated in this study
ΔP	Sustainable pressure buildup	Mpa				15		calculated in this study

Table A.10. Formation J

Symbol	Parameters	Units	Formula for Uncertainty	Uncertainty	Minimum	Baseline	Maximum	Source
H	Net aquifer thickness	m	$\psi=\Delta P/P$	0.2	540	600	660	Szulczewski et al. (2012)
L_T	Length of trapping-model domain	m	$\psi=\Delta P/P$	0.1	57000	60000	63000	Szulczewski et al. (2012)
W	Width of well array	m	$\psi=\Delta P/P$	0.1	95000	100000	105000	Szulczewski et al. (2012)
ϕ	Porosity		$\psi=\Delta P/P$	0.4	0.064	0.08	0.096	Szulczewski et al. (2012)
ρ_g	CO_2 density	kg/m^3	ΔP	20	490	500	510	Szulczewski et al. (2012)
S_{wc}	Connate water saturation		ΔP	0.2	0.3	0.4	0.5	Szulczewski et al. (2012)
k_{aq}	Aquifer permeability	mD	Ψ	0.03	56	60	64	Szulczewski et al. (2012)
T_s	Surface temperature	^oC				6		Szulczewski et al. (2012)
G_T	Geothermal gradient	$^oC/km$				40		Szulczewski et al. (2012)
D	depth to top of aquifer	m				3000		Szulczewski et al. (2012)
ρ_w	Brine density	kg/m^3				1000		Szulczewski et al. (2012)
s	Salinity	g/L				200		Szulczewski et al. (2012)
H_{gross}	Gross aquifer thickness	m	$\psi=\Delta P/P$	0.2	1525	1694	1864	calculated in this study
B_p	Pore compressibility	Pa^{-1}			1E-10	3E-10	5E-10	calculated in this study
B_w	Brine compressibility	Pa^{-1}			4.3E-10	4.7E-10	5.1E-10	Battistelli et al. (1997)
G_P	Pressure gradient for fresh water	MPa/m				0.009792		Schlumberger Oilfield Glossary
P	Hydrostatic pressure	MPa				29		calculated in this study
ΔP	Sustainable pressure buildup	Mpa				15		calculated in this study

Table A.11. Formation K

Symbol	Parameters	Units	Formula for Uncertainty	Uncertainty	Minimum	Baseline	Maximum	Source
H	Net aquifer thickness	m	$\psi=\Delta P/P$	0.2	180	200	220	Szulczewski et al. (2012)
L_T	Length of trapping-model domain	m	$\psi=\Delta P/P$	0.1	47500	50000	52500	Szulczewski et al. (2012)
W	Width of well array	m	$\psi=\Delta P/P$	0.1	95000	100000	105000	Szulczewski et al. (2012)
ϕ	Porosity		$\psi=\Delta P/P$	0.4	0.16	0.2	0.24	Szulczewski et al. (2012)
ρ_g	CO_2 density	kg/m^3	ΔP	20	590	600	610	Szulczewski et al. (2012)
S_{wc}	Connate water saturation		ΔP	0.2	0.3	0.4	0.5	Szulczewski et al. (2012)
k_{aq}	Aquifer permeability	mD			40	100	4000	Szulczewski et al. (2012)
T_s	Surface temperature	^oC				10		Szulczewski et al. (2012)
G_T	Geothermal gradient	$^oC/km$				30		Szulczewski et al. (2012)
D	depth to top of aquifer	m				3000		Szulczewski et al. (2012)
ρ_w	Brine density	kg/m^3				1000		Szulczewski et al. (2012)
s	Salinity	g/L				35		Szulczewski et al. (2012)
H_{gross}	Gross aquifer thickness	m	$\psi=\Delta P/P$	0.2	374	416	457	calculated in this study
B_p	Pore compressibility	Pa^{-1}			1E-10	3E-10	5E-10	calculated in this study
B_w	Brine compressibility	Pa^{-1}			4.8E-10	4.9E-10	5.1E-10	Battistelli et al. (1997)
G_P	Pressure gradient for fresh water	MPa/m				0.009792		Schlumberger Oilfield Glossary
P	Hydrostatic pressure	MPa				29		calculated in this study
ΔP	Sustainable pressure buildup	Mpa				15		calculated in this study

Table A.12. Formation L

Symbol	Parameters	Units	Formula for Uncertainty	Uncertainty	Minimum	Baseline	Maximum	Source
H	Net aquifer thickness	m	$\psi=\Delta P/P$	0.2	13.5	15	16.5	Szulczewski et al. (2012)
L_T	Length of trapping-model domain	m	$\psi=\Delta P/P$	0.1	66500	70000	73500	Szulczewski et al. (2012)
W	Width of well array	m	$\psi=\Delta P/P$	0.1	76000	80000	84000	Szulczewski et al. (2012)
ϕ	Porosity		$\psi=\Delta P/P$	0.4	0.16	0.2	0.24	Szulczewski et al. (2012)
ρ_g	CO_2 density	kg/m^3	ΔP	20	590	600	610	Szulczewski et al. (2012)
S_{wc}	Connate water saturation		ΔP	0.2	0.3	0.4	0.5	Szulczewski et al. (2012)
k_{aq}	Aquifer permeability	mD	Ψ	0.03	275	300	327	Szulczewski et al. (2012)
T_s	Surface temperature	^oC				20		Szulczewski et al. (2012)
G_T	Geothermal gradient	$^oC/km$				30		Szulczewski et al. (2012)
D	depth to top of aquifer	m				2000		Szulczewski et al. (2012)
ρ_w	Brine density	kg/m^3				1000		Szulczewski et al. (2012)
s	Salinity	g/L				100		Szulczewski et al. (2012)
H_{gross}	Gross aquifer thickness	m	$\psi=\Delta P/P$	0.2	28	31	34	calculated in this study
B_p	Pore compressibility	Pa^{-1}			1E-10	3E-10	5E-10	calculated in this study
B_w	Brine compressibility	Pa^{-1}			3.9E-10	3.9E-10	3.9E-10	Battistelli et al. (1997)
G_P	Pressure gradient for fresh water	MPa/m				0.009792		Schlumberger Oilfield Glossary
P	Hydrostatic pressure	MPa				20		calculated in this study
ΔP	Sustainable pressure buildup	Mpa				10		calculated in this study

Table A.13. Formation M

Symbol	Parameters	Units	Formula for Uncertainty	Uncertainty	Minimum	Baseline	Maximum	Source
H	Net aquifer thickness	m	$\psi=\Delta P/P$	0.2	36	40	44	Szulczewski et al. (2012)
L_T	Length of trapping-model domain	m	$\psi=\Delta P/P$	0.1	95000	100000	105000	Szulczewski et al. (2012)
W	Width of well array	m	$\psi=\Delta P/P$	0.1	95000	100000	105000	Szulczewski et al. (2012)
ϕ	Porosity		$\psi=\Delta P/P$	0.4	0.048	0.06	0.072	Szulczewski et al. (2012)
ρ_g	CO_2 density	kg/m^3	ΔP	20	790	800	810	Szulczewski et al. (2012)
S_{wc}	Connate water saturation		ΔP	0.2	0.3	0.4	0.5	Szulczewski et al. (2012)
k_{aq}	Aquifer permeability	mD	Ψ	0.03	47	50	53	Szulczewski et al. (2012)
T_s	Surface temperature	^oC				10		Szulczewski et al. (2012)
G_T	Geothermal gradient	$^oC/km$				20		Szulczewski et al. (2012)
D	depth to top of aquifer	m				2000		Szulczewski et al. (2012)
ρ_w	Brine density	kg/m^3				1000		Szulczewski et al. (2012)
s	Salinity	g/L				100		Szulczewski et al. (2012)
H_{gross}	Gross aquifer thickness	m	$\psi=\Delta P/P$	0.2	75	83	91	calculated in this study
B_p	Pore compressibility	Pa^{-1}			1E-10	3E-10	5E-10	calculated in this study
B_w	Brine compressibility	Pa^{-1}			3.6E-10	3.6E-10	3.6E-10	Battistelli et al. (1997)
G_P	Pressure gradient for fresh water	MPa/m				0.009792		Schlumberger Oilfield Glossary
P	Hydrostatic pressure	MPa				20		calculated in this study
ΔP	Sustainable pressure buildup	Mpa				10		calculated in this study

APPENDIX B:

GoldSim Model of DOE-NETL Atlas I, II (2007, 2008) and DOE-NETL Atlas III, IV (2010, 2012) methods:

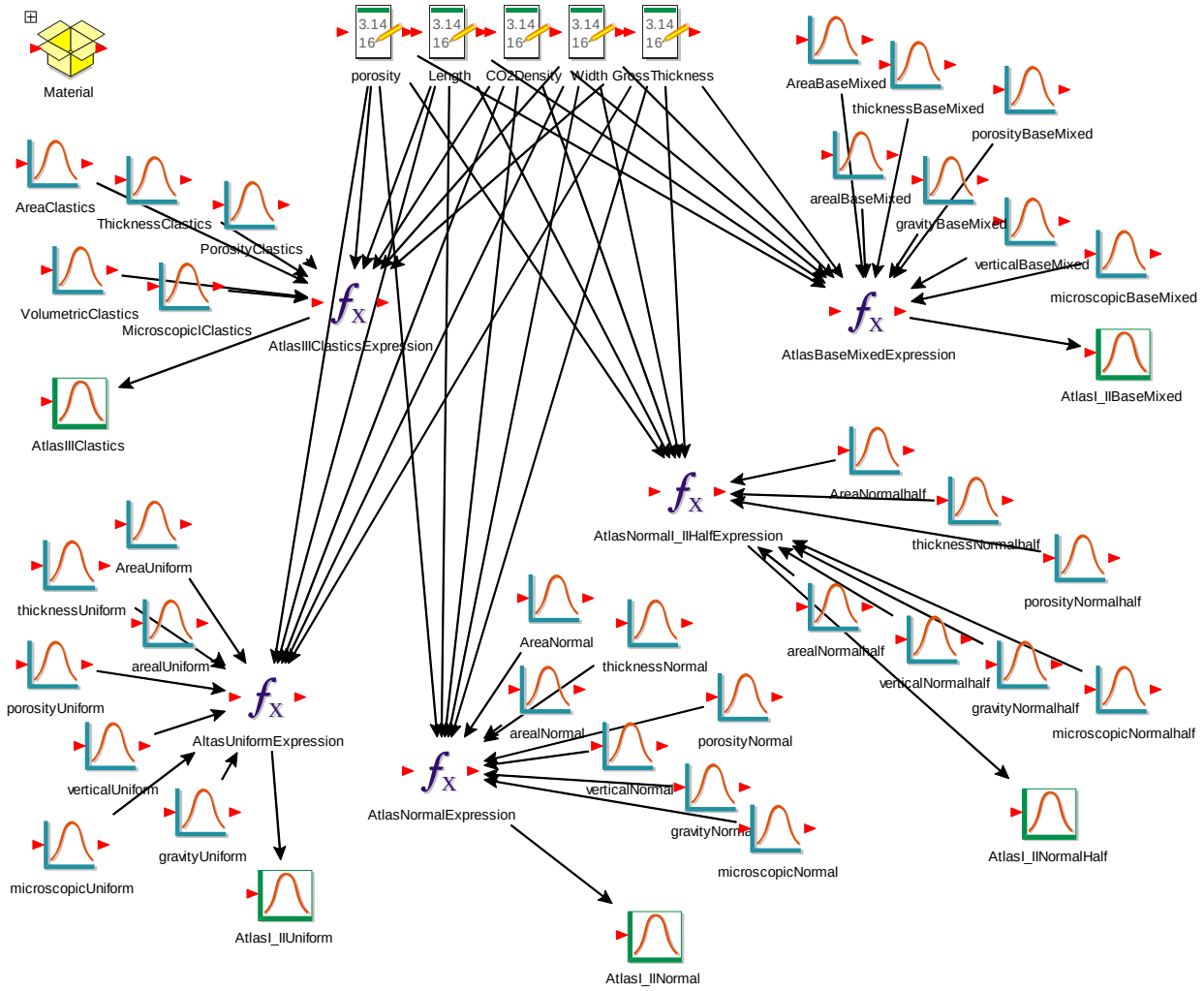

This page intentionally left blank.

APPENDIX C:

GoldSim Model of USGS: Brennan et al. (2010) Method (upper right) and GoldSim Model of Zhou et al. (2008) Method (bottom left):

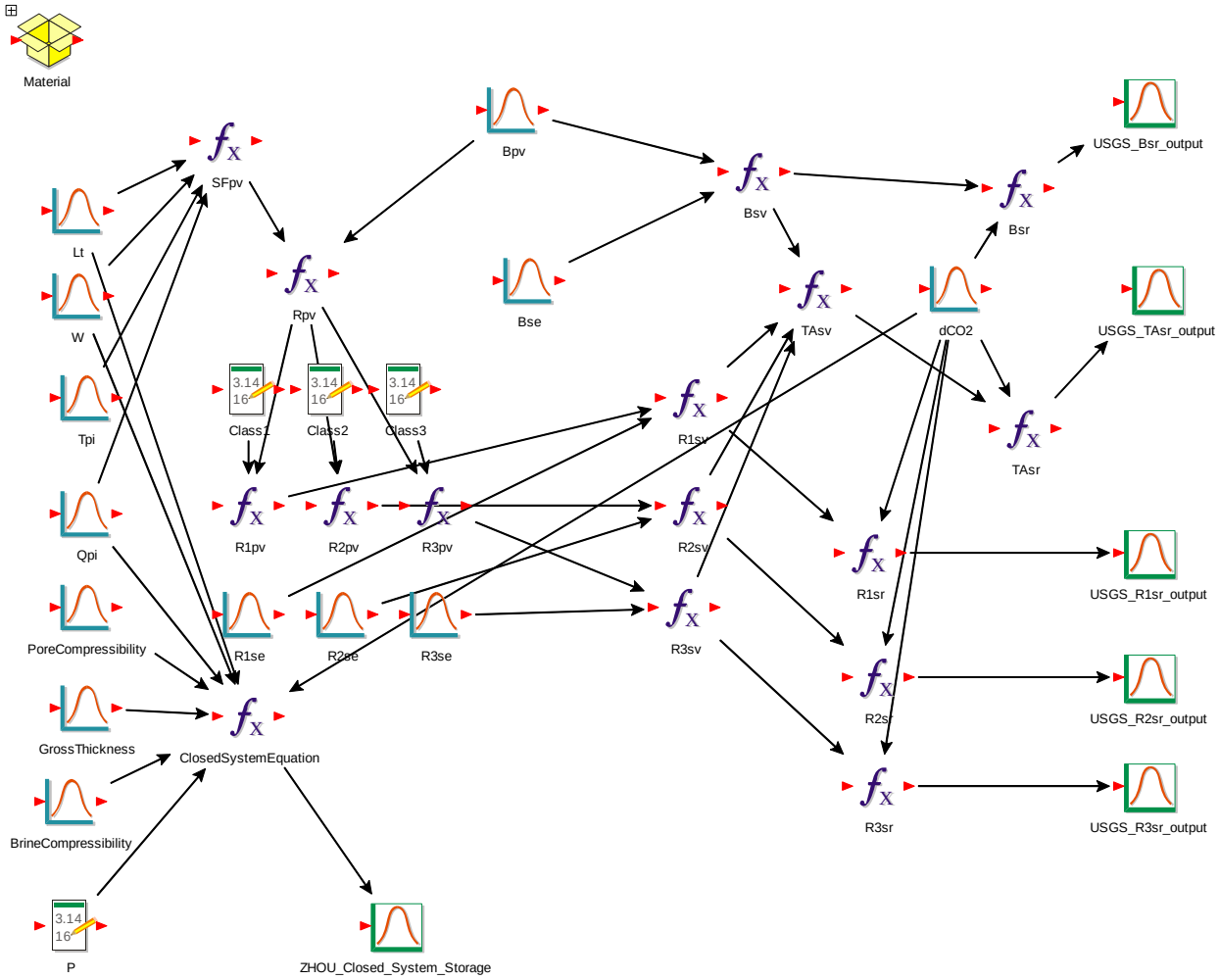

This page intentionally left blank.

APPENDIX D:

The following table compiles resource estimates (GT) between the 5th and 95th percentiles. The methods by CSLF: Bachu et al. (2007), DOE-NETL Atlas III, IV (2010, 2012), and Zhou et al. (2008) produce CO_2 storage resource at the 10th, 50th, and 90th percentiles. The method by DOE-NETL Atlas I, II (2007, 2008) produces CO_2 storage resource values at the 15th, 50th, and 85th percentiles. The method by USGS: Brennan et al. (2010) produces CO_2 storage resource values at the 5th, 50th, and 95th percentiles. The method by Szulczewski et al. (2012) produces a low, baseline, and high storage estimate where one standard deviation is used as an appropriate measure of uncertainty from the probability density function. Because of the assumed normality of the distribution, one standard deviation was taken to be the half-range of the 16th and 84th percentiles of the storage values.

Prospective CO_2 Storage Resource Estimates (GT)							
Formation	Percentile	CSLF: Bachu et al. (2007) open	DOE-NETL: Altas I, II (2007, 2008) open	DOE-NETL: Atlas III, IV (2010, 2012) open	USGS: Brennan et al. (2010) open	Szulczewski et al. (2012) migration-limited	Zhou et al. (2008) closed
A	P_5				**38.2**		
	P_{10}	**49.5**	15.1	**14.2**	49.1	5.2	**13.8**
	P_{15}		**20.2**				
	P_{16}		21.2	19.5	58.7	**6.7**	14.5
	P_{50}	**71.8**	**54.8**	**52.4**	**95.5**	**10.0**	**17.2**
	P_{84}		120.4	117.2	138.3	**13.3**	20.2
	P_{85}		**124.1**				
	P_{90}	**159.6**	147.7	**142.8**	150.5	17.0	**21.1**
	P_{95}				**165.1**		
B	P_5				**33.5**		
	P_{10}	**43.3**	13.2	**12.4**	43.0	47.7	**12.4**
	P_{15}		**17.7**				
	P_{16}		18.5	17.0	51.5	**61.0**	13.0
	P_{50}	**62.8**	**47.9**	**45.8**	**83.6**	**88.0**	**15.4**
	P_{84}		105.3	102.4	121.0	**120.0**	17.9
	P_{85}		**108.5**				
	P_{90}	**139.6**	129.1	**124.8**	131.5	153.6	**18.7**
	P_{95}				**144.4**		

Formation	Percentile	CSLF: Bachu et al. (2007) open	DOE-NETL: Altas I, II (2007, 2008) open	DOE-NETL: Atlas III, IV (2010, 2012) open	USGS: Brennan et al. (2010) open	Szulczewski et al. (2012) migration-limited	Zhou et al. (2008) closed
C	P_5				**30.0**		
	P_{10}	**38.7**	11.8	**11.1**	38.4	7.7	**7.0**
	P_{15}		**15.8**				
	P_{16}		16.5	15.2	46.0	**9.9**	7.4
	P_{50}	**56.1**	**42.8**	**40.9**	**74.6**	**18.0**	**8.7**
	P_{84}		94.0	91.5	108.0	**26.2**	10.2
	P_{85}		**96.9**				
	P_{90}	**124.7**	115.3	**111.5**	117.4	33.5	**10.6**
	P_{95}				**128.9**		
D	P_5				**25.2**		
	P_{10}	**32.5**	9.9	**9.3**	32.3	9.9	**4.4**
	P_{15}		**13.3**				
	P_{16}		13.9	12.8	38.6	**12.7**	4.6
	P_{50}	**47.1**	**36.0**	**34.4**	**62.7**	**17.0**	**5.5**
	P_{84}		79.0	76.9	90.8	**22.2**	6.4
	P_{85}		**81.5**				
	P_{90}	**104.7**	96.9	**93.7**	98.6	28.4	**6.7**
	P_{95}				**108.3**		
E	P_5				**10.8**		
	P_{10}	**13.9**	4.3	**4.0**	13.8	2.9	**2.3**
	P_{15}		**5.7**				
	P_{16}		5.9	5.5	16.6	**3.7**	2.4
	P_{50}	**20.2**	**15.4**	**14.7**	**26.9**	**8.6**	**2.8**
	P_{84}		33.8	32.9	38.9	**12.3**	3.2
	P_{85}		**34.9**				
	P_{90}	**44.9**	41.5	**40.1**	42.3	15.7	**3.3**
	P_{95}				**46.4**		
F	P_5				**10.6**		
	P_{10}	**13.5**	4.1	**3.9**	13.5	5.2	**2.0**

Formation	Percentile	CSLF: Bachu et al. (2007) open	DOE-NETL: Altas I, II (2007, 2008) open	DOE-NETL: Atlas III, IV (2010, 2012) open	USGS: Brennan et al. (2010) open	Szulczewski et al. (2012) migration-limited	Zhou et al. (2008) closed
F	P_{15}		**5.5**				
	P_{16}		5.8	5.3	16.0	**6.6**	2.1
	P_{50}	**19.6**	**15.0**	**14.3**	**26.1**	**12.0**	**2.5**
	P_{84}		32.9	32.0	37.9	**17.4**	2.9
	P_{85}		**33.9**				
	P_{90}	**43.6**	40.4	**39.0**	41.3	22.3	**3.0**
	P_{95}				**44.9**		
G	P_{5}				**10.8**		
	P_{10}	**14.3**	5.8	**4.2**	13.8	3.0	**6.8**
	P_{15}		**7.7**				
	P_{16}		8.1	5.8	16.6	**3.8**	7.1
	P_{50}	**20.7**	**20.9**	**15.2**	**26.9**	**6.6**	**8.2**
	P_{84}		46.0	33.2	38.9	**9.2**	9.5
	P_{85}		**47.4**				
	P_{90}	**33.2**	56.4	**40.3**	42.3	11.8	**9.8**
	P_{95}				**46.4**		
H	P_{5}				**7.5**		
	P_{10}	**9.7**	3.0	**2.8**	9.7	8.3	**1.4**
	P_{15}		**4.0**				
	P_{16}		4.2	3.8	11.6	**10.6**	1.5
	P_{50}	**14.1**	**10.8**	**10.3**	**18.8**	**14.0**	**1.8**
	P_{84}		23.7	23.1	27.2	**17.4**	2.0
	P_{85}		**24.4**				
	P_{90}	**31.4**	29.1	**28.1**	29.6	22.3	**2.1**
	P_{95}				**32.5**		
I	P_{5}				**4.4**		
	P_{10}	**5.6**	1.7	**1.6**	5.5	2.1	**2.9**
	P_{15}		**2.3**				
	P_{16}		2.4	2.2	6.6	**2.7**	3.0

Formation	Percentile	CSLF: Bachu et al. (2007) open	DOE-NETL: Altas I, II (2007, 2008) open	DOE-NETL: Atlas III, IV (2010, 2012) open	USGS: Brennan et al. (2010) open	Szulczewski et al. (2012) migration-limited	Zhou et al. (2008) closed
I	P_{50}	**8.1**	**6.2**	**5.9**	**10.5**	**5.1**	**3.5**
	P_{84}		13.5	13.2	15.1	**7.5**	4.0
	P_{85}		**14.0**				
	P_{90}	**18.0**	16.6	**16.1**	16.4	9.6	**4.2**
	P_{95}				**18.0**		
J	P_{5}				**4.3**		
	P_{10}	**5.7**	2.3	**1.7**	5.5	2.6	**3.9**
	P_{15}		**3.1**				
	P_{16}		3.2	2.3	6.6	**3.3**	4.0
	P_{50}	**8.3**	**8.4**	**6.1**	**10.7**	**5.3**	**4.7**
	P_{84}		18.4	13.3	15.6	**7.5**	5.4
	P_{85}		**19.0**				
	P_{90}	**13.3**	22.6	**16.1**	16.9	9.6	**5.6**
	P_{95}				**18.6**		
K	P_{5}				**3.7**		
	P_{10}	**4.6**	1.4	**1.3**	4.6	2.0	**2.4**
	P_{15}		**1.9**				
	P_{16}		2.0	1.8	5.5	**2.6**	2.5
	P_{50}	**6.7**	**5.1**	**4.9**	**8.8**	**4.0**	**2.9**
	P_{84}		11.3	11.0	12.6	**5.4**	3.4
	P_{85}		**11.6**				
	P_{90}	**15.0**	13.8	**13.4**	13.7	6.9	**3.5**
	P_{95}				**15.0**		
L	P_{5}				**0.3**		
	P_{10}	**0.4**	0.1	**0.1**	0.4	0.8	**0.1**
	P_{15}		**0.2**				
	P_{16}		0.2	0.2	0.5	**1.0**	0.1
	P_{50}	**0.6**	**0.4**	**0.4**	**0.8**	**1.5**	**0.1**
	P_{84}		0.9	0.9	1.1	**2.0**	0.2

Formation	Percentile	CSLF: Bachu et al. (2007) open	DOE-NETL: Altas I, II (2007, 2008) open	DOE-NETL: Atlas III, IV (2010, 2012) open	USGS: Brennan et al. (2010) open	Szulczewski et al. (2012) migration-limited	Zhou et al. (2008) closed
L	P_{85}		**1.0**				
	P_{90}	**1.3**	1.2	**1.1**	1.2	2.6	**0.2**
	P_{95}				**1.3**		
M	P_{5}				**0.6**		
	P_{10}	**0.7**	0.2	**0.2**	0.7	1.0	**0.2**
	P_{15}		**0.3**				
	P_{16}		0.3	0.3	0.9	**1.2**	0.2
	P_{50}	**1.1**	**0.8**	**0.8**	**1.4**	**1.6**	**0.3**
	P_{84}		1.8	1.8	2.1	**2.0**	0.3
	P_{85}		**1.9**				
	P_{90}	**2.4**	2.2	**2.1**	2.3	2.5	**0.3**
	P_{95}				**2.5**		

This page intentionally left blank.

APPENDIX E:

Example R script used to compare differences in CO_2 storage resource computed using different methods with stochastic inputs. All pairwise comparisons are made using the Šidák inequality to control for false positives arising from multiple comparisons within each site.

Input data for the method by CSLF: Bachu et al. (2007) with limited stochastic input was represented by a loglogistic distribution for sandstone lithology and lognormal for limestone lithology.

Input data for the method by Szulczewski et al. (2012) with limited stochastic input was represented by a normal distribution.

Input data for methods by DOE-NETL Atlas I, II (2007, 2008), DOE-NETL Atlas III, IV (2010, 2012), USGS: Brennan et al. (2010), and Zhou et al. (2008) with full stochastic input was empirically represented by 50 000 realizations generated by the Monte Carlo program, GoldSim.

```
# R script to compare carbon sequestration capacities computed using
# different methods with stochastic inputs. All pairwise comparisons
# are made using the Sidak inequality to control for false positives
# arising from multiple comparison.
#
# Author: Will Guthrie, 2012-10-12
# Last Change: 2012-10-21
#######################################################################

# read in and setup data for computation
# user input potentially required in each section
#####

# formation name
formation.name <- "friob"

# read input values from methods with full stochastic output into R
input.initial <- read.table("simulation-data-friob-six-
methods.txt",header=T)

# combine or transform initial input as necessary
```

```
# generate input values from methods with limited stochastic input
atlas3 <- input.initial[,1]/10^9
usgs <- input.initial[,2]/10^9
atlas12 <- apply(input.initial[,3:6],1,mean)/10^9
zhou <- input.initial[,7]/10^9
library(FAdist)
cslf <-
pmin(signif(rllog3(dim(input.initial)[1],0.62,2.13,11.77),5),179.54)
mit <- signif(rnorm(dim(input.initial)[1],mean=8.60,sd=4.30),5)

# put all input values into a single dataframe for analysis
input.final <-
data.frame(usgs=usgs,cslf=cslf,atlas12=atlas12,atlas3=atlas3,mit=mit,z
hou=zhou)

# desired family-wise confidence level for each set of comparisons
fwcl <- 0.95

# output file for simulated pairwise differences
differences.filename <- "simulated-differences-friob-six-methods.txt"

# indicator to select between plotting to a file or screen
ptf <- T

# output file name for graphical output
graphics.filename <- "comparison-results-friob-six-methods.pdf"

# output filename for uncertainty bounds
uncertainty.bounds.filename <- "uncertainty-bounds-friob-six-
methods.txt"

# computations - no user input needed from here on
#####
```

```
# compute number of methods and get method names
n.m <- dim(input.final)[2]
method.names <- dimnames(input.final)[[2]]

#compute pair-wise confidence level for each comparison using the
# Sidak inequality
pwcl <- fwcl^(1/choose(n.m,2))

# loop through methods and compute differences for each pair
for(i in 1:(n.m-1))
{
for(j in (i+1):n.m)
{

# compute simulated differences in methods from simulated input values
# for each method
vn <- paste("delta.",method.names[i],".",method.names[j],sep="")
assign(vn,with(input.final,get(method.names[i]))-
with(input.final,get(method.names[j])))
if(i==1 & j==2) diff.values <- data.frame(get(vn)) else
                diff.values <- data.frame(diff.values,get(vn))
dimnames(diff.values)[[2]][dim(diff.values)[2]] <- vn
if(i==1 & j==2) dens.values <- data.frame(density(get(vn))$y) else
                dens.values <-
data.frame(dens.values,density(get(vn))$y)
}
}

# write out raw differences for use in other programs and/or for
# documentation
orig.width <- options()$width
options(width=1000)
```

```
sink(differences.filename)
print(diff.values)
sink()
options(width=orig.width)

# loop through methods and carry out computations for each pair of
# methods
if(ptf) pdf(graphics.filename) else par(ask=T)
cnt <- 1
uncertainty.bounds <- matrix(NA,nrow=choose(n.m,2),ncol=3)
for(i in 1:(n.m-1))
{
for(j in (i+1):n.m)
{

# assign current difference to a temporary variable with a standard
# name for convenience
cdiff <-
get(paste("delta.",method.names[i],".",method.names[j],sep=""))

# approximate the probability density function
kde <- density(cdiff)

# compute the median of the distribution for each difference and
# the associated uncertainty bounds
md <- median(cdiff)
ub <- quantile(cdiff,c(1/2-pwcl/2,1/2+pwcl/2))
uncertainty.bounds[cnt,] <- c(ub[1],md,ub[2])

# plot the results
plot(kde,lwd=3,col="blue",xlim=range(diff.values),ylim=c(0-
0.01*max(dens.values),max(dens.values)),xlab="(Difference in CO2
```

```
Storage)/GT",ylab="Probability Density",main=paste("Difference
Between",method.names[i],"and",method.names[j],"\n",formation.name))

# draw red lines indicating lower uncertainty bound, median, and upper
# uncertainty bound on plot
segments(kde$x[which.min((md-kde$x)^2)],0,kde$x[which.min((md-
kde$x)^2)],kde$y[which.min((md-kde$x)^2)],col="red",lwd=3)
lines(kde,lwd=3,col="blue")
segments(kde$x[which.min((ub[1]-kde$x)^2)],0,kde$x[which.min((ub[1]-
kde$x)^2)],kde$y[which.min((ub[1]-kde$x)^2)],col="red",lwd=4)
segments(kde$x[which.min((ub[2]-kde$x)^2)],0,kde$x[which.min((ub[2]-
kde$x)^2)],kde$y[which.min((ub[2]-kde$x)^2)],col="red",lwd=4)

# write values of lower uncertainty bound, median, and upper
# uncertainty bound on plot
text(kde$x[which.min((ub[1]-kde$x)^2)],-
0.04*max(dens.values)/2,round(ub[1],1),cex=0.75,col="red")
text(kde$x[which.min((md-kde$x)^2)],-
0.04*max(dens.values)/2,round(md,1),cex=0.75,col="red")
text(kde$x[which.min((ub[2]-kde$x)^2)],-
0.04*max(dens.values)/2,round(ub[2],1),cex=0.75,col="red")

# add a dotted reference line at zero
segments(0,0,0,kde$y[which.min((0-kde$x)^2)],lty=3)
cnt <- cnt+1
}
}

# add row and column labels to uncertainty.bounds
dimnames(uncertainty.bounds)[[1]] <- dimnames(diff.values)[[2]]
dimnames(uncertainty.bounds)[[2]] <- c("Lower Bound","Median","Upper
Bound")

# write out uncertainty.bounds to a file
```

```
sink(uncertainty.bounds.filename)
print(uncertainty.bounds)
sink()

# add a summary plot to the results that compares the uncertainty
# intervals for each pair of methods
plot(rep(1:choose(n.m,2),3),uncertainty.bounds,type="n",xlab="Method
Differences",ylab="(Difference CO2 Storage)/GT")
segments(1:choose(n.m,2),uncertainty.bounds[,1],1:choose(n.m,2),uncert
ainty.bounds[,3],lwd=3,col="gray")
points(1:choose(n.m,2),uncertainty.bounds[,2],pch=18,cex=1.5)
abline(h=0,lty=3)
title(paste("Simultaneous",fwcl*100,"% Uncertainty Intervals\nfor All
Pairwise Differences Between Methods"))
if(ptf) dev.off()
```

APPENDIX F:

Individual 95% uncertainty intervals for all possible pair-wise difference comparisons between methods for Formations A through M.

Key:

Methods applied in this study	"The R Project for Statistical Computing" designation of each method
CSLF: Bachu et al. (2007)	cslf
DOE-NETL Atlas I, II (2007, 2008)	altas12
DOE-NETL Atlas III, IV (2010, 2012)	altas3
Szulczewski et al. (2012)	mit
USGS: Brennan et al. (2010)	usgs
Zhou et al. (2008)	zhou

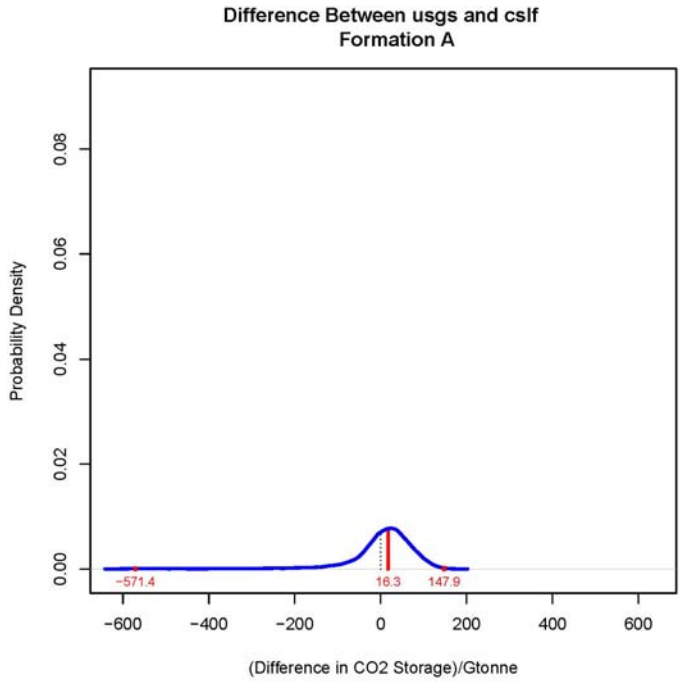
Difference Between usgs and cslf
Formation A
Probability Density
0.00
0.02
0.04
0.06
0.08
-571.4
16.3
147.9
-600
-400
-200
0
200
400
600
(Difference in CO2 Storage)/Gtonne

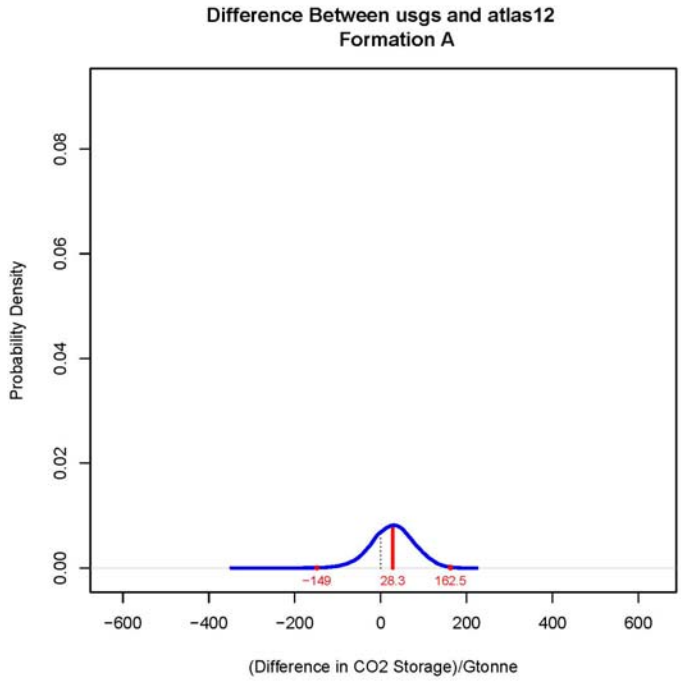
Difference Between usgs and atlas12
Formation A
Probability Density
0.00
0.02
0.04
0.06
0.08
-149
28.3
162.5
-600
-400
-200
0
200
400
600
(Difference in CO2 Storage)/Gtonne

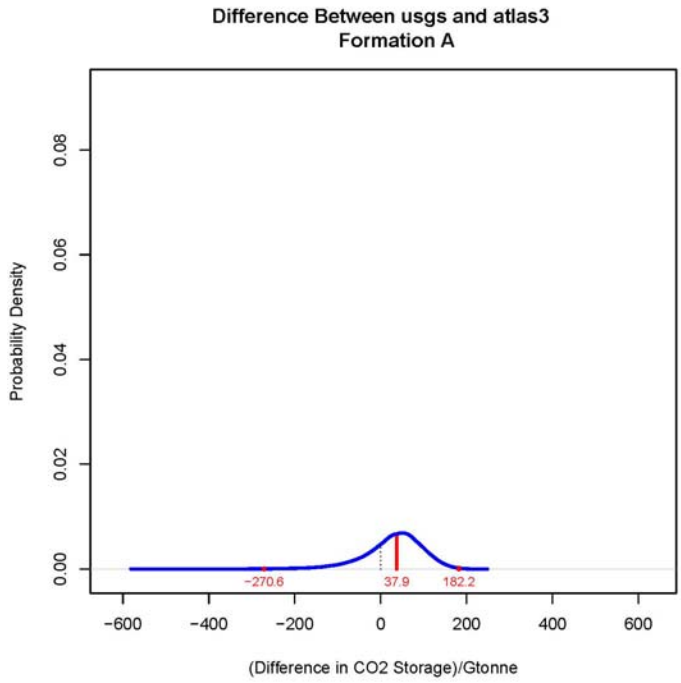
Difference Between usgs and atlas3
Formation A
Probability Density
0.00
0.02
0.04
0.06
0.08
-270.6
37.9
182.2
-600
-400
-200
0
200
400
600
(Difference in CO2 Storage)/Gtonne

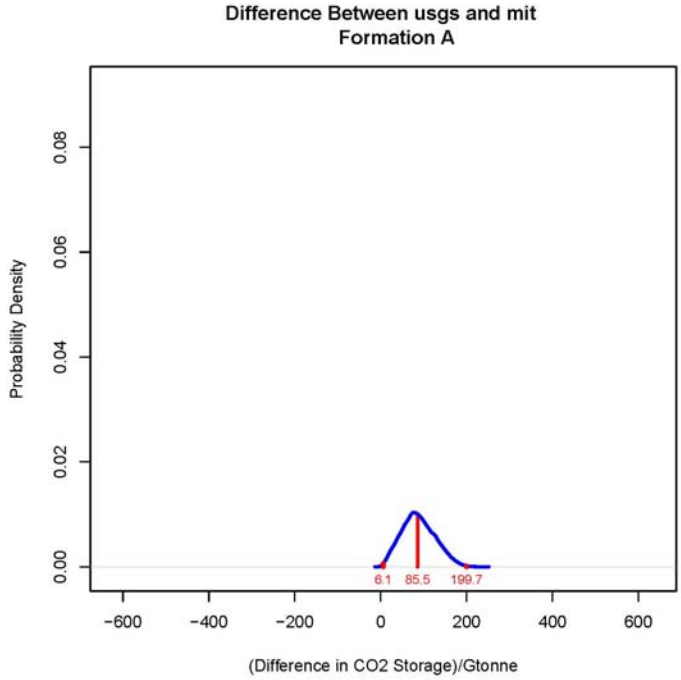
Difference Between usgs and mit
Formation A
Probability Density
0.00
0.02
0.04
0.06
0.08
6.1
85.5
199.7
-600
-400
-200
0
200
400
600
(Difference in CO2 Storage)/Gtonne

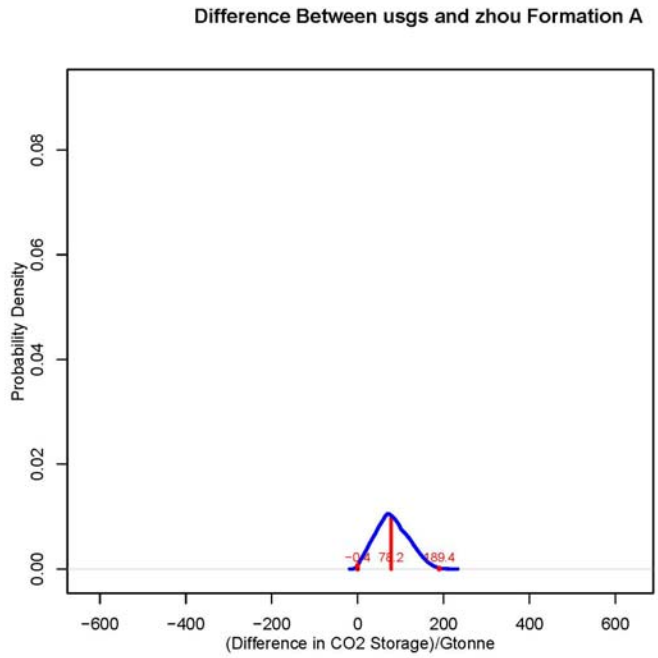
Difference Between usgs and zhou Formation A
Probability Density
0.00
0.02
0.04
0.06
0.08
-600
-400
-200
0
200
400
600
(Difference in CO2 Storage)/Gtonne
189.4

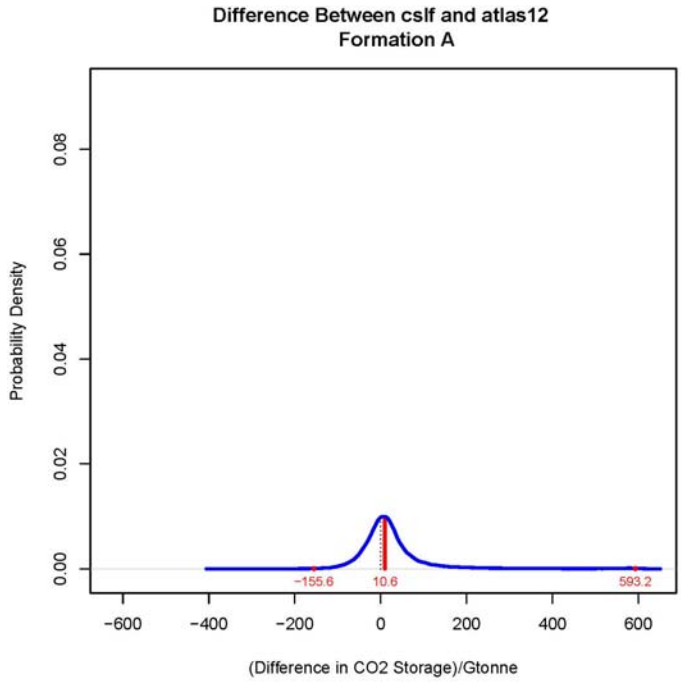
Difference Between cslf and atlas12
Formation A
Probability Density
0.00
0.02
0.04
0.06
0.08
-155.6
10.6
593.2
-600
-400
-200
0
200
400
600
(Difference in CO2 Storage)/Gtonne

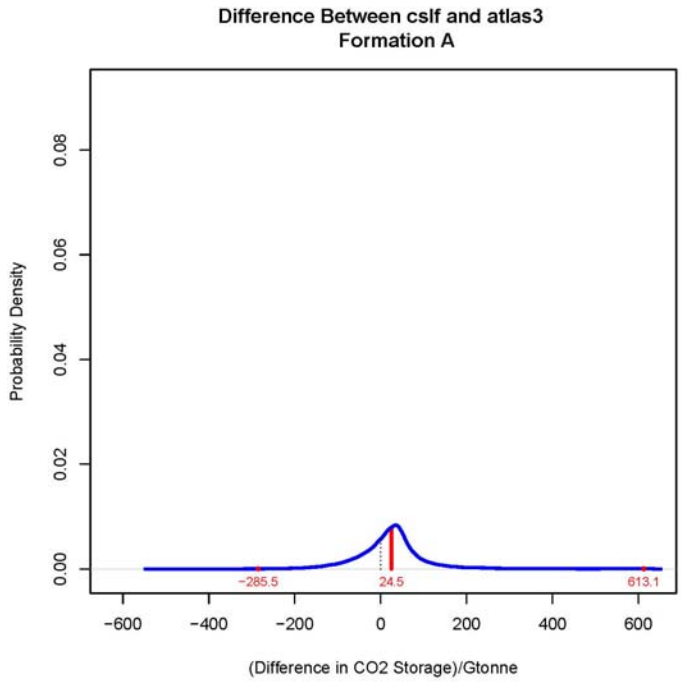
Difference Between cslf and atlas3
Formation A
Probability Density
0.00
0.02
0.04
0.06
0.08
-285.5
24.5
613.1
-600
-400
-200
0
200
400
600
(Difference in CO2 Storage)/Gtonne

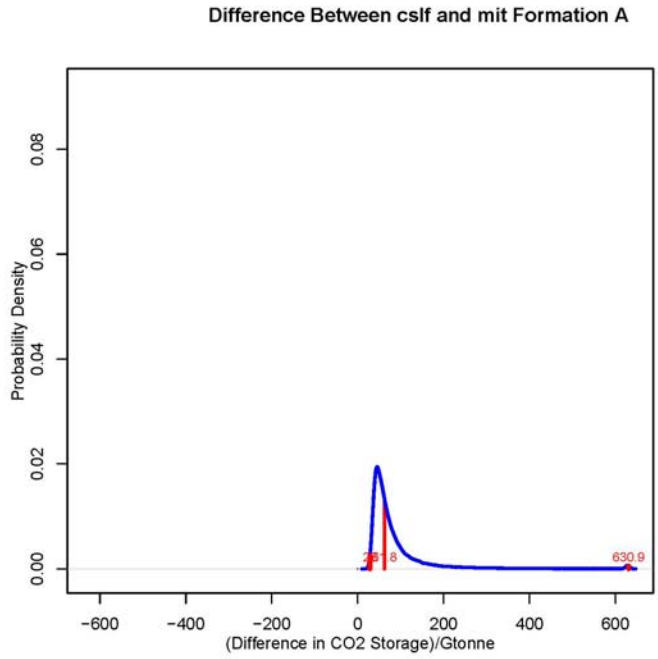
Difference Between cslf and mit Formation A
Probability Density
0.00
0.02
0.04
0.06
0.08
630.9
-600
-400
-200
0
200
400
600
(Difference in CO2 Storage)/Gtonne

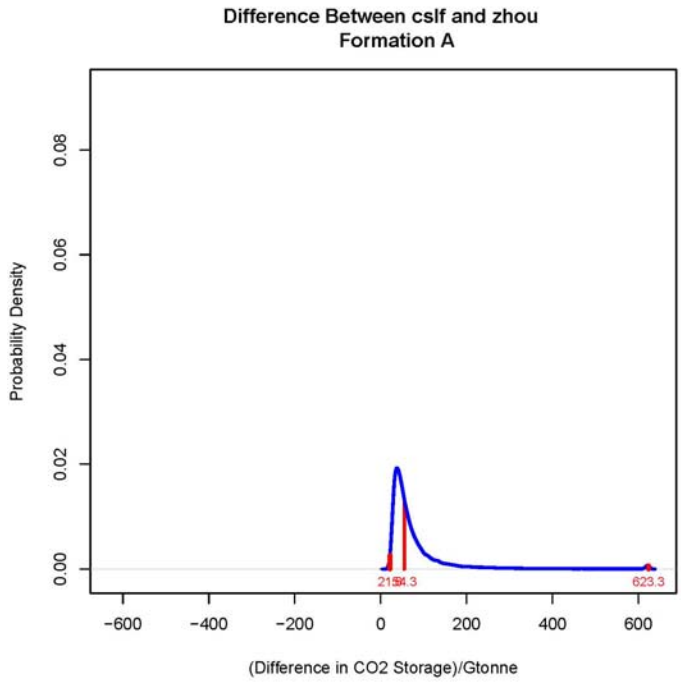
Difference Between cslf and zhou
Formation A
Probability Density
0.00
0.02
0.04
0.06
0.08
623.3
-600
-400
-200
0
200
400
600
(Difference in CO2 Storage)/Gtonne

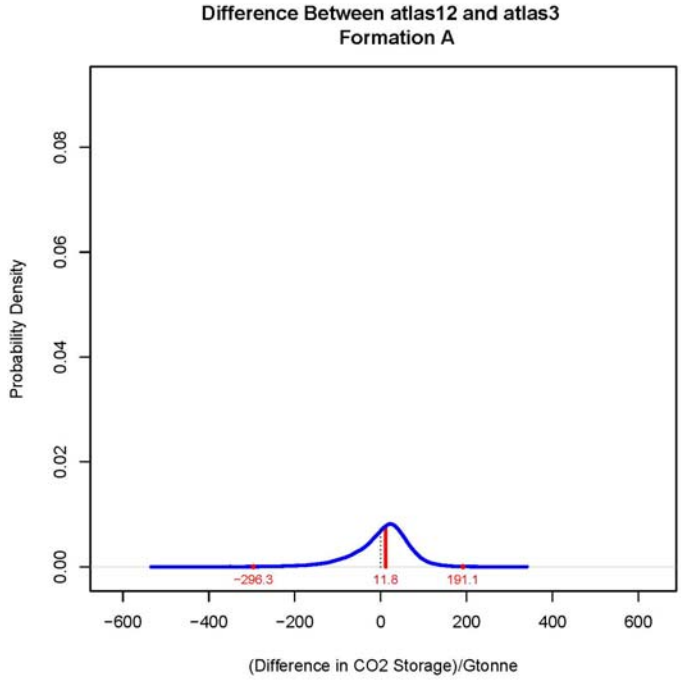
Difference Between atlas12 and atlas3
Formation A
Probability Density
0.00
0.02
0.04
0.06
0.08
-296.3
11.8
191.1
-600
-400
-200
0
200
400
600
(Difference in CO2 Storage)/Gtonne

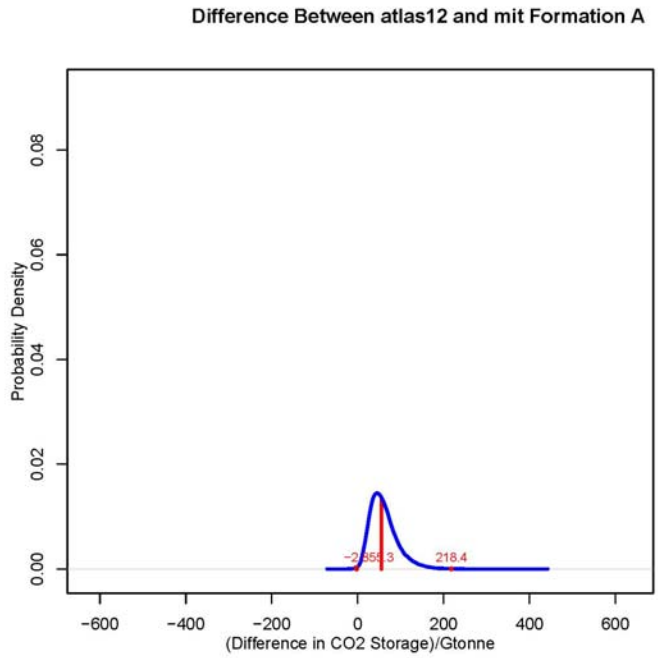
Difference Between atlas12 and mit Formation A
Probability Density
0.00
0.02
0.04
0.06
0.08
-2,858.3
218.4
-600
-400
-200
0
200
400
600
(Difference in CO2 Storage)/Gtonne

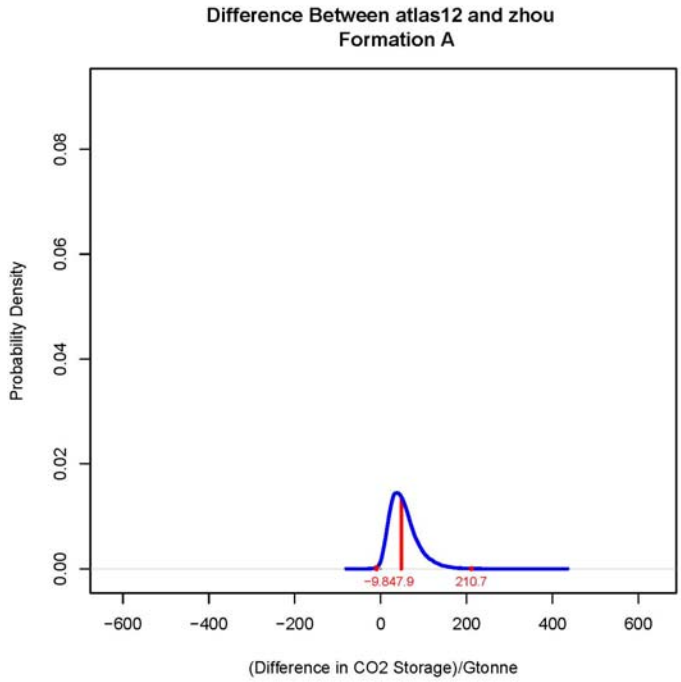
Difference Between atlas12 and zhou
Formation A
Probability Density
0.00
0.02
0.04
0.06
0.08
-9,847.9
210.7
-600
-400
-200
0
200
400
600
(Difference in CO2 Storage)/Gtonne

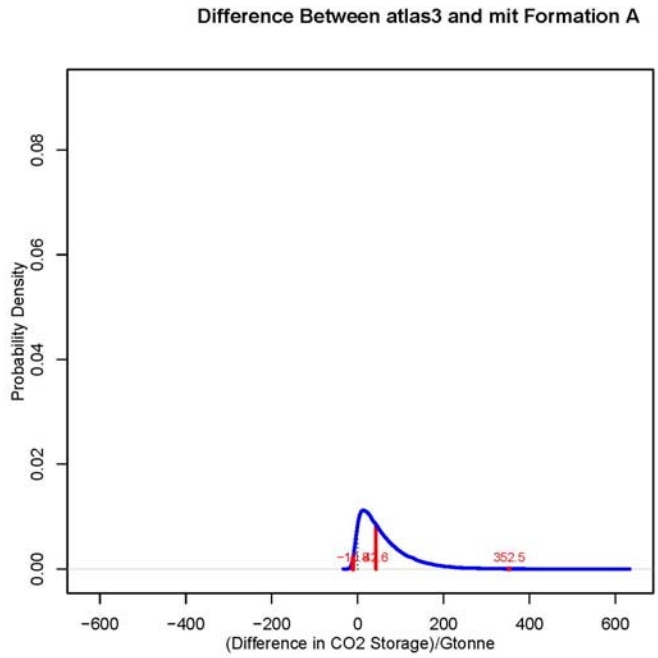
Difference Between atlas3 and mit Formation A
Probability Density
0.00
0.02
0.04
0.06
0.08
352.5
−600
−400
−200
0
200
400
600
(Difference in CO2 Storage)/Gtonne

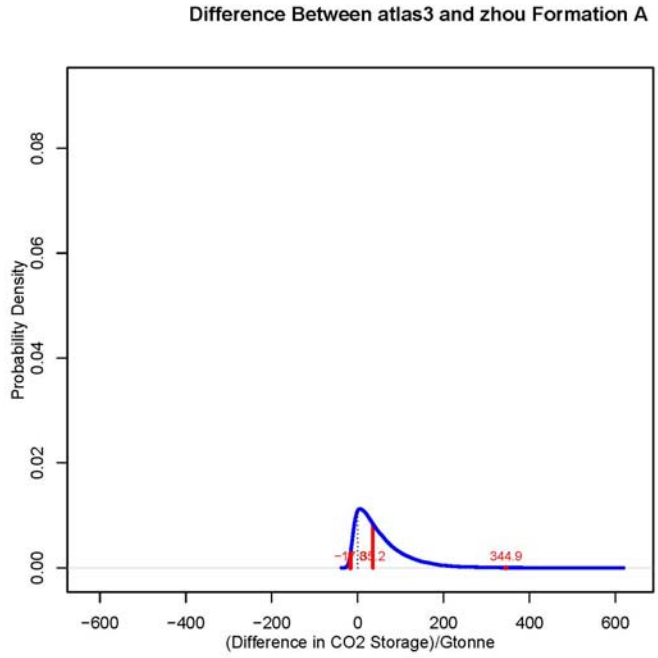
Difference Between atlas3 and zhou Formation A
Probability Density
0.00
0.02
0.04
0.06
0.08
344.9
−600
−400
−200
0
200
400
600
(Difference in CO2 Storage)/Gtonne

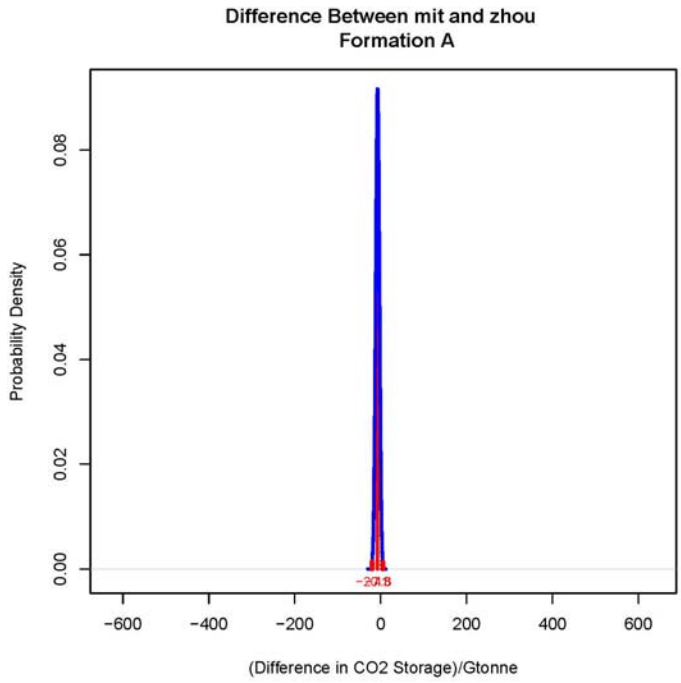
Difference Between mit and zhou
Formation A
Probability Density
0.00
0.02
0.04
0.06
0.08
−600
−400
−200
0
200
400
600
(Difference in CO2 Storage)/Gtonne

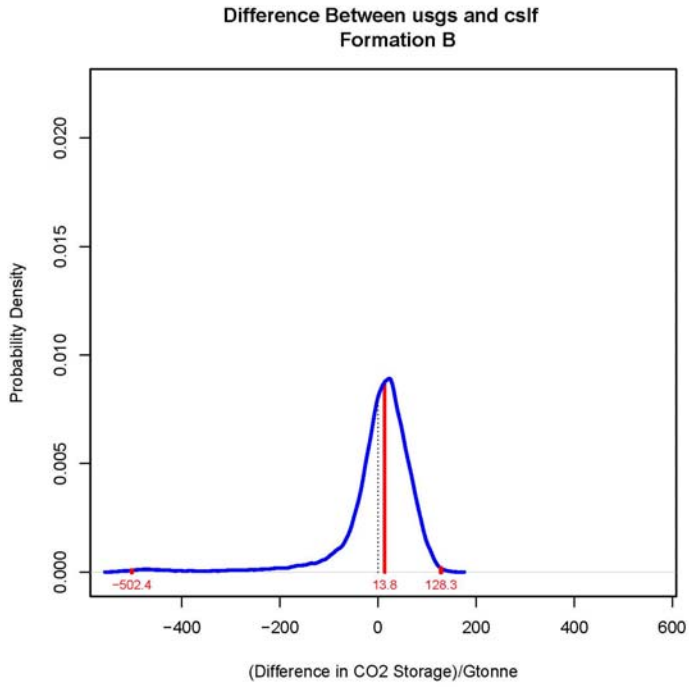
Difference Between usgs and cslf
Formation B
Probability Density
0.000
0.005
0.010
0.015
0.020
−502.4
13.8
128.3
−400
−200
0
200
400
600
(Difference in CO2 Storage)/Gtonne

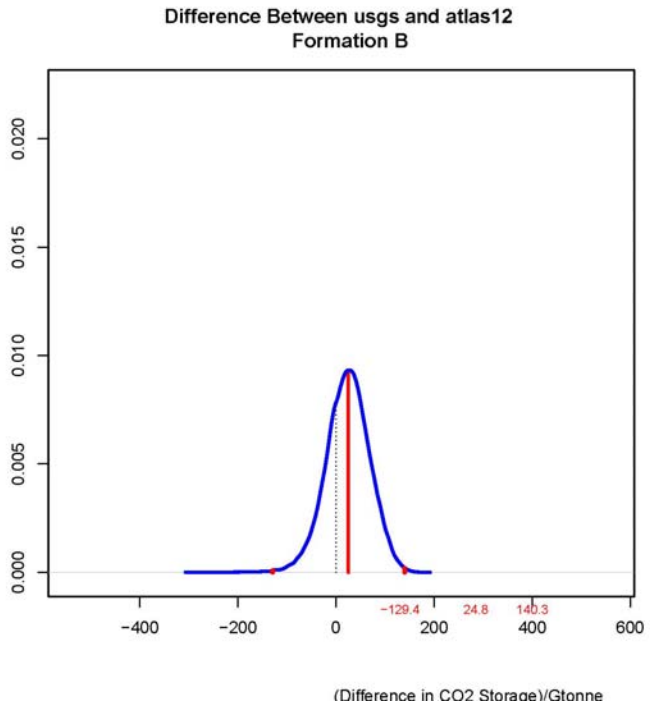
Difference Between usgs and atlas12
Formation B
0.020
0.015
0.010
0.005
0.000
-129.4
24.8
140.3
-400
-200
0
200
400
600
(Difference in CO2 Storage)/Gtonne

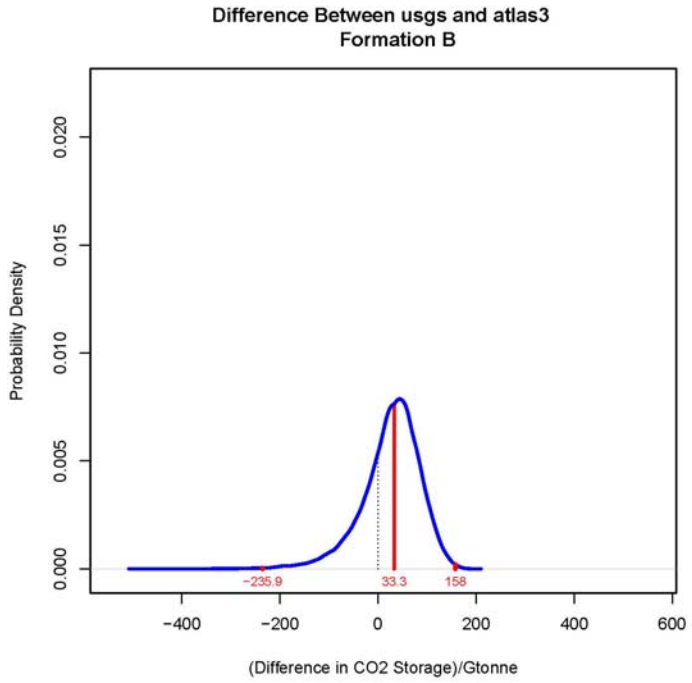
Difference Between usgs and atlas3
Formation B
Probability Density
0.020
0.015
0.010
0.005
0.000
-235.9
33.3
158
-400
-200
0
200
400
600
(Difference in CO2 Storage)/Gtonne

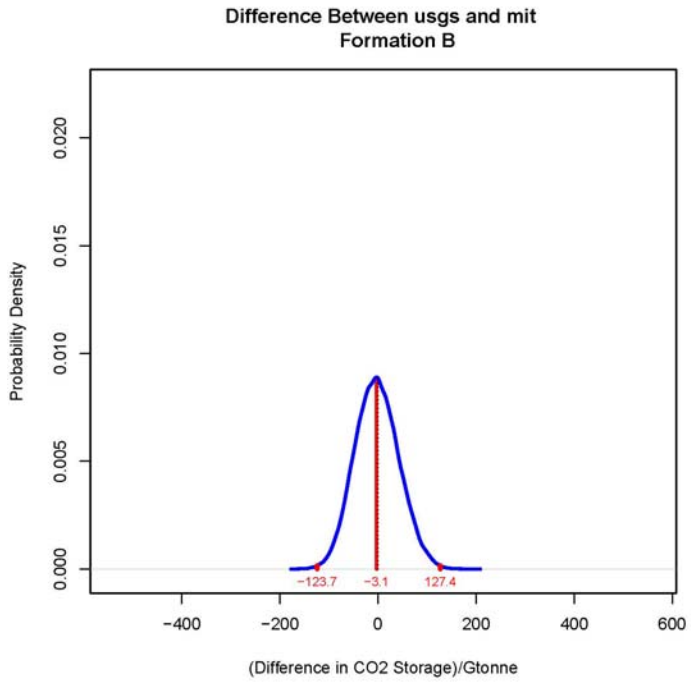
Difference Between usgs and mit
Formation B
Probability Density
0.000
0.005
0.010
0.015
0.020
−123.7
−3.1
127.4
−400
−200
0
200
400
600
(Difference in CO2 Storage)/Gtonne

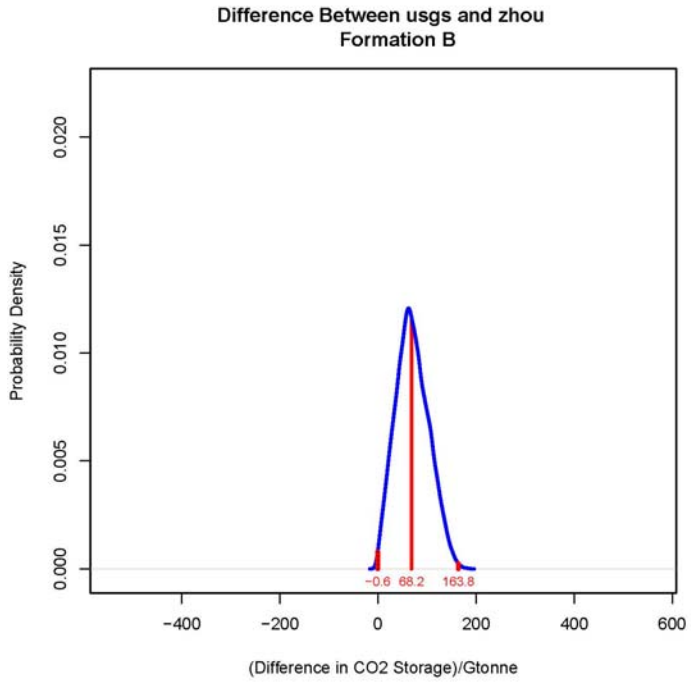
Difference Between usgs and zhou
Formation B
Probability Density
0.000
0.005
0.010
0.015
0.020
−0.6
68.2
163.8
−400
−200
0
200
400
600
(Difference in CO2 Storage)/Gtonne

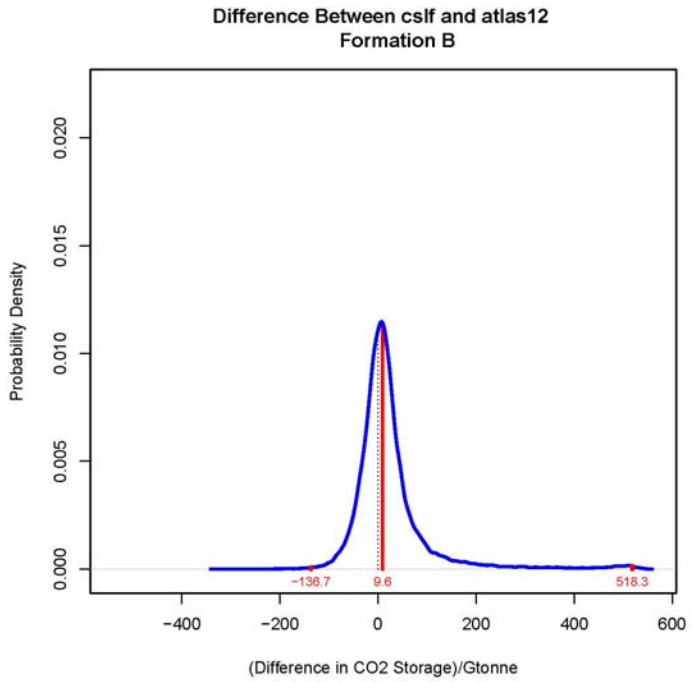
Difference Between cslf and atlas12
Formation B
Probability Density
0.000
0.005
0.010
0.015
0.020
−136.7
9.6
518.3
−400
−200
0
200
400
600
(Difference in CO2 Storage)/Gtonne

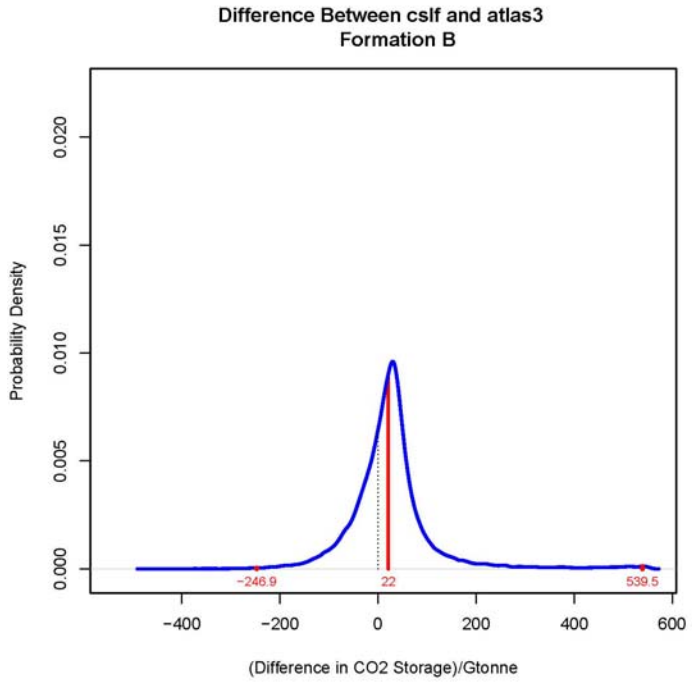
Difference Between cslf and atlas3
Formation B
Probability Density
0.000
0.005
0.010
0.015
0.020
−246.9
22
539.5
−400
−200
0
200
400
600
(Difference in CO2 Storage)/Gtonne

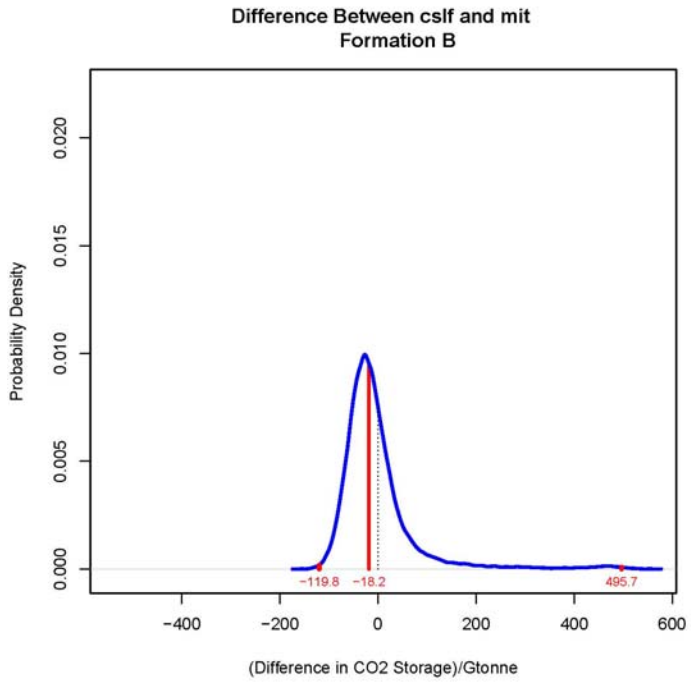
Difference Between cslf and mit
Formation B
Probability Density
0.000
0.005
0.010
0.015
0.020
−119.8
−18.2
495.7
−400
−200
0
200
400
600
(Difference in CO2 Storage)/Gtonne

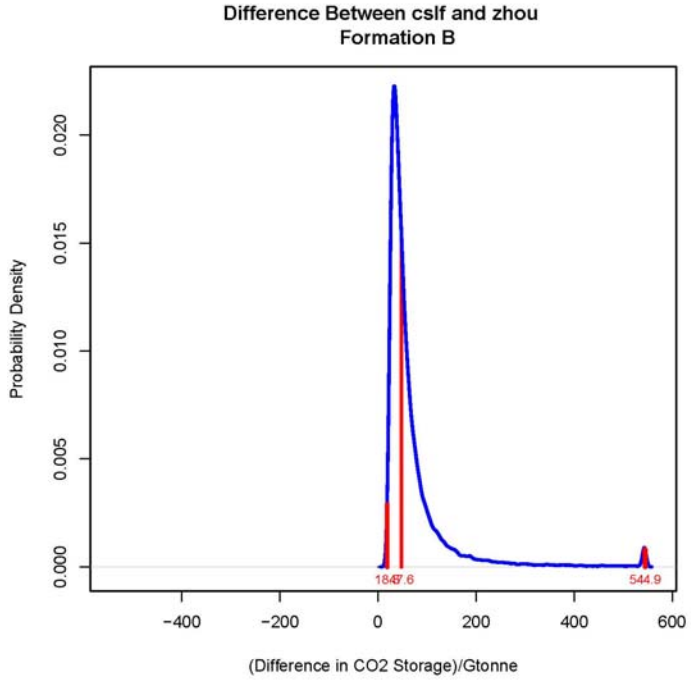
Difference Between cslf and zhou
Formation B
Probability Density
0.000
0.005
0.010
0.015
0.020
18.4
37.6
544.9
−400
−200
0
200
400
600
(Difference in CO2 Storage)/Gtonne

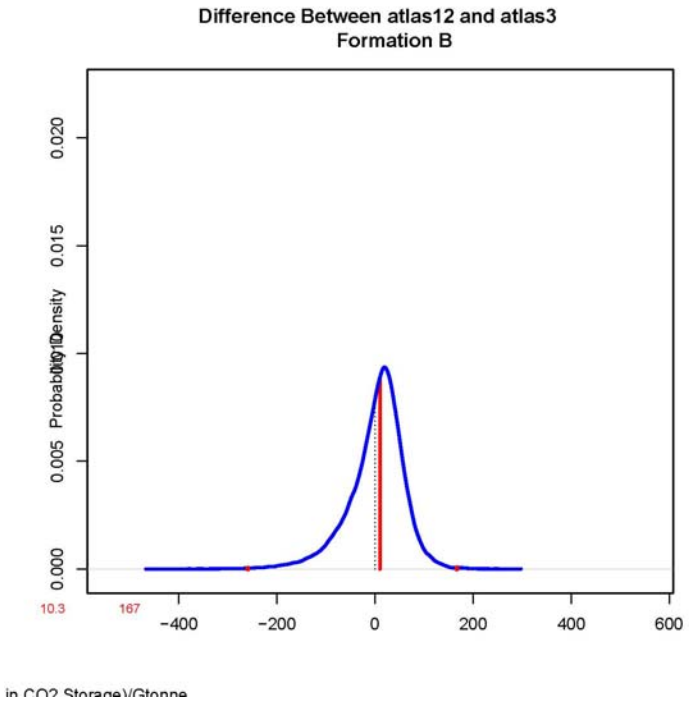
Difference Between atlas12 and atlas3
Formation B
0.020
0.015
0.010
0.005
0.000
10.3
167
−400
−200
0
200
400
600

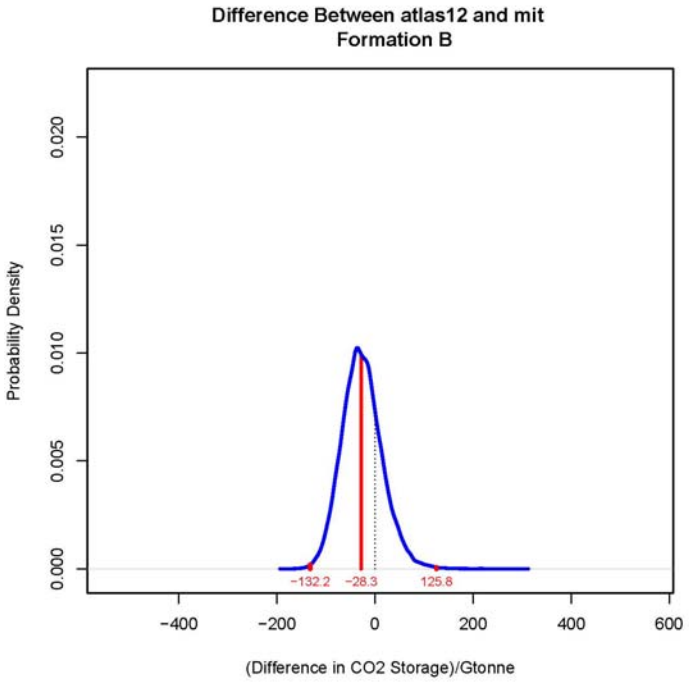
Difference Between atlas12 and mit
Formation B
Probability Density
0.020
0.015
0.010
0.005
0.000
−132.2
−28.3
125.8
−400
−200
0
200
400
600
(Difference in CO2 Storage)/Gtonne

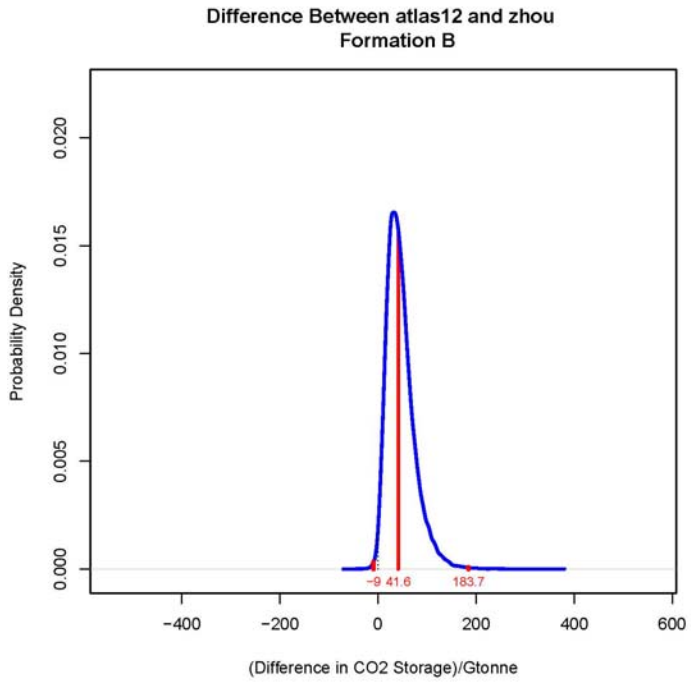
Difference Between atlas12 and zhou
Formation B
Probability Density
0.000
0.005
0.010
0.015
0.020
−9
41.6
183.7
−400
−200
0
200
400
600
(Difference in CO2 Storage)/Gtonne

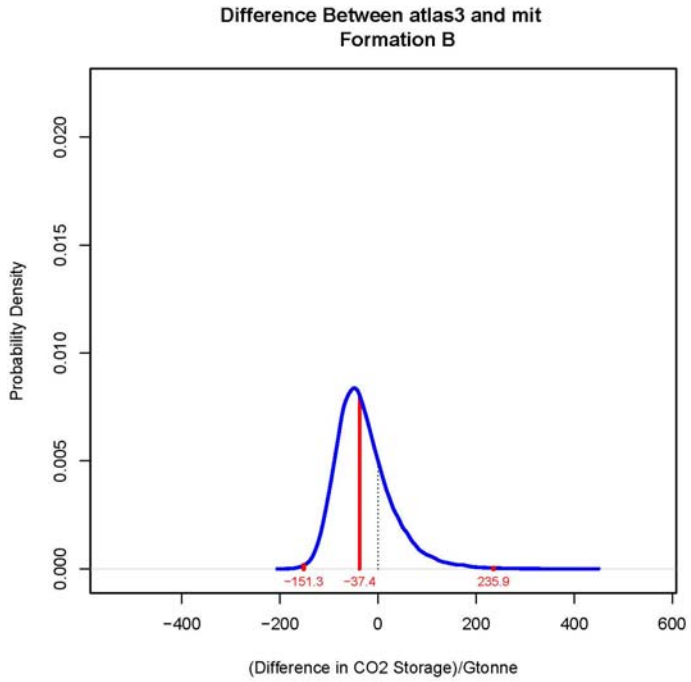
Difference Between atlas3 and mit
Formation B
Probability Density
0.000
0.005
0.010
0.015
0.020
−151.3
−37.4
235.9
−400
−200
0
200
400
600
(Difference in CO2 Storage)/Gtonne

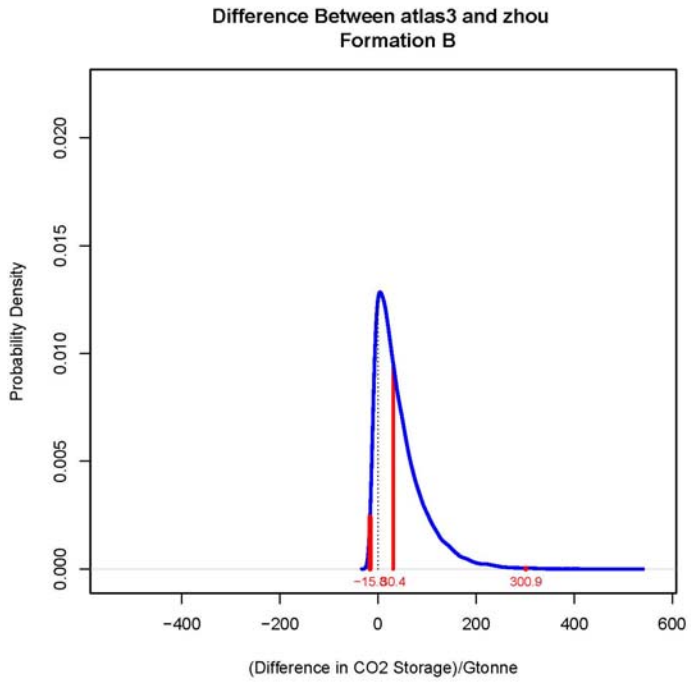
Difference Between atlas3 and zhou
Formation B
Probability Density
0.000
0.005
0.010
0.015
0.020
−15.8
0.4
300.9
−400
−200
0
200
400
600
(Difference in CO2 Storage)/Gtonne

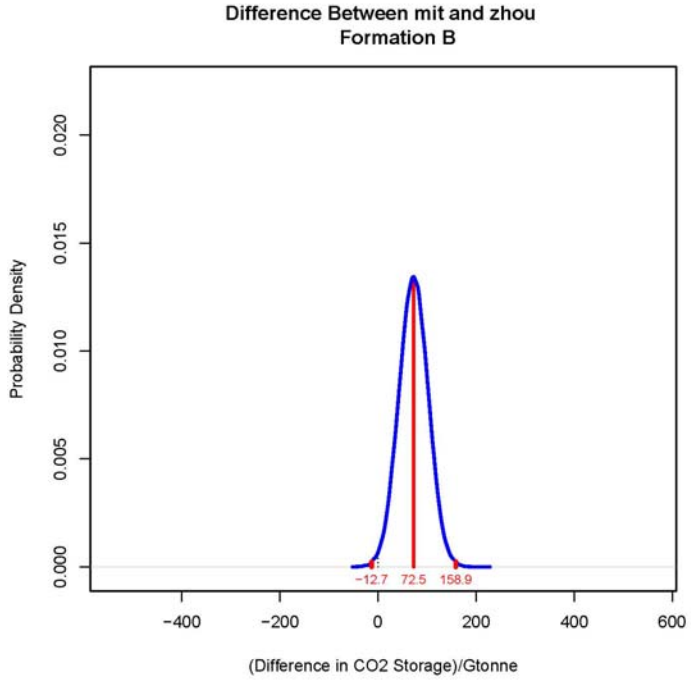
Difference Between mit and zhou
Formation B
Probability Density
0.000
0.005
0.010
0.015
0.020
−12.7
72.5
158.9
−400
−200
0
200
400
600
(Difference in CO2 Storage)/Gtonne

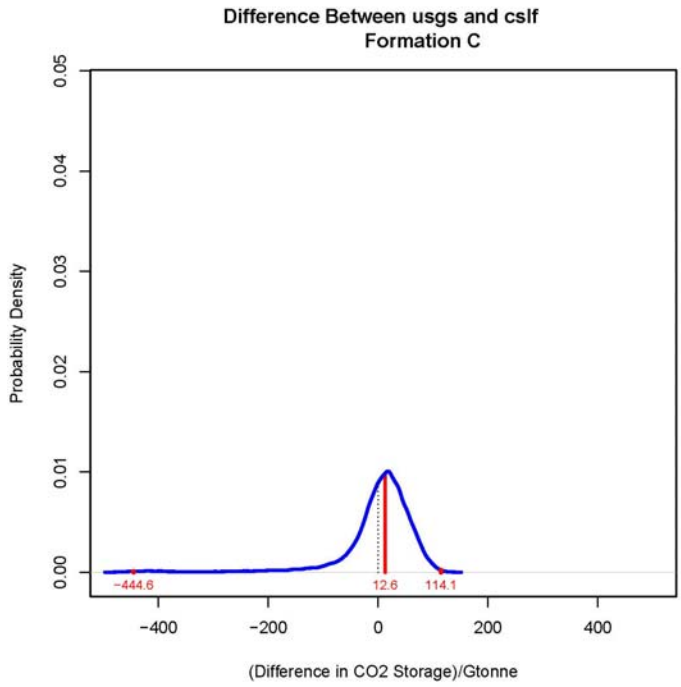
Difference Between usgs and cslf
Formation C
Probability Density
0.00
0.01
0.02
0.03
0.04
0.05
−444.6
12.6
114.1
−400
−200
0
200
400
(Difference in CO2 Storage)/Gtonne

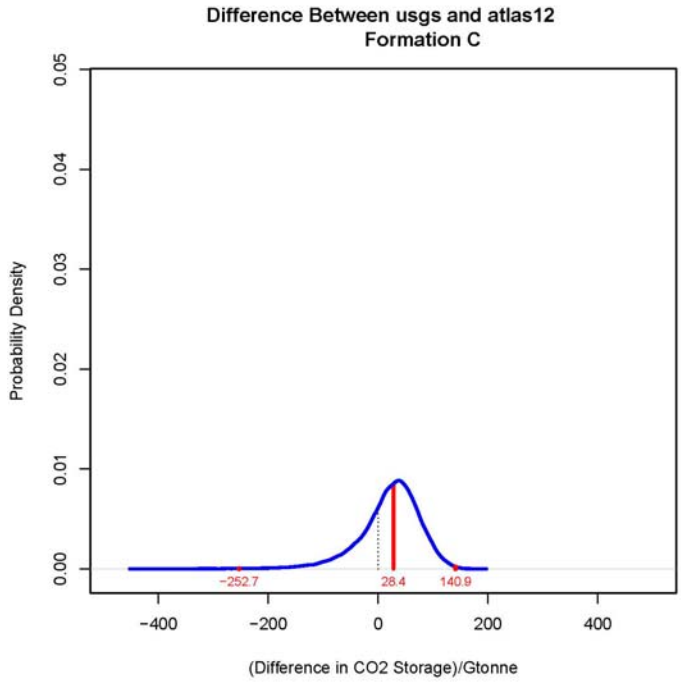
Difference Between usgs and atlas12
Formation C
Probability Density
0.00
0.01
0.02
0.03
0.04
0.05
−252.7
28.4
140.9
−400
−200
0
200
400
(Difference in CO2 Storage)/Gtonne

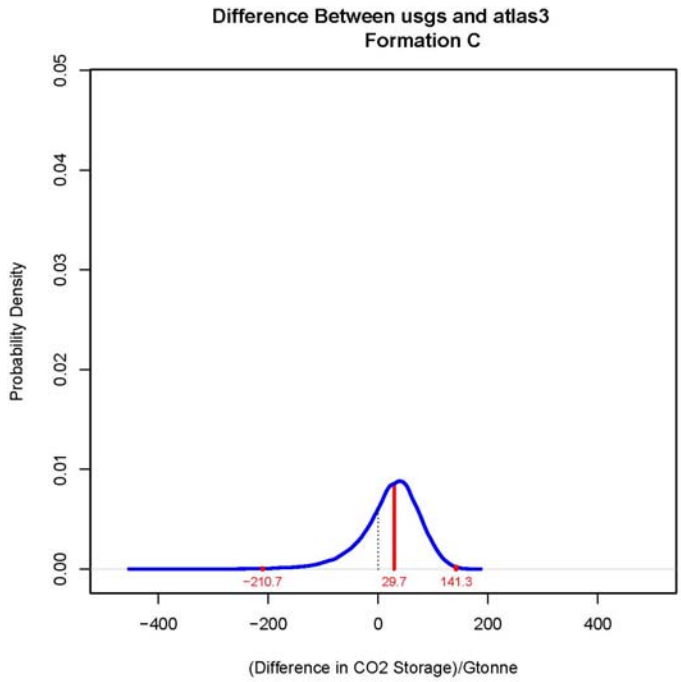
Difference Between usgs and atlas3
Formation C
Probability Density
0.00
0.01
0.02
0.03
0.04
0.05
−210.7
29.7
141.3
−400
−200
0
200
400
(Difference in CO2 Storage)/Gtonne

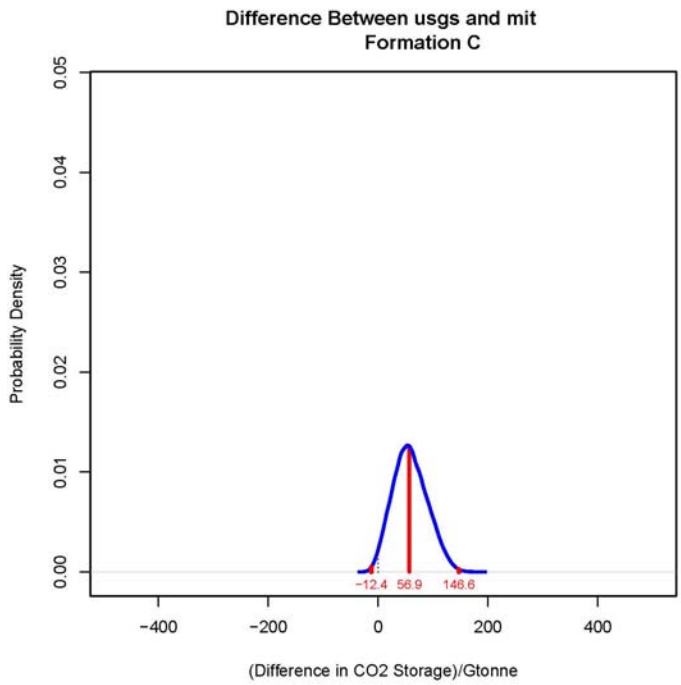
Difference Between usgs and mit
Formation C
Probability Density
0.00
0.01
0.02
0.03
0.04
0.05
−12.4
56.9
146.6
−400
−200
0
200
400
(Difference in CO2 Storage)/Gtonne

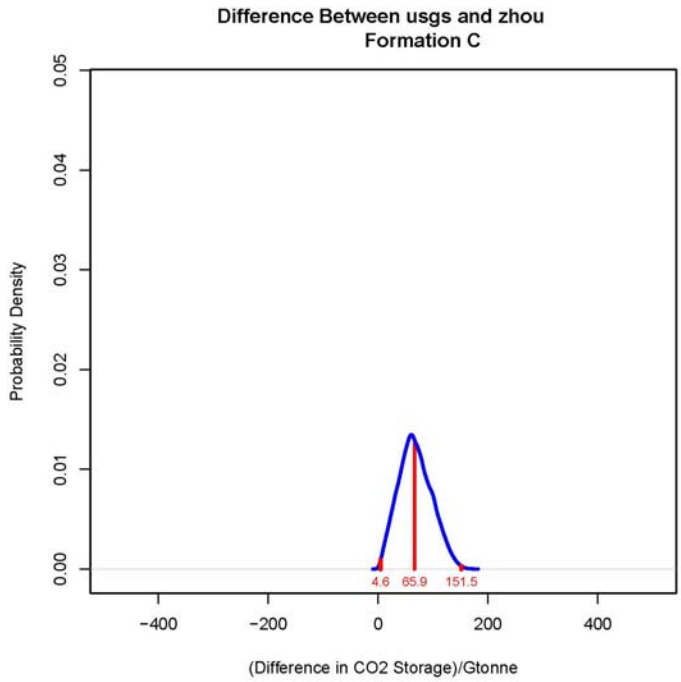
Difference Between usgs and zhou
Formation C
Probability Density
0.00
0.01
0.02
0.03
0.04
0.05
4.6
65.9
151.5
−400
−200
0
200
400
(Difference in CO2 Storage)/Gtonne

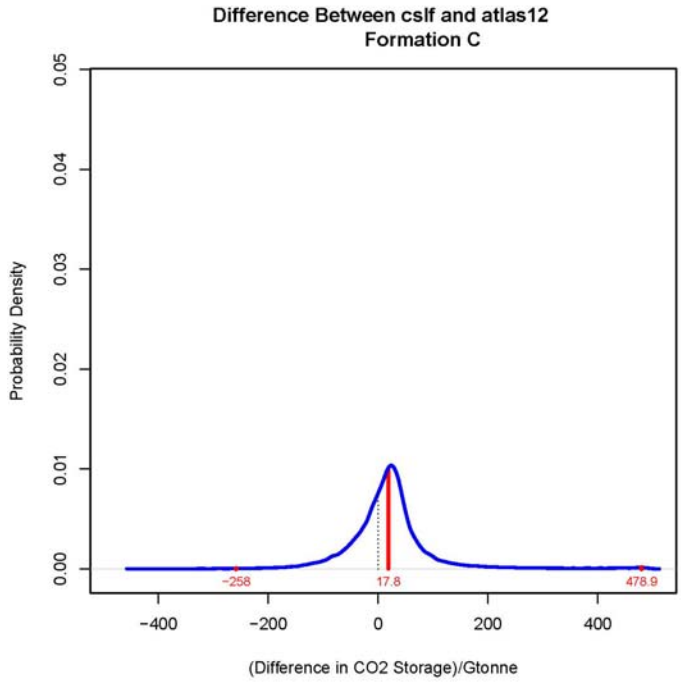
Difference Between cslf and atlas12
Formation C
Probability Density
0.00
0.01
0.02
0.03
0.04
0.05
−258
17.8
478.9
−400
−200
0
200
400
(Difference in CO2 Storage)/Gtonne

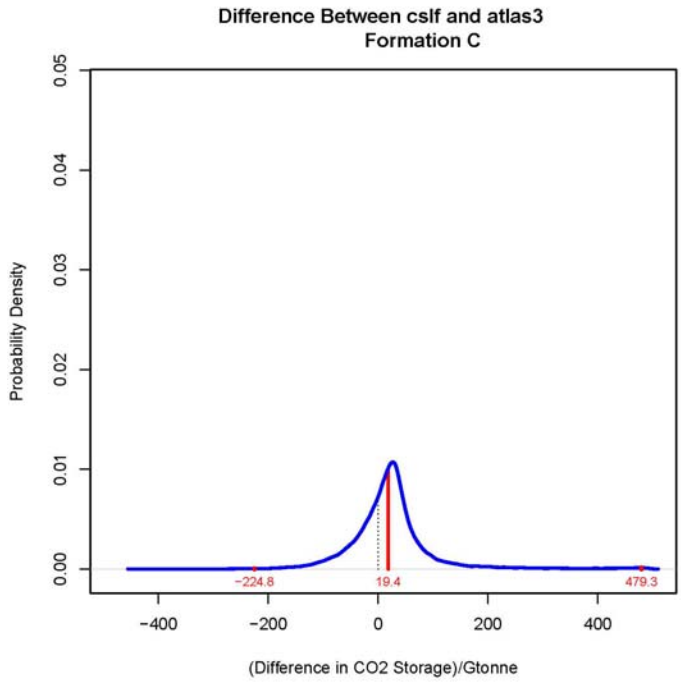
Difference Between cslf and atlas3
Formation C
Probability Density
0.00
0.01
0.02
0.03
0.04
0.05
−224.8
19.4
479.3
−400
−200
0
200
400
(Difference in CO2 Storage)/Gtonne

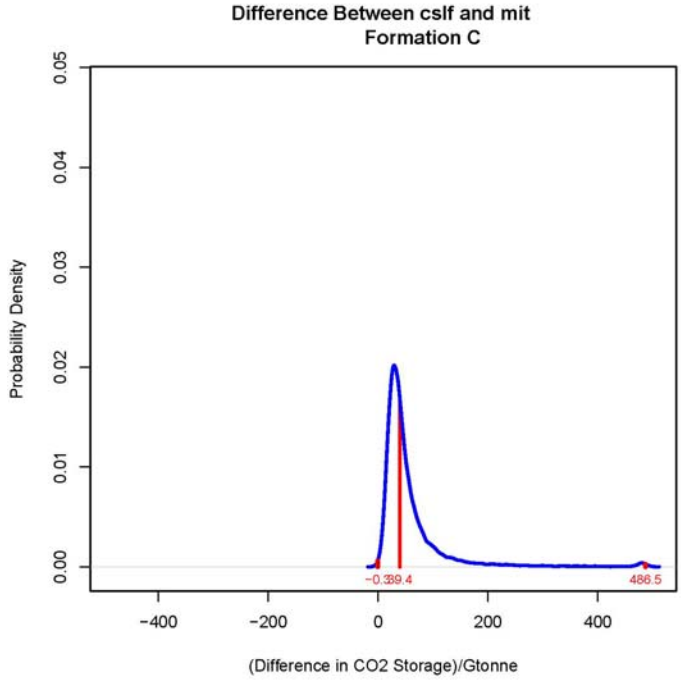
Difference Between cslf and mit
Formation C
Probability Density
0.00
0.01
0.02
0.03
0.04
0.05
−0.3
39.4
486.5
−400
−200
0
200
400
(Difference in CO2 Storage)/Gtonne

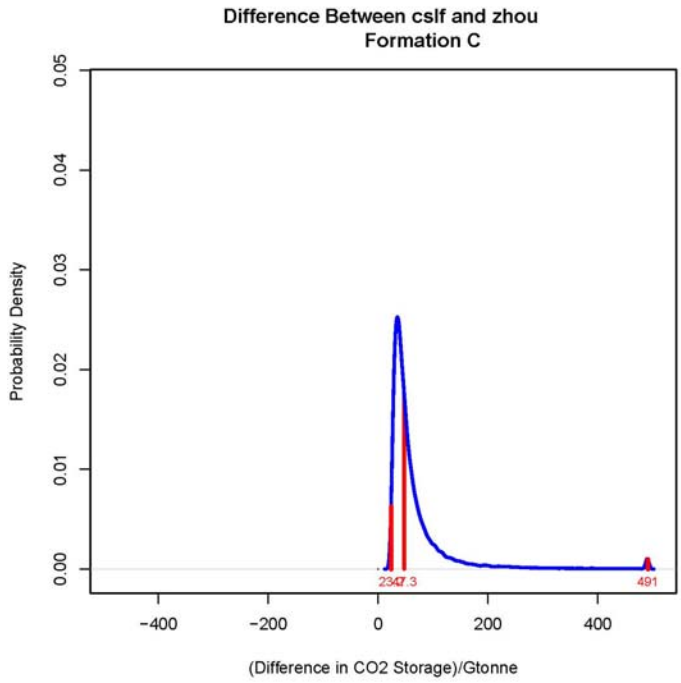
Difference Between cslf and zhou
Formation C
Probability Density
0.00
0.01
0.02
0.03
0.04
0.05
23
47.3
491
−400
−200
0
200
400
(Difference in CO2 Storage)/Gtonne

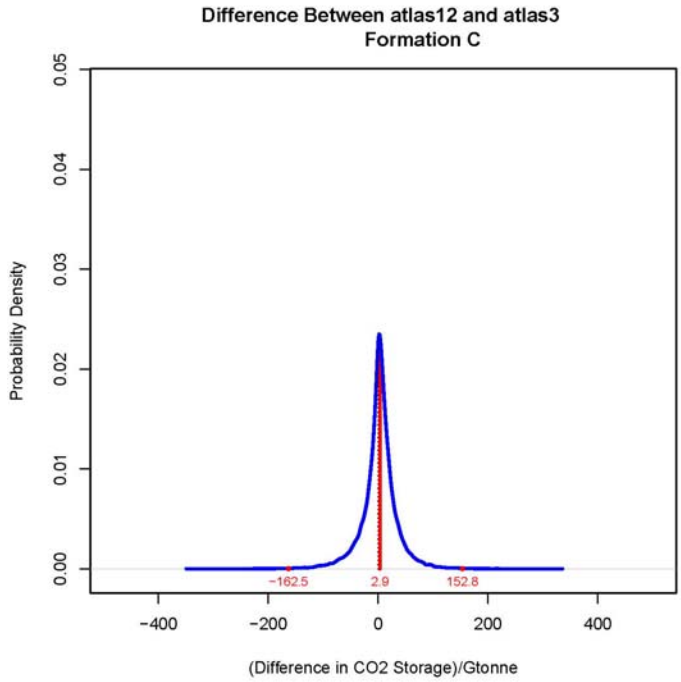
Difference Between atlas12 and atlas3
Formation C
Probability Density
0.00
0.01
0.02
0.03
0.04
0.05
−162.5
2.9
152.8
−400
−200
0
200
400
(Difference in CO2 Storage)/Gtonne

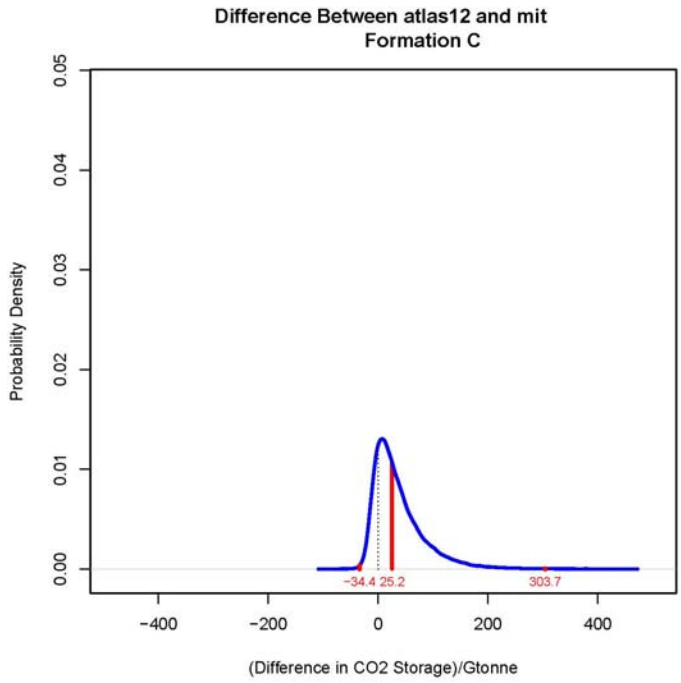
Difference Between atlas12 and mit
Formation C
Probability Density
0.00
0.01
0.02
0.03
0.04
0.05
−34.4
25.2
303.7
−400
−200
0
200
400
(Difference in CO2 Storage)/Gtonne

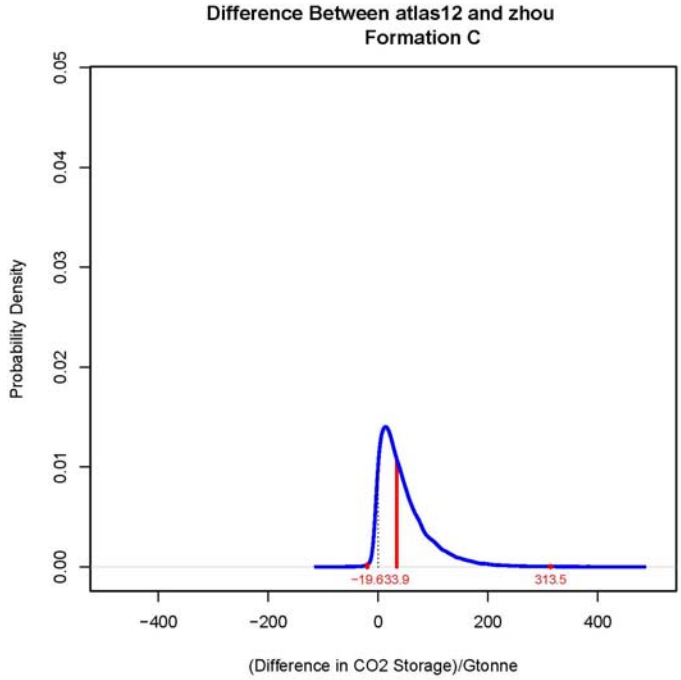
Difference Between atlas12 and zhou
Formation C
Probability Density
0.00
0.01
0.02
0.03
0.04
0.05
−19.633.9
313.5
−400
−200
0
200
400
(Difference in CO2 Storage)/Gtonne

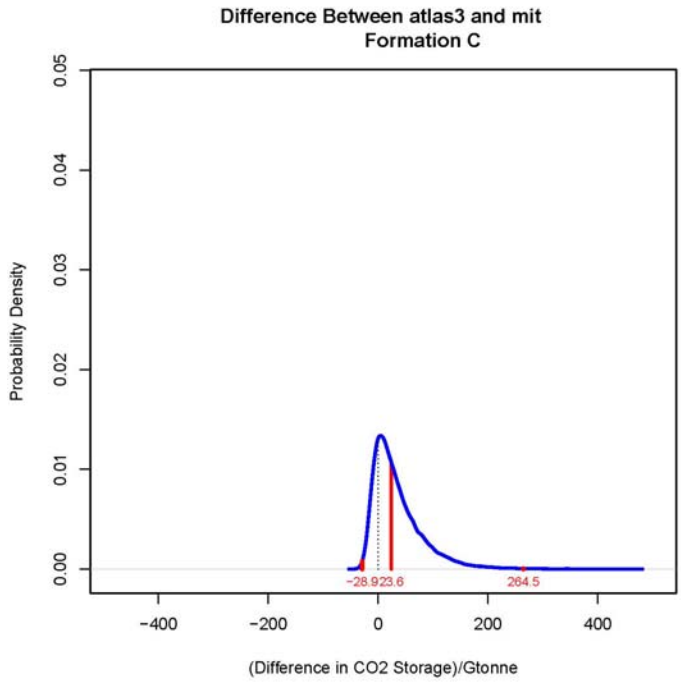
Difference Between atlas3 and mit
Formation C
Probability Density
0.00
0.01
0.02
0.03
0.04
0.05
−28.9
23.6
264.5
−400
−200
0
200
400
(Difference in CO2 Storage)/Gtonne

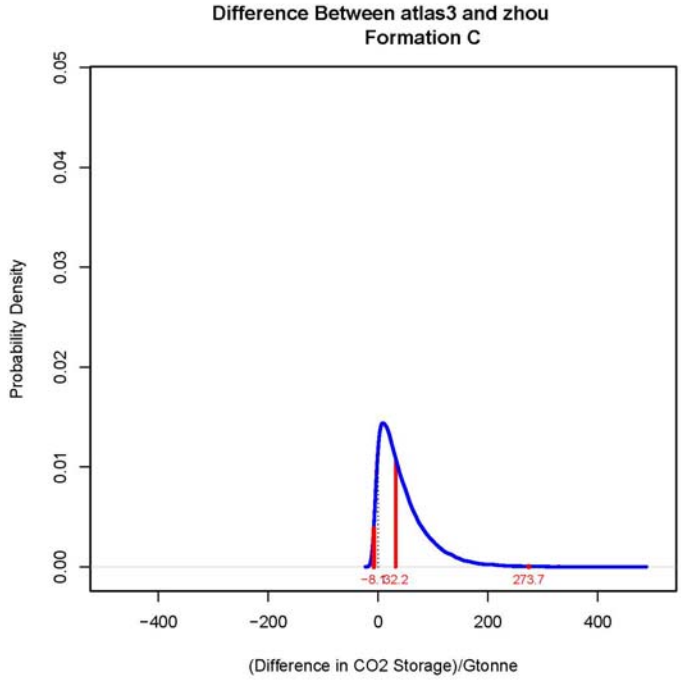
Difference Between atlas3 and zhou
Formation C
Probability Density
0.00
0.01
0.02
0.03
0.04
0.05
−8.1
32.2
273.7
−400
−200
0
200
400
(Difference in CO2 Storage)/Gtonne

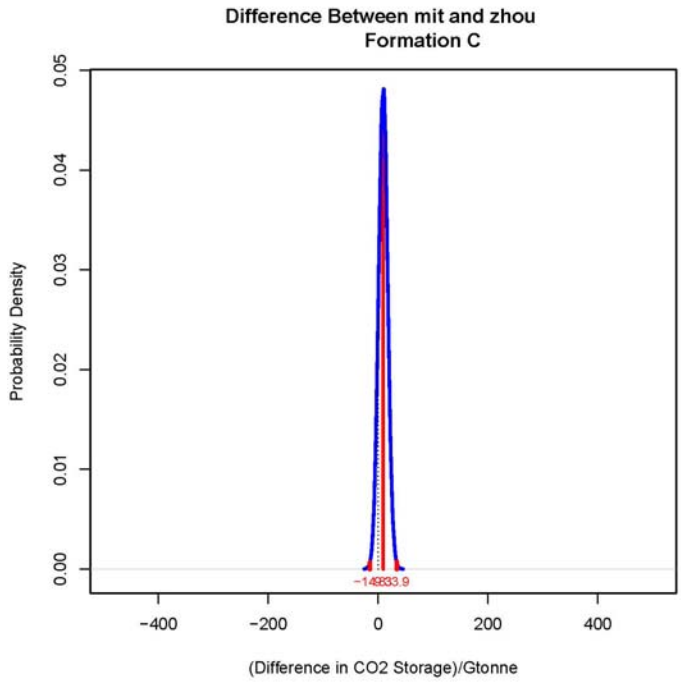
Difference Between mit and zhou
Formation C
Probability Density
0.00
0.01
0.02
0.03
0.04
0.05
−14833.9
−400
−200
0
200
400
(Difference in CO2 Storage)/Gtonne

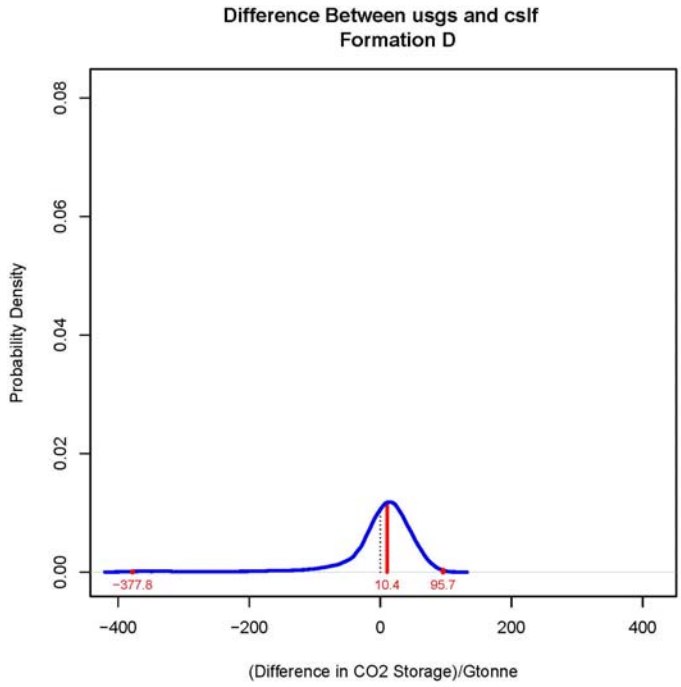
Difference Between usgs and cslf
Formation D
Probability Density
0.00
0.02
0.04
0.06
0.08
−377.8
10.4
95.7
−400
−200
0
200
400
(Difference in CO2 Storage)/Gtonne

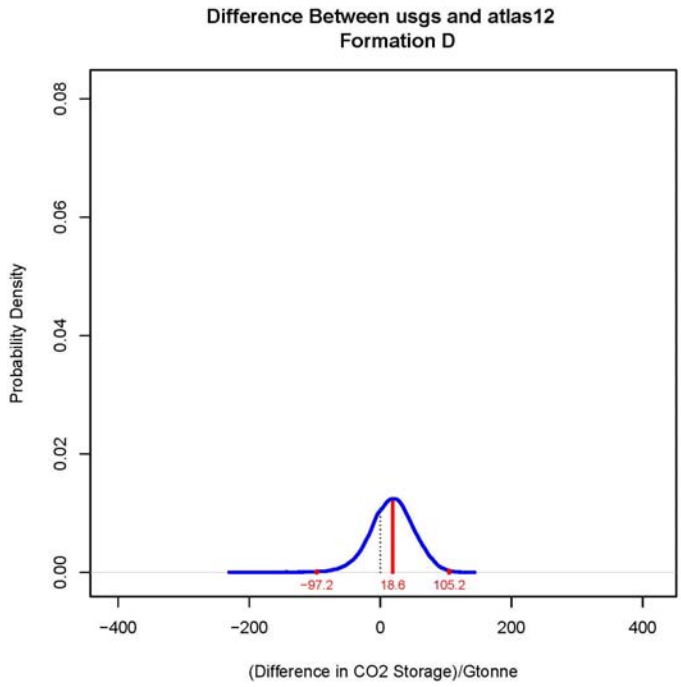
Difference Between usgs and atlas12
Formation D
Probability Density
0.00
0.02
0.04
0.06
0.08
−97.2
18.6
105.2
−400
−200
0
200
400
(Difference in CO2 Storage)/Gtonne

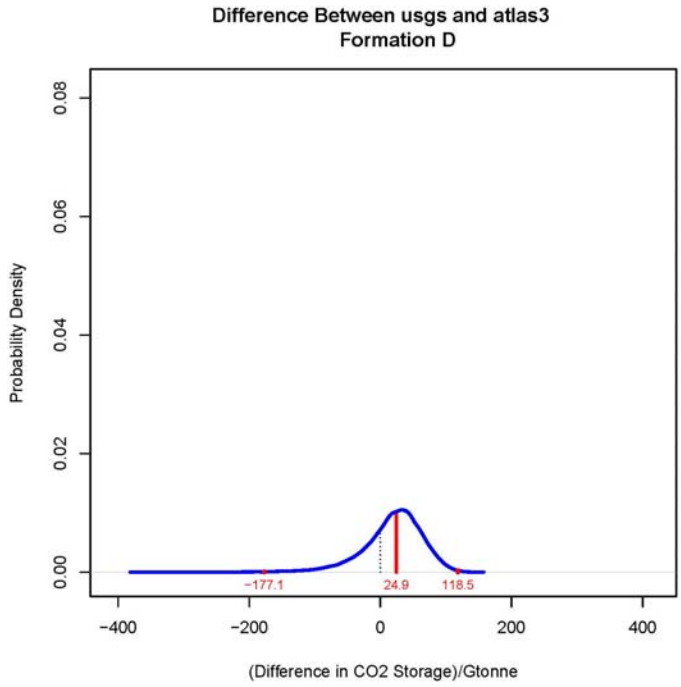
Difference Between usgs and atlas3
Formation D
Probability Density
0.00
0.02
0.04
0.06
0.08
−177.1
24.9
118.5
−400
−200
0
200
400
(Difference in CO2 Storage)/Gtonne

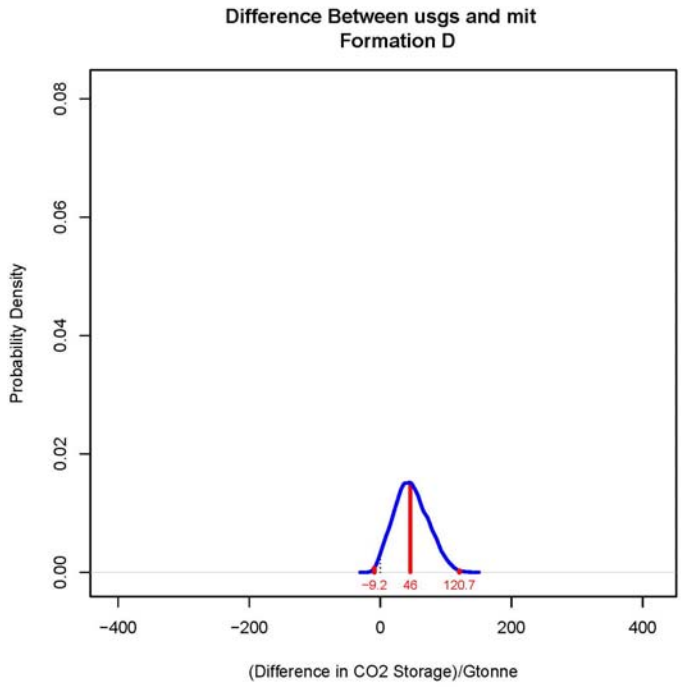
Difference Between usgs and mit
Formation D
Probability Density
0.00
0.02
0.04
0.06
0.08
-9.2
46
120.7
-400
-200
0
200
400
(Difference in CO2 Storage)/Gtonne

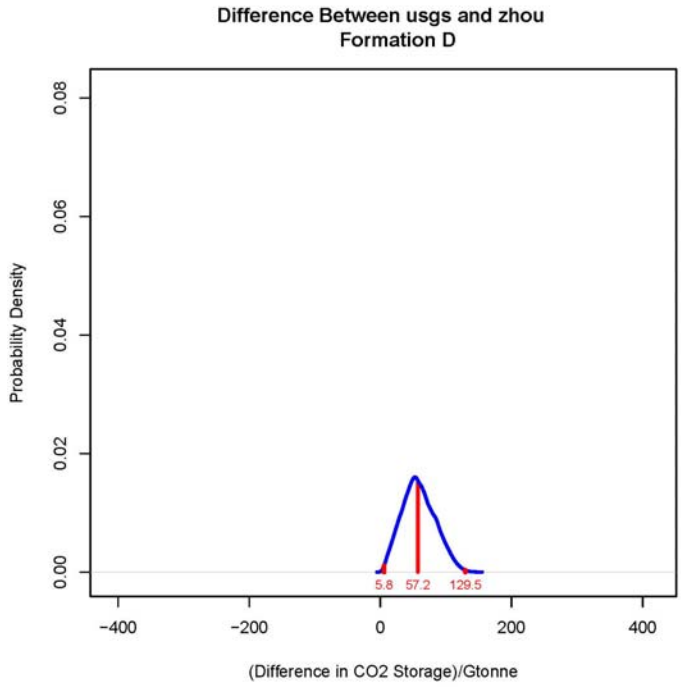
Difference Between usgs and zhou
Formation D
Probability Density
0.00
0.02
0.04
0.06
0.08
5.8
57.2
129.5
-400
-200
0
200
400
(Difference in CO2 Storage)/Gtonne

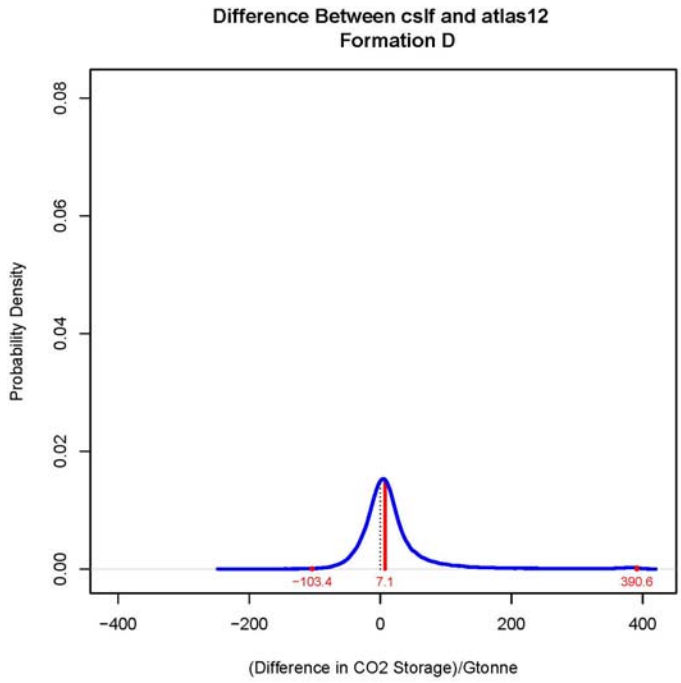
Difference Between cslf and atlas12
Formation D
Probability Density
0.00
0.02
0.04
0.06
0.08
−103.4
7.1
390.6
−400
−200
0
200
400
(Difference in CO2 Storage)/Gtonne

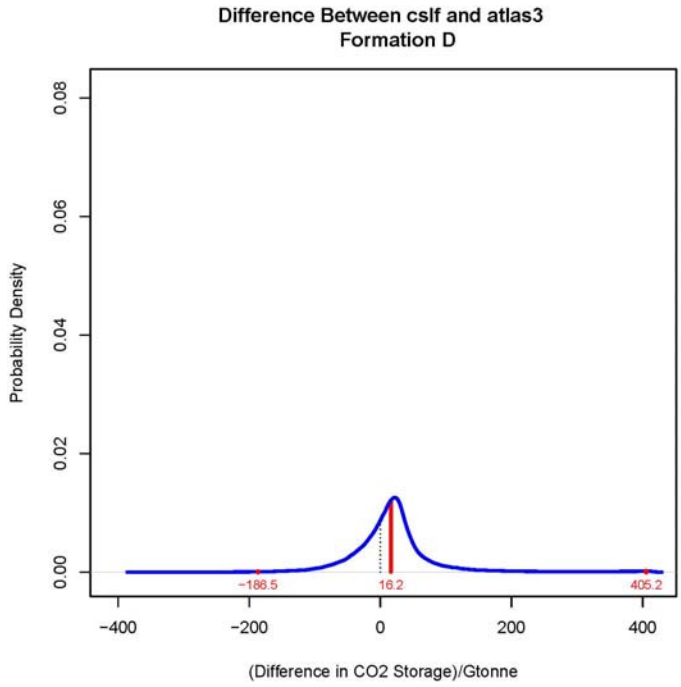
Difference Between cslf and atlas3
Formation D
Probability Density
0.00
0.02
0.04
0.06
0.08
−186.5
16.2
405.2
−400
−200
0
200
400
(Difference in CO2 Storage)/Gtonne

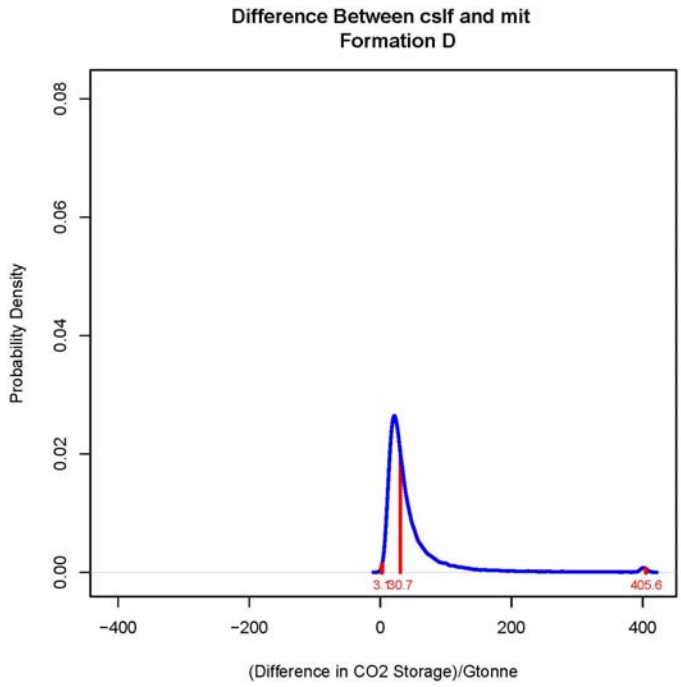
Difference Between cslf and mit
Formation D
Probability Density
0.00
0.02
0.04
0.06
0.08
3.130.7
405.6
−400
−200
0
200
400
(Difference in CO2 Storage)/Gtonne

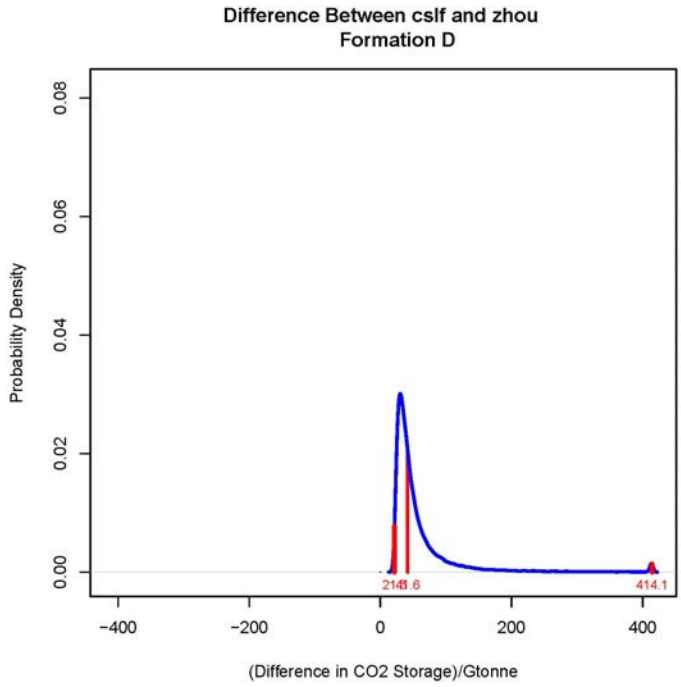
Difference Between cslf and zhou
Formation D
Probability Density
0.00
0.02
0.04
0.06
0.08
214.6
414.1
−400
−200
0
200
400
(Difference in CO2 Storage)/Gtonne

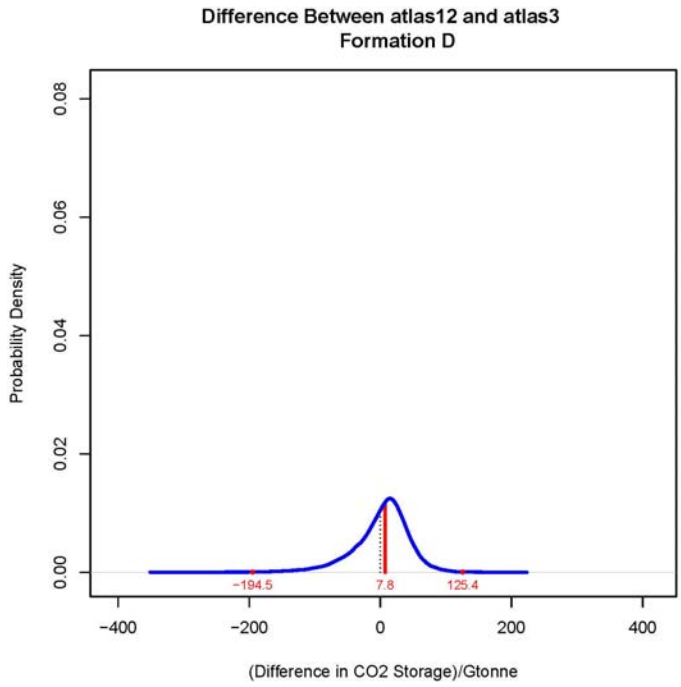
Difference Between atlas12 and atlas3
Formation D
Probability Density
0.00
0.02
0.04
0.06
0.08
−194.5
7.8
125.4
−400
−200
0
200
400
(Difference in CO2 Storage)/Gtonne

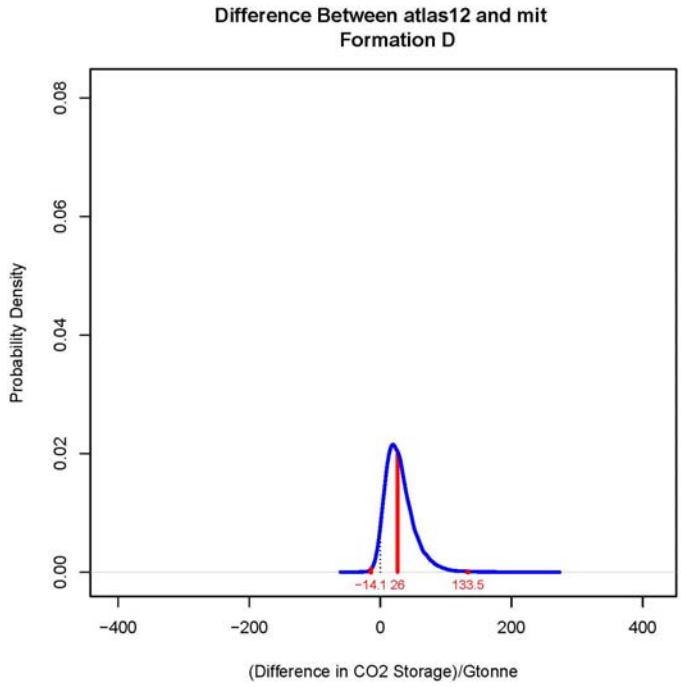
Difference Between atlas12 and mit
Formation D
Probability Density
0.00
0.02
0.04
0.06
0.08
−14.1
26
133.5
−400
−200
0
200
400
(Difference in CO2 Storage)/Gtonne

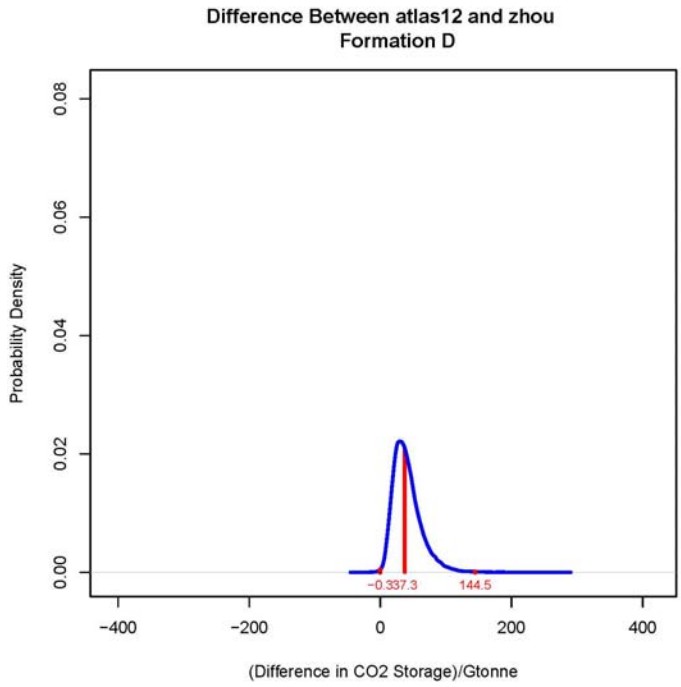
Difference Between atlas12 and zhou
Formation D
Probability Density
0.00
0.02
0.04
0.06
0.08
−0.337.3
144.5
−400
−200
0
200
400
(Difference in CO2 Storage)/Gtonne

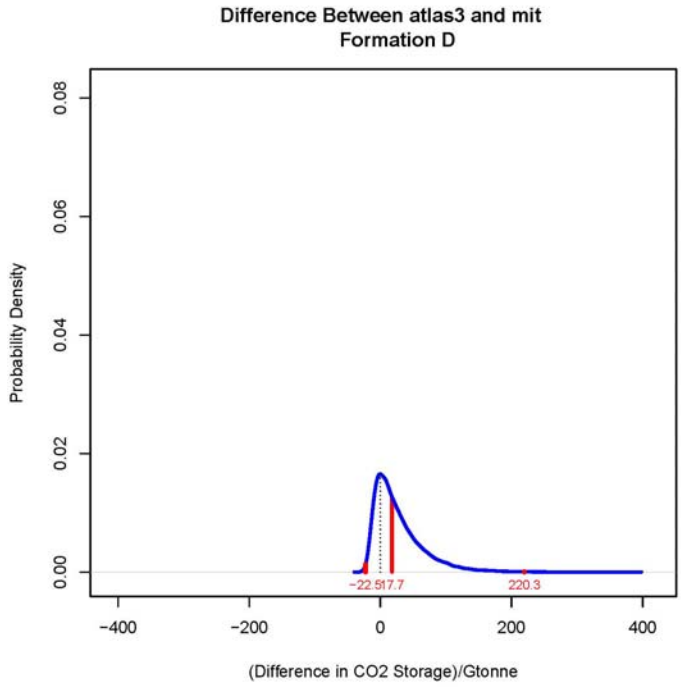
Difference Between atlas3 and mit
Formation D
Probability Density
0.00
0.02
0.04
0.06
0.08
−22.517.7
220.3
−400
−200
0
200
400
(Difference in CO2 Storage)/Gtonne

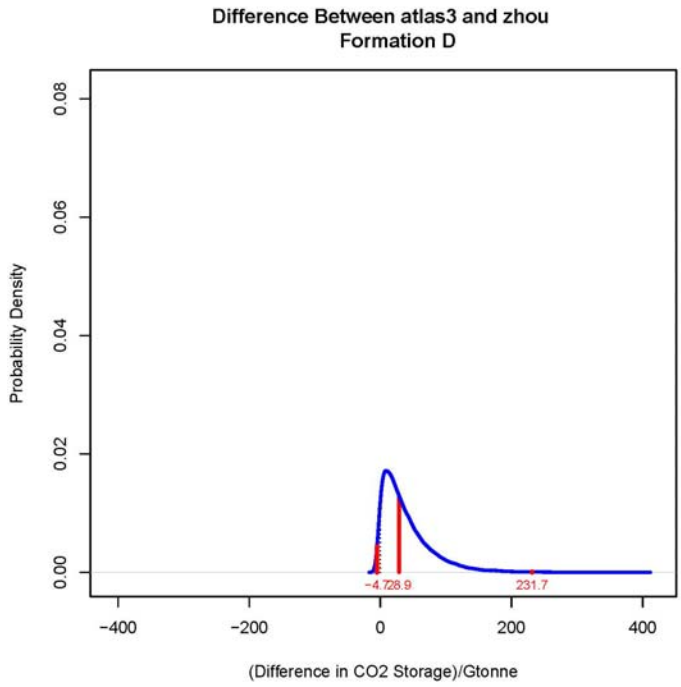
Difference Between atlas3 and zhou
Formation D
Probability Density
0.00
0.02
0.04
0.06
0.08
−4.7
28.9
231.7
−400
−200
0
200
400
(Difference in CO2 Storage)/Gtonne

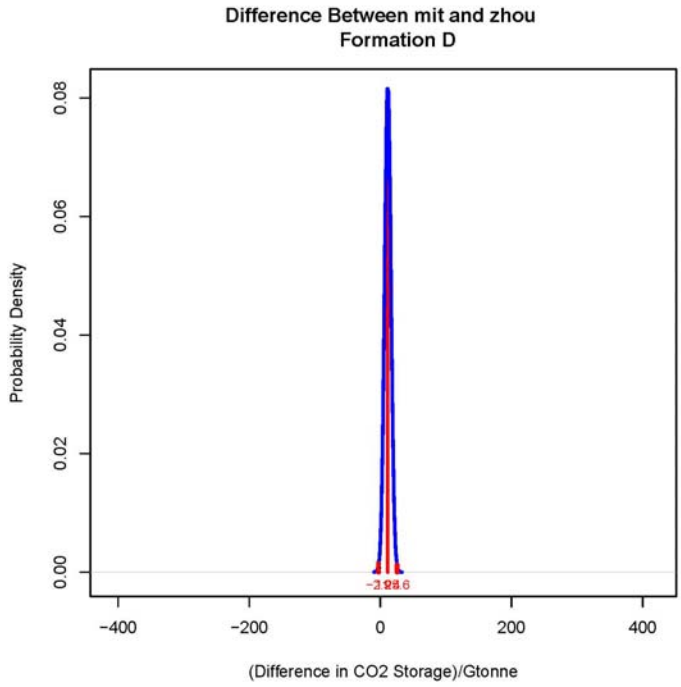
Difference Between mit and zhou
Formation D
Probability Density
0.00
0.02
0.04
0.06
0.08
−400
−200
0
200
400
(Difference in CO2 Storage)/Gtonne

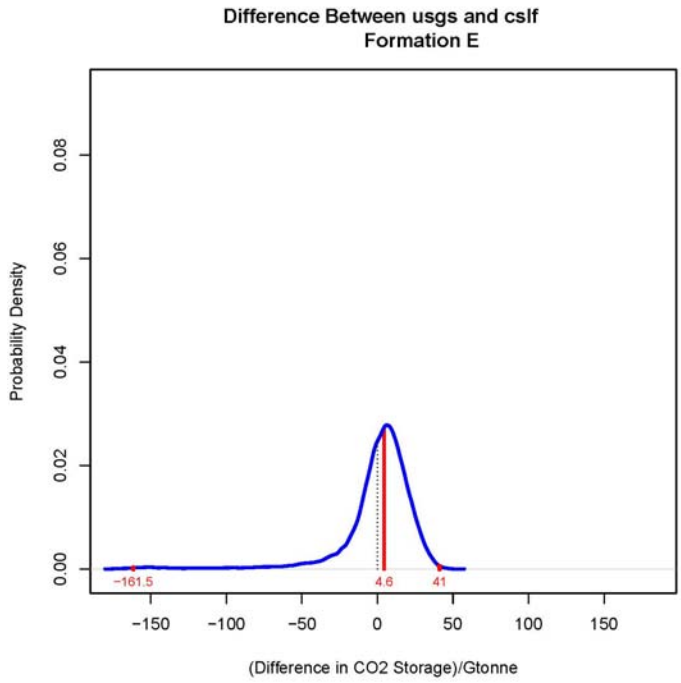
Difference Between usgs and cslf
Formation E
Probability Density
0.00
0.02
0.04
0.06
0.08
−161.5
4.6
41
−150
−100
−50
0
50
100
150
(Difference in CO2 Storage)/Gtonne

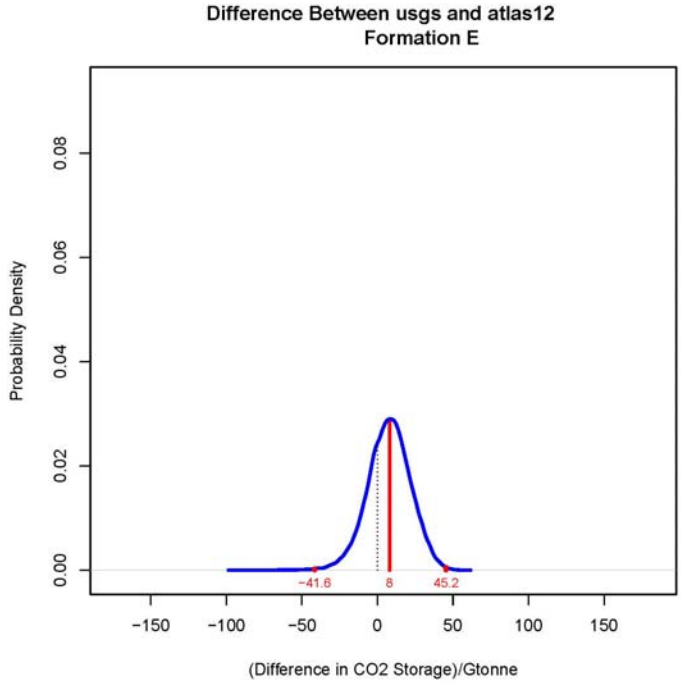
Difference Between usgs and atlas12
Formation E
Probability Density
0.00
0.02
0.04
0.06
0.08
−41.6
8
45.2
−150
−100
−50
0
50
100
150
(Difference in CO2 Storage)/Gtonne

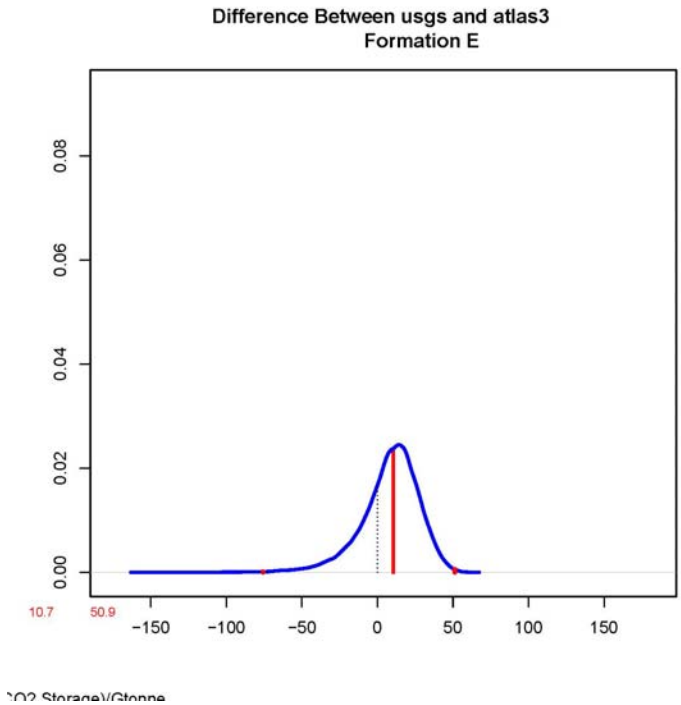
Difference Between usgs and atlas3
Formation E
0.08
0.06
0.04
0.02
0.00
10.7
50.9
−150
−100
−50
0
50
100
150

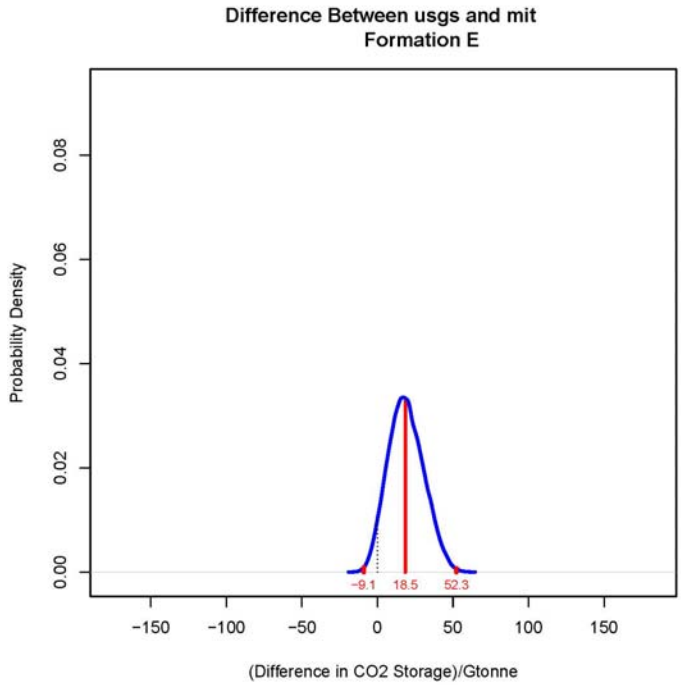
Difference Between usgs and mit
Formation E
Probability Density
0.08
0.06
0.04
0.02
0.00
−9.1
18.5
52.3
−150
−100
−50
0
50
100
150
(Difference in CO2 Storage)/Gtonne

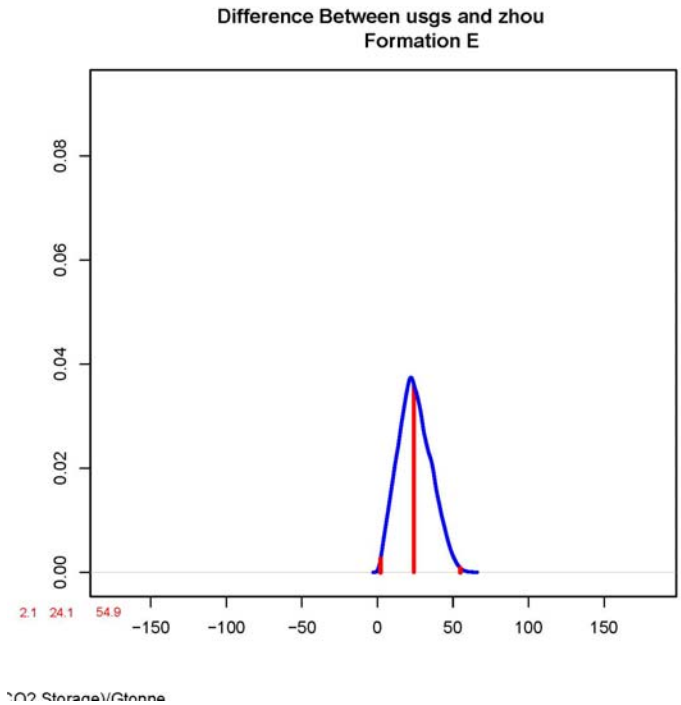
Difference Between usgs and zhou
Formation E
0.08
0.06
0.04
0.02
0.00
2.1
24.1
54.9
−150
−100
−50
0
50
100
150

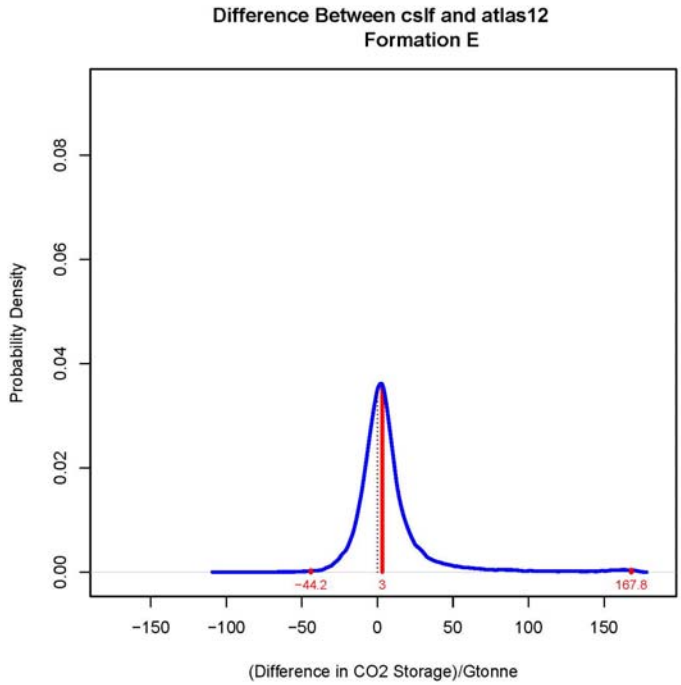
Difference Between cslf and atlas12
Formation E
Probability Density
0.08
0.06
0.04
0.02
0.00
−44.2
3
167.8
−150
−100
−50
0
50
100
150
(Difference in CO2 Storage)/Gtonne

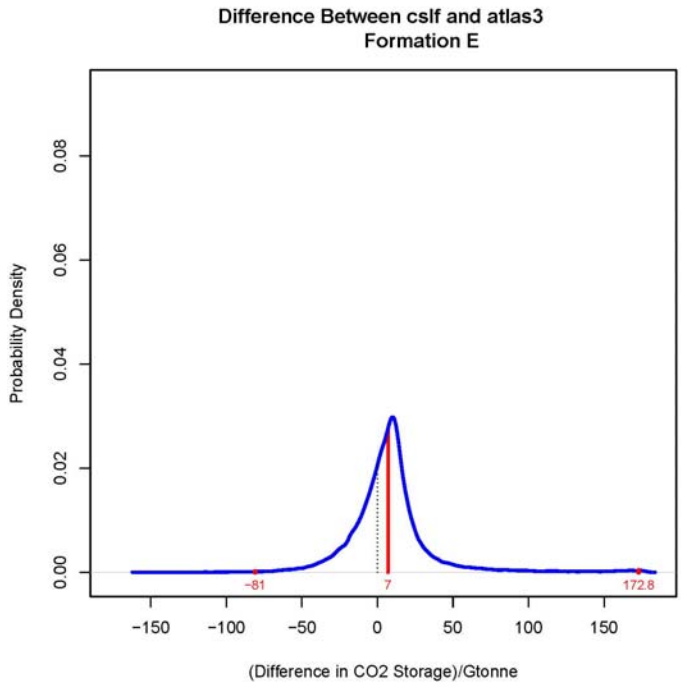
Difference Between cslf and atlas3
Formation E
Probability Density
0.00
0.02
0.04
0.06
0.08
−81
7
172.8
−150
−100
−50
0
50
100
150
(Difference in CO2 Storage)/Gtonne

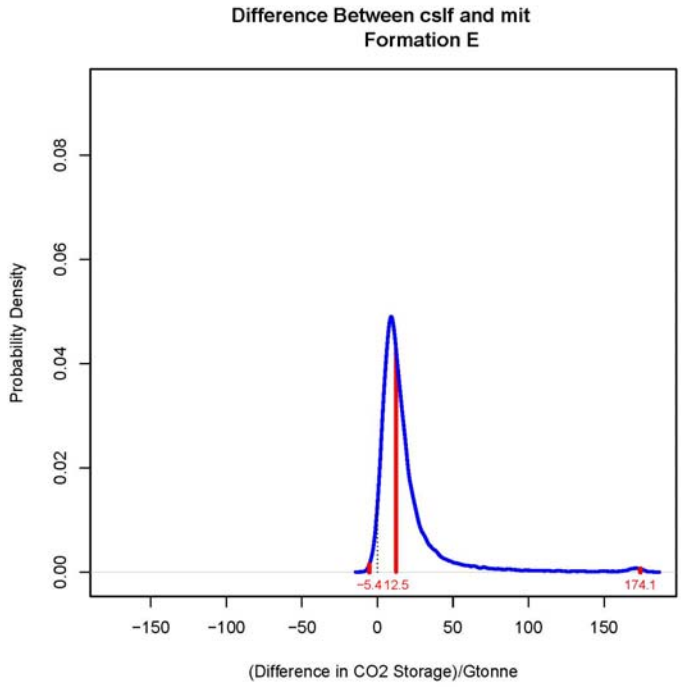
Difference Between cslf and mit
Formation E
Probability Density
0.00
0.02
0.04
0.06
0.08
−5.4
12.5
174.1
−150
−100
−50
0
50
100
150
(Difference in CO2 Storage)/Gtonne

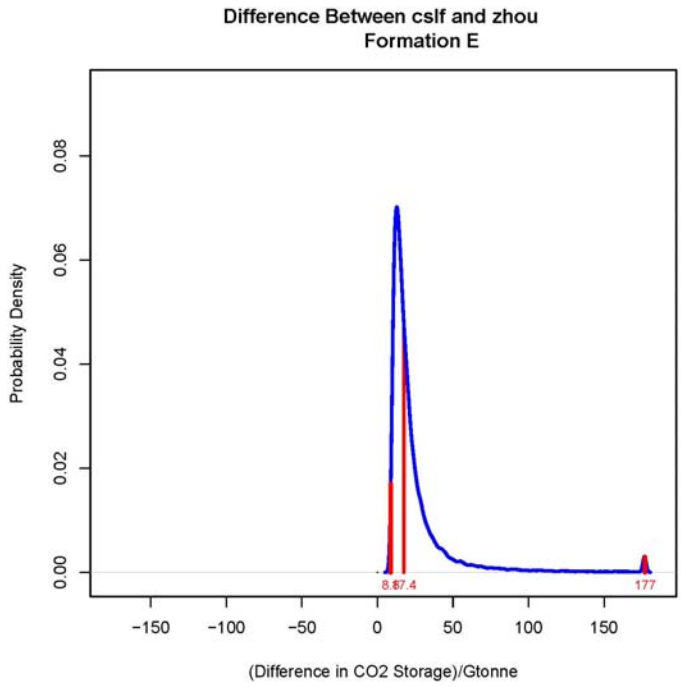
Difference Between cslf and zhou
Formation E
Probability Density
0.00
0.02
0.04
0.06
0.08
8.8
7.4
177
−150
−100
−50
0
50
100
150
(Difference in CO2 Storage)/Gtonne

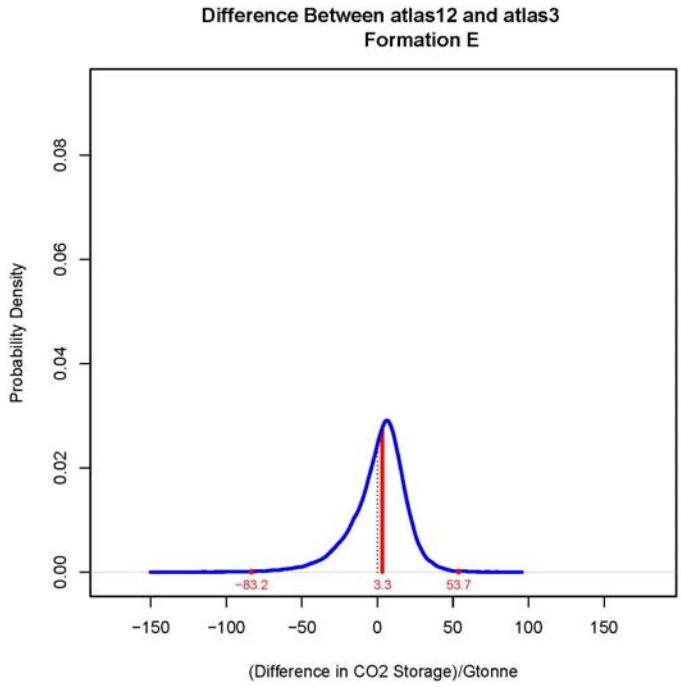
Difference Between atlas12 and atlas3
Formation E
Probability Density
0.00
0.02
0.04
0.06
0.08
−83.2
3.3
53.7
−150
−100
−50
0
50
100
150
(Difference in CO2 Storage)/Gtonne

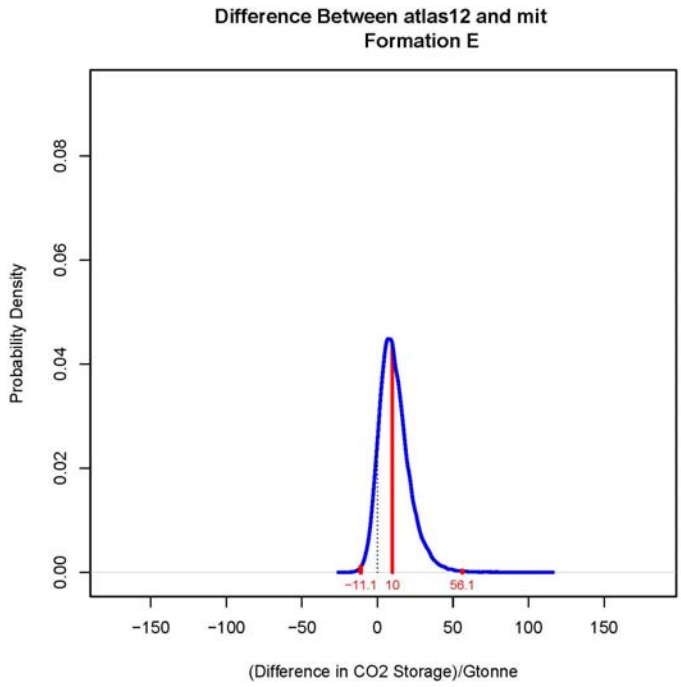
Difference Between atlas12 and mit
Formation E
Probability Density
0.00
0.02
0.04
0.06
0.08
−11.1
10
56.1
−150
−100
−50
0
50
100
150
(Difference in CO2 Storage)/Gtonne

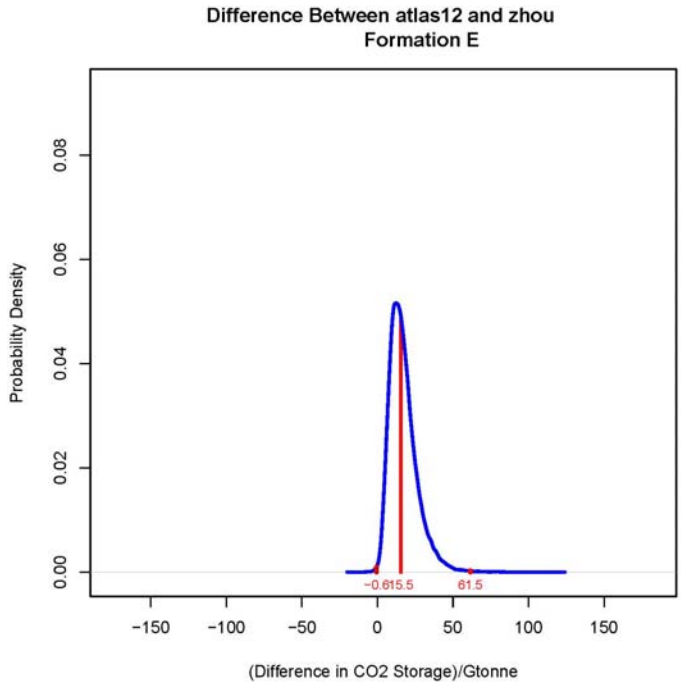
Difference Between atlas12 and zhou
Formation E
Probability Density
0.00
0.02
0.04
0.06
0.08
−0.615.5
61.5
−150
−100
−50
0
50
100
150
(Difference in CO2 Storage)/Gtonne

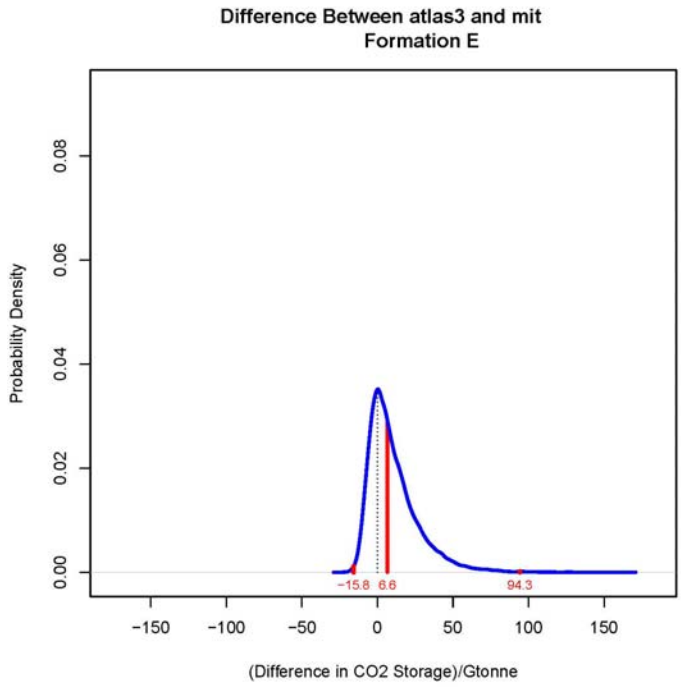
Difference Between atlas3 and mit
Formation E
Probability Density
0.00
0.02
0.04
0.06
0.08
−15.8
6.6
94.3
−150
−100
−50
0
50
100
150
(Difference in CO2 Storage)/Gtonne

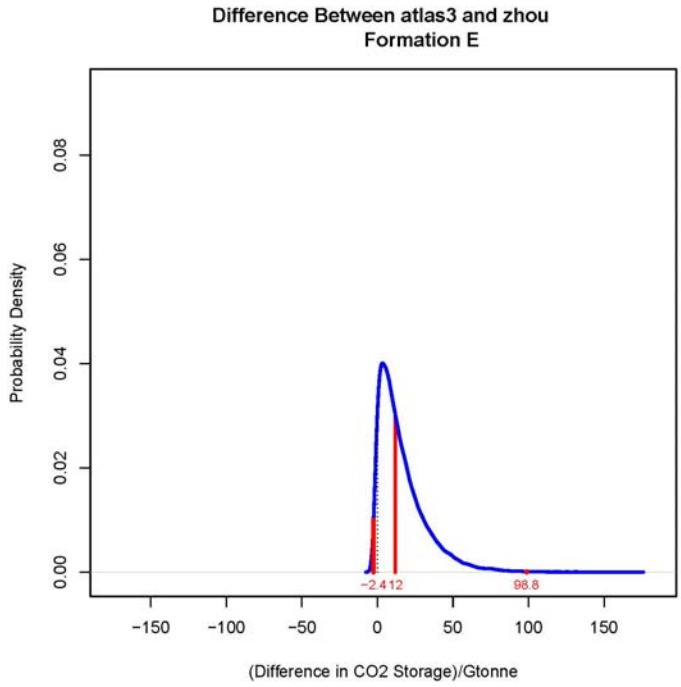
Difference Between atlas3 and zhou
Formation E
Probability Density
0.00
0.02
0.04
0.06
0.08
−2.412
98.8
−150
−100
−50
0
50
100
150
(Difference in CO2 Storage)/Gtonne

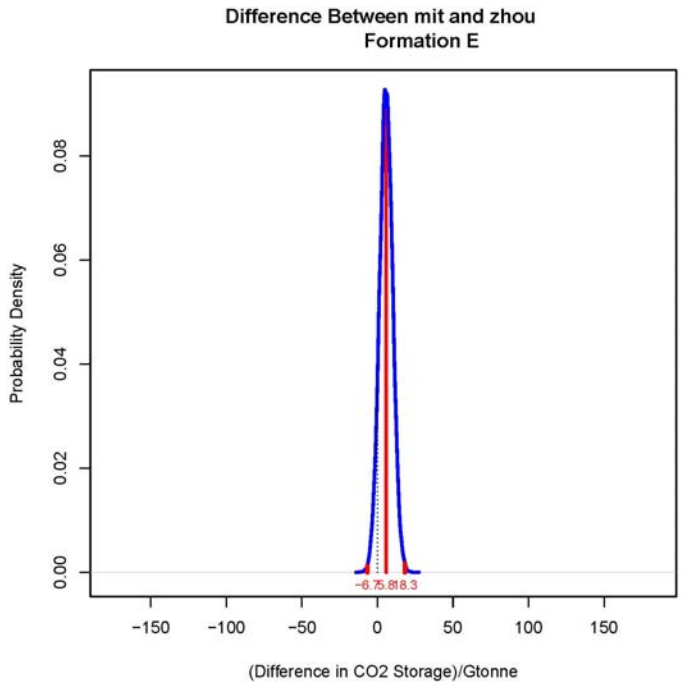
Difference Between mit and zhou
Formation E
Probability Density
0.00
0.02
0.04
0.06
0.08
−6.7 5.8 18.3
−150
−100
−50
0
50
100
150
(Difference in CO2 Storage)/Gtonne

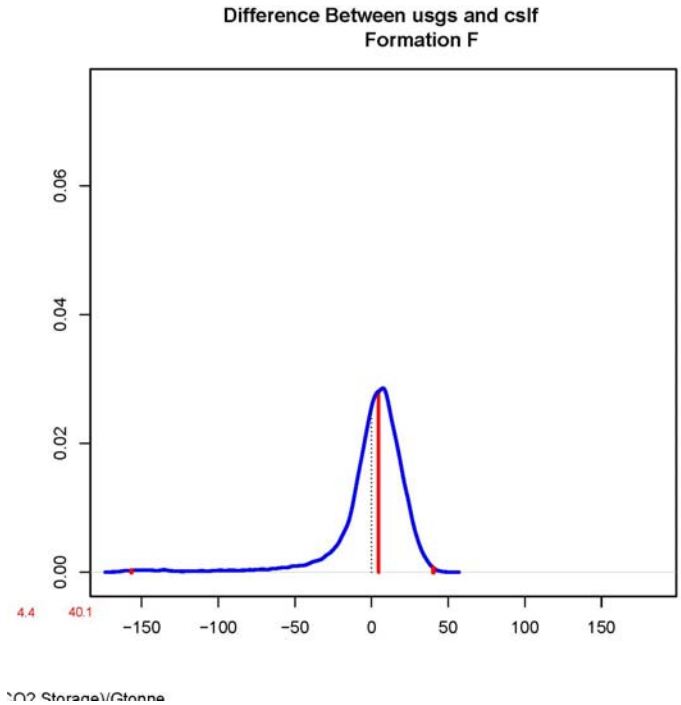
Difference Between usgs and cslf
Formation F
0.00
0.02
0.04
0.06
4.4
40.1
−150
−100
−50
0
50
100
150

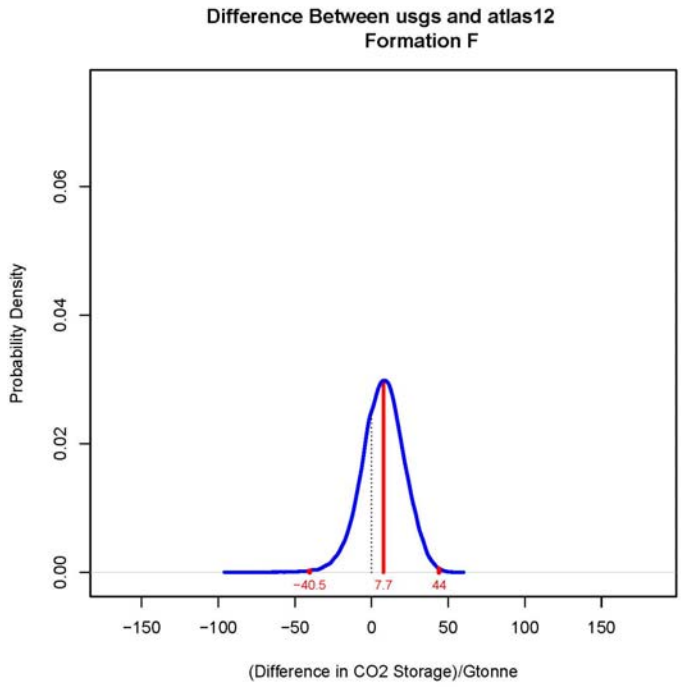
Difference Between usgs and atlas12
Formation F
Probability Density
0.00
0.02
0.04
0.06
−40.5
7.7
44
−150
−100
−50
0
50
100
150
(Difference in CO2 Storage)/Gtonne

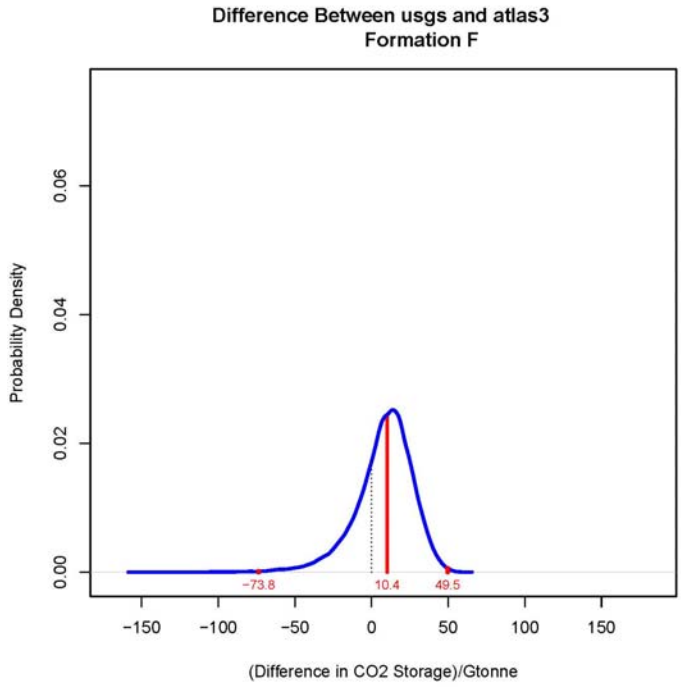
Difference Between usgs and atlas3
Formation F
Probability Density
0.00
0.02
0.04
0.06
−73.8
10.4
49.5
−150
−100
−50
0
50
100
150
(Difference in CO2 Storage)/Gtonne

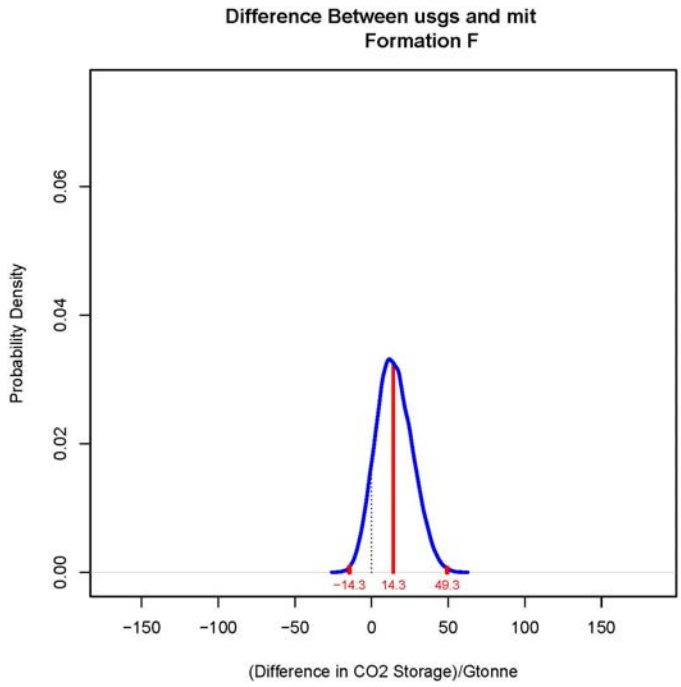
Difference Between usgs and mit
Formation F
Probability Density
0.00
0.02
0.04
0.06
−14.3
14.3
49.3
−150
−100
−50
0
50
100
150
(Difference in CO2 Storage)/Gtonne

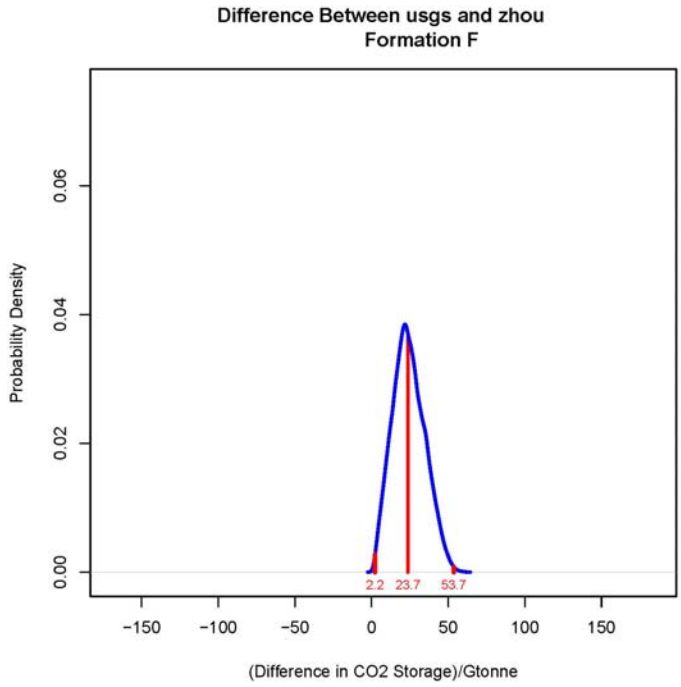
Difference Between usgs and zhou
Formation F
Probability Density
0.00
0.02
0.04
0.06
2.2
23.7
53.7
−150
−100
−50
0
50
100
150
(Difference in CO2 Storage)/Gtonne

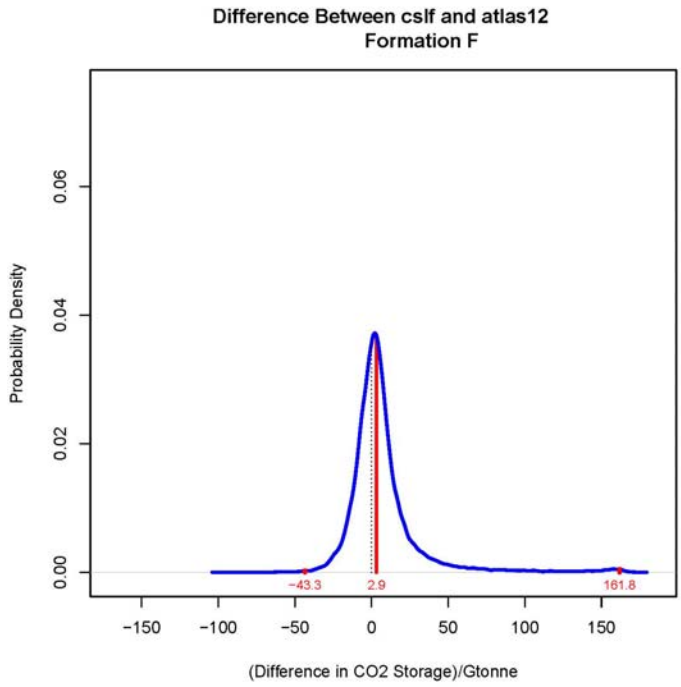
Difference Between cslf and atlas12
Formation F
Probability Density
0.00
0.02
0.04
0.06
−43.3
2.9
161.8
−150
−100
−50
0
50
100
150
(Difference in CO2 Storage)/Gtonne

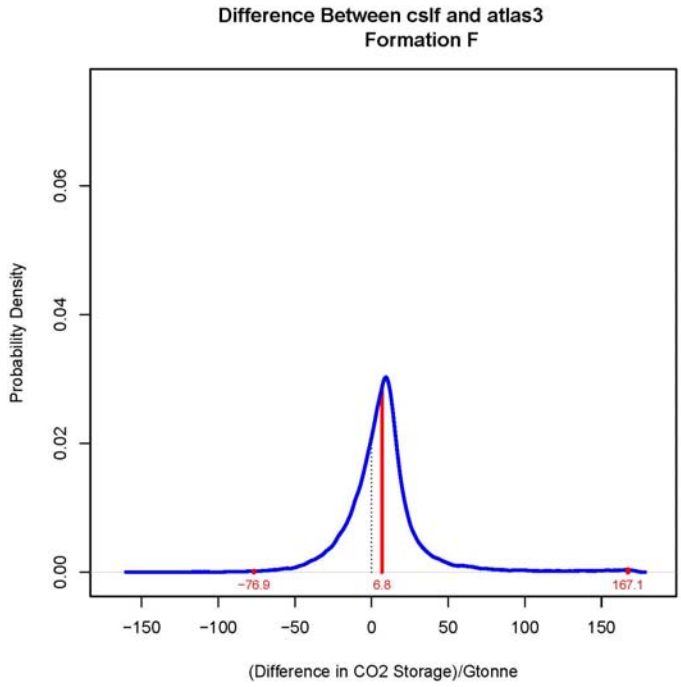
Difference Between cslf and atlas3
Formation F
Probability Density
0.00
0.02
0.04
0.06
−76.9
6.8
167.1
−150
−100
−50
0
50
100
150
(Difference in CO2 Storage)/Gtonne

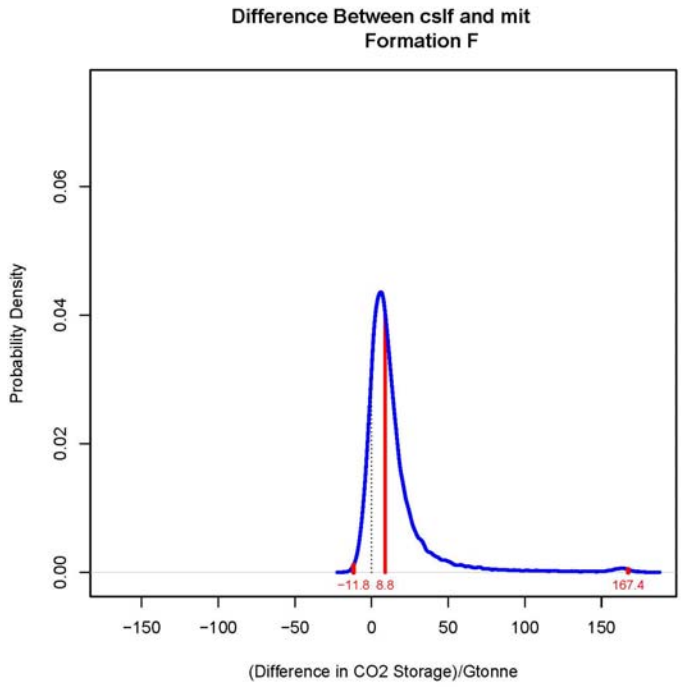
Difference Between cslf and mit
Formation F
Probability Density
0.00
0.02
0.04
0.06
−11.8
8.8
167.4
−150
−100
−50
0
50
100
150
(Difference in CO2 Storage)/Gtonne

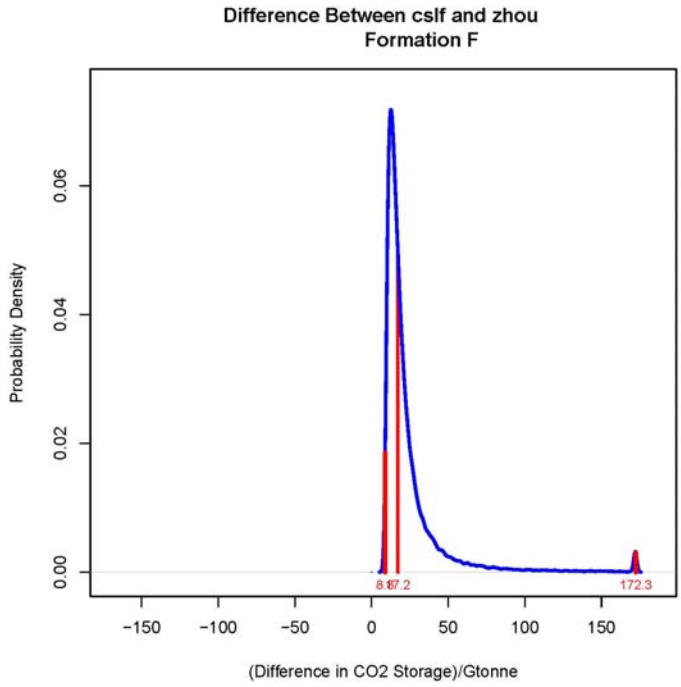
Difference Between cslf and zhou
Formation F
Probability Density
0.00
0.02
0.04
0.06
8.8
7.2
172.3
−150
−100
−50
0
50
100
150
(Difference in CO2 Storage)/Gtonne

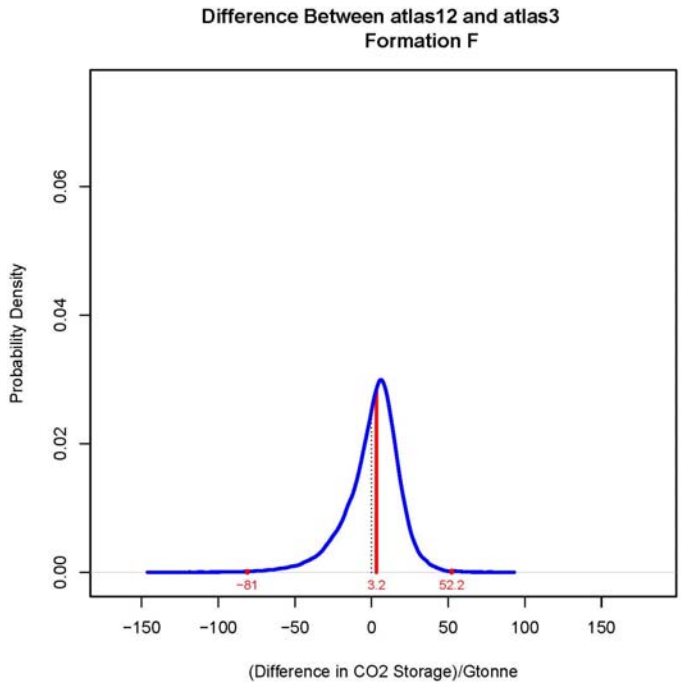
Difference Between atlas12 and atlas3
Formation F
Probability Density
0.00
0.02
0.04
0.06
−81
3.2
52.2
−150
−100
−50
0
50
100
150
(Difference in CO2 Storage)/Gtonne

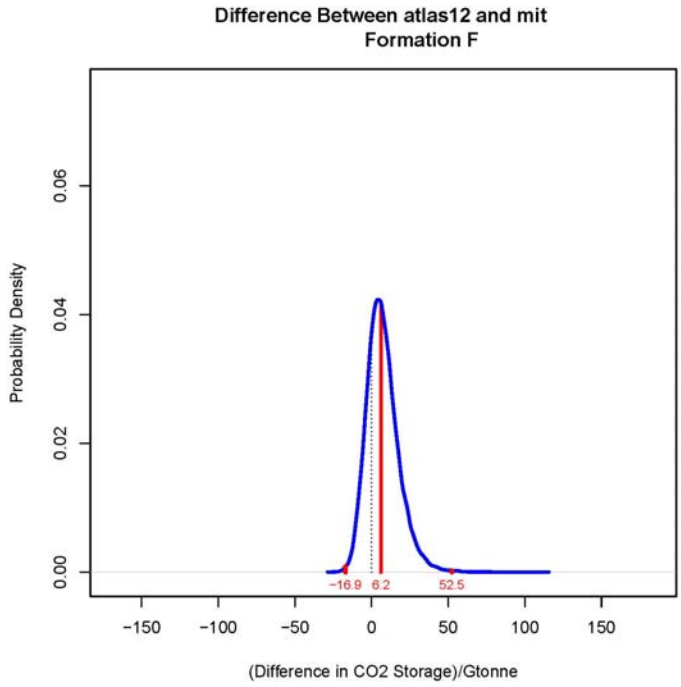
Difference Between atlas12 and mit
Formation F
Probability Density
0.00
0.02
0.04
0.06
−16.9
6.2
52.5
−150
−100
−50
0
50
100
150
(Difference in CO2 Storage)/Gtonne

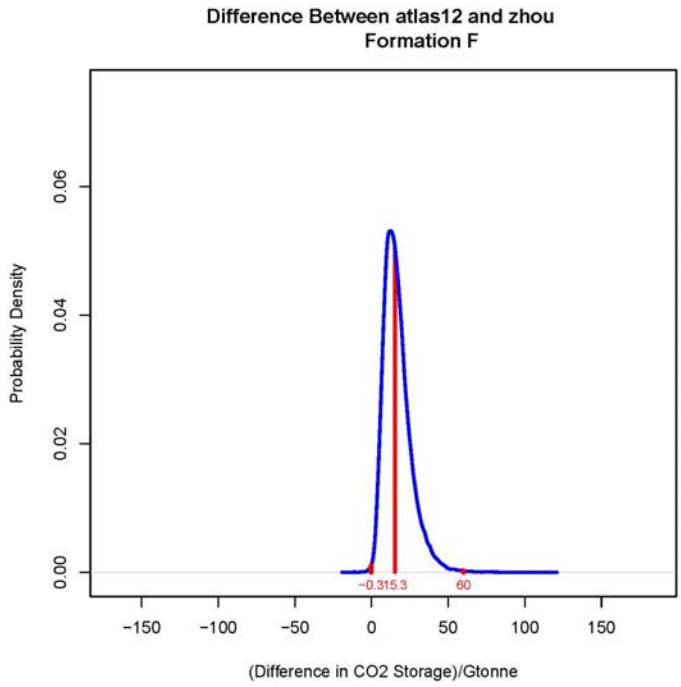
Difference Between atlas12 and zhou
Formation F
Probability Density
0.00
0.02
0.04
0.06
−0.315.3
60
−150
−100
−50
0
50
100
150
(Difference in CO2 Storage)/Gtonne

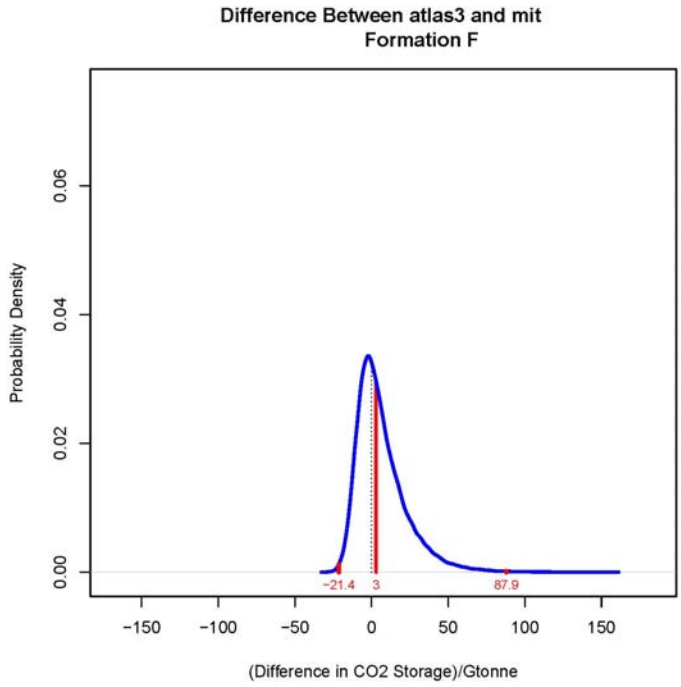
Difference Between atlas3 and mit
Formation F
Probability Density
0.00
0.02
0.04
0.06
−21.4
3
87.9
−150
−100
−50
0
50
100
150
(Difference in CO2 Storage)/Gtonne

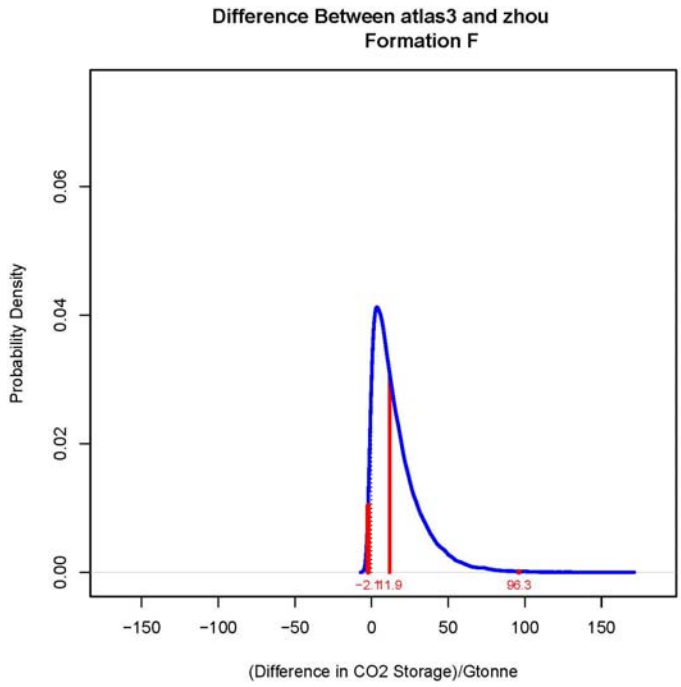
Difference Between atlas3 and zhou
Formation F
Probability Density
0.00
0.02
0.04
0.06
−2.1
11.9
96.3
−150
−100
−50
0
50
100
150
(Difference in CO2 Storage)/Gtonne

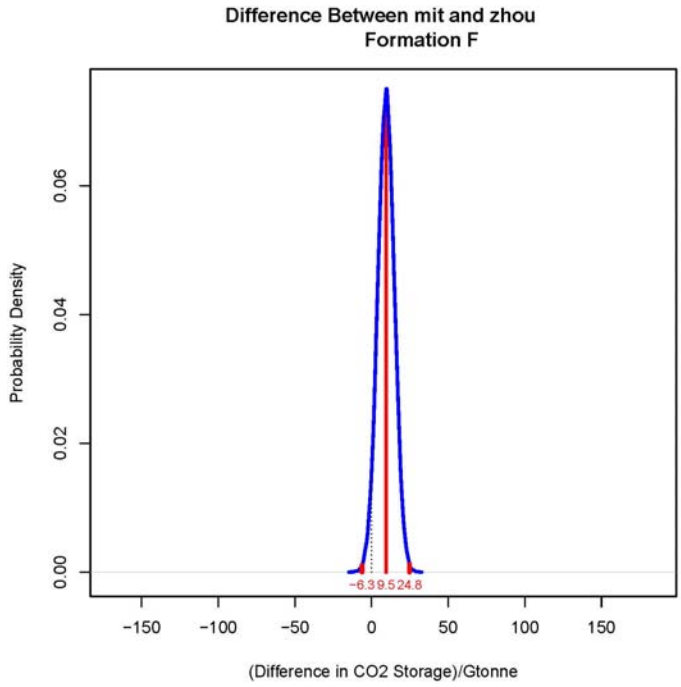
Difference Between mit and zhou
Formation F
Probability Density
0.00
0.02
0.04
0.06
−6.3
9.5
24.8
−150
−100
−50
0
50
100
150
(Difference in CO2 Storage)/Gtonne

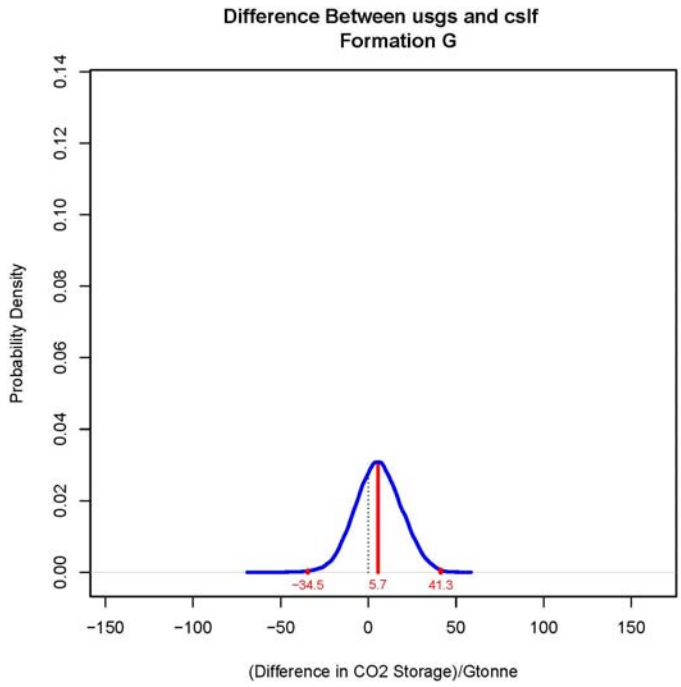
Difference Between usgs and cslf
Formation G
Probability Density
0.00
0.02
0.04
0.06
0.08
0.10
0.12
0.14
−34.5
5.7
41.3
−150
−100
−50
0
50
100
150
(Difference in CO2 Storage)/Gtonne

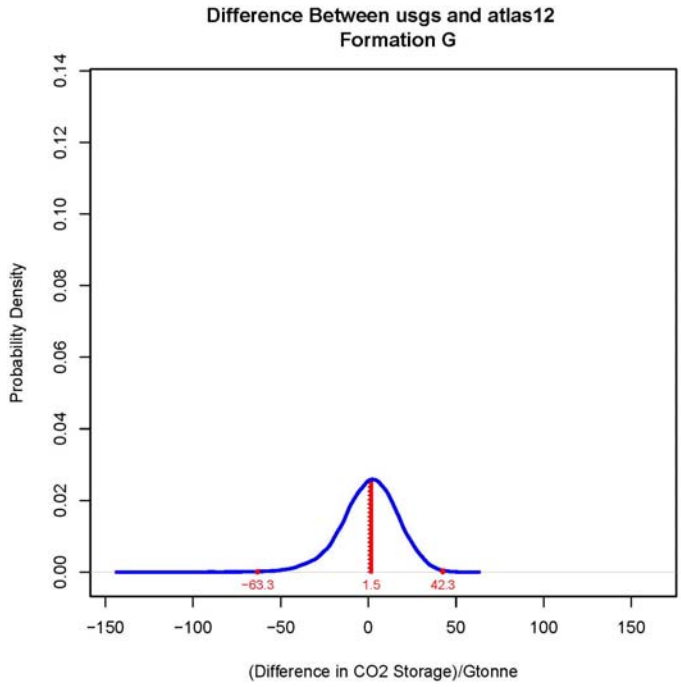
Difference Between usgs and atlas12
Formation G
Probability Density
0.00
0.02
0.04
0.06
0.08
0.10
0.12
0.14
−63.3
1.5
42.3
−150
−100
−50
0
50
100
150
(Difference in CO2 Storage)/Gtonne

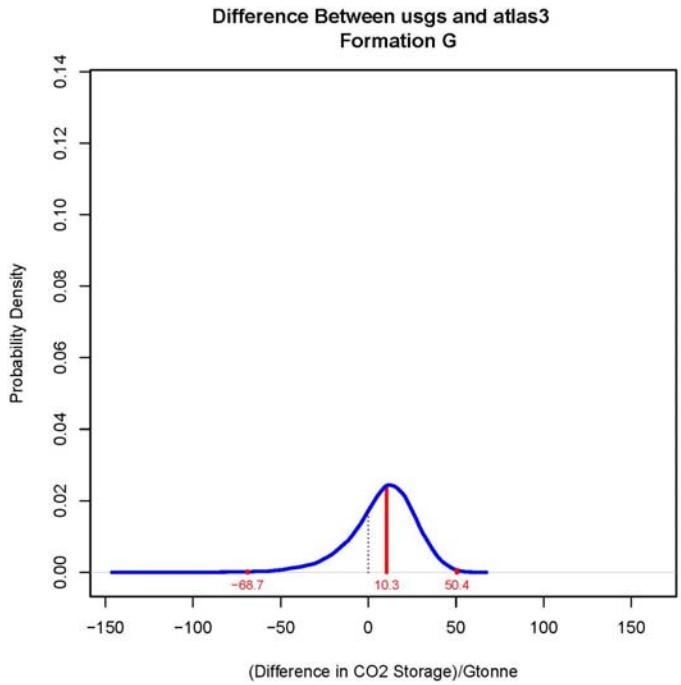
Difference Between usgs and atlas3
Formation G
Probability Density
0.00
0.02
0.04
0.06
0.08
0.10
0.12
0.14
−68.7
10.3
50.4
−150
−100
−50
0
50
100
150
(Difference in CO2 Storage)/Gtonne

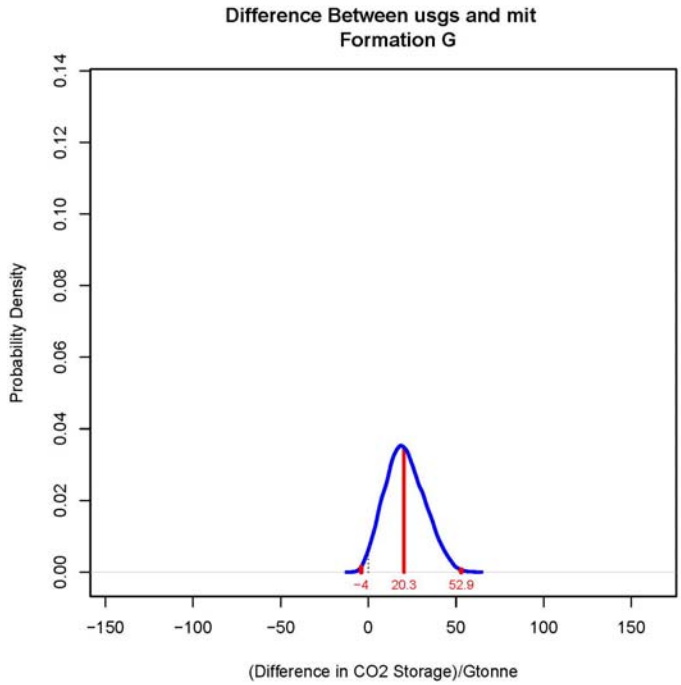
Difference Between usgs and mit
Formation G
Probability Density
0.00
0.02
0.04
0.06
0.08
0.10
0.12
0.14
−4
20.3
52.9
−150
−100
−50
0
50
100
150
(Difference in CO2 Storage)/Gtonne

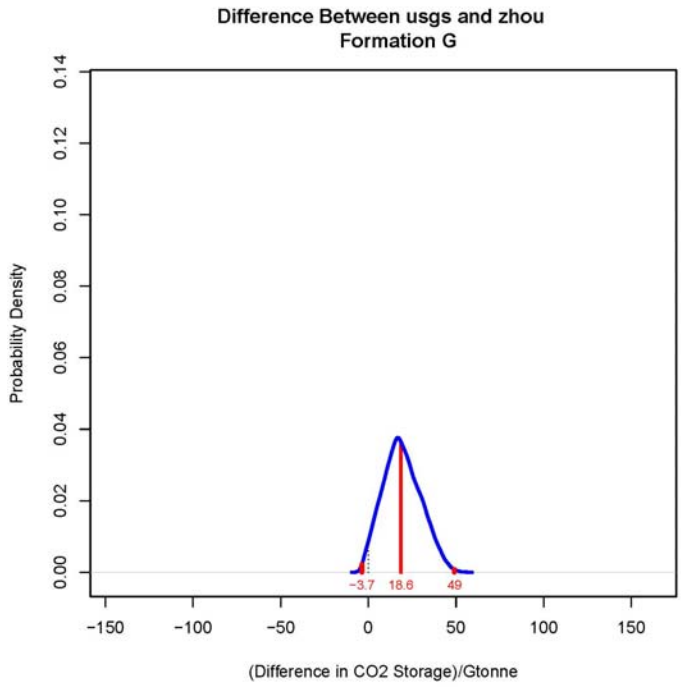
Difference Between usgs and zhou
Formation G
Probability Density
0.00
0.02
0.04
0.06
0.08
0.10
0.12
0.14
−3.7
18.6
49
−150
−100
−50
0
50
100
150
(Difference in CO2 Storage)/Gtonne

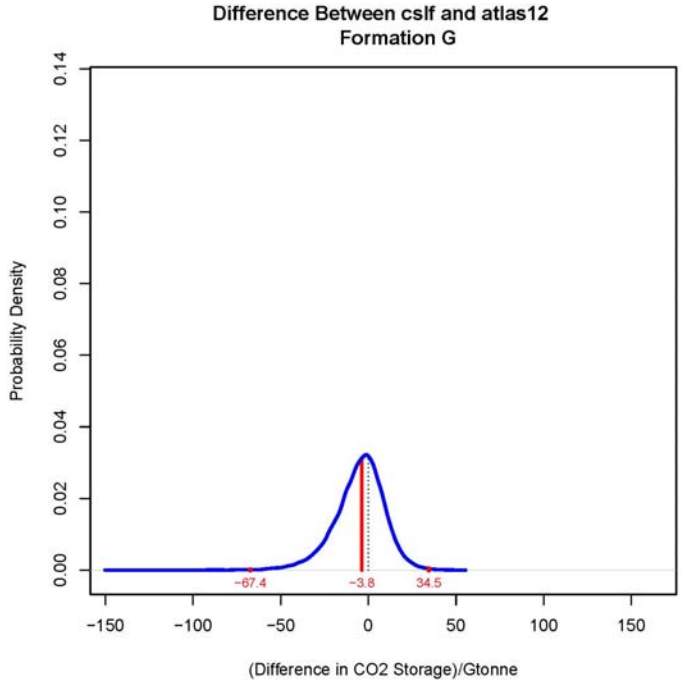
Difference Between cslf and atlas12
Formation G
Probability Density
0.00
0.02
0.04
0.06
0.08
0.10
0.12
0.14
−67.4
−3.8
34.5
−150
−100
−50
0
50
100
150
(Difference in CO2 Storage)/Gtonne

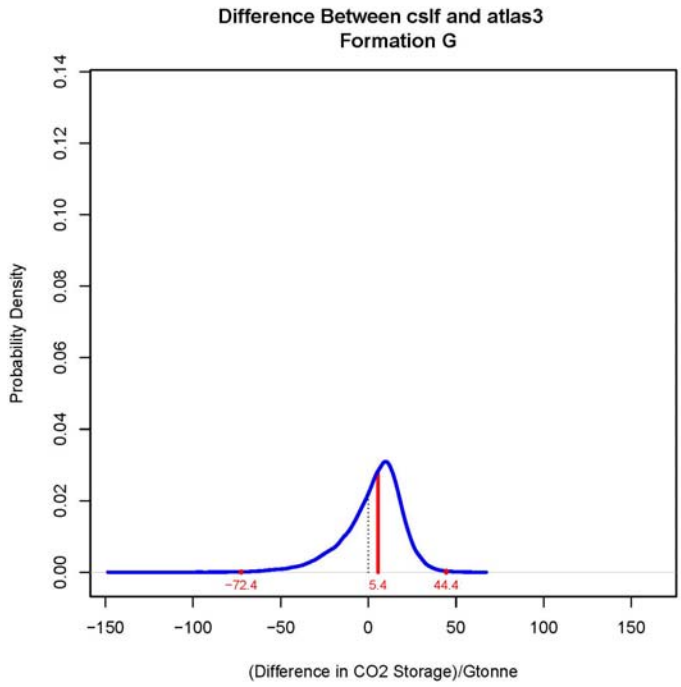
Difference Between cslf and atlas3
Formation G
Probability Density
0.00
0.02
0.04
0.06
0.08
0.10
0.12
0.14
−72.4
5.4
44.4
−150
−100
−50
0
50
100
150
(Difference in CO2 Storage)/Gtonne

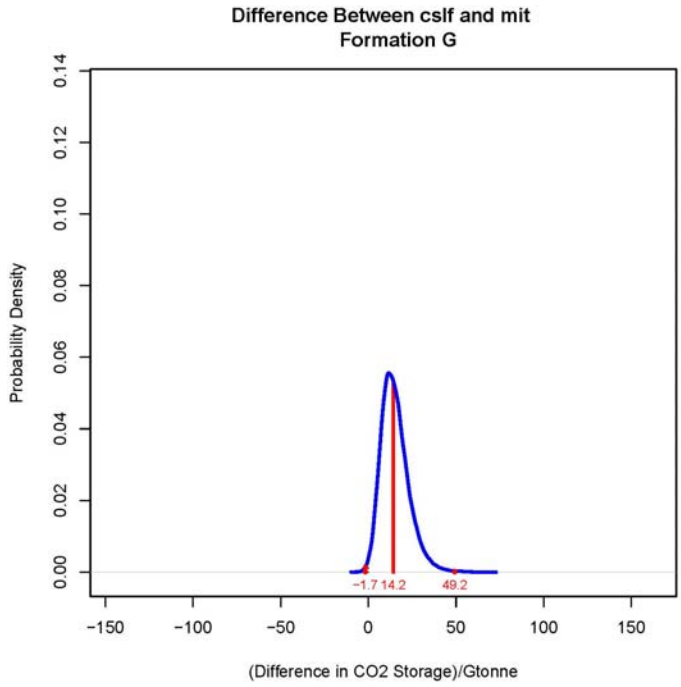
Difference Between cslf and mit
Formation G
Probability Density
0.00
0.02
0.04
0.06
0.08
0.10
0.12
0.14
−1.7
14.2
49.2
−150
−100
−50
0
50
100
150
(Difference in CO2 Storage)/Gtonne

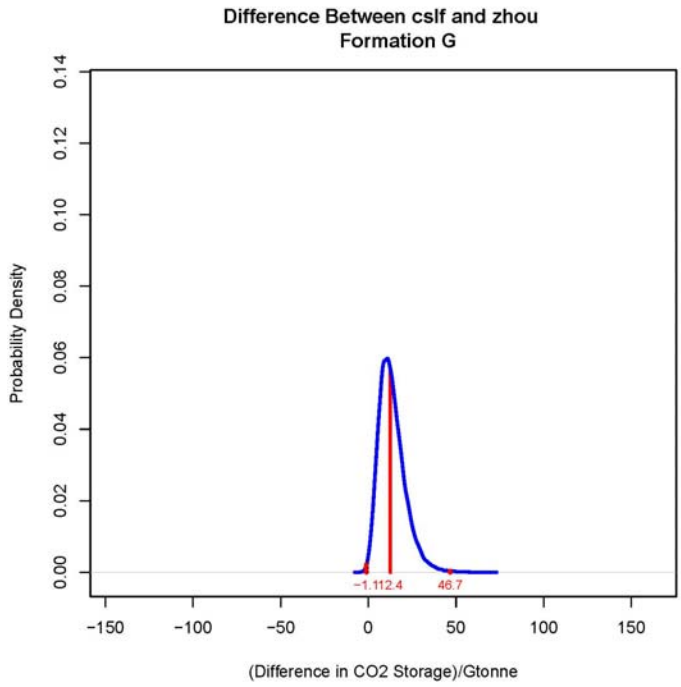
Difference Between cslf and zhou
Formation G
Probability Density
0.00
0.02
0.04
0.06
0.08
0.10
0.12
0.14
−1.112.4
46.7
−150
−100
−50
0
50
100
150
(Difference in CO2 Storage)/Gtonne

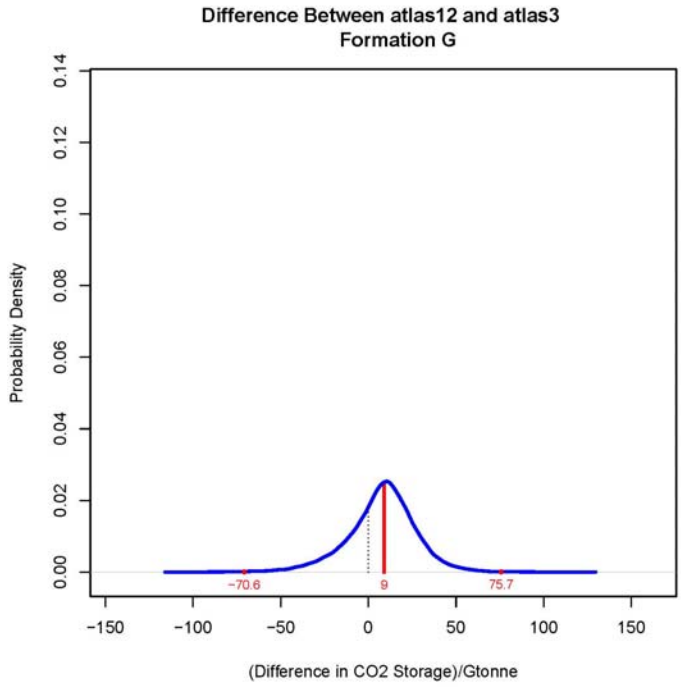
Difference Between atlas12 and atlas3
Formation G
Probability Density
0.00
0.02
0.04
0.06
0.08
0.10
0.12
0.14
−70.6
9
75.7
−150
−100
−50
0
50
100
150
(Difference in CO2 Storage)/Gtonne

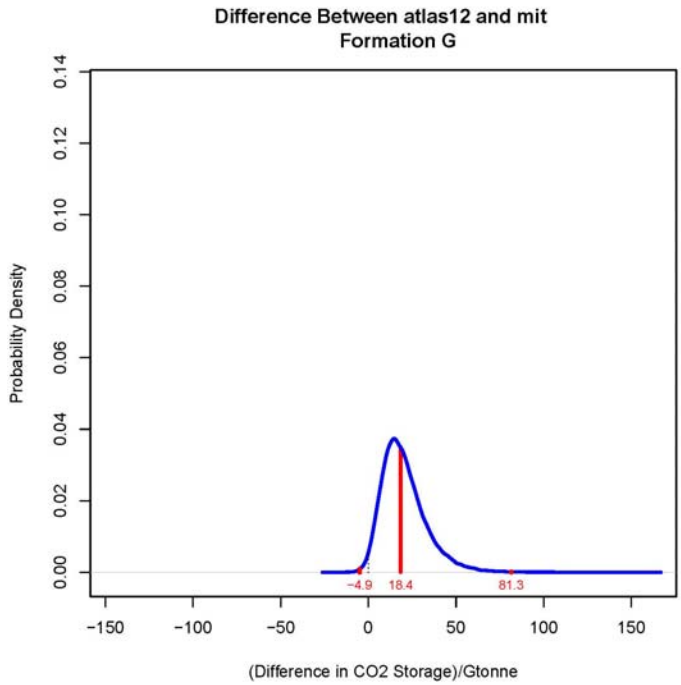
Difference Between atlas12 and mit
Formation G
Probability Density
0.00
0.02
0.04
0.06
0.08
0.10
0.12
0.14
−4.9
18.4
81.3
−150
−100
−50
0
50
100
150
(Difference in CO2 Storage)/Gtonne

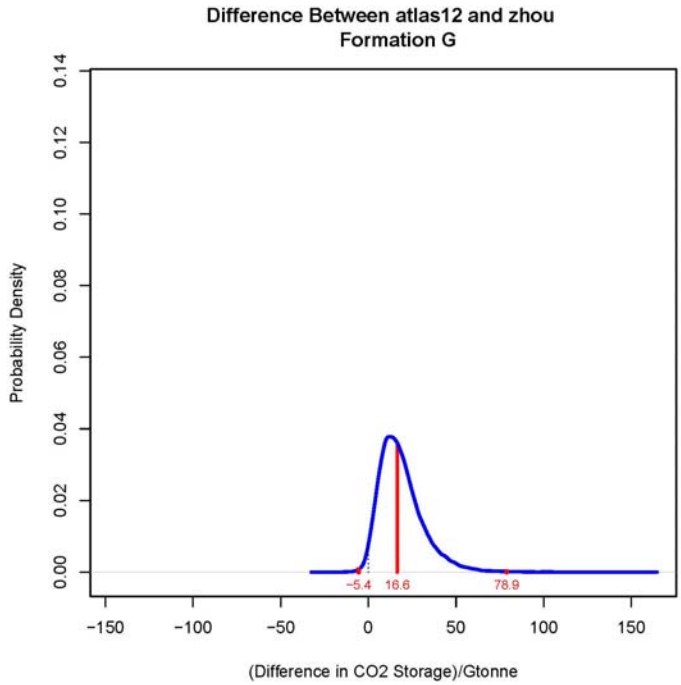
Difference Between atlas12 and zhou
Formation G
Probability Density
0.00
0.02
0.04
0.06
0.08
0.10
0.12
0.14
−5.4
16.6
78.9
−150
−100
−50
0
50
100
150
(Difference in CO2 Storage)/Gtonne

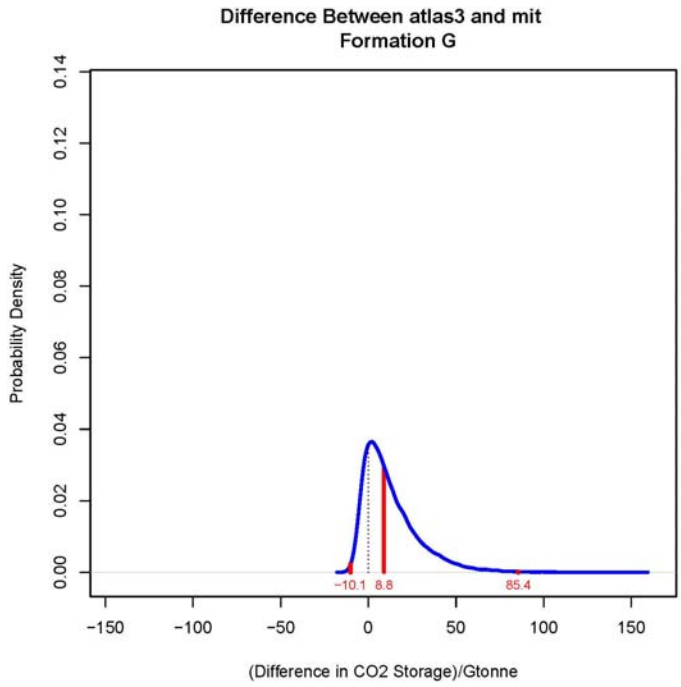
Difference Between atlas3 and mit
Formation G
Probability Density
0.00
0.02
0.04
0.06
0.08
0.10
0.12
0.14
−10.1
8.8
85.4
−150
−100
−50
0
50
100
150
(Difference in CO2 Storage)/Gtonne

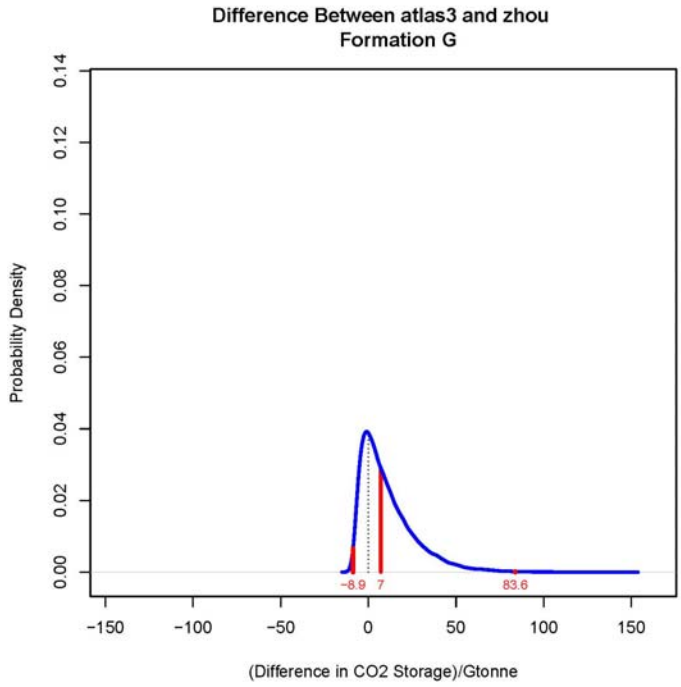
Difference Between atlas3 and zhou
Formation G
Probability Density
0.00
0.02
0.04
0.06
0.08
0.10
0.12
0.14
−8.9
7
83.6
−150
−100
−50
0
50
100
150
(Difference in CO2 Storage)/Gtonne

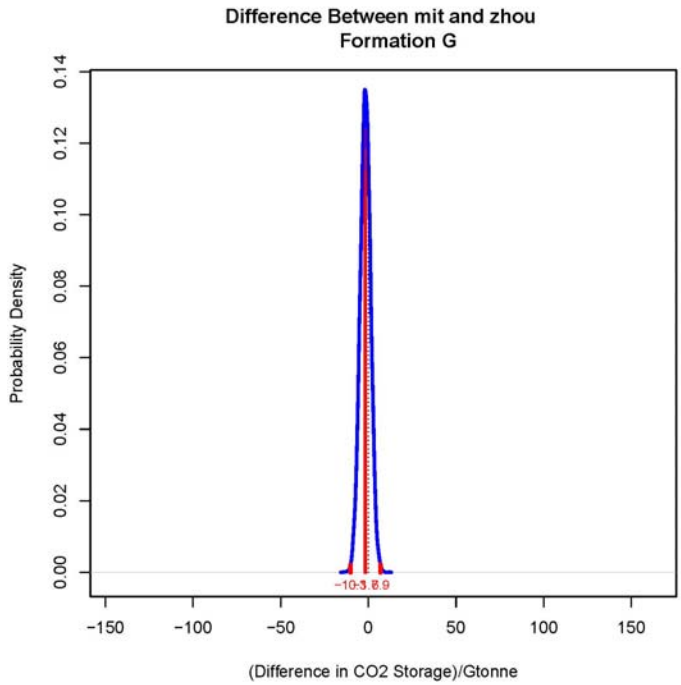
Difference Between mit and zhou
Formation G
Probability Density
0.00
0.02
0.04
0.06
0.08
0.10
0.12
0.14
−10
−3.8
8.9
−150
−100
−50
0
50
100
150
(Difference in CO2 Storage)/Gtonne

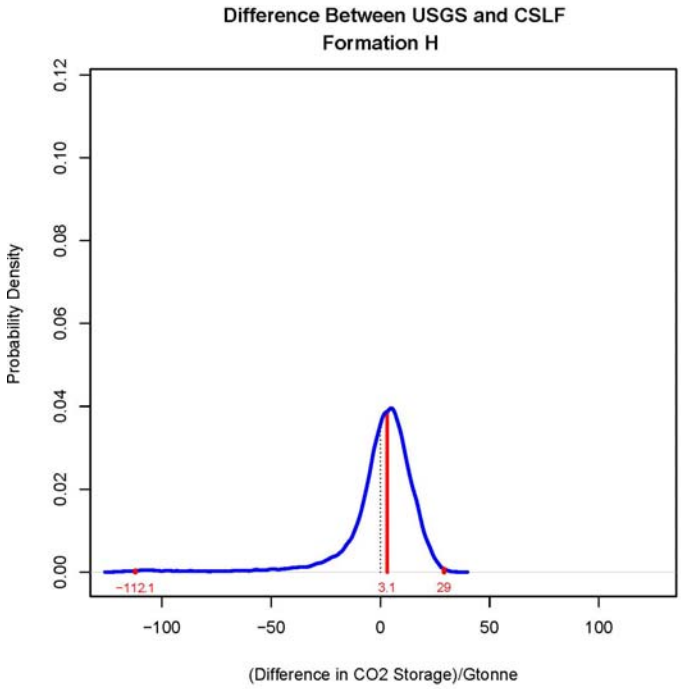
Difference Between USGS and CSLF
Formation H
Probability Density
0.00
0.02
0.04
0.06
0.08
0.10
0.12
−112.1
3.1
29
−100
−50
0
50
100
(Difference in CO2 Storage)/Gtonne

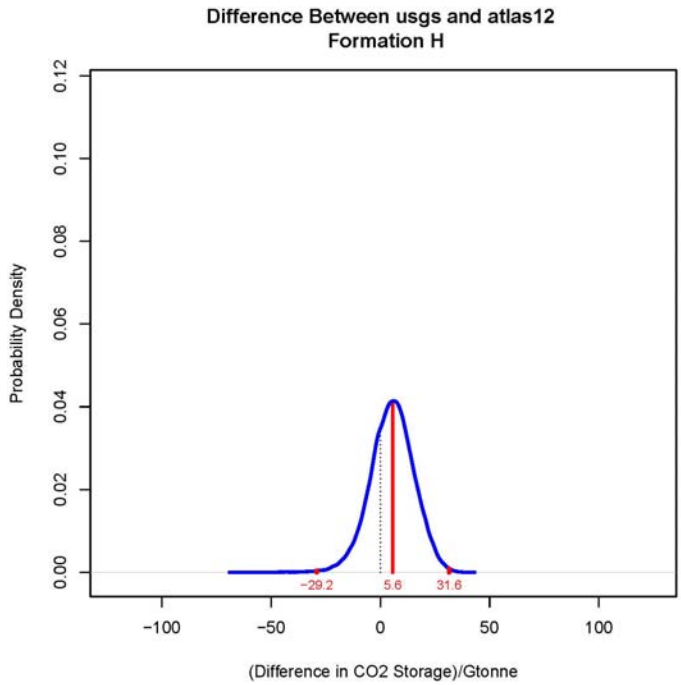
Difference Between usgs and atlas12
Formation H
Probability Density
0.00
0.02
0.04
0.06
0.08
0.10
0.12
−29.2
5.6
31.6
−100
−50
0
50
100
(Difference in CO2 Storage)/Gtonne

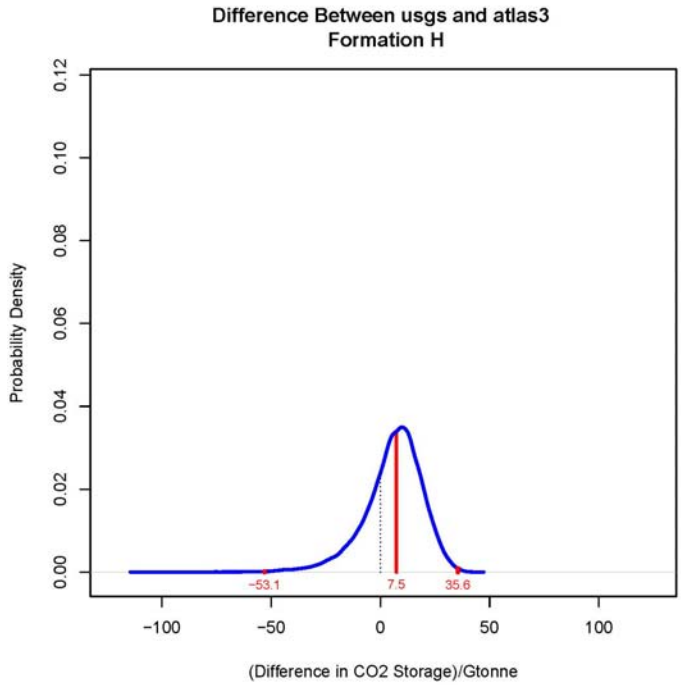
Difference Between usgs and atlas3
Formation H
Probability Density
0.00
0.02
0.04
0.06
0.08
0.10
0.12
−53.1
7.5
35.6
−100
−50
0
50
100
(Difference in CO2 Storage)/Gtonne

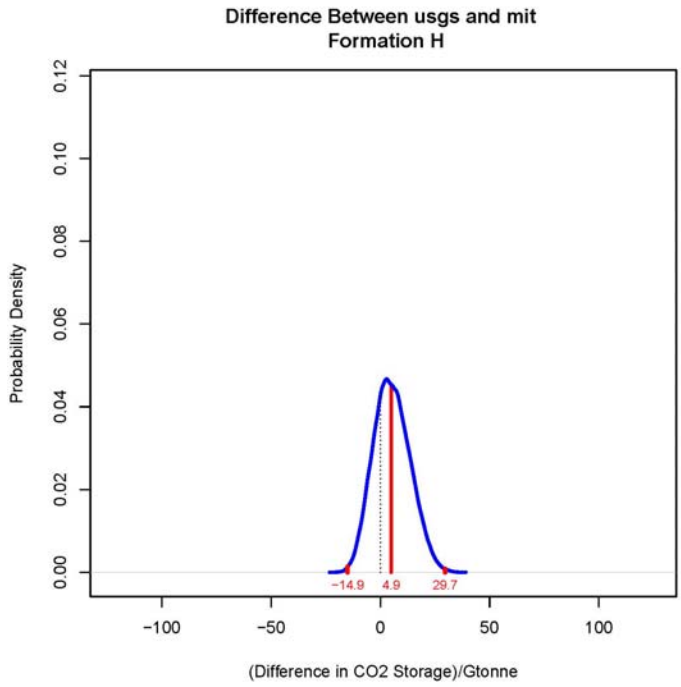
Difference Between usgs and mit
Formation H
Probability Density
0.00
0.02
0.04
0.06
0.08
0.10
0.12
−14.9
4.9
29.7
−100
−50
0
50
100
(Difference in CO2 Storage)/Gtonne

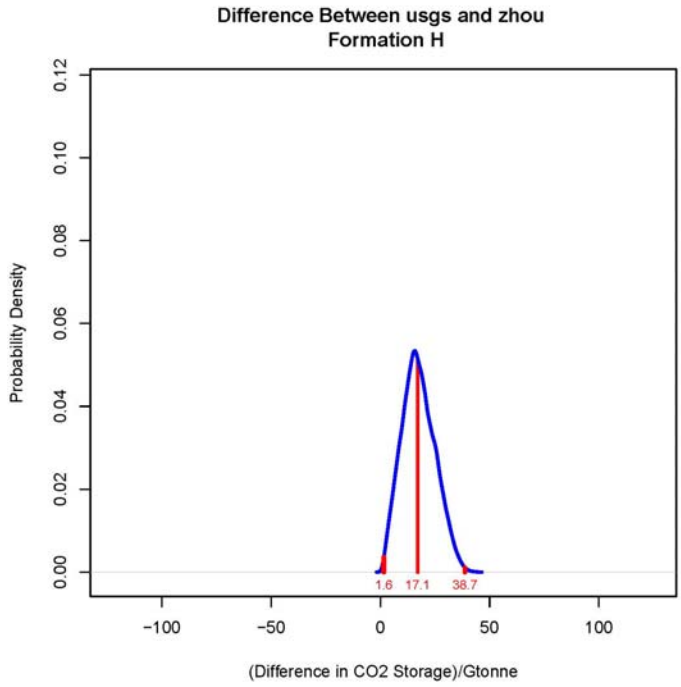
Difference Between usgs and zhou
Formation H
Probability Density
0.00
0.02
0.04
0.06
0.08
0.10
0.12
1.6
17.1
38.7
−100
−50
0
50
100
(Difference in CO2 Storage)/Gtonne

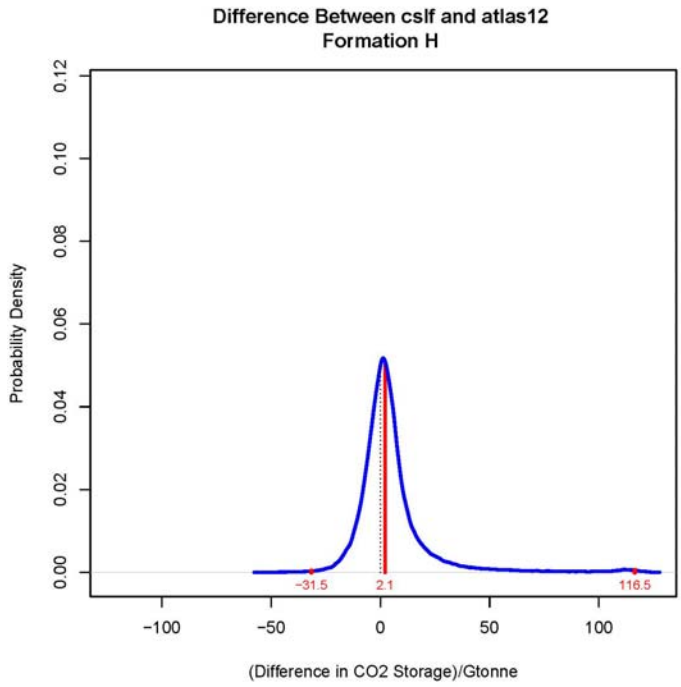
Difference Between cslf and atlas12
Formation H
Probability Density
0.00
0.02
0.04
0.06
0.08
0.10
0.12
−31.5
2.1
116.5
−100
−50
0
50
100
(Difference in CO2 Storage)/Gtonne

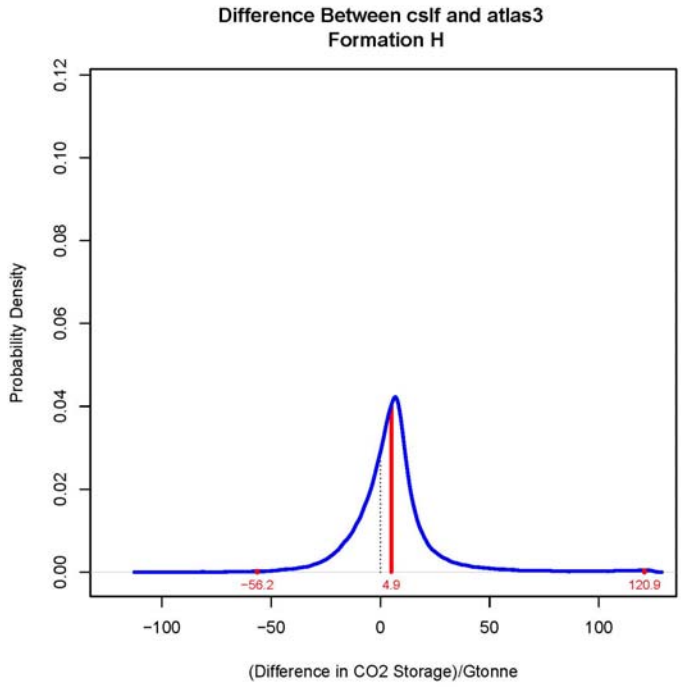
Difference Between cslf and atlas3
Formation H
Probability Density
0.00
0.02
0.04
0.06
0.08
0.10
0.12
−56.2
4.9
120.9
−100
−50
0
50
100
(Difference in CO2 Storage)/Gtonne

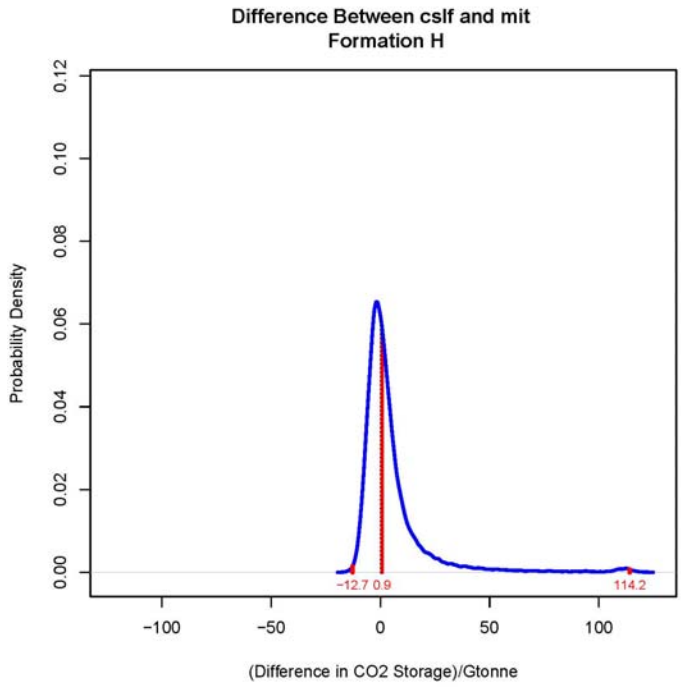
Difference Between cslf and mit
Formation H
Probability Density
0.00
0.02
0.04
0.06
0.08
0.10
0.12
−12.7
0.9
114.2
−100
−50
0
50
100
(Difference in CO2 Storage)/Gtonne

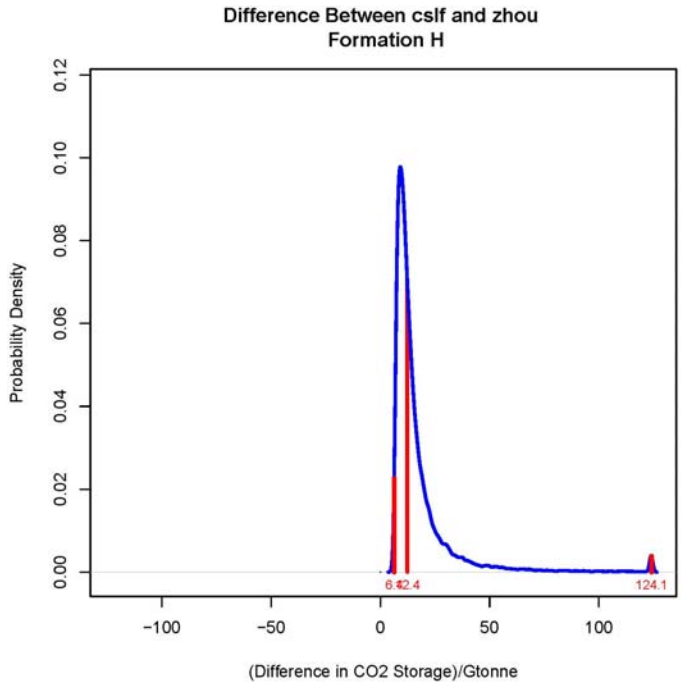
Difference Between cslf and zhou
Formation H
Probability Density
0.00
0.02
0.04
0.06
0.08
0.10
0.12
6.4
2.4
124.1
−100
−50
0
50
100
(Difference in CO2 Storage)/Gtonne

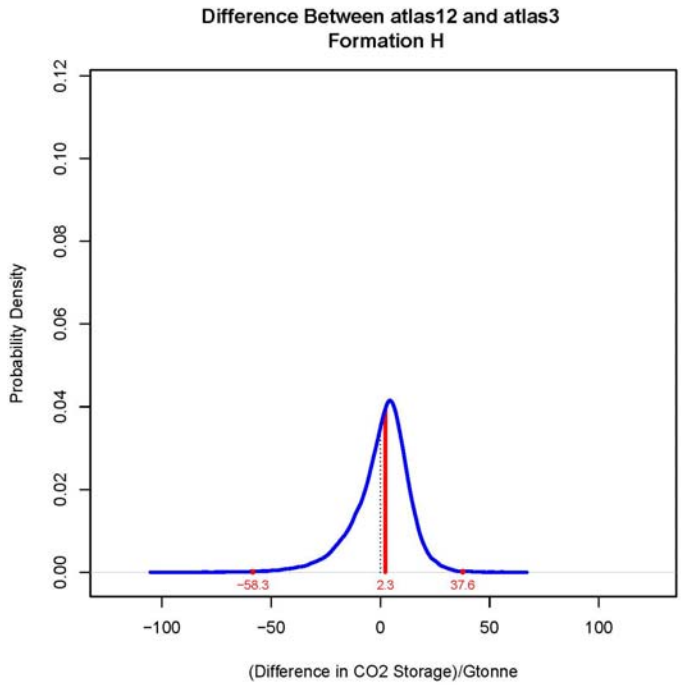
Difference Between atlas12 and atlas3
Formation H
Probability Density
0.00
0.02
0.04
0.06
0.08
0.10
0.12
−58.3
2.3
37.6
−100
−50
0
50
100
(Difference in CO2 Storage)/Gtonne

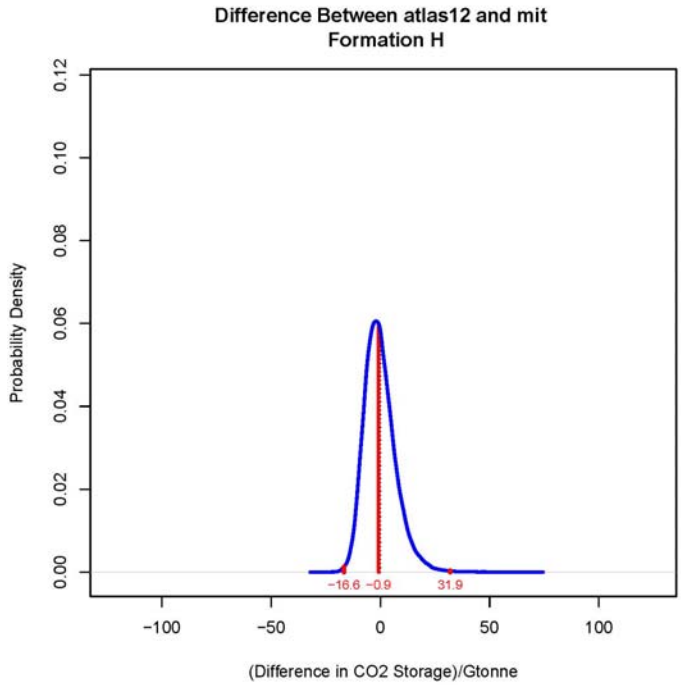
Difference Between atlas12 and mit
Formation H
Probability Density
0.00
0.02
0.04
0.06
0.08
0.10
0.12
−16.6
−0.9
31.9
−100
−50
0
50
100
(Difference in CO2 Storage)/Gtonne

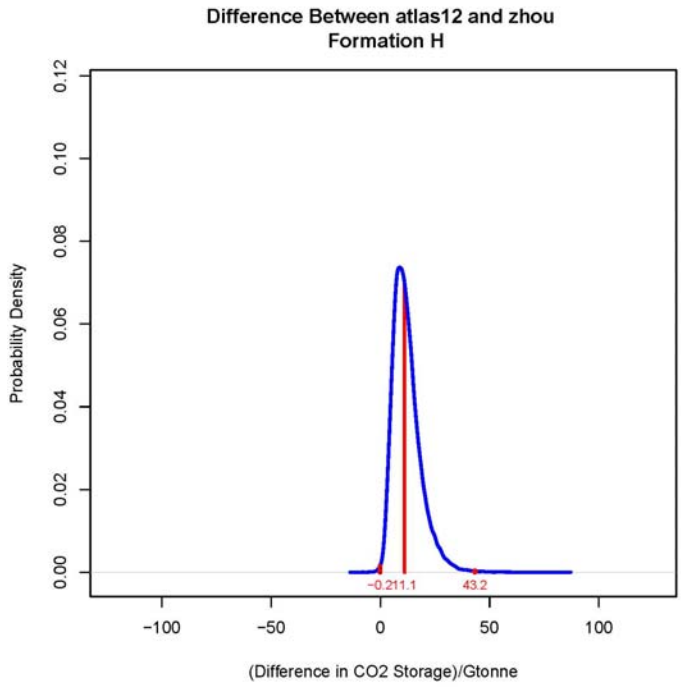
Difference Between atlas12 and zhou
Formation H
Probability Density
0.00
0.02
0.04
0.06
0.08
0.10
0.12
−0.2
11.1
43.2
−100
−50
0
50
100
(Difference in CO2 Storage)/Gtonne

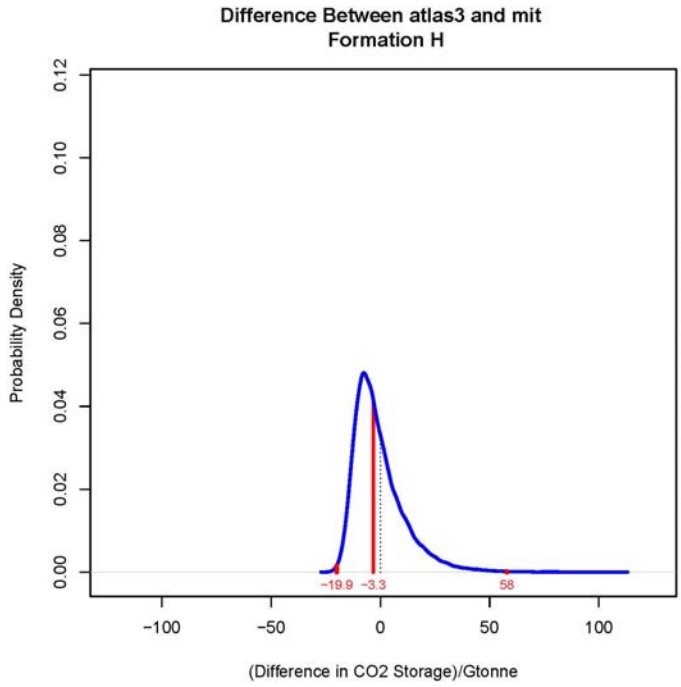
Difference Between atlas3 and mit
Formation H
Probability Density
0.00
0.02
0.04
0.06
0.08
0.10
0.12
−19.9
−3.3
58
−100
−50
0
50
100
(Difference in CO2 Storage)/Gtonne

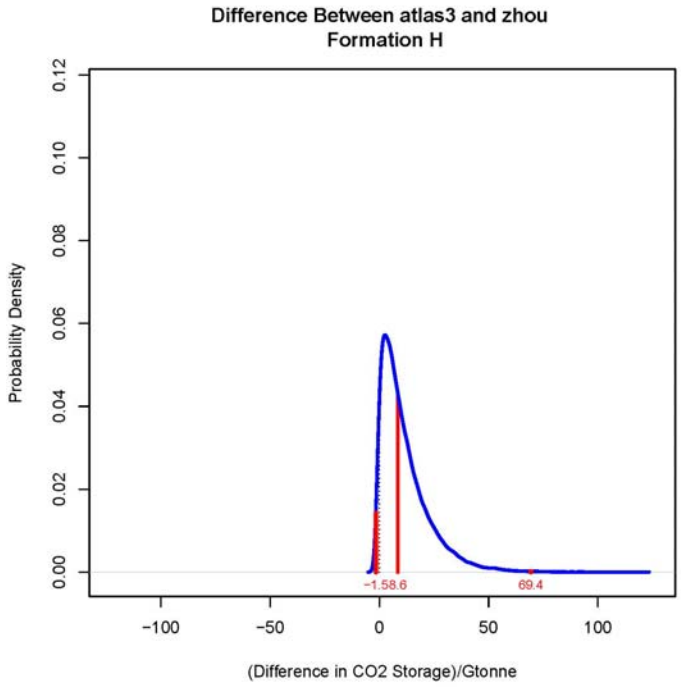
Difference Between atlas3 and zhou
Formation H
Probability Density
0.00
0.02
0.04
0.06
0.08
0.10
0.12
−1.58.6
69.4
−100
−50
0
50
100
(Difference in CO2 Storage)/Gtonne

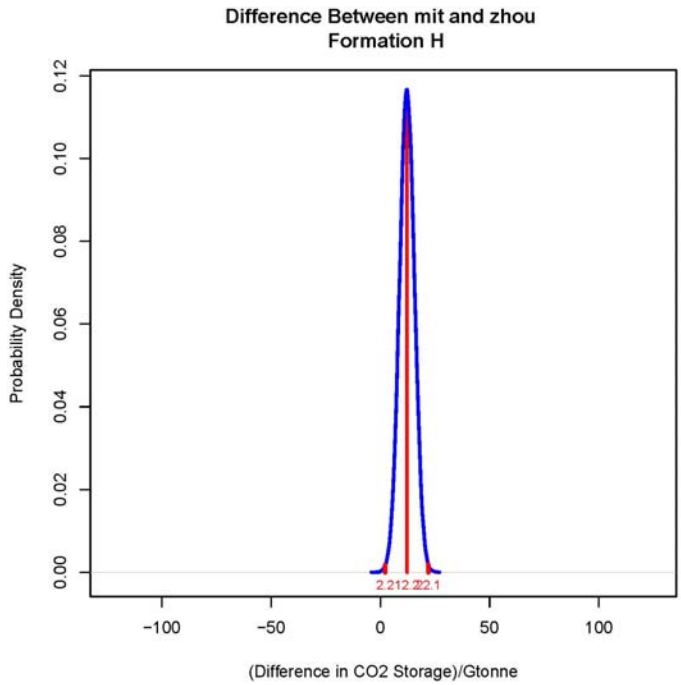
Difference Between mit and zhou
Formation H
Probability Density
0.00
0.02
0.04
0.06
0.08
0.10
0.12
2.212.222.1
−100
−50
0
50
100
(Difference in CO2 Storage)/Gtonne

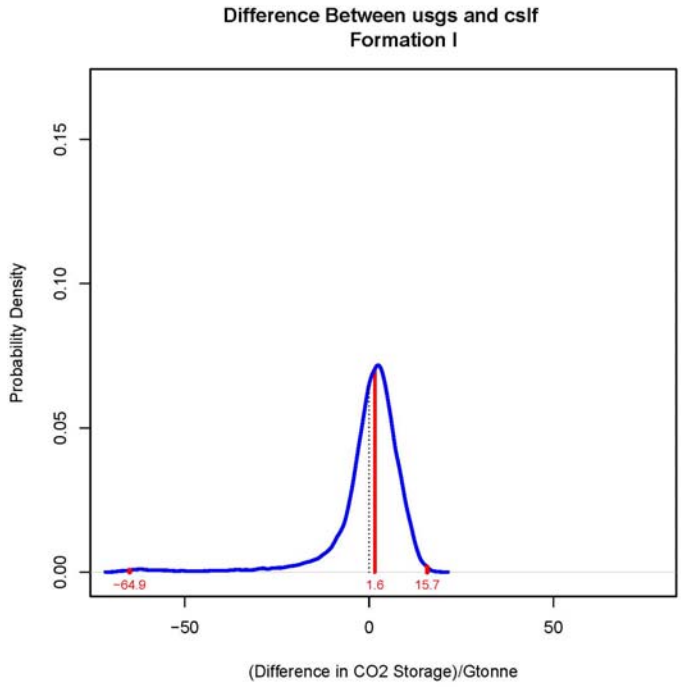
Difference Between usgs and cslf
Formation I
Probability Density
0.00
0.05
0.10
0.15
-64.9
1.6
15.7
-50
0
50
(Difference in CO2 Storage)/Gtonne

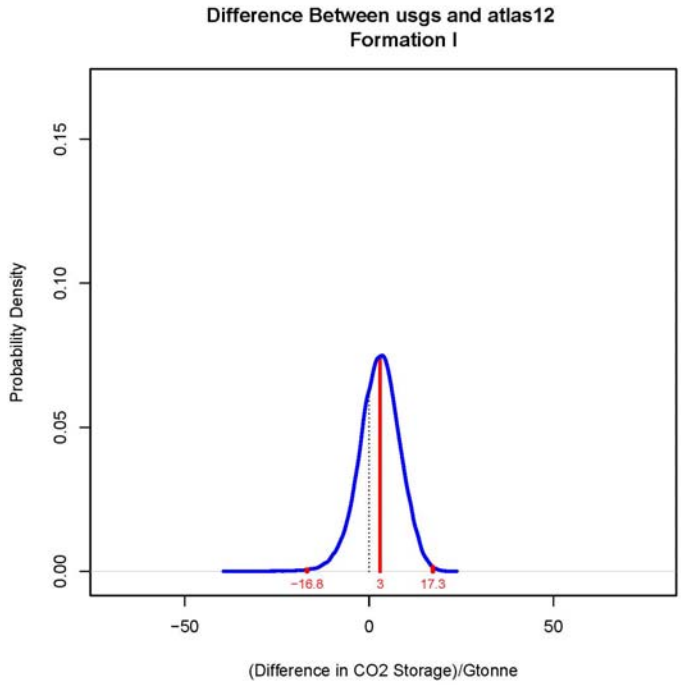
Difference Between usgs and atlas12
Formation I
Probability Density
0.00
0.05
0.10
0.15
-16.8
3
17.3
-50
0
50
(Difference in CO2 Storage)/Gtonne

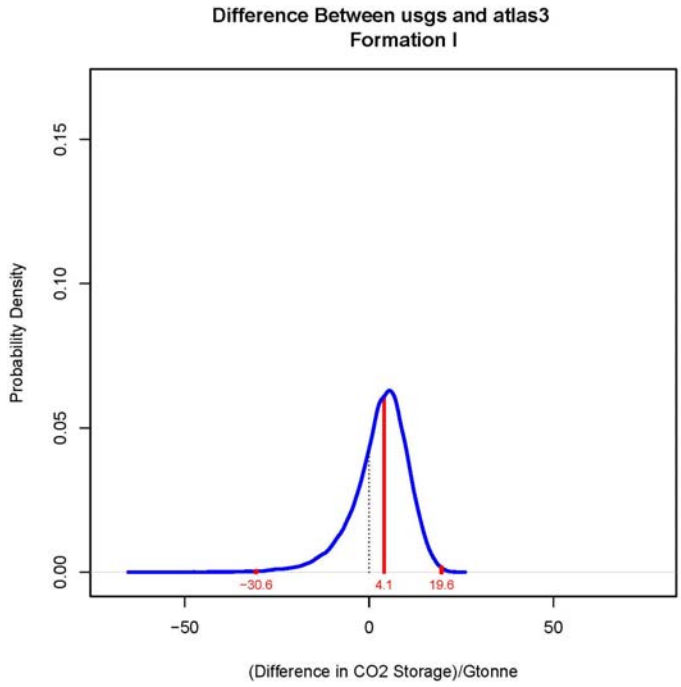
Difference Between usgs and atlas3
Formation I
Probability Density
0.00
0.05
0.10
0.15
−30.6
4.1
19.6
−50
0
50
(Difference in CO2 Storage)/Gtonne

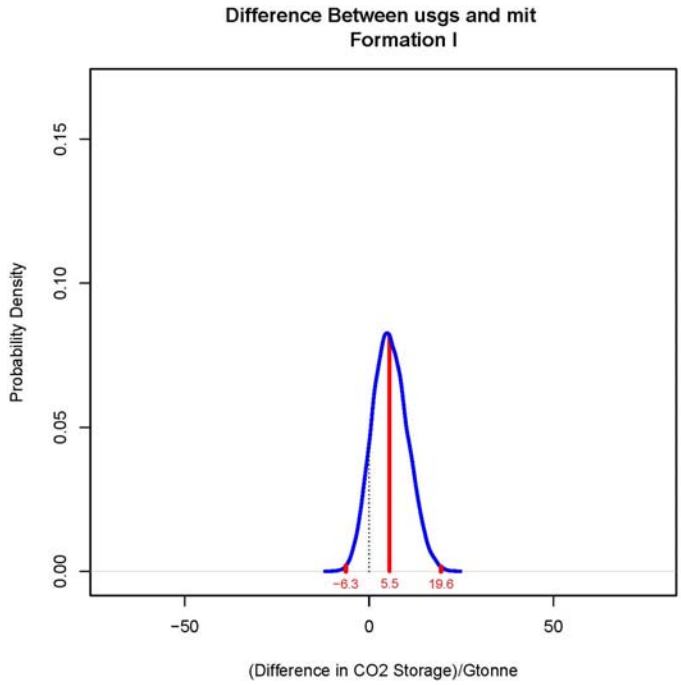
Difference Between usgs and mit
Formation I
Probability Density
0.00
0.05
0.10
0.15
−6.3
5.5
19.6
−50
0
50
(Difference in CO2 Storage)/Gtonne

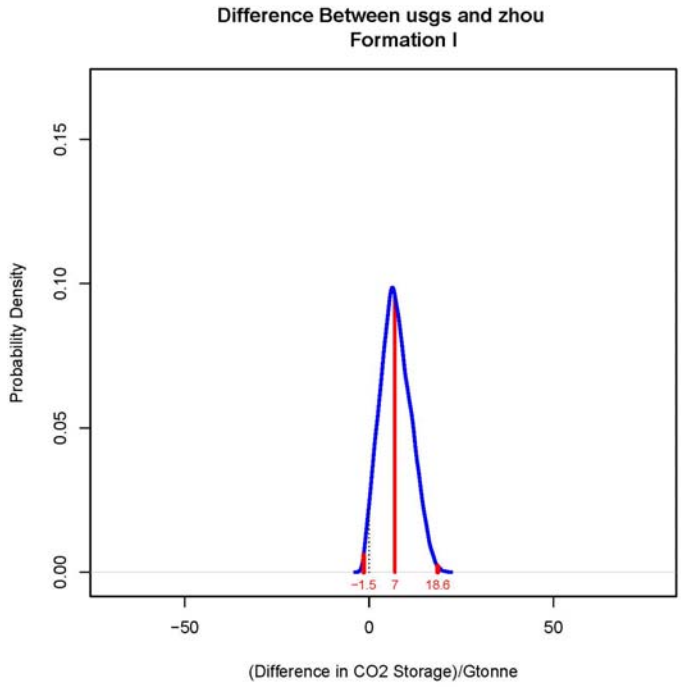
Difference Between usgs and zhou
Formation I
Probability Density
0.00
0.05
0.10
0.15
−1.5
7
18.6
−50
0
50
(Difference in CO2 Storage)/Gtonne

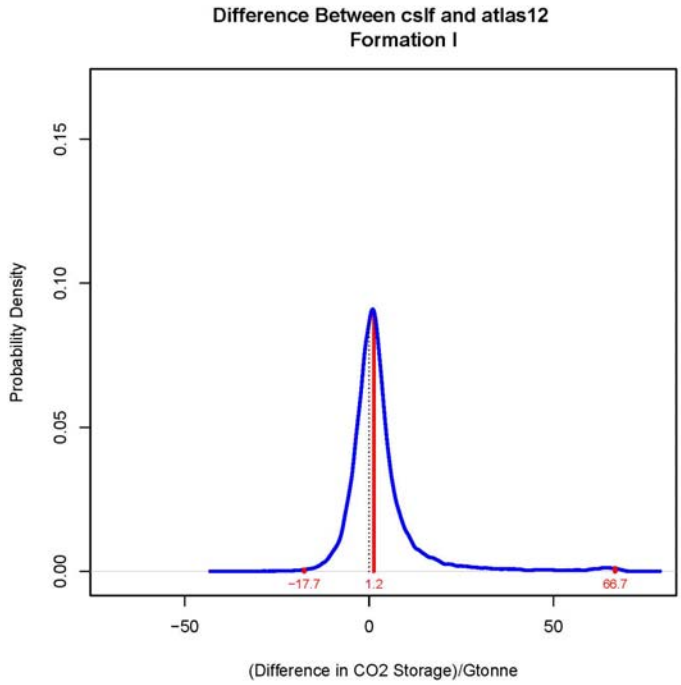
Difference Between cslf and atlas12
Formation I
Probability Density
0.00
0.05
0.10
0.15
−17.7
1.2
66.7
−50
0
50
(Difference in CO2 Storage)/Gtonne

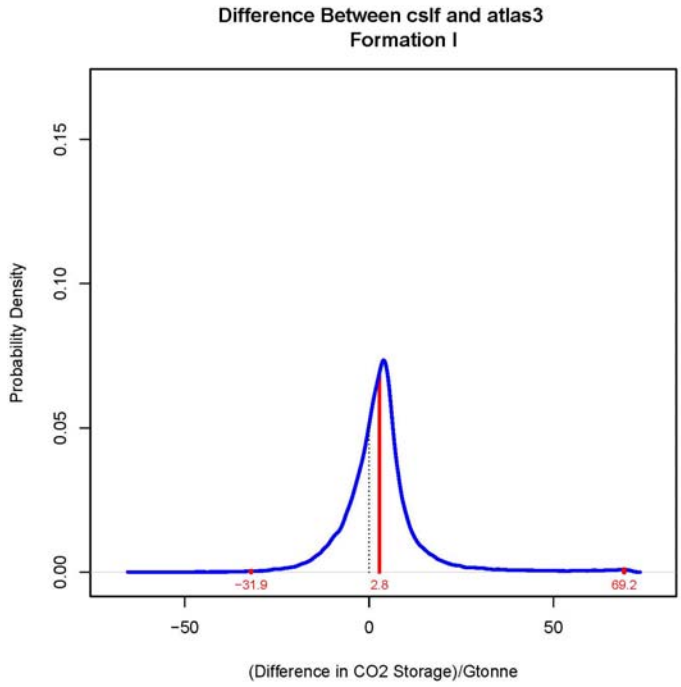
Difference Between cslf and atlas3
Formation I
Probability Density
0.00
0.05
0.10
0.15
−31.9
2.8
69.2
−50
0
50
(Difference in CO2 Storage)/Gtonne

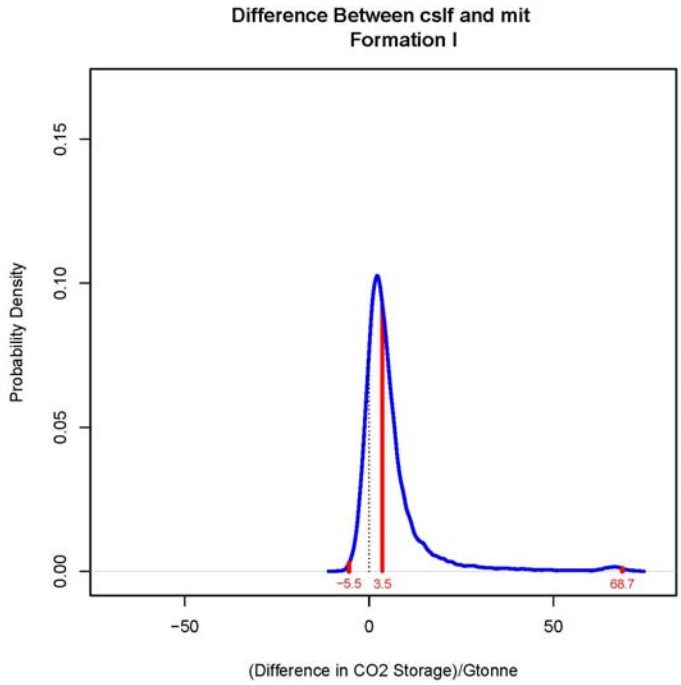
Difference Between cslf and mit
Formation I
Probability Density
0.00
0.05
0.10
0.15
−5.5
3.5
68.7
−50
0
50
(Difference in CO2 Storage)/Gtonne

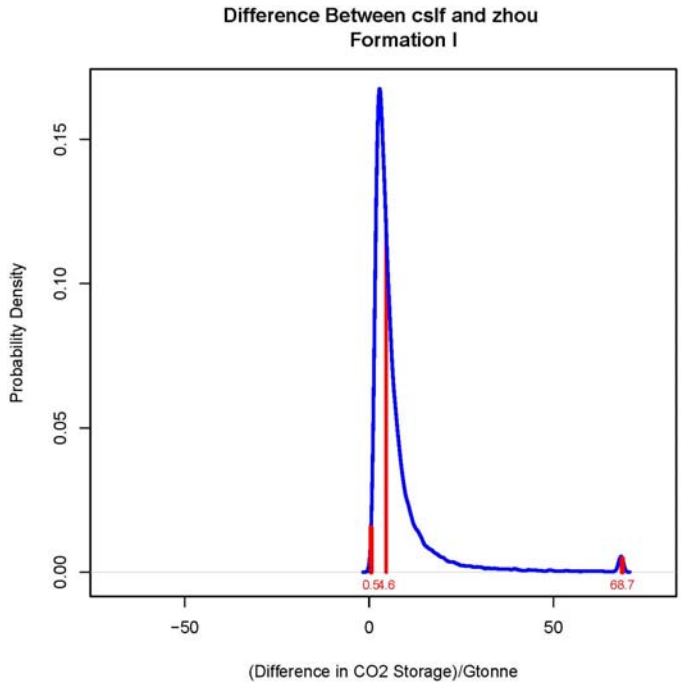
Difference Between cslf and zhou
Formation I
Probability Density
0.00
0.05
0.10
0.15
0.5
4.6
68.7
−50
0
50
(Difference in CO2 Storage)/Gtonne

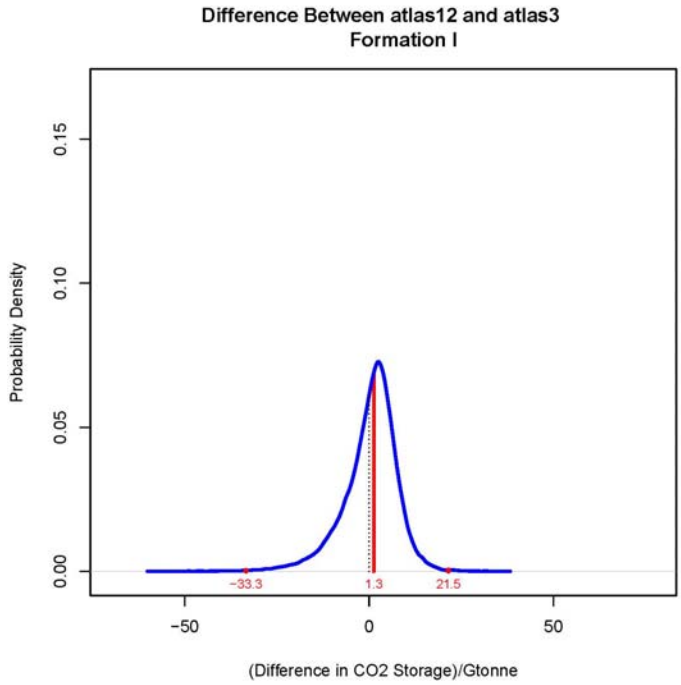
Difference Between atlas12 and atlas3
Formation I
Probability Density
0.00
0.05
0.10
0.15
−33.3
1.3
21.5
−50
0
50
(Difference in CO2 Storage)/Gtonne

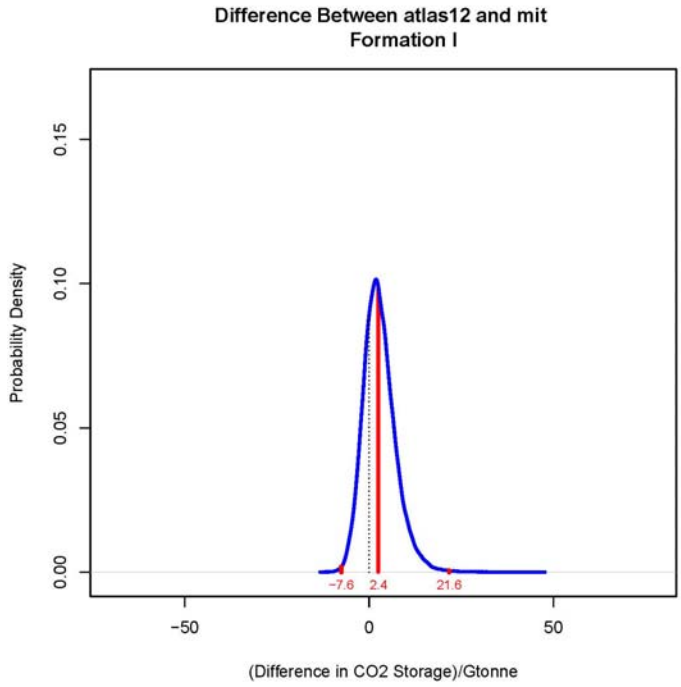
Difference Between atlas12 and mit
Formation I
Probability Density
0.00
0.05
0.10
0.15
−7.6
2.4
21.6
−50
0
50
(Difference in CO2 Storage)/Gtonne

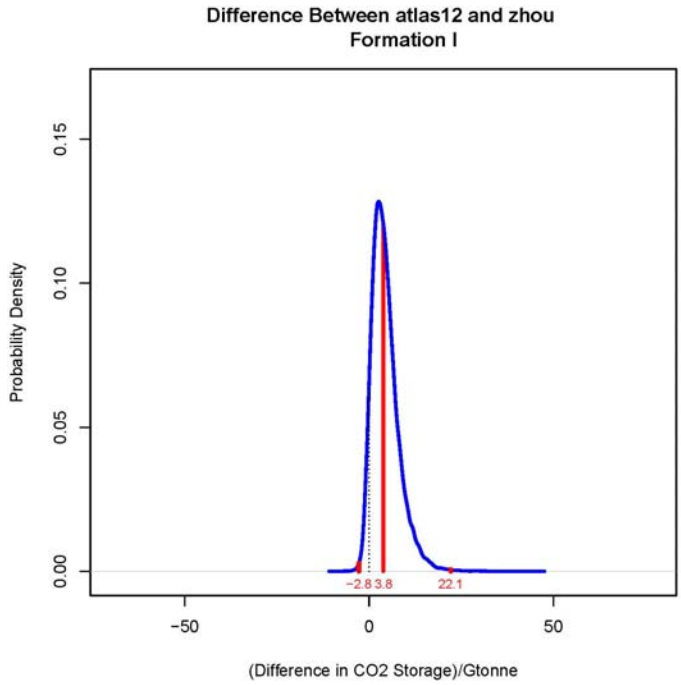
Difference Between atlas12 and zhou
Formation I
Probability Density
0.00
0.05
0.10
0.15
−2.8
3.8
22.1
−50
0
50
(Difference in CO2 Storage)/Gtonne

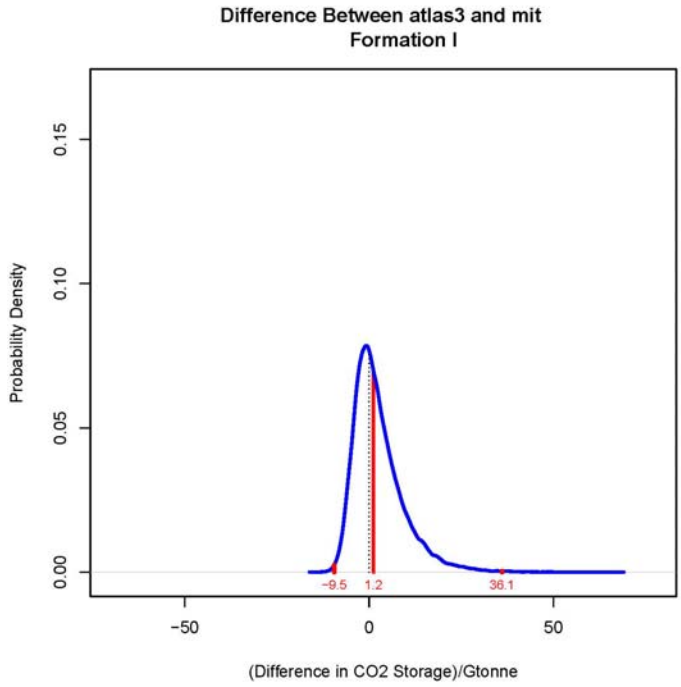
Difference Between atlas3 and mit
Formation I
Probability Density
0.00
0.05
0.10
0.15
−9.5
1.2
36.1
−50
0
50
(Difference in CO2 Storage)/Gtonne

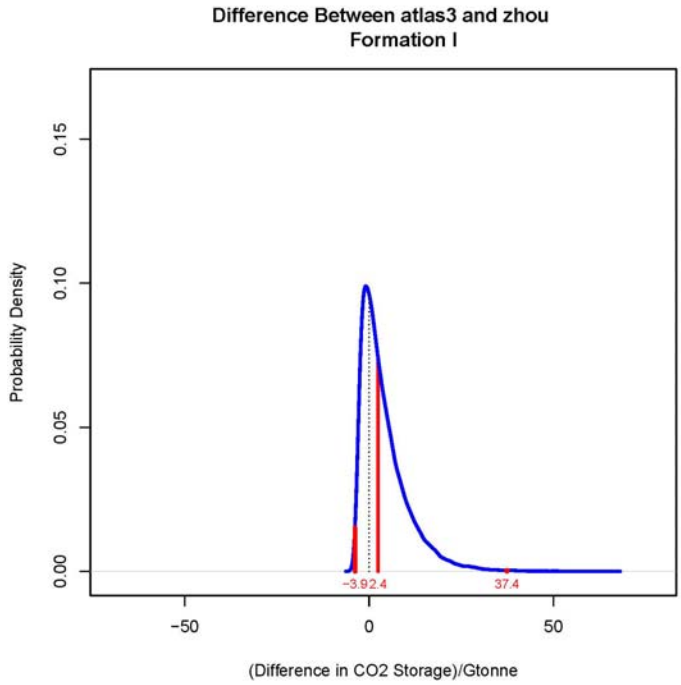
Difference Between atlas3 and zhou
Formation I
Probability Density
0.00
0.05
0.10
0.15
−3.9
2.4
37.4
−50
0
50
(Difference in CO2 Storage)/Gtonne

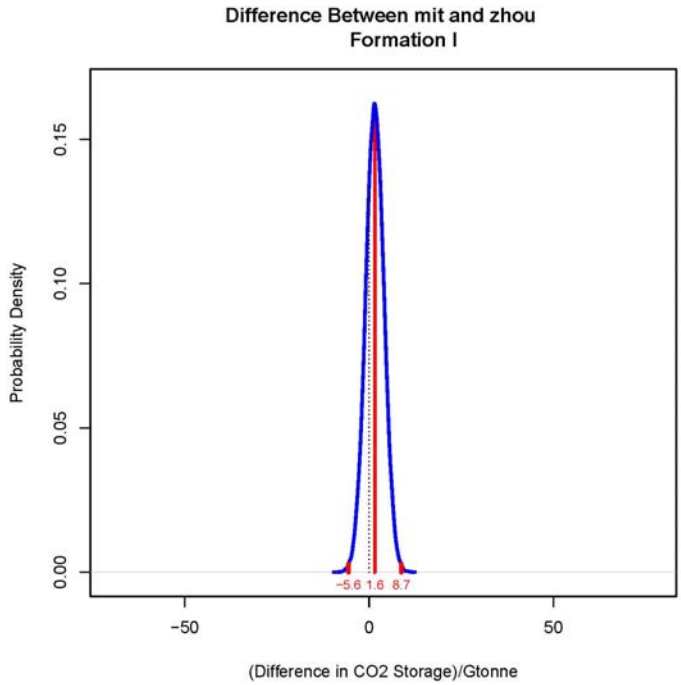
Difference Between mit and zhou
Formation I
Probability Density
0.00
0.05
0.10
0.15
−5.6 1.6 8.7
−50
0
50
(Difference in CO2 Storage)/Gtonne

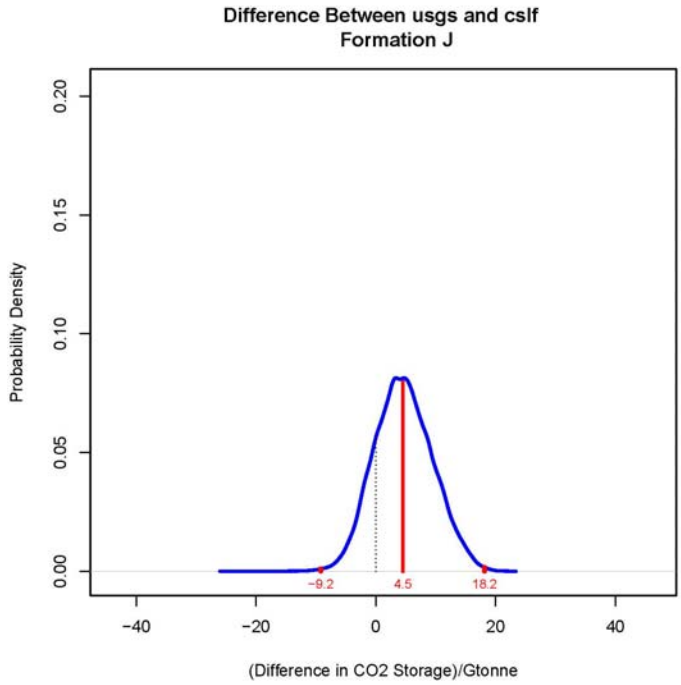
Difference Between usgs and cslf
Formation J
Probability Density
0.00
0.05
0.10
0.15
0.20
−9.2
4.5
18.2
−40
−20
0
20
40
(Difference in CO2 Storage)/Gtonne

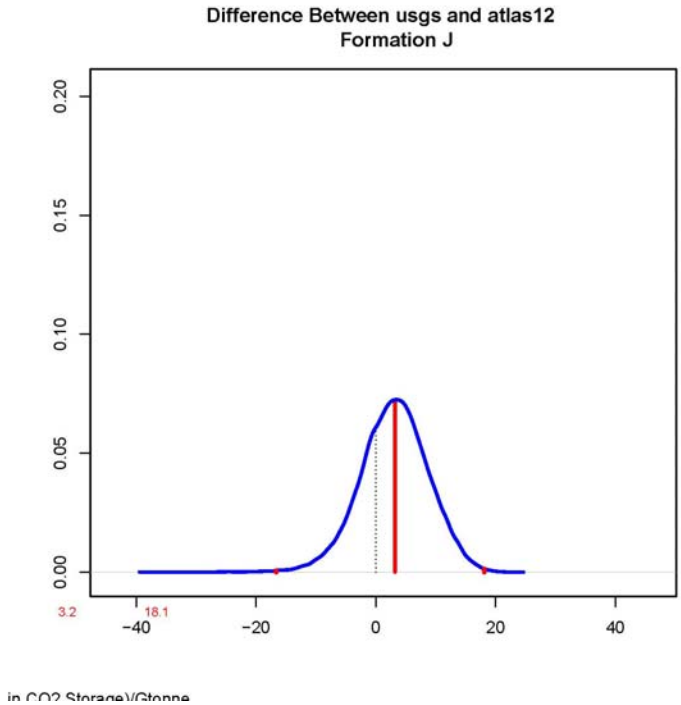
Difference Between usgs and atlas12
Formation J
0.20
0.15
0.10
0.05
0.00
3.2
18.1
−40
−20
0
20
40
in CO2 Storage)/Gtonne

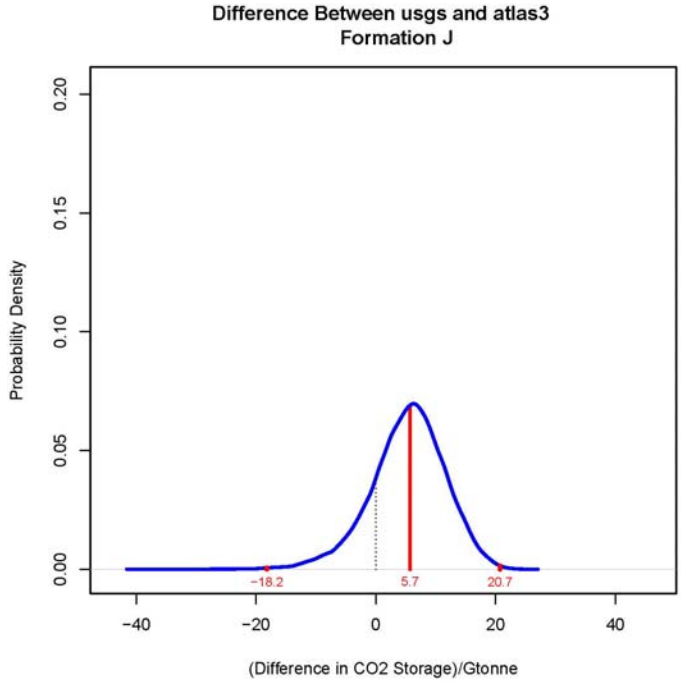
Difference Between usgs and atlas3
Formation J
Probability Density
0.20
0.15
0.10
0.05
0.00
−18.2
5.7
20.7
−40
−20
0
20
40
(Difference in CO2 Storage)/Gtonne

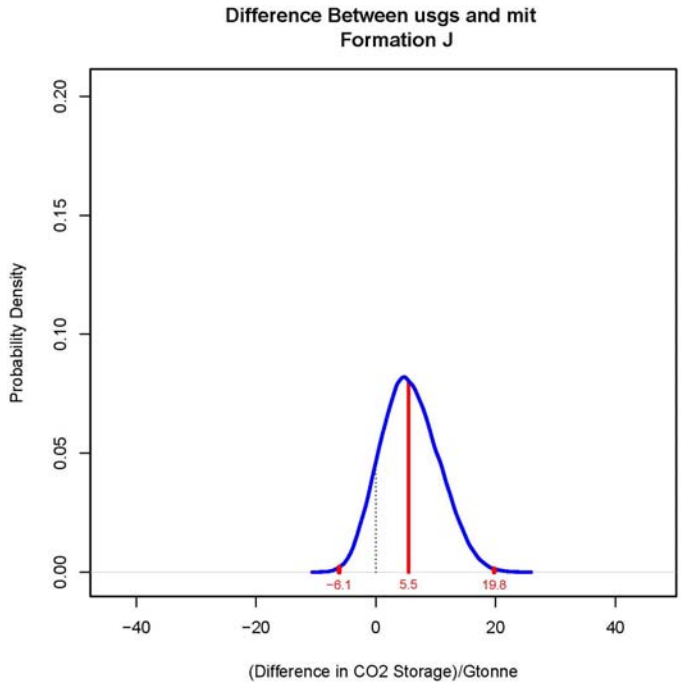
Difference Between usgs and mit
Formation J
Probability Density
0.00
0.05
0.10
0.15
0.20
−6.1
5.5
19.8
−40
−20
0
20
40
(Difference in CO2 Storage)/Gtonne

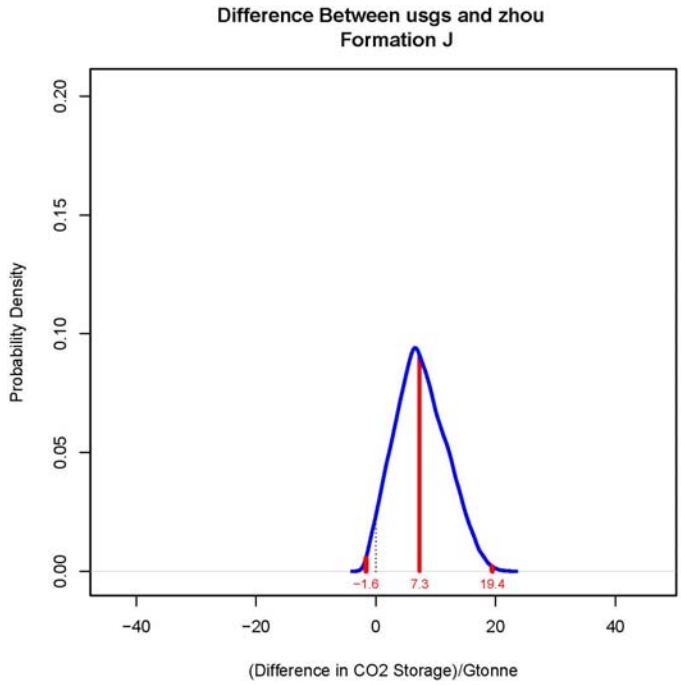
Difference Between usgs and zhou
Formation J
Probability Density
0.00
0.05
0.10
0.15
0.20
−1.6
7.3
19.4
−40
−20
0
20
40
(Difference in CO2 Storage)/Gtonne

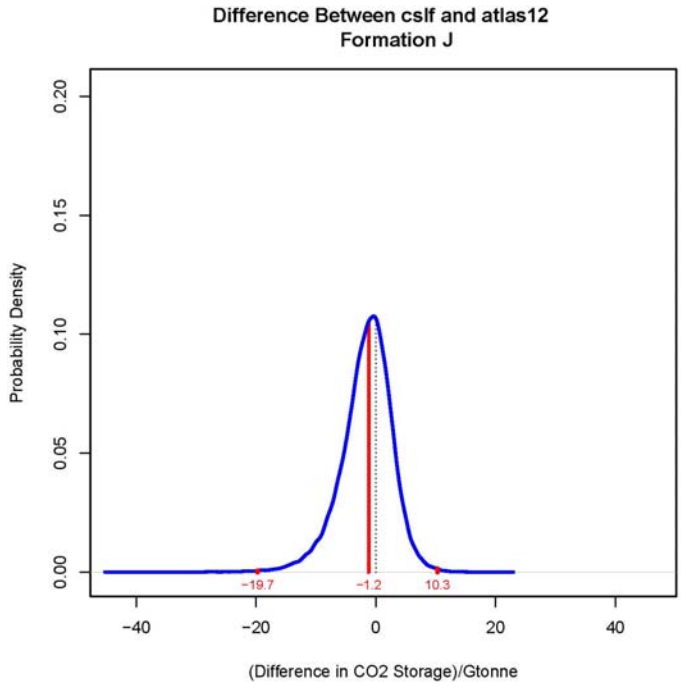
Difference Between cslf and atlas12
Formation J
Probability Density
0.00
0.05
0.10
0.15
0.20
−19.7
−1.2
10.3
−40
−20
0
20
40
(Difference in CO2 Storage)/Gtonne

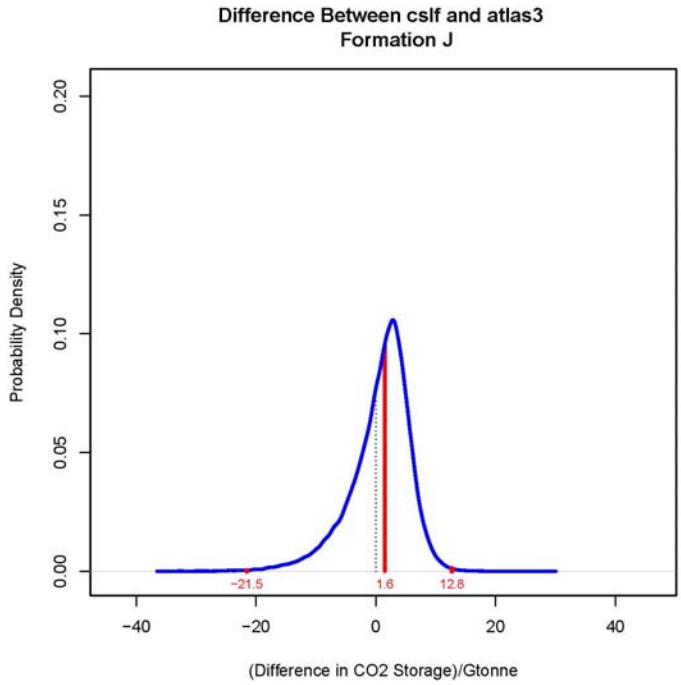
Difference Between cslf and atlas3
Formation J
Probability Density
0.00
0.05
0.10
0.15
0.20
−21.5
1.6
12.8
−40
−20
0
20
40
(Difference in CO2 Storage)/Gtonne

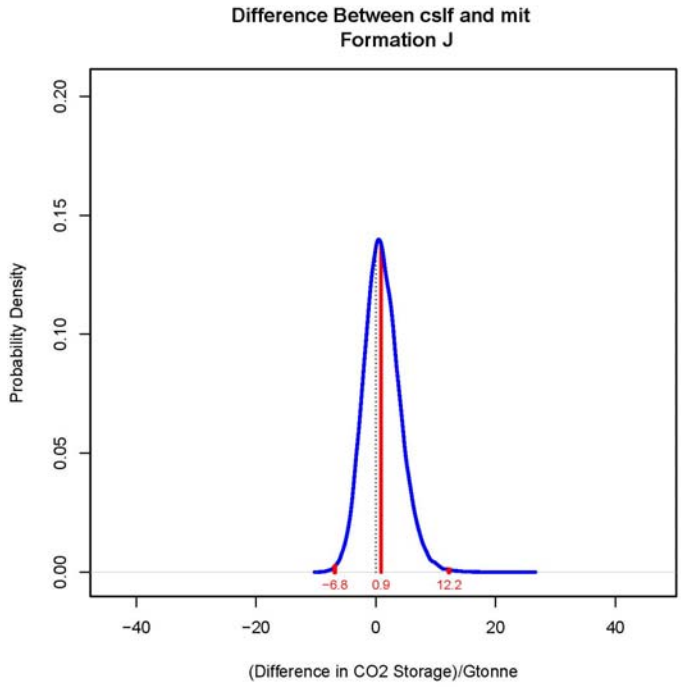
Difference Between cslf and mit
Formation J
Probability Density
0.00
0.05
0.10
0.15
0.20
−6.8
0.9
12.2
−40
−20
0
20
40
(Difference in CO2 Storage)/Gtonne

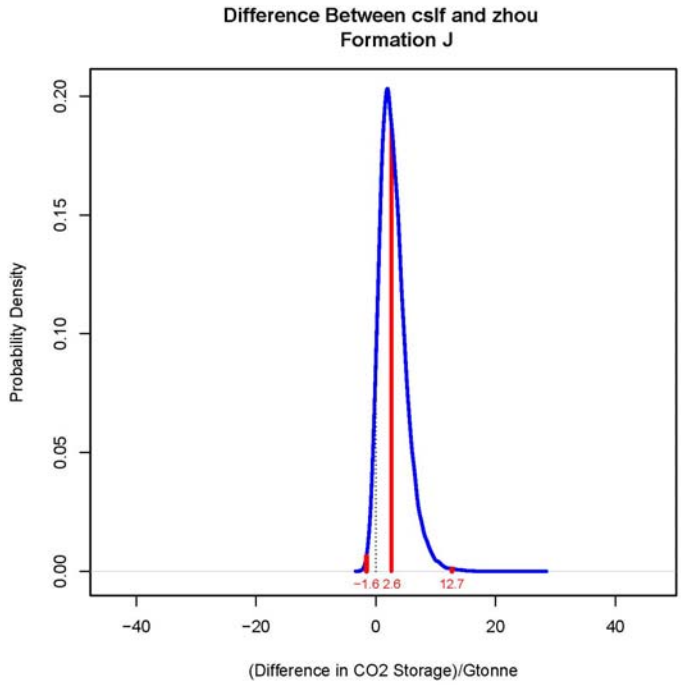
Difference Between cslf and zhou
Formation J
Probability Density
0.00
0.05
0.10
0.15
0.20
−1.6
2.6
12.7
−40
−20
0
20
40
(Difference in CO2 Storage)/Gtonne

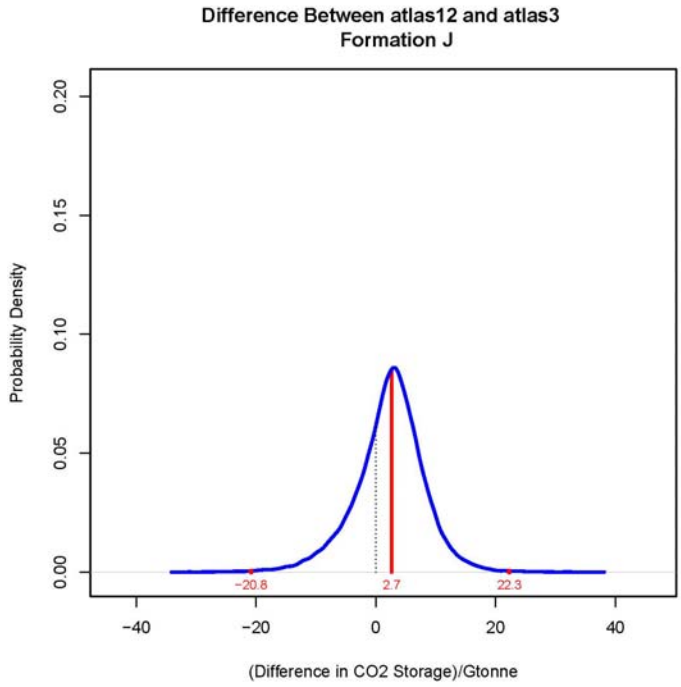
Difference Between atlas12 and atlas3
Formation J
Probability Density
0.00
0.05
0.10
0.15
0.20
−20.8
2.7
22.3
−40
−20
0
20
40
(Difference in CO2 Storage)/Gtonne

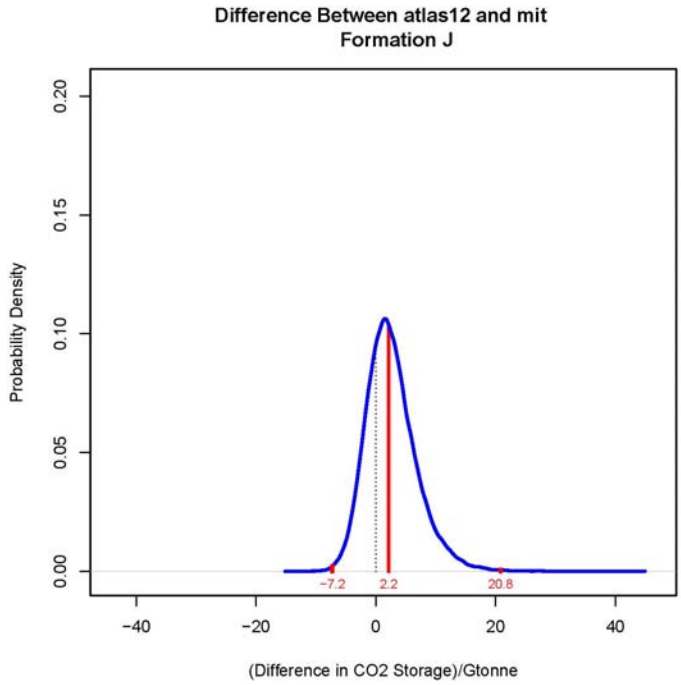
Difference Between atlas12 and mit
Formation J
Probability Density
0.00
0.05
0.10
0.15
0.20
−7.2
2.2
20.8
−40
−20
0
20
40
(Difference in CO2 Storage)/Gtonne

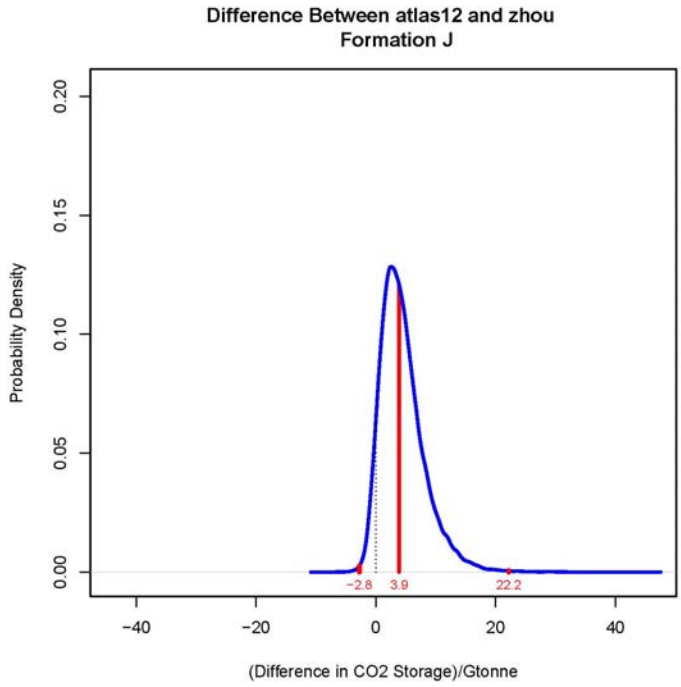
Difference Between atlas12 and zhou
Formation J
Probability Density
0.00
0.05
0.10
0.15
0.20
−2.8
3.9
22.2
−40
−20
0
20
40
(Difference in CO2 Storage)/Gtonne

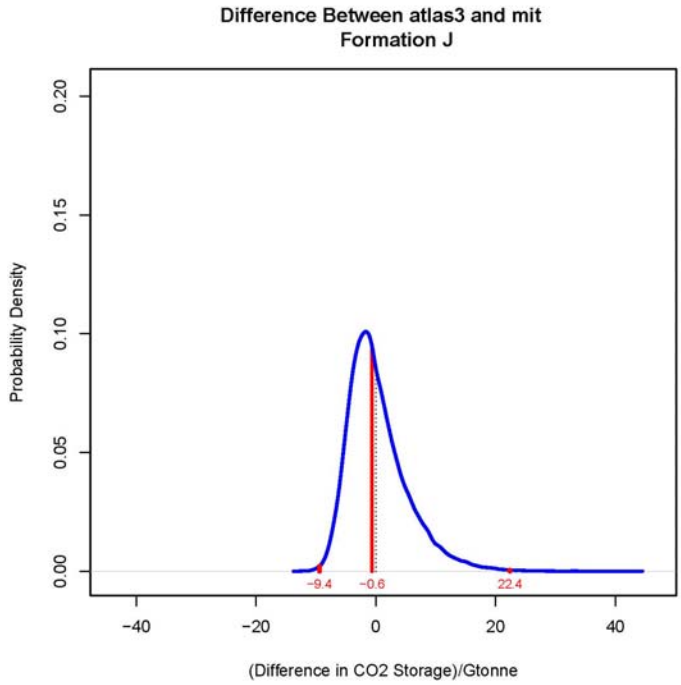
Difference Between atlas3 and mit
Formation J
Probability Density
0.00
0.05
0.10
0.15
0.20
−9.4
−0.6
22.4
−40
−20
0
20
40
(Difference in CO2 Storage)/Gtonne

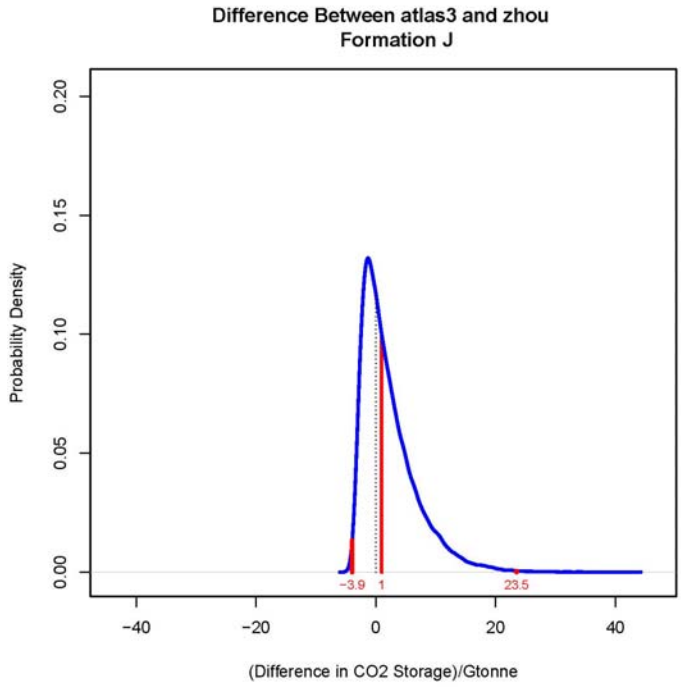
Difference Between atlas3 and zhou
Formation J
Probability Density
0.00
0.05
0.10
0.15
0.20
−3.9
1
23.5
−40
−20
0
20
40
(Difference in CO2 Storage)/Gtonne

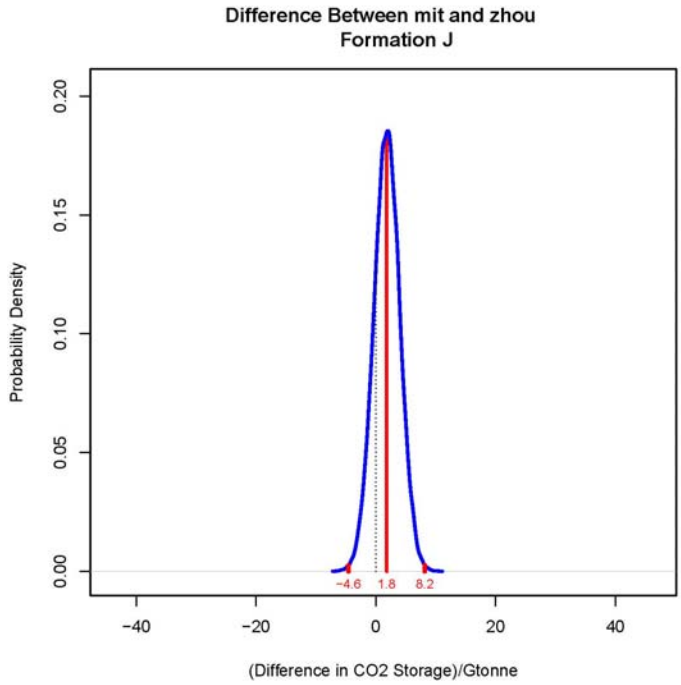
Difference Between mit and zhou
Formation J
Probability Density
0.00
0.05
0.10
0.15
0.20
−4.6
1.8
8.2
−40
−20
0
20
40
(Difference in CO2 Storage)/Gtonne

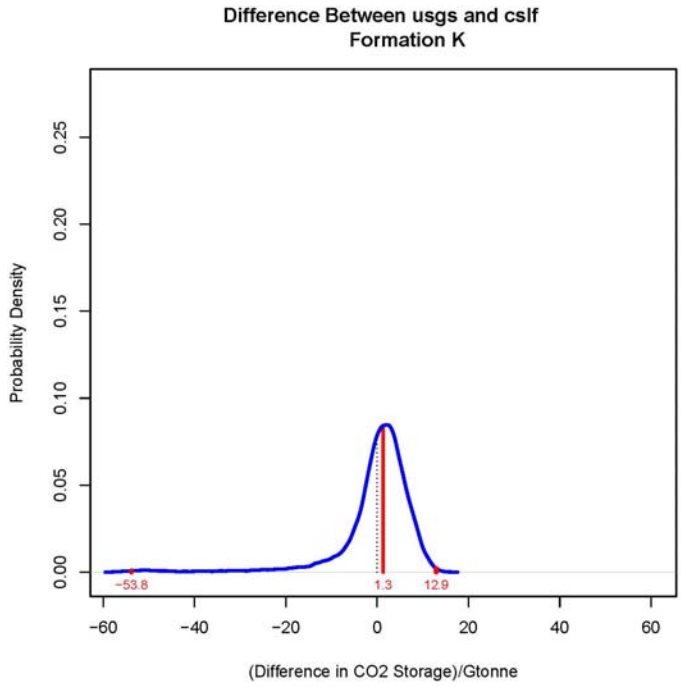
Difference Between usgs and cslf
Formation K
Probability Density
0.00
0.05
0.10
0.15
0.20
0.25
−53.8
1.3
12.9
−60
−40
−20
0
20
40
60
(Difference in CO2 Storage)/Gtonne

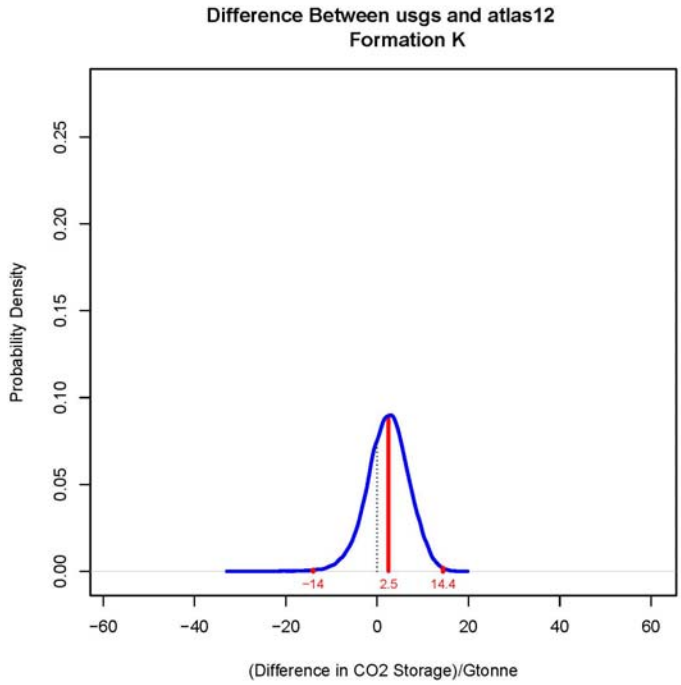
Difference Between usgs and atlas12
Formation K
Probability Density
0.00
0.05
0.10
0.15
0.20
0.25
−14
2.5
14.4
−60
−40
−20
0
20
40
60
(Difference in CO2 Storage)/Gtonne

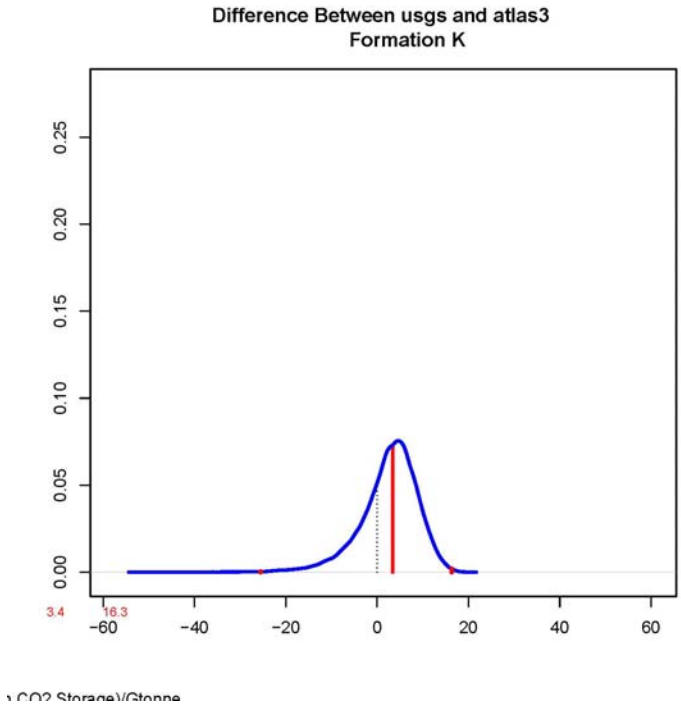
Difference Between usgs and atlas3
Formation K
0.25
0.20
0.15
0.10
0.05
0.00
3.4
16.3
−60
−40
−20
0
20
40
60

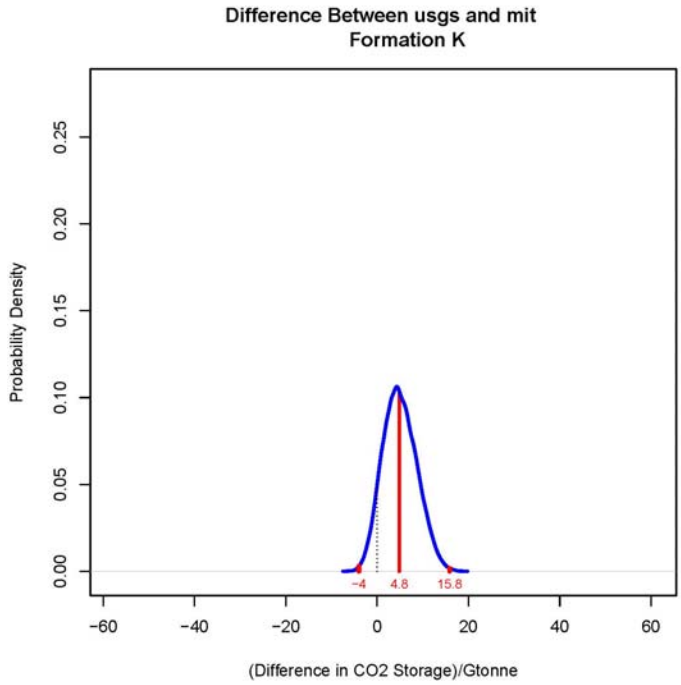
Difference Between usgs and mit
Formation K
Probability Density
0.25
0.20
0.15
0.10
0.05
0.00
−4
4.8
15.8
−60
−40
−20
0
20
40
60
(Difference in CO2 Storage)/Gtonne

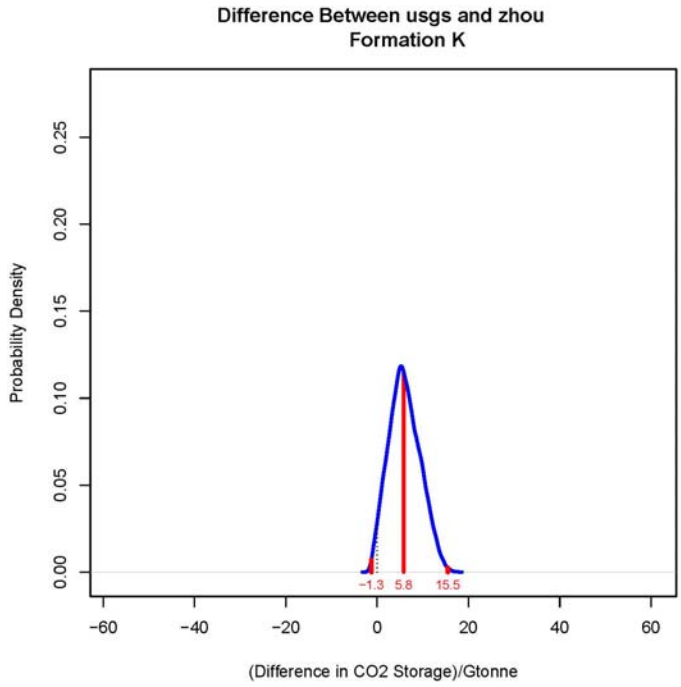
Difference Between usgs and zhou
Formation K
Probability Density
0.00
0.05
0.10
0.15
0.20
0.25
−1.3
5.8
15.5
−60
−40
−20
0
20
40
60
(Difference in CO2 Storage)/Gtonne

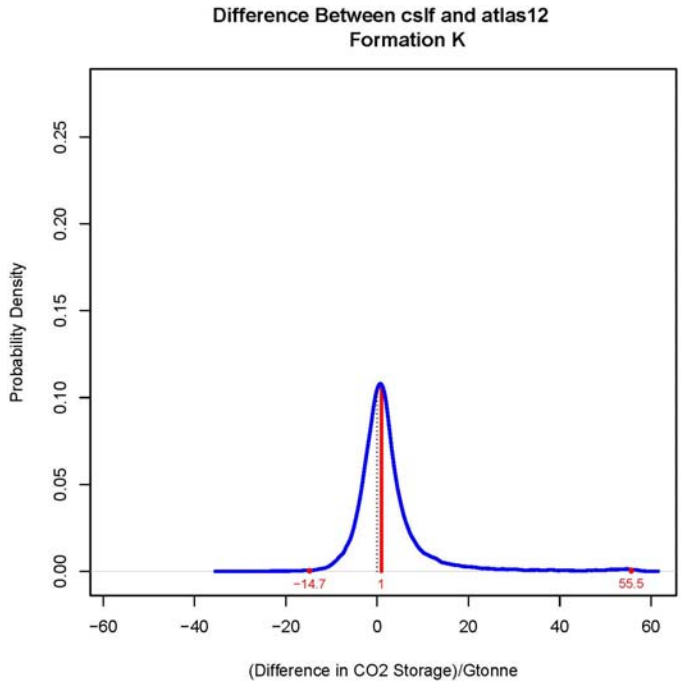
Difference Between cslf and atlas12
Formation K
Probability Density
0.00
0.05
0.10
0.15
0.20
0.25
−14.7
1
55.5
−60
−40
−20
0
20
40
60
(Difference in CO2 Storage)/Gtonne

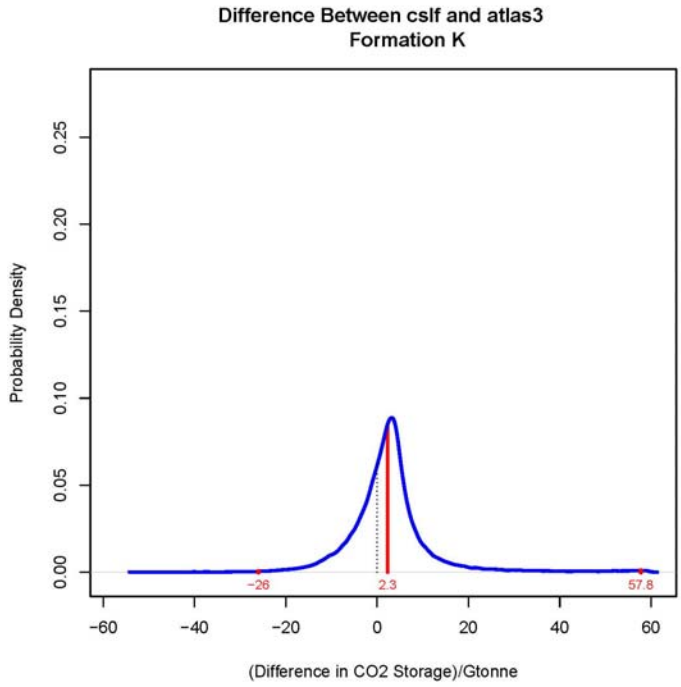
Difference Between cslf and atlas3
Formation K
Probability Density
0.00
0.05
0.10
0.15
0.20
0.25
−26
2.3
57.8
−60
−40
−20
0
20
40
60
(Difference in CO2 Storage)/Gtonne

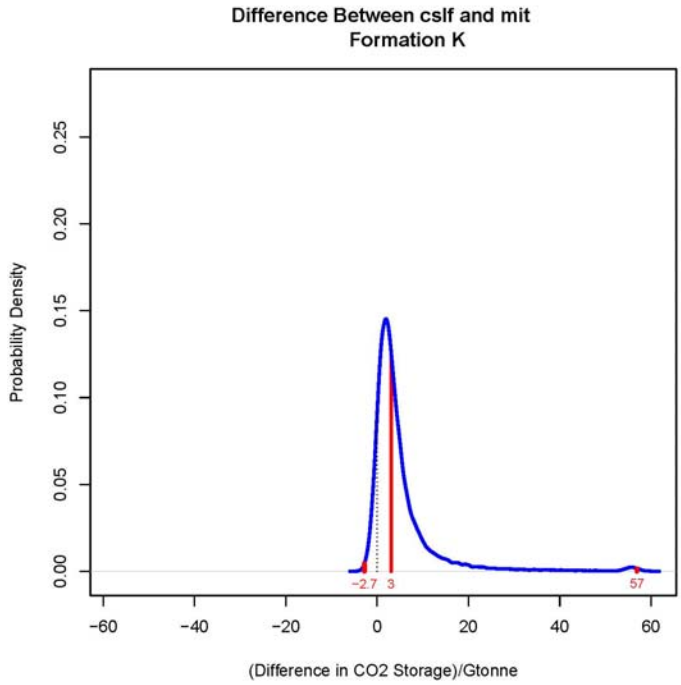
Difference Between cslf and mit
Formation K
Probability Density
0.00
0.05
0.10
0.15
0.20
0.25
−2.7
3
57
−60
−40
−20
0
20
40
60
(Difference in CO2 Storage)/Gtonne

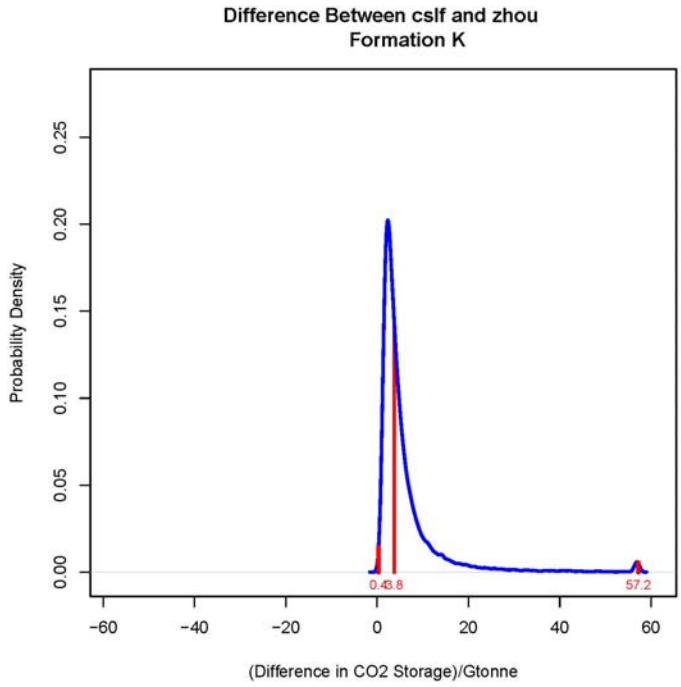
Difference Between cslf and zhou
Formation K
Probability Density
0.00
0.05
0.10
0.15
0.20
0.25
0.4
3.8
57.2
−60
−40
−20
0
20
40
60
(Difference in CO2 Storage)/Gtonne

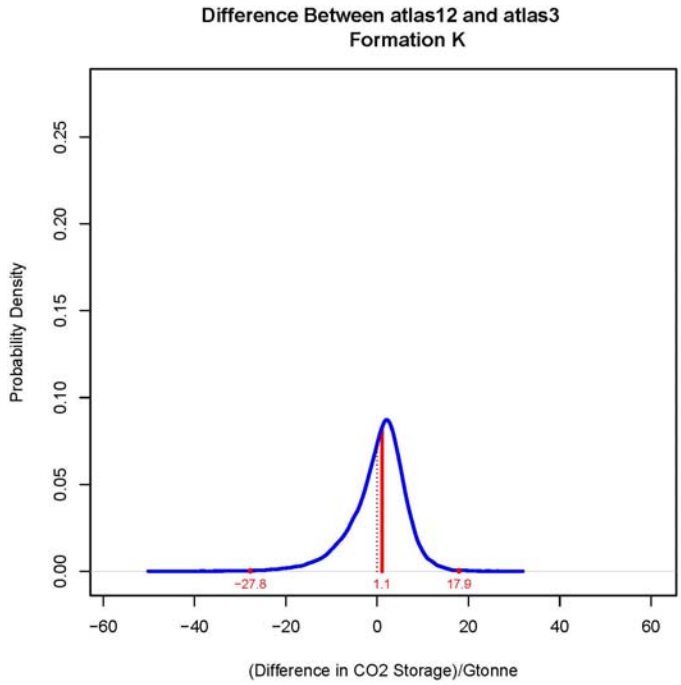
Difference Between atlas12 and atlas3
Formation K
Probability Density
0.00
0.05
0.10
0.15
0.20
0.25
−27.8
1.1
17.9
−60
−40
−20
0
20
40
60
(Difference in CO2 Storage)/Gtonne

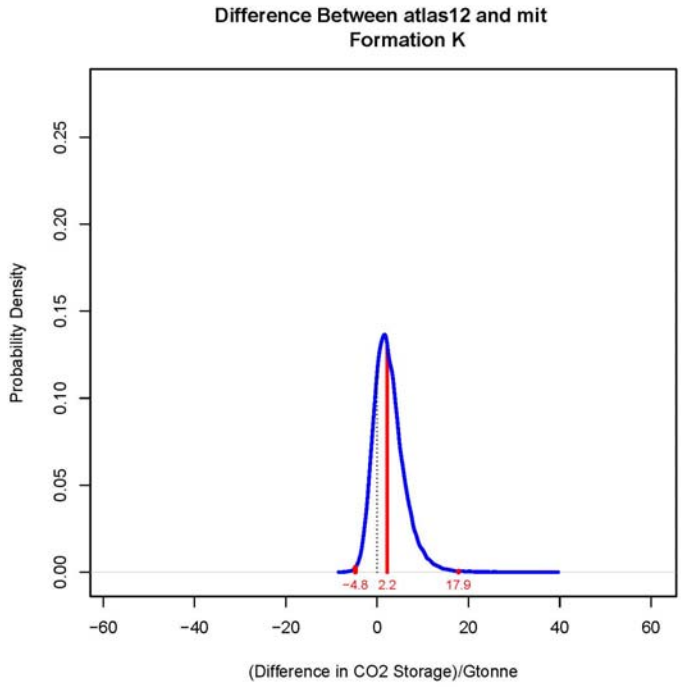
Difference Between atlas12 and mit
Formation K
Probability Density
0.00
0.05
0.10
0.15
0.20
0.25
−4.8
2.2
17.9
−60
−40
−20
0
20
40
60
(Difference in CO2 Storage)/Gtonne

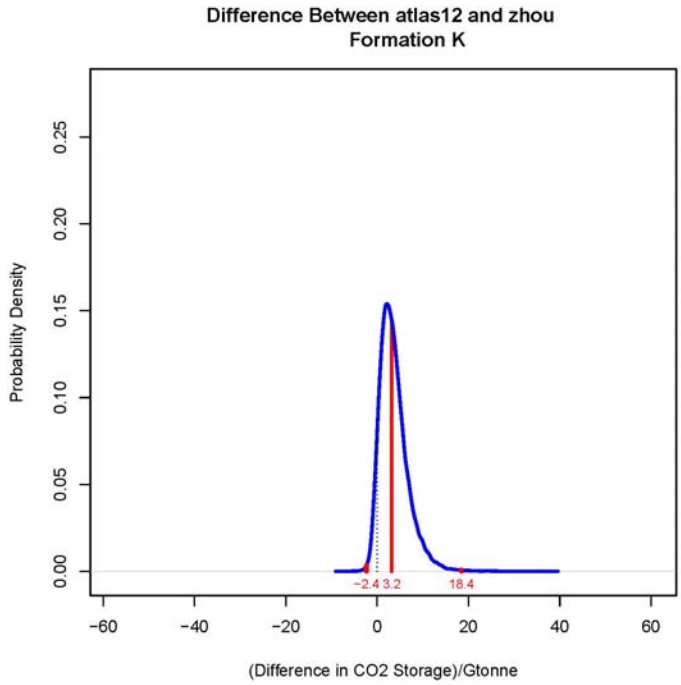
Difference Between atlas12 and zhou
Formation K
Probability Density
0.00
0.05
0.10
0.15
0.20
0.25
−2.4
3.2
18.4
−60
−40
−20
0
20
40
60
(Difference in CO2 Storage)/Gtonne

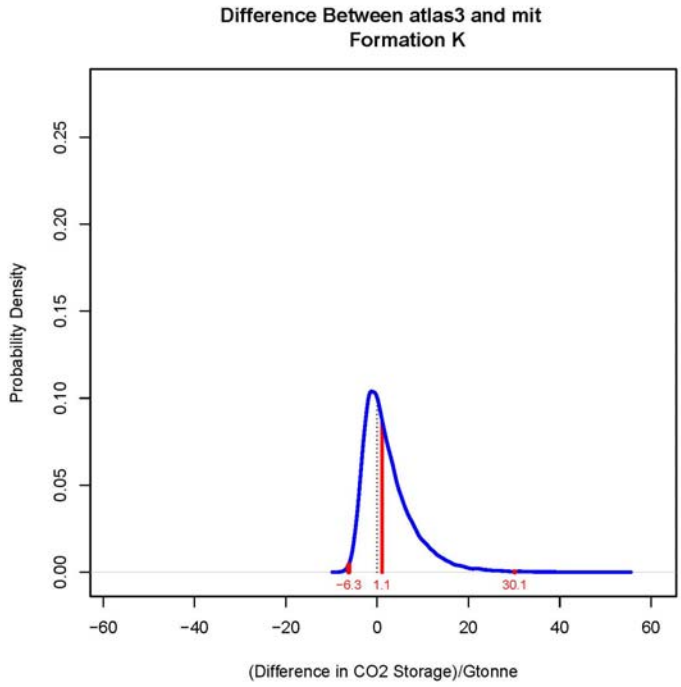
Difference Between atlas3 and mit
Formation K
Probability Density
0.00
0.05
0.10
0.15
0.20
0.25
−6.3
1.1
30.1
−60
−40
−20
0
20
40
60
(Difference in CO2 Storage)/Gtonne

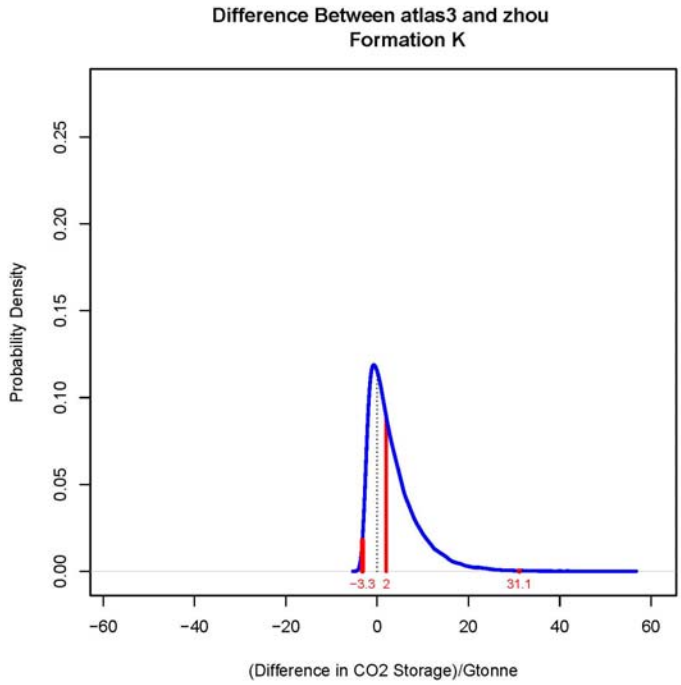
Difference Between atlas3 and zhou
Formation K
Probability Density
0.00
0.05
0.10
0.15
0.20
0.25
−3.3
2
31.1
−60
−40
−20
0
20
40
60
(Difference in CO2 Storage)/Gtonne

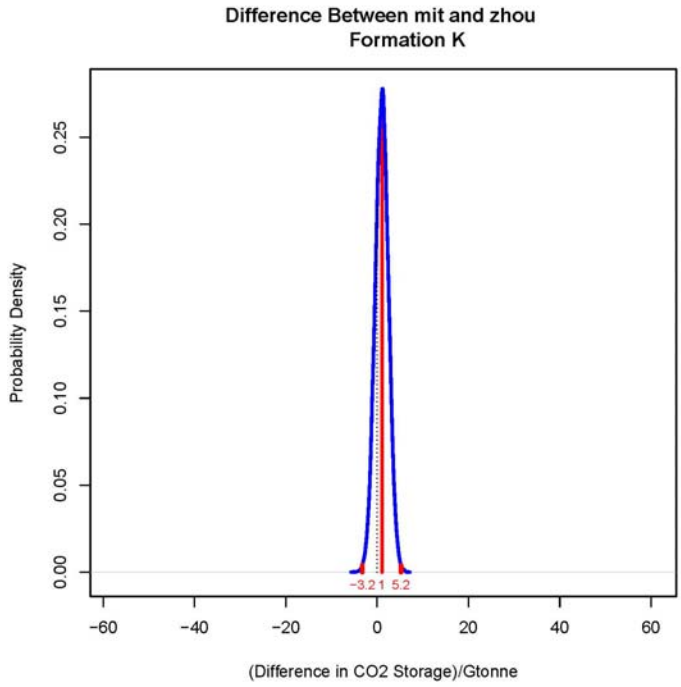
Difference Between mit and zhou
Formation K
Probability Density
0.00
0.05
0.10
0.15
0.20
0.25
−3.2
1
5.2
−60
−40
−20
0
20
40
60
(Difference in CO2 Storage)/Gtonne

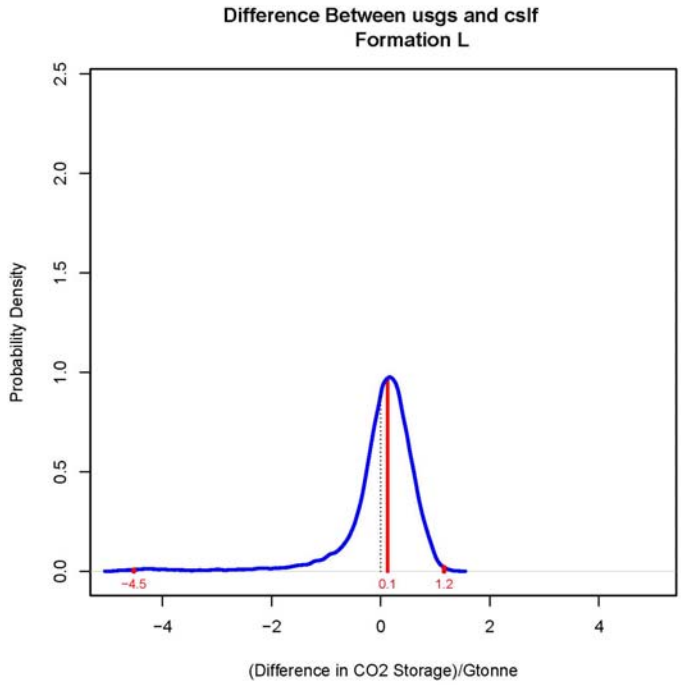
Difference Between usgs and cslf
Formation L
Probability Density
0.0
0.5
1.0
1.5
2.0
2.5
−4.5
0.1
1.2
−4
−2
0
2
4
(Difference in CO2 Storage)/Gtonne

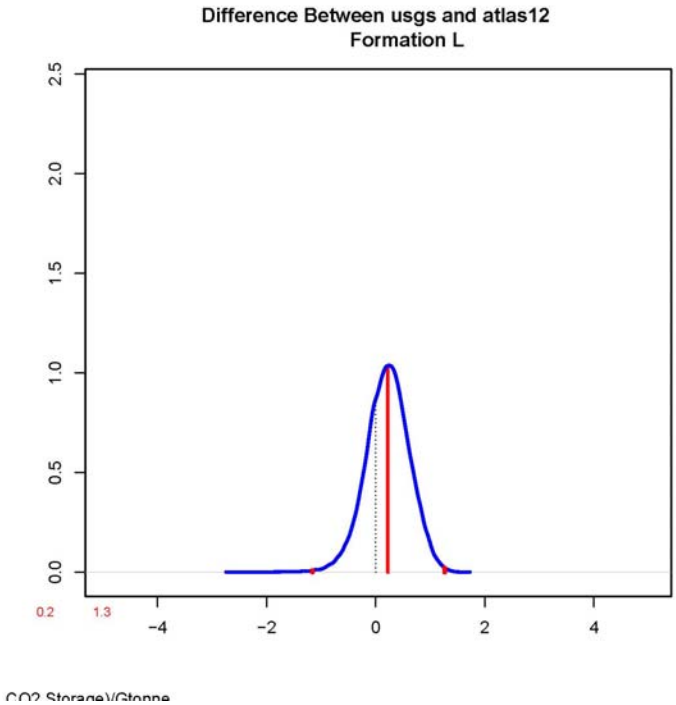
Difference Between usgs and atlas12
Formation L
0.2
1.3
CO2 Storage)/Gtonne

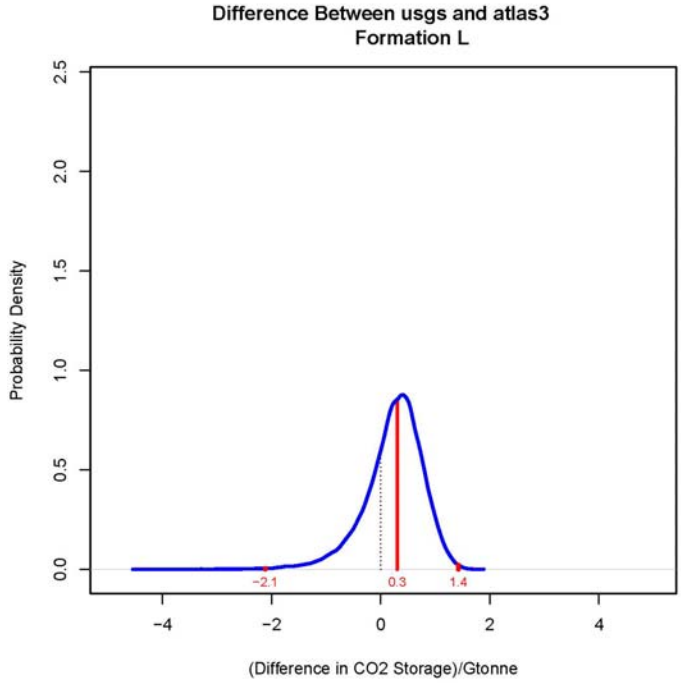
Difference Between usgs and atlas3
Formation L
Probability Density
-2.1
0.3
1.4
(Difference in CO2 Storage)/Gtonne

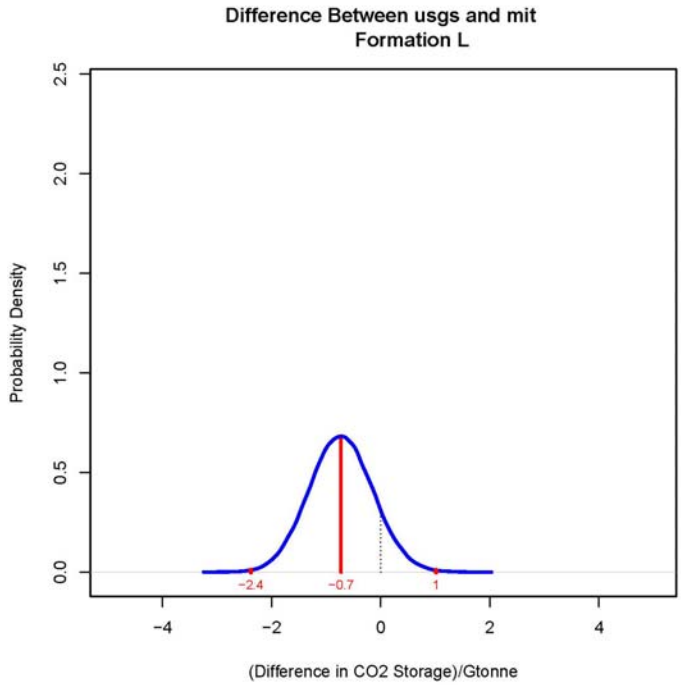
Difference Between usgs and mit
Formation L
Probability Density
0.0
0.5
1.0
1.5
2.0
2.5
−2.4
−0.7
1
−4
−2
0
2
4
(Difference in CO2 Storage)/Gtonne

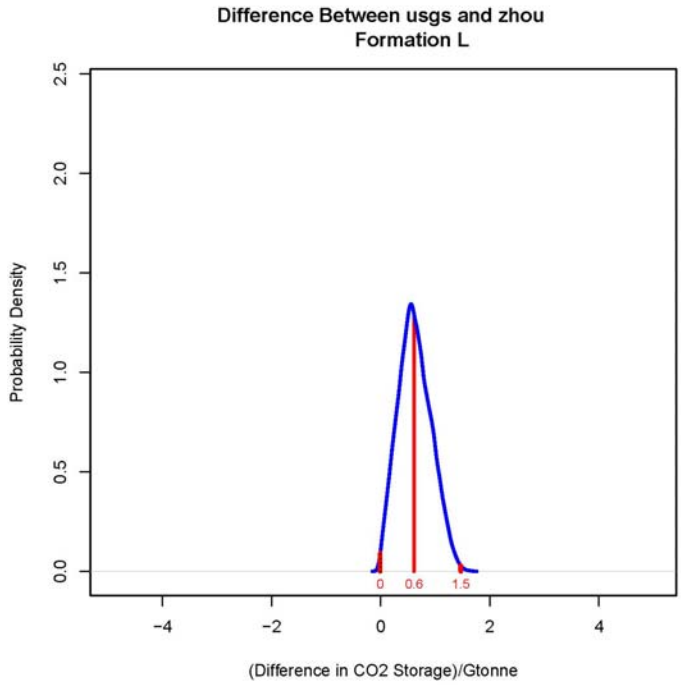
Difference Between usgs and zhou
Formation L
Probability Density
0.0
0.5
1.0
1.5
2.0
2.5
0
0.6
1.5
−4
−2
0
2
4
(Difference in CO2 Storage)/Gtonne

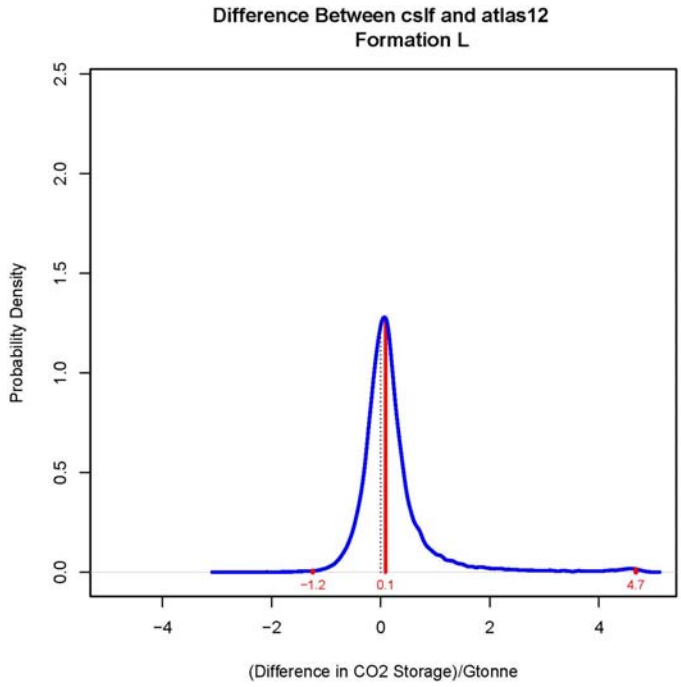
Difference Between cslf and atlas12
Formation L
Probability Density
0.0
0.5
1.0
1.5
2.0
2.5
−1.2
0.1
4.7
−4
−2
0
2
4
(Difference in CO2 Storage)/Gtonne

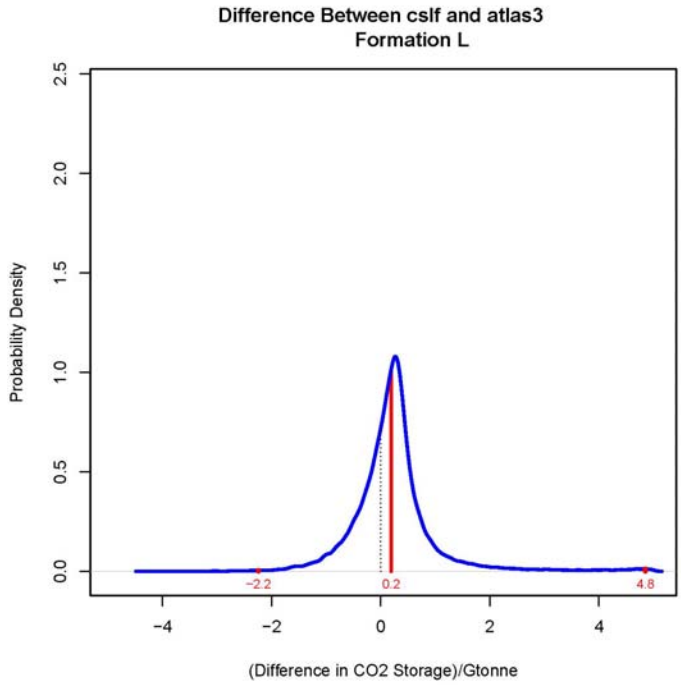
Difference Between cslf and atlas3
Formation L
Probability Density
0.0
0.5
1.0
1.5
2.0
2.5
−2.2
0.2
4.8
−4
−2
0
2
4
(Difference in CO2 Storage)/Gtonne

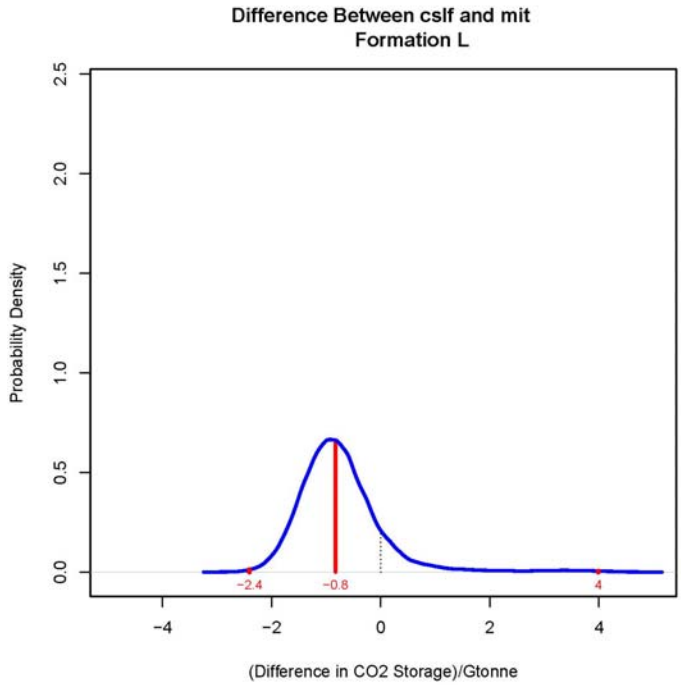
Difference Between cslf and mit
Formation L
Probability Density
0.0
0.5
1.0
1.5
2.0
2.5
−2.4
−0.8
4
−4
−2
0
2
4
(Difference in CO2 Storage)/Gtonne

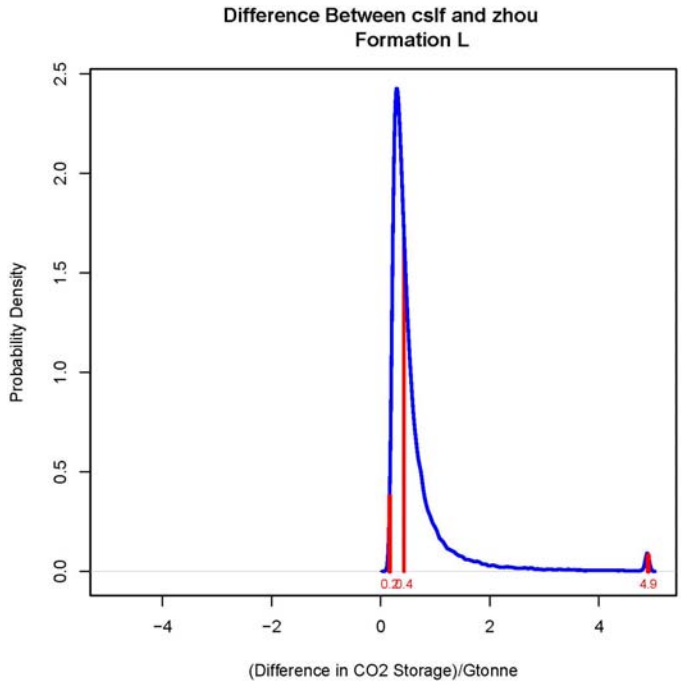
Difference Between cslf and zhou
Formation L
Probability Density
0.0
0.5
1.0
1.5
2.0
2.5
0.2
0.4
4.9
−4
−2
0
2
4
(Difference in CO2 Storage)/Gtonne

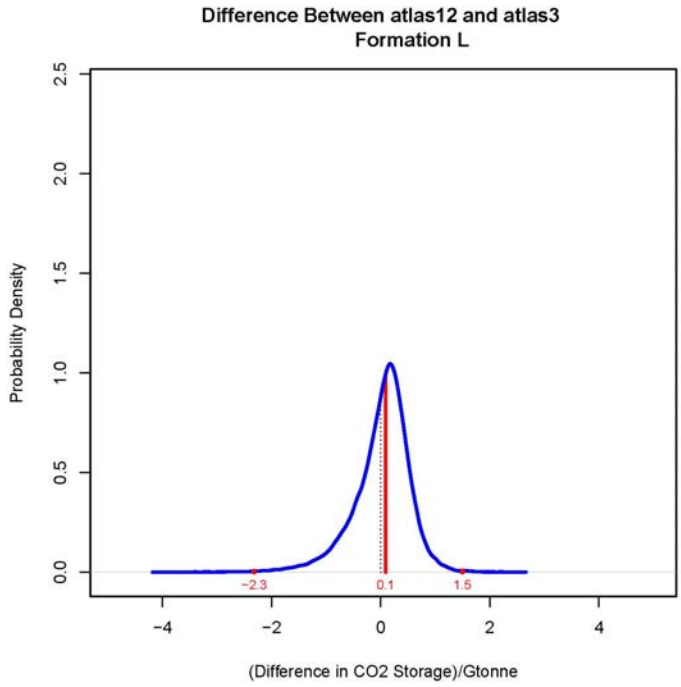
Difference Between atlas12 and atlas3
Formation L
Probability Density
0.0
0.5
1.0
1.5
2.0
2.5
−2.3
0.1
1.5
−4
−2
0
2
4
(Difference in CO2 Storage)/Gtonne

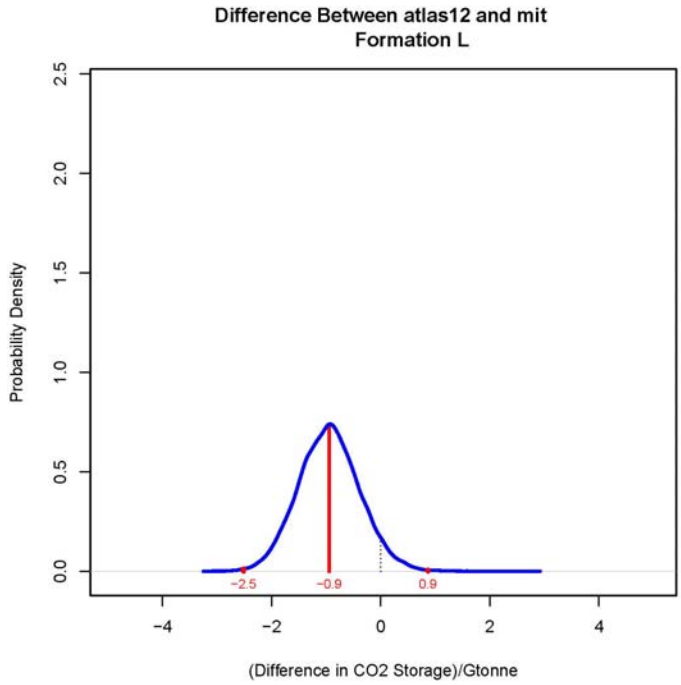
Difference Between atlas12 and mit
Formation L
Probability Density
0.0
0.5
1.0
1.5
2.0
2.5
−2.5
−0.9
0.9
−4
−2
0
2
4
(Difference in CO2 Storage)/Gtonne

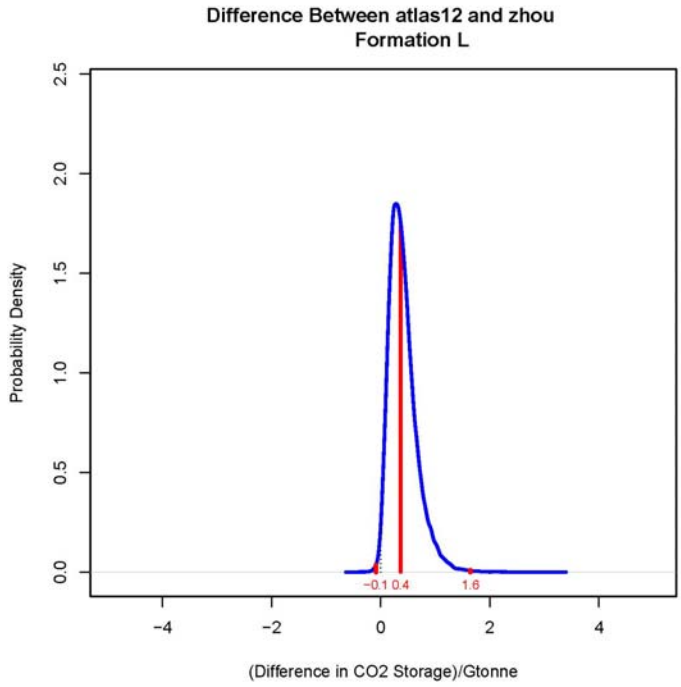
Difference Between atlas12 and zhou
Formation L
Probability Density
0.0
0.5
1.0
1.5
2.0
2.5
−0.1 0.4
1.6
−4
−2
0
2
4
(Difference in CO2 Storage)/Gtonne

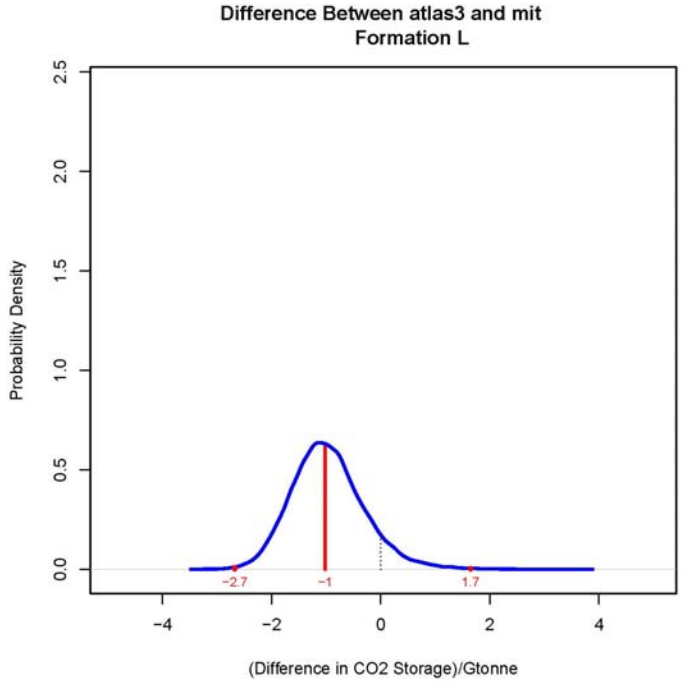
Difference Between atlas3 and mit
Formation L
Probability Density
0.0
0.5
1.0
1.5
2.0
2.5
−2.7
−1
1.7
−4
−2
0
2
4
(Difference in CO2 Storage)/Gtonne

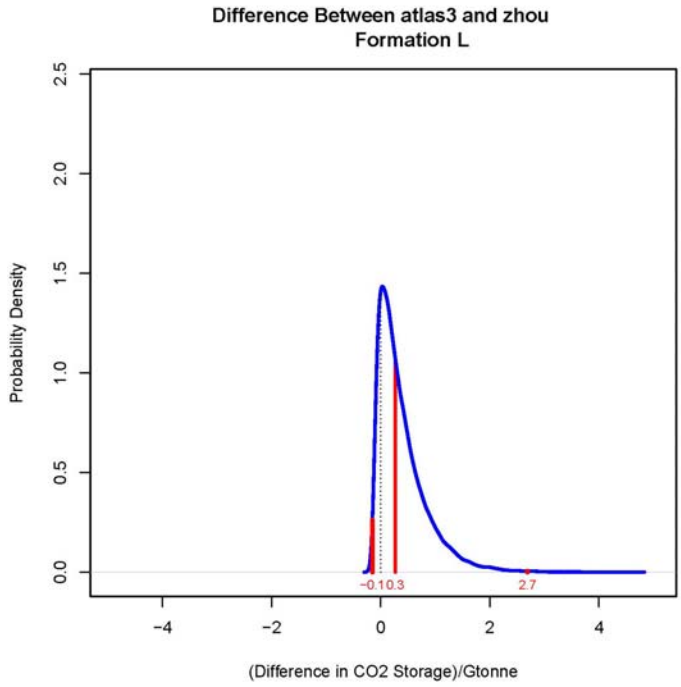
Difference Between atlas3 and zhou
Formation L
Probability Density
0.0
0.5
1.0
1.5
2.0
2.5
−0.1
0.3
2.7
−4
−2
0
2
4
(Difference in CO2 Storage)/Gtonne

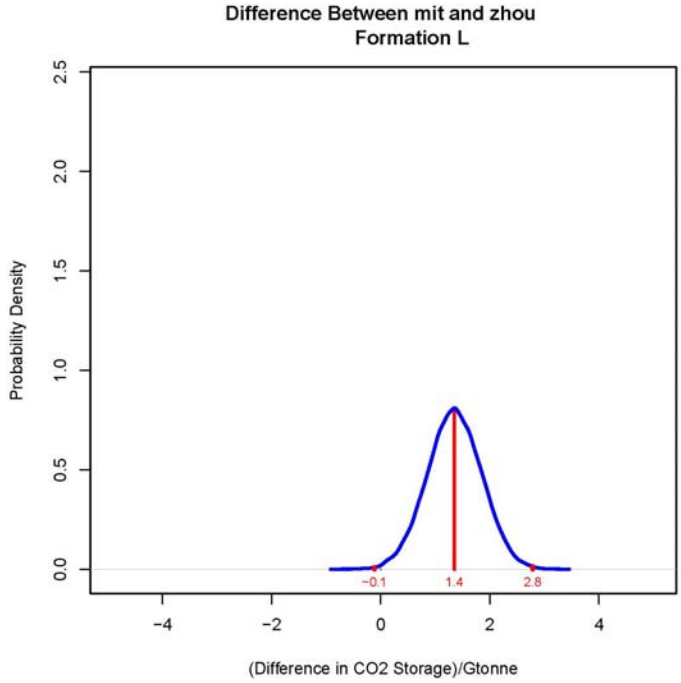
Difference Between mit and zhou
Formation L
Probability Density
0.0
0.5
1.0
1.5
2.0
2.5
−0.1
1.4
2.8
−4
−2
0
2
4
(Difference in CO2 Storage)/Gtonne

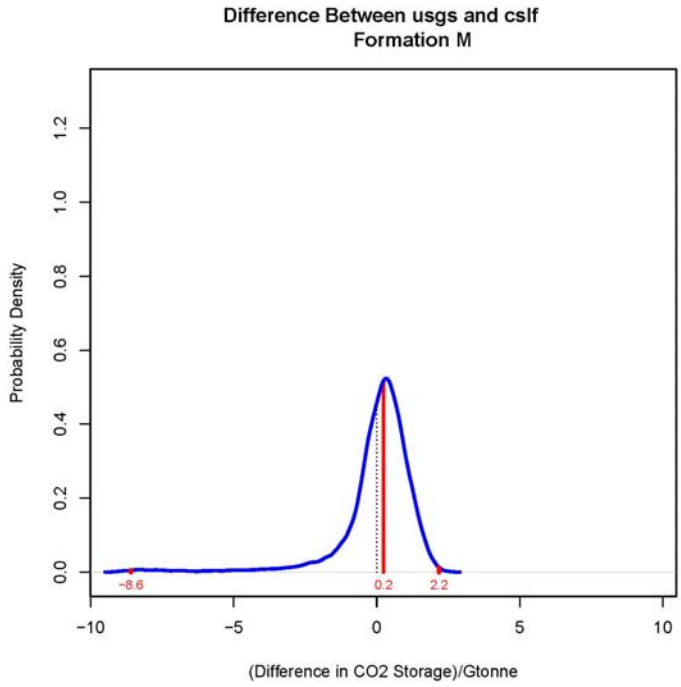
Difference Between usgs and cslf
Formation M
Probability Density
0.0
0.2
0.4
0.6
0.8
1.0
1.2
−8.6
0.2
2.2
−10
−5
0
5
10
(Difference in CO2 Storage)/Gtonne

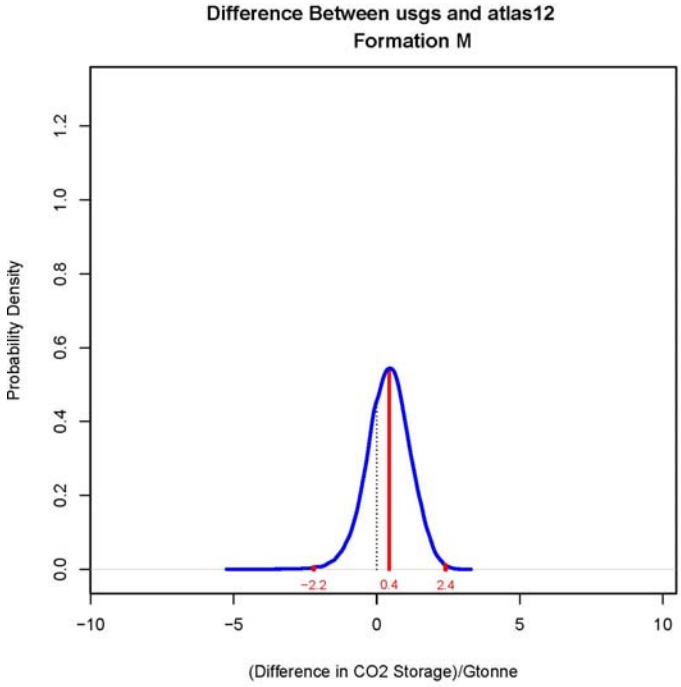
Difference Between usgs and atlas12
Formation M
Probability Density
0.0
0.2
0.4
0.6
0.8
1.0
1.2
−2.2
0.4
2.4
−10
−5
0
5
10
(Difference in CO2 Storage)/Gtonne

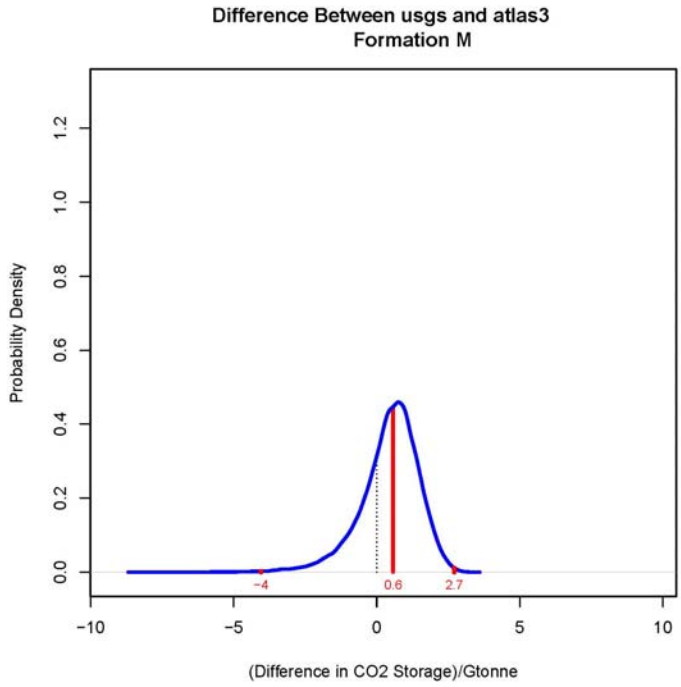
Difference Between usgs and atlas3
Formation M
Probability Density
0.0
0.2
0.4
0.6
0.8
1.0
1.2
−4
0.6
2.7
−10
−5
0
5
10
(Difference in CO2 Storage)/Gtonne

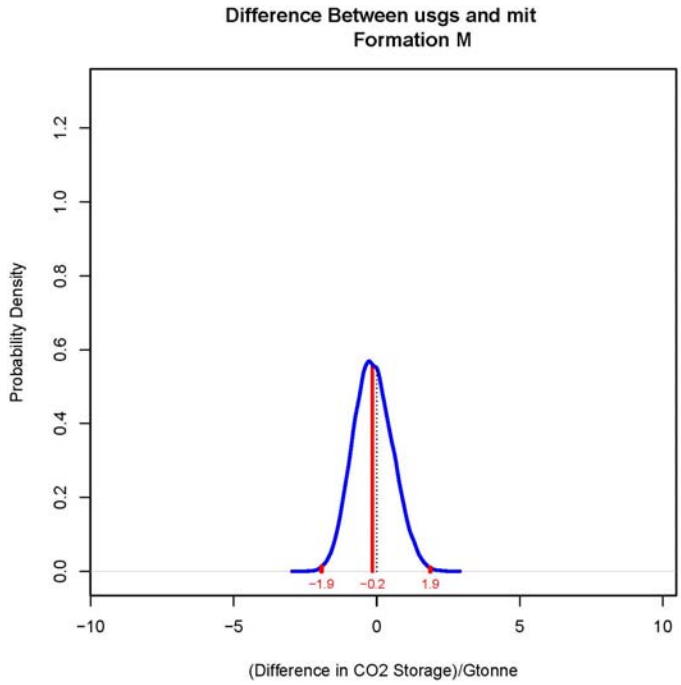
Difference Between usgs and mit
Formation M
Probability Density
0.0
0.2
0.4
0.6
0.8
1.0
1.2
−1.9
−0.2
1.9
−10
−5
0
5
10
(Difference in CO2 Storage)/Gtonne

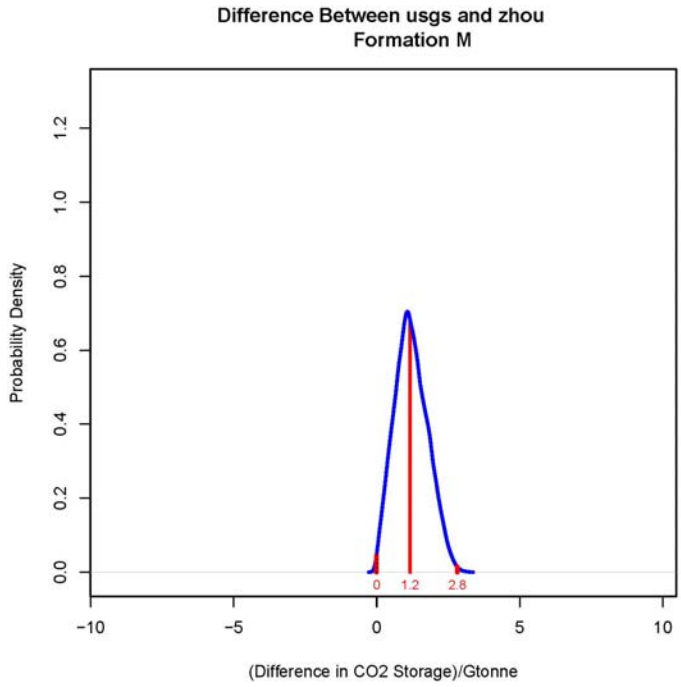
Difference Between usgs and zhou
Formation M
Probability Density
0.0
0.2
0.4
0.6
0.8
1.0
1.2
0
1.2
2.8
−10
−5
0
5
10
(Difference in CO2 Storage)/Gtonne

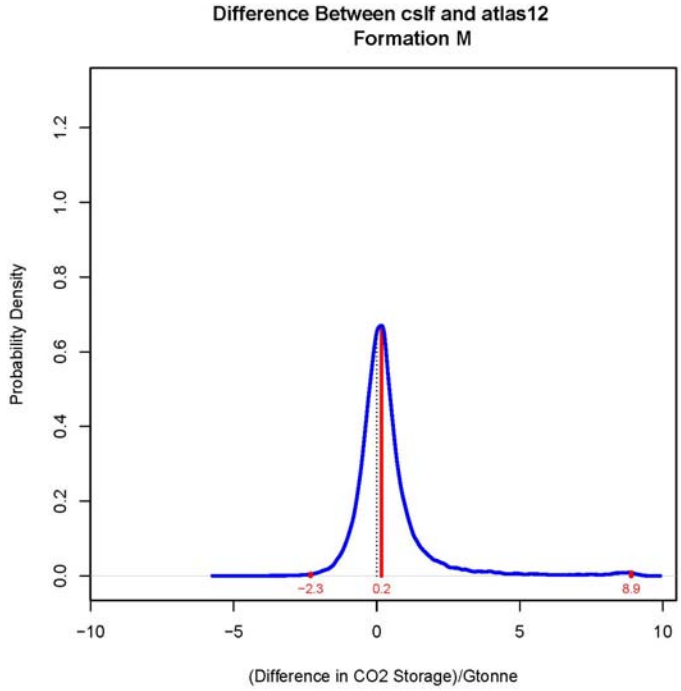
Difference Between cslf and atlas12
Formation M
Probability Density
0.0
0.2
0.4
0.6
0.8
1.0
1.2
−2.3
0.2
8.9
−10
−5
0
5
10
(Difference in CO2 Storage)/Gtonne

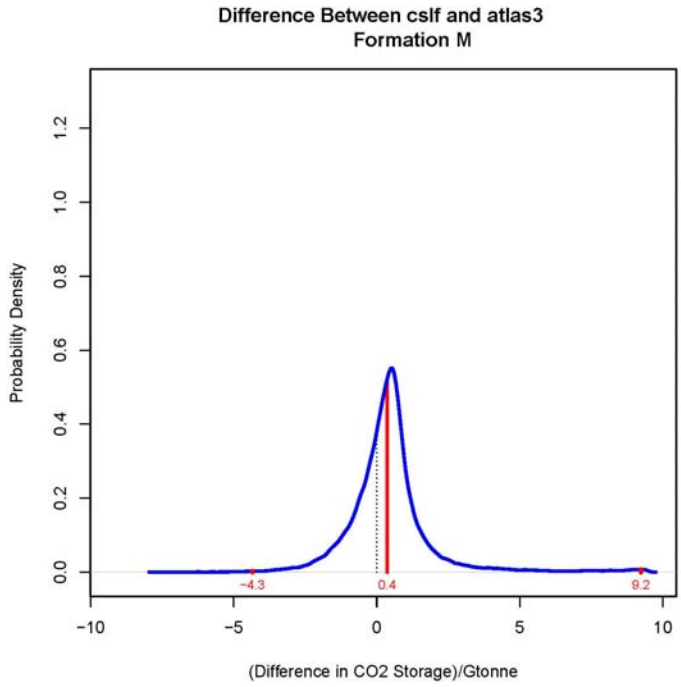
Difference Between cslf and atlas3
Formation M
Probability Density
0.0
0.2
0.4
0.6
0.8
1.0
1.2
−4.3
0.4
9.2
−10
−5
0
5
10
(Difference in CO2 Storage)/Gtonne

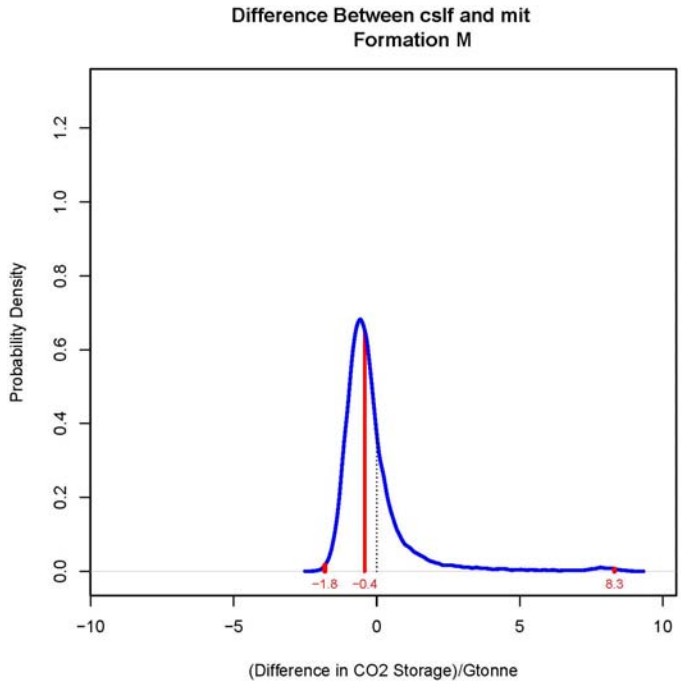
Difference Between cslf and mit
Formation M
Probability Density
0.0
0.2
0.4
0.6
0.8
1.0
1.2
−1.8
−0.4
8.3
−10
−5
0
5
10
(Difference in CO2 Storage)/Gtonne

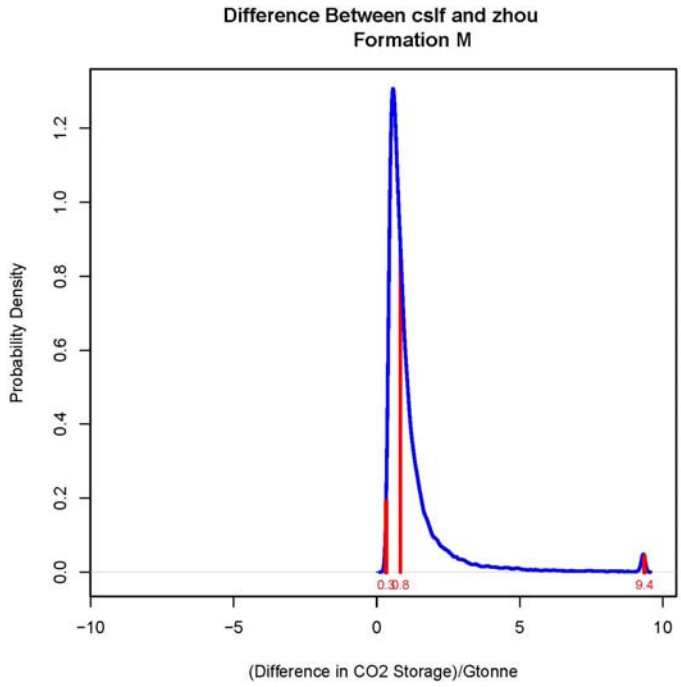
Difference Between cslf and zhou
Formation M
Probability Density
0.0
0.2
0.4
0.6
0.8
1.0
1.2
0.3
0.8
9.4
−10
−5
0
5
10
(Difference in CO2 Storage)/Gtonne

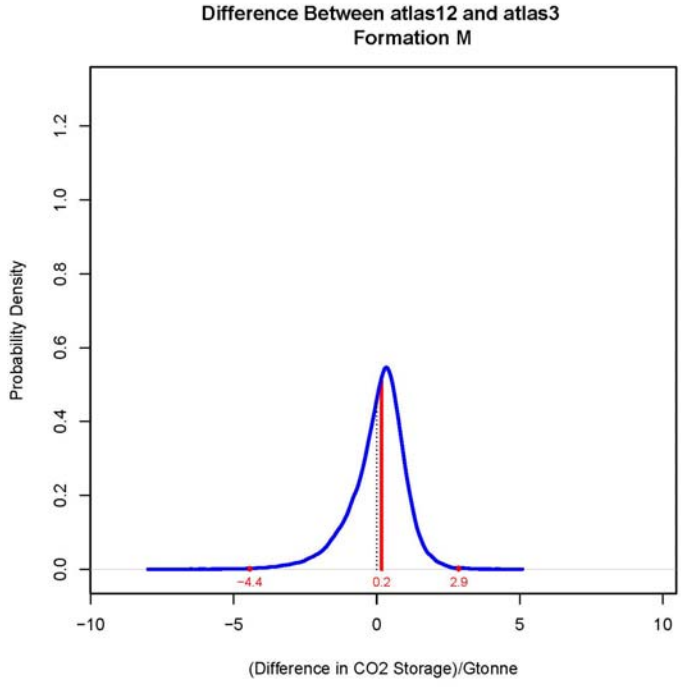
Difference Between atlas12 and atlas3
Formation M
Probability Density
0.0
0.2
0.4
0.6
0.8
1.0
1.2
−4.4
0.2
2.9
−10
−5
0
5
10
(Difference in CO2 Storage)/Gtonne

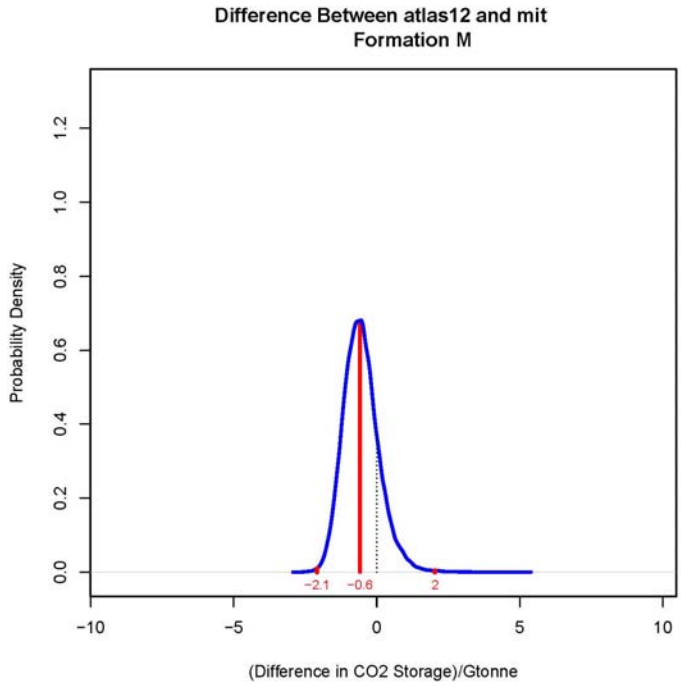
Difference Between atlas12 and mit
Formation M
Probability Density
0.0
0.2
0.4
0.6
0.8
1.0
1.2
−2.1
−0.6
2
−10
−5
0
5
10
(Difference in CO2 Storage)/Gtonne

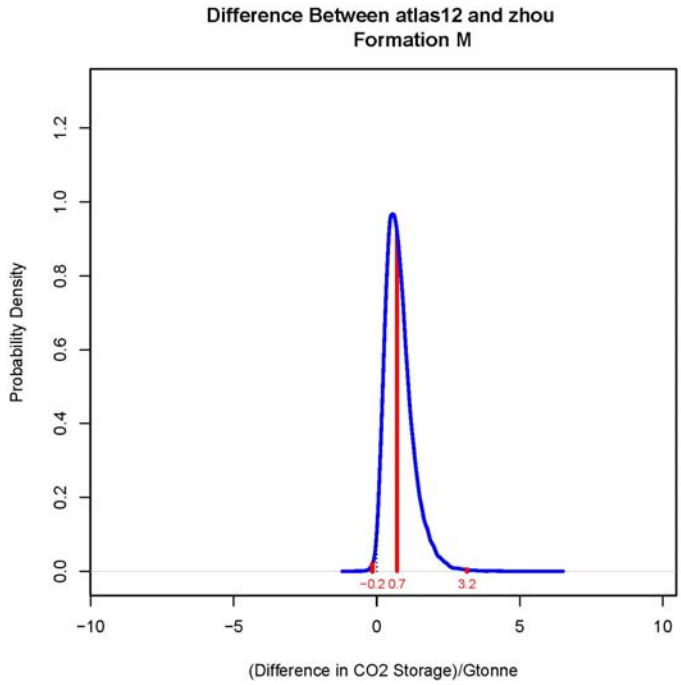
Difference Between atlas12 and zhou
Formation M
Probability Density
0.0
0.2
0.4
0.6
0.8
1.0
1.2
−0.2
0.7
3.2
−10
−5
0
5
10
(Difference in CO2 Storage)/Gtonne

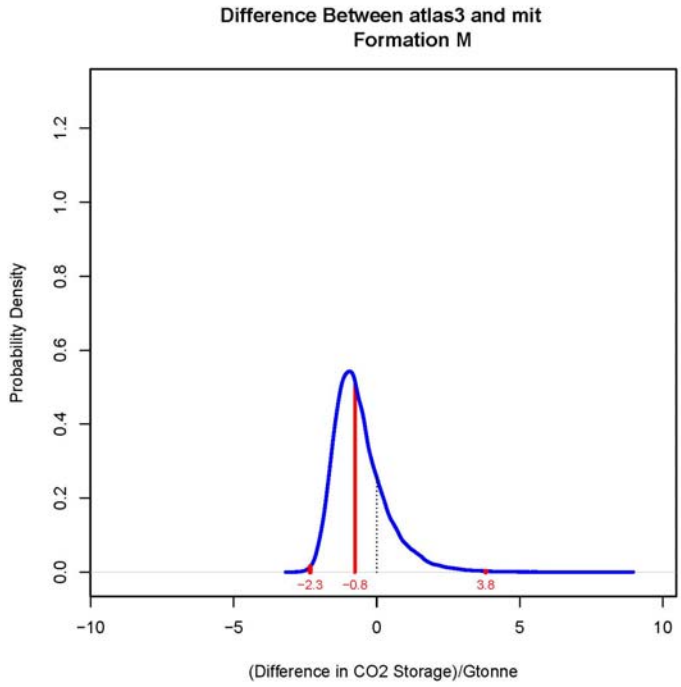
Difference Between atlas3 and mit
Formation M
Probability Density
0.0
0.2
0.4
0.6
0.8
1.0
1.2
−2.3
−0.8
3.8
−10
−5
0
5
10
(Difference in CO2 Storage)/Gtonne

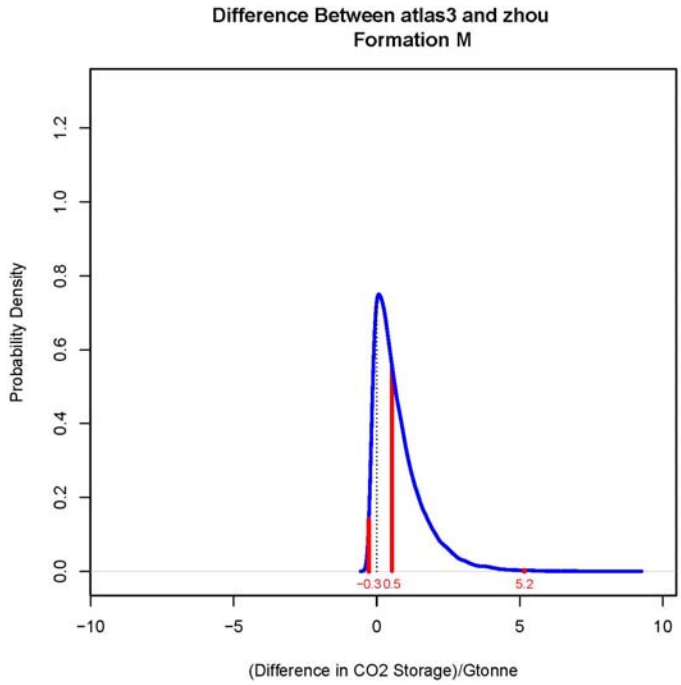
Difference Between atlas3 and zhou
Formation M
Probability Density
0.0
0.2
0.4
0.6
0.8
1.0
1.2
−0.3
0.5
5.2
−10
−5
0
5
10
(Difference in CO2 Storage)/Gtonne

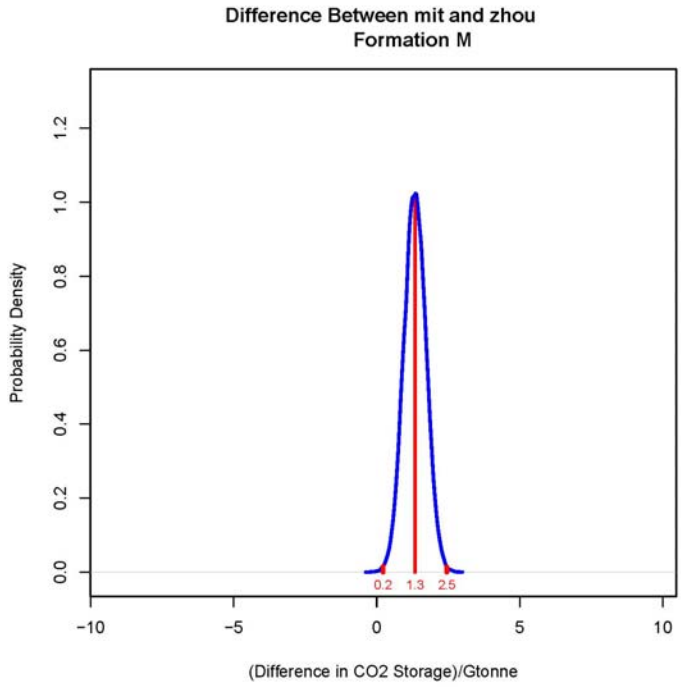
Difference Between mit and zhou
Formation M
Probability Density
0.0
0.2
0.4
0.6
0.8
1.0
1.2
0.2
1.3
2.5
−10
−5
0
5
10
(Difference in CO2 Storage)/Gtonne

This page intentionally left blank.

APPENDIX G:

Overall storage efficiency (%) compiled at the10th, 50th, and 90th percentiles.

CO_2 Storage Efficiency (%)							
Formation	Percentile	CSLF: Bachu et al. (2007) open	DOE-NETL: Altas I, II (2007, 2008) open	DOE-NETL: Atlas III, IV (2010, 2012) open	USGS: Brennan et al. (2010) open	Szulczewski et al. (2012) migration-limited	Zhou et al. (2008) closed
A	P_{10}	1.9	0.6	0.5	1.8	0.2	0.5
	P_{50}	2.7	2.1	2.0	3.6	0.4	0.6
	P_{90}	6.0	5.6	5.4	5.7	0.6	0.8
B	P_{10}	1.9	0.6	0.5	1.8	2.0	0.5
	P_{50}	2.7	2.1	2.0	3.6	3.8	0.6
	P_{90}	6.0	5.5	5.4	5.6	6.6	0.8
C	P_{10}	1.9	0.6	0.5	1.8	0.4	0.4
	P_{50}	2.7	2.1	2.0	3.6	0.9	0.4
	P_{90}	6.0	5.5	5.4	5.6	1.6	0.5
D	P_{10}	1.9	0.6	0.5	1.8	0.6	0.3
	P_{50}	2.7	2.1	2.0	3.6	1.0	0.3
	P_{90}	6.0	5.6	5.4	5.6	1.6	0.4
E	P_{10}	1.9	0.6	0.5	1.8	0.4	0.3
	P_{50}	2.7	2.1	2.0	3.6	1.1	0.4
	P_{90}	6.0	5.5	5.4	5.6	2.1	0.4
F	P_{10}	1.9	0.6	0.5	1.8	0.7	0.3
	P_{50}	2.7	2.1	2.0	3.6	1.6	0.3
	P_{90}	6.0	5.6	5.4	5.7	3.1	0.4
G	P_{10}	1.4	0.6	0.4	1.4	0.3	0.7
	P_{50}	2.0	2.1	1.5	2.6	0.6	0.8
	P_{90}	3.3	5.5	4.0	4.2	1.2	1.0
H	P_{10}	1.9	0.6	0.5	1.8	1.6	0.3
	P_{50}	2.7	2.1	2.0	3.6	2.7	0.3
	P_{90}	6.0	5.6	5.4	5.6	4.3	0.4

Formation	Percentile	CSLF: Bachu et al. (2007) open	DOE-NETL: Altas I, II (2007, 2008) open	DOE-NETL: Atlas III, IV (2010, 2012) open	USGS: Brennan et al. (2010) open	Szulczewski et al. (2012) migration-limited	Zhou et al. (2008) closed
I	P_{10}	1.9	0.6	0.5	1.9	0.7	1.0
	P_{50}	2.7	2.1	2.0	3.5	1.7	1.2
	P_{90}	6.0	5.6	5.4	5.5	3.2	1.4
J	P_{10}	1.4	0.6	0.4	1.4	0.6	1.0
	P_{50}	2.0	2.1	1.5	2.6	1.3	1.2
	P_{90}	3.3	5.5	4.0	4.2	2.4	1.4
K	P_{10}	1.9	0.6	0.5	1.9	0.8	1.0
	P_{50}	2.7	2.1	2.0	3.5	1.6	1.2
	P_{90}	6.0	5.6	5.4	5.5	2.8	1.4
L	P_{10}	1.9	0.6	0.5	1.8	3.7	0.6
	P_{50}	2.7	2.0	2.0	3.6	7.2	0.7
	P_{90}	6.0	5.5	5.3	5.6	12.2	0.8
M	P_{10}	1.9	0.6	0.5	1.8	2.4	0.5
	P_{50}	2.7	2.1	2.0	3.6	4.0	0.7
	P_{90}	6.0	5.5	5.4	5.6	6.4	0.8

The National Energy Technology Laboratory (NETL) conducts cutting-edge energy research and technology development and analyzes energy systems and international energy issues for the U.S. Department of Energy. The NETL-Regional University Alliance (NETL-RUA) is an applied research collaboration that combines NETL's energy research expertise with the broad capabilities of five nationally recognized, regional universities: Carnegie Mellon University (CMU), The Pennsylvania State University (PSU), the University of Pittsburgh (Pitt), Virginia Tech (VT), and West Virginia University (WVU), and the engineering and construction expertise of an industry partner (URS). The NETL-RUA leverages its expertise with current fossil energy sources to discover and develop sustainable energy systems of the future, introduce new technology, and boost economic development and national security.

Sean Plasynski
Deputy Director
Strategic Center for Coal
National Energy Technology Laboratory
U.S. Department of Energy

Jared Ciferno
Director
Office of Coal and Power R&D
National Energy Technology Laboratory
U.S. Department of Energy

Traci Rodosta
Technology Manager
Office of Coal and Power R&D
National Energy Technology Laboratory
U.S. Department of Energy

Mark Ackiewicz
Director
Division of Carbon Capture and Storage
Office of Fossil Energy
U.S. Department of Energy

Cynthia Powell
Director
Office of Research and Development
National Energy Technology Laboratory
U.S. Department of Energy

Timothy McNulty
Associate Vice-President for
Government Relations
Carnegie Mellon University

Henry Foley
Vice President for Research
The Pennsylvania State University

George Klinzing
Vice Provost for Research
University of Pittsburgh

Robert Walters
Vice President for Research
Virginia Polytechnic Institute and State
University

Fred King
Vice President for Research and
Economic Development
West Virginia University

Kevin Donovan
RES Program Manager
URS Corporation